Design and analysis of resilient state estimators for linear discrete-time systems

Alexandre Kircher

N° d'ordre NNT : 2021LYSEC21

Thèse de Doctorat de l'Université de Lyon
opérée au sein de l'École Centrale de Lyon

École Doctorale N° 160 Électronique, Électrotechnique et Automatique (EEA)

Spécialité de doctorat : Automatique

préparée au Laboratoire Ampère, UMR CNRS 5005

Design and Analysis of Resilient state estimators for Linear Discrete-Time systems

---

par Alexandre KIRCHER

Soutenue le 15 juin 2021 devant le jury composé de :

Président	M. Vincent Andrieu	Directeur de Recherche CNRS, LAGEPP
Rapporteur	M. Angelo Alessandri	Professeur Associé, Université de Gênes
Rapporteur	M. Michel Zasadzinski	Professeur des Universités, Université de Lorraine
Examinatrice	Mme Suzanne Lesecq	Directrice de Recherche, CEA LETI
Examinateur	M. Qinghua Zhang	Directeur de Recherche, INRIA
Directeur de thèse	M. Laurent Bako	Maître de Conférences (HDR), Ampère
Encadrant de thèse	M. Mohamed Benallouch	Enseignant Chercheur, ECAM Lyon
Encadrant de thèse	M. Éric Blanco	Maître de Conférences, Ampère

Abstract of the thesis

Given the role of state space representations in engineering methods linked with the control of systems, it is important to know the state of a system, *i.e.* a set of variable describing the system configuration, at all time. However, there are systems for which the state is not directly accessible through measurement. The *state estimation problem* then consists in reconstructing the state of the system through the model of the system (*prior knowledge*) and accessible system measurement (*posterior knowledge*). Moreover, this reconstruction must be performed without knowing the exact values of the disturbances which can be present in the system.

In this PhD work, we will focus on state estimation in the presence of *impulsive noises*. This type of noise is characterised by having most of its entries equal to zero, but its nonzero entries can take arbitrarily large values. Impulsive noises can model a wide range of disturbances, from the temporary loss of sensors to potential attacks on the system.

More precisely, we aim at designing and analysing state estimators able to reconstruct the state of a system despite the presence of impulsive noises. To do so, we will assess if the estimators verify the *resilience property*, which characterises an estimator whose performances are insensitive to a given class of disturbances. We will also investigate the *approximate resilience property*, a weaker version of resilience characterising when a given class of disturbances, potentially unbounded, have a bounded impact on the performances of the estimator.

Every estimator considered in this manuscript will be defined through the *optimal estimation framework*. An *optimal state estimator* will be defined through the minimisation of a given cost function. The role of this cost function is to weight every hypothetical trajectory that the system state can take. The estimator then returns the best state trajectories with respect to this cost function.

The choice of the cost functions is the first problem addressed in this manuscript. After reviewing the state of the art, we focus our attention on two types of state estimators which could be resilient to impulsive noises. The estimators originating from the compressed sensing methods, which use norms in their cost function, form the first type. The second type refers to estimators deriving from the Maximum Correntropy Criterion (MCC) framework. These estimators are defined through cost functions presenting a saturation due to the presence of exponential terms with negative arguments in their expression.

In order for the analysis to cover many estimators, the elements of these classes were defined through their properties, and not through a specific closed-form algebraic expression.

These classes were then analysed. The main theoretical results obtained in this PhD work are upper bounds on the norm of the estimation error, *i.e.* the difference between the real trajectory and the estimated trajectory. The existence of these bounds is guaranteed through sufficient conditions linked to the observability of the

system, to properties verified by the cost function, and to the number of nonzero entries in the impulsive noises. Moreover, these bounds have two main advantages. First of all, they do not depend on the extreme values taken by the impulsive noises. Secondly, they are explicitly expressed with the help of the different parameters of the estimators. This allows us to discuss how these parameters impact the quality of the estimation.

Finally, we will deal with the implementation of the estimators defined in this thesis. Given that they are defined through the solution of an optimisation problem, these state estimators can be complicated to implement. In the case where the estimator is defined through a convex cost function, it can be directly implemented through an algorithm using convex optimisation methods. We also derived several algorithms in order to approximately implement estimators defined through non convex cost function with exponential losses. In addition, we considered the recursive implementation of our estimators and derived Kalman-like recursive algorithms by applying the Forward Dynamic Programming (FDP) framework.

The performances of all the algorithms defined were assessed in simulation. In particular, we displayed four typical cases of applications. These cases, all linked to actual engineering problems, aim at showcasing the versatility of the frameworks developed in this PhD work, and how they can be adapted and implemented to solve these problems.

Keywords : Resilient State Estimation, Secured State Estimation, Optimal estimation, Recursive estimator, Forward Dynamic Programming, Impulsive noise, Sparse noise, Cyber-Physical Systems, Maximum Correntropy Criterion.

Résumé de la thèse

Du fait de la place des représentations d'état dans les méthodes d'ingénierie liées au contrôle des systèmes, il est important de connaître à tout instant l'état d'un système, c'est-à-dire un ensemble de variables décrivant sa configuration. Cependant, cet état n'est pas toujours mesurable directement par le biais de capteurs. Le problème de l'estimation d'état consiste donc à reconstruire l'état du système à partir d'un modèle du système (connaissance *a priori*) et de données mesurables dans le système (connaissance *a posteriori*). En outre, cette reconstruction doit se réaliser sans connaître la valeur exacte des perturbations qui peuvent avoir lieu dans le système.

Cette thèse est consacrée au problème de l'estimation d'état en présence de *bruits impulsifs*. Les bruits impulsifs sont des perturbations dont la caractéristique principale est d'être égales à zéro la plupart du temps, mais leurs valeurs non nulles peuvent être arbitrairement grandes. Ce genre de perturbations se retrouve dans de nombreux systèmes, que ce soit pour modéliser des dysfonctionnements temporaires de capteurs, ou bien des attaques sur le système.

Notre but est de développer et d'analyser des estimateurs pouvant reconstruire l'état d'un système malgré la présence de bruits impulsifs. Pour cela, nous allons étudier la propriété de *résilience* des estimateurs, c'est-à-dire la capacité à produire une erreur d'estimation qui est insensible à la présence d'une classe de perturbations donnée. Nous aborderons aussi la propriété de *résilience approchée* d'un estimateur, qui caractérise le cas où une classe de perturbations, bien qu'à valeurs potentiellement non bornées, a un impact borné sur les performances de l'estimateur.

Le cadre donné aux estimateurs considérés dans ce document est le cadre de l'*estimation optimale*. Ainsi, un estimateur est défini comme l'ensemble des arguments minimisants d'une fonction coût. Cette fonction coût sert à discriminer toutes les trajectoires que l'état du système peut potentiellement emprunter sur un horizon de temps donné. L'estimateur retourne donc les meilleures trajectoires au regard de cette fonction coût.

Une première question abordée dans ce manuscrit est celle du choix de la fonction coût. Après un état de l'art, nous isolons deux types d'estimateurs optimaux pouvant être résilients aux bruits impulsifs. D'une part, les estimateurs dérivés des méthodes d'acquisition compressée, sont définis par des fonctions coûts mettant en œuvre des normes. D'autre part, les estimateurs issus du cadre du *critère de correntropie maximale* (ou *Maximum Correntropy Criterion* (MCC)), sont définis par des fonctions coûts qui saturent via la présence de termes exponentiels avec un argument négatif.

Ces deux types d'estimateurs ont ainsi servi de base aux classes d'estimateurs principales considérées dans ce document. Afin de donner une plus grande portée à l'analyse de ces classes, les fonctions coûts des estimateurs qui les composent ne sont pas définies par une expression algébrique précise mais par un ensemble de propriétés qu'elles doivent vérifier.

L'analyse des propriétés de résilience stricte et de résilience approchée de ces estimateurs est ensuite effectuée. Les principaux résultats théoriques obtenus dans cette thèse sont des bornes sur la norme de l'erreur d'estimation. L'existence de ces bornes est garantie lorsque des conditions, liées à l'observabilité des systèmes considérés, aux propriétés de la fonction coût de l'estimateur, ainsi qu'au nombre d'occurrences du bruit impulsif, sont vérifiées. Par ailleurs, ces bornes ont un intérêt double : elles ne dépendent pas des valeurs extrêmes prises par le bruit impulsif, et elles s'expriment explicitement en fonction des paramètres du système et de l'estimateur. Ce dernier point permet d'analyser l'impact de ces différents paramètres sur la qualité de l'estimation.

Pour finir, la question de l'implémentation des estimateurs d'état définis dans cette thèse est traitée. En effet, du fait de leur définition en tant que solution d'un problème d'optimisation sur un horizon de temps donné, ces estimateurs d'état ne sont pas forcément implémentables directement. Certains d'entre eux sont définis par des fonctions coûts convexes, ce qui rend possible leur implémentation par résolution directe via des algorithmes d'optimisation convexe. Nous avons également développé des algorithmes afin d'implémenter une version approchée de certains estimateurs définis par des fonctions coûts non convexes. Enfin, des algorithmes récursifs, semblables à des filtres de Kalman, ont été proposés pour ces estimateurs via le cadre du Forward Dynamic Programming.

Les performances de l'ensemble de ces algorithmes ont par ailleurs été étudiées, et ce notamment par le biais de quatre cas d'application. Ces cas, tous tirés de problématiques d'ingénierie réelles, montrent la polyvalence du cadre d'estimation développé, et comment il est capable de répondre à des cas pratiques.

Mots clés : Estimation d'état résiliente, Estimation d'état sécurisée, Estimation d'état optimale, Estimateur récursif, Forward Dynamic Programming, Bruit impulsif, Système cyber-physique, Maximum Correntropy Criterion.

Acknowledgements

Nothing means finishing your Ph.D. quite as much as writing its *Acknowledgements* section. For this last challenge, I will try to not forget all the people whom I met over the last three and a half years and who participated, directly or indirectly, to the present document.

First of all, I would like to thank all the members of the Ph.D. committee who accepted to assess my work and attend its defence. Indeed, I am grateful to Prof. Angelo Alessandri and Prof. Michel Zasadzinski for doing me the honour of reviewing my manuscript, and the present document would not be as rigorous if it was not for their remarks and suggestions. My sincere thanks to Dr. Vincent Andrieu who accepted to be the president of this Ph.D. committee despite how difficult and unusual an exclusively online Ph.D. defence can be. I would also like to express my gratitude to Dr. Suzanne Lesecq and Dr. Qinghua Zhang for completing the committee: their questions during the defence allowed for really interesting discussions and prospects around the topic of resilient state estimation.

Moreover, I owe a lot to my three supervisors, Laurent Bako, Mohamed Benallouch and Eric Blanco. During the past three and a half years, they have been of unfailing support and helped me tremendously through all of our interactions, including the meetings, discussions, but also their numerous ideas and remarks. I am grateful for their trust, and it is not an exaggeration to say that I would not have been able to finish this Ph.D. and this manuscript if they were not there, especially when my motivation waned during the context we all know too well.

More specifically, I would like to thank Laurent for his guidance. I learned a lot by working with him, and the way he shared his theoretical knowledge in Automatic Control inspired so many ideas in my work that I cannot count them. I am all the more thankful as he was assuming the really difficult role of being the main supervisor of a Ph.D. student for the first time. I hope this first experience was not too difficult.

I thank Eric for doing his best to bring Laurent and I back on earth when we were losing ourselves in endless theoretical discussions. His more grounded approach and his ability to find practical examples turned out to be invaluable for my understanding of my Ph.D. topic. It is also worth noting that my (humble) first experience in research was also under his supervision, in a study project concerning the design of a guitar effect pedal in 2013. What a long way we have come.

Even if Mohamed might not have been as involved in this Ph.D. as he would have liked to, I still am really grateful for all the refreshing interactions we had over these years. Having his more external point of view gave me perspective on what I was doing and taught me to be as pedagogic as possible when presenting my work. I also would like to thank him for his enthusiasm and optimism regarding the quality of my results, which eventually helped me being proud of what I achieved.

This manuscript would not have been the same without the direct contributions of two teams of the Ampère Laboratory who were kind enough to grant me access to

some of the data they measured.

Indeed, in the first place, I would like to thank Malorie Carpentier's Ph.D. team, through Hubert Razic and Guy Clerc, who gave me access to measurements she made for her thesis, constituting the example provided in Section 4.1 of Chapter 4. Special thanks to Guy Clerc who took the time to explain me the context of this work and how resilient estimation could be relevant for it: the discourse of Section 4.1 owes him a lot.

In the second place, I also thank Jérémy Barra and his PhD team (CEA and Ampère Laboratory) for letting me use their measurements as well as their model for the estimation of a drone position presented in Section 4.4 of Chapter 4. Jérémy explained me thoroughly the issue at stake, walked me through the scripts he provided me and even gave me feedback once I implemented my solution. For this, I am very grateful.

The course of my Ph.D. would also have been very different if I did not have the chance to do it at the Ampère Laboratory, on the ECL site. I would therefore like to show my greatest appreciation to all the members of the Ampère Laboratory whom I have been able to meet during these years.

In particular, I am grateful to Julien Huillery and Gérard Scorletti who were the first to welcome me into this big family in April 2017 for my final year internship, during which we worked on the stability of Linear Time-Varying Systems. Not only did this first experience give me a good overview of research, which eventually led me to pursue a Ph.D., but it also allowed me to discover the atmosphere of the laboratory which suited me so much that I decided to spend three and a half years there.

I also owe a lot to Anton Korniienko who, in addition to his enthusiastic nature, was most helpful to the Ph.D. student with limited financial resources that I was when I had to publish my ACC paper.

Obviously, I could not write this section without acknowledging some of the Ph.D. students who constituted the core of my everyday interactions since April 2017. I will start with some of the "old geezers", those who where already there and mostly done when I arrived: François, Khaled, Sérgio, Zhao, Arbi, among others. Thank you very much for showing me how friendly and supportive a Ph.D. student should be to their peers, in a spirit that my fellow Ph.D. colleagues and I tried to preserve as much as possible. The only thing for which I am not grateful is how most of you finished your Ph.D. in four years, setting a bad example that I unfortunately followed.

I have been really lucky to spend these years with many wonderful Ph.D. students. I would like to thank the *salle Poitou* gang, Wassim, Yanis, Hussein, Debou, and the many guests it welcomed, such as Nicolas, or Hadiseh. Sharing this office was an honour and I wish you all the best in your future endeavours.

I also acknowledge our rivals, the NEXT4MEMS gang, namely Kevin, Federico, Jorge, Fabricio and Eva who infiltrated their office despite not working on their project anymore. We definitely beat you in terms of coffee break length, but most of you beat us to the Ph.D. graduation, so I would call this a draw.

Many other students do not fit in those two groups, but their presence and our discussions helped me a lot. This includes many great people such as Arthur, Grégory, Sigurd, Marion, Abdelghani, Fatma, Jérémy B. or Quentin.

Finally, my deepest appreciation goes to all my friends and relatives who were there to support me during this especially hard journey. I am incredibly lucky to

have been well surrounded all those years and I would not have been able to make it without them.

I would therefore like to thank my parents who have always encouraged me to study, and provided me with everything I needed in order to succeed in higher education. In addition, I thank my brother Nicolas, my grandparents, uncles, aunts and cousins for all they have done for me, and wanting to make them proud turned out to be a huge drive for this work.

I am also grateful to the many people and acquaintances I have met over the last few years:

- my friends from ECL, with a special thanks to Antoine, Nicolas and Vincent for tolerating me as a flatmate from 2016 to 2019,
- my friends from Metz and its surroundings whom I have not been able to see in ages because of this work,
- Arnaud, (he has got a bullet point just for him, how lucky)
- all my friends from Asperly, LFR, LC, HKSRC, and CF (cryptic acronyms, I know).

And I could not acknowledge my friends and families without talking about my partner of more than five years, Camille. I will be forever indebted to her for everything she has done for me. The last year before I turned in my manuscript was especially hard for the both of us, and I hope I will be able to pay off all the support she gave me.

Last but not least, I will NOT thank our cat, Paprika, who found a safe haven in my desk and napped there more often than not. The extra months that this manuscript took can solely be explained by the fact that she was just too cute to be displaced (see Figure 0).

FIGURE 0: A blissful cat preventing an honest Ph.D. student from completing their manuscript

Contents

List of Figures

Glossary

Disturbance	A disturbance is a signal that tends to adversely affect the value of the output of a system [Oga09, Sec.1-1].
Model	Set of mathematical variables and relations which represent a system and its internal behaviours in order to link its inputs and outputs.
Offline state estimator	An estimator which reconstructs the state trajectory of a system based on all the measurements available on the same time-horizon.
Online state estimator	An estimator which reconstructs the state of a system while receiving the data available from the system.
Outlier	Aberrant value which differs significantly from the rest of the values in terms of magnitude order.
State	The state of a system is a variable or a set of variables which contribute to the description of the configuration in which a system is at a given instant of time. [Sim06]
State estimator	Algorithm which aims at reconstructing the state of a system through the use of a model and accessible system measurements.
Resilience	Property of an estimator which induces an estimation error insensitive to the presence of a given class of disturbances.
Sparsity	Characteristic of an object (noise, matrix, vector, etc.) whose entries are almost all equal to zero.
System	A system is a combination of components that act together and perform a certain objective. It need not to be physical and the concept can be applied to abstract phenomenons such as those encountered in economics. [Oga09, Sec. 1-1]

Nomenclature

Symbols

$\mathbb{R}$	Set of real numbers
$\mathbb{R}_{\geq 0}$ $(\mathbb{R}_{\leq 0})$	Set of non-negative (resp. non-positive) real numbers
$\mathbb{R}_{>0}$ $(\mathbb{R}_{<0})$	Set of positive (resp. negative) real numbers
$\mathbb{N}$	Set of natural numbers
$\mathbb{N}_{\neq 0}$	Notation for $\mathbb{N} \setminus \{0\}$
$\mathbb{K}^{a \times b}$	Set of matrices with a rows et b columns whose values are in the field $\mathbb{K}$
$\mathbb{K}^{a}$	Set of column vectors with a elements within $\mathbb{K}$
$\mathbb{R}^{a}_{\geq 0}$ $(\mathbb{R}^{a}_{>0})$	Set of vectors with a nonnegative (resp. positive) elements
$\mathcal{S}^{+}_{a}(\mathbb{K})$	Set of positive definite matrices with a rows whose values are in $\mathbb{K}$
$\lvert\mathcal{S}\rvert$	Designates the cardinality, *i.e.* the number of elements, of the set $\mathcal{S}$
$\mathcal{P}(\mathcal{S})$	Power set of set $\mathcal{S}$, *i.e.* the collection of subsets of $\mathcal{S}$
I_a	Identity (square) matrix with a rows
$\mathbb{0}_{a \times b}$	Zero matrix with a rows and b columns
$\mathbf{diag}(z_1, ..., z_n)$	Diagonal matrix from $\mathbb{R}^{n \times n}$ which has the (ordered) values z_1,..., z_n on its diagonal
$M^{\top}$	Transposed matrix of matrix M
t	Time variable. Without any explicit statement, it will be supposed to be *discrete* and within $\mathbb{N}$
$\xi^{(k)}$	k-th time derivative of function ξ
ξ^{-1}	Inverse function of function ξ
$\nabla\xi$	Gradient of function ξ
$\mathcal{K}_{\infty}$	Set of continuous and increasing functions g from $\mathbb{R}_{\geq 0}$ to $\mathbb{R}_{\geq 0}$ such that $g(0) = 0$ and $g(\lambda) \to \infty$ when $\lambda \to \infty$
$\mathbb{I}$	Set of state indexes
$\mathbb{J}$	Set of sensor indexes
$\mathbb{T}$	Set of time indexes

$\|\cdot\|_p$	The ℓ_p norm (for $p \geq 1$) or pseudo-norm (for $0 < p < 1$) such that for any z in $\mathbb{R}^a$, $\|z\|_p = (\|z_1\|^p + \cdots + \|z_a\|^p)^{1/p}$ where z_i is the i-th component of z.
$\|\cdot\|_0$	The ℓ_0-norm which returns the number of non-zero entries of its argument.
$\|\cdot\|_M^2$	The quadratic form weighted by $M \in \mathcal{S}_a^+(\mathbb{R})$, such that for all z in $\mathbb{R}^a$, $\|z\|_M^2 = z^\top M z$
$\|\cdot\|_\infty$	The infinity norm which returns the biggest component of its argument.
$\mathbf{vec}(Z)$	For a matrix $Z = \begin{pmatrix} z_1 & z_2 & \cdots & z_b \end{pmatrix} \in \mathbb{R}^{a \times b}$ ($z_i \in \mathbb{R}^a$), designates its vectorization, *i.e.* the vector $\begin{pmatrix} z_1^\top & z_2^\top & \cdots & z_b^\top \end{pmatrix}^\top$ from $\mathbb{R}^{(ab)}$

Acronyms

CPS	**C**yber-**P**hysical **S**ystem
FDP	**F**orward **D**ynamic **P**rogramming
LHS	**L**eft-**H**and **S**ide
LSE	**L**east **S**quares **E**stimator
LTI	**L**inear **T**ime-**I**nvariant
LTV	**L**inear **T**ime-**V**arying
MCC	**M**aximum **C**orrentropy **C**riterion
REE	**R**elative **E**stimation **E**rror
RHS	**R**ight-**H**and **S**ide

Linear Time-Varying (LTV) Discrete-time State-Space representation:

$$\Sigma : \begin{cases} x_{t+1} &= A_t x_t + w_t \\ y_t &= C_t x_t + f_t \end{cases} \quad \text{with } x_0 \in \mathbb{R}^n \text{ initial state of the system.}$$

with

$$\begin{array}{ll} x_0 \in \mathbb{R}^n & : \text{Initial state of the system} \\ x_t \in \mathbb{R}^n & : \text{State vector} \\ A_t \in \mathbb{R}^{n \times n} & : \text{State matrix at time } t \\ w_t \in \mathbb{R}^n & : \text{Unknown process disturbance} \\ y_t \in \mathbb{R}^m & : \text{Measurement vector} \\ C_t \in \mathbb{R}^{m \times n} & : \text{Measurement matrix at time } t \\ f_t \in \mathbb{R}^m & : \text{Unknown output disturbance} \end{array} \tag{0.1}$$

Supremum: Given a function f over $\mathbb{R}^a$ and a subset $\mathcal{S}$ of $\mathbb{R}^a$, the notation

$$\sup_{z \in \mathcal{S}} f(z) < b, \tag{0.2}$$

with $b \in \mathbb{R}$, will mean that for all z in $\mathcal{S}$, $f(z) < b$. This notation includes the case where the supremum is b but is not attained by any element of $\mathcal{S}$.

General Introduction

Context and purpose of this thesis

In this manuscript, we will investigate the problem of *estimating the state of a system*. From a conceptual point of view, a *system* is a combination of components that act together and perform a certain objective [Oga09, Sec. 1-1]. A car, an electrical network, or a chemical process, are three examples of system, which shows the versatility of the notion and how central it is in the field of modern engineering.

From an analytical point of view, a system can be described by a *model*, which is a set of equations and parameters describing its internal behaviour as well as the interactions with its environment. A possible model structure is the *state-space representation*, which is of the form

$$\begin{aligned} x_{t+1} &= g(x_t, u_t, w_t) \\ y_t &= h(x_t, u_t, f_t), \end{aligned}$$

with u_t the known inputs of the system, w_t and f_t unknown inputs disturbing the system, y_t the outputs of the system, and g a function describing the system dynamics and h a function describing the measurement process. In this structure, we see that x_t plays a central role, as the way it evolves over time determines completely the dynamics of the system, and it makes the connection between the inputs and the outputs of the system. x_t is called the *state of a system*, and it is relative to the state-space model displayed above.

The state of a system is a variable or a set of variables contributing to the description of the system at a given instant of time [Sim06]. A state therefore describes the evolution of different quantities involved in the system, and depends on the considered model. For a car, possible state variables are its position and its velocity. In an electrical network, the state can gather the voltage in each branch. In a chemical process, it can represent the amount of substance of each component involved in the chemical reaction.

Describing a system through a state-space representation is an interesting approach, given that state-space representations are at the core of many engineering methods, such as feedback control [AJ05], health monitoring [Sah09], failure detection [Man12] or target tracking [Cha84]. Successfully operating a system then requires to know the evolution of the system state in order to be able to use these methods.

However, in some engineering systems, the state cannot be directly measured. Several reasons can explain that:

- The state cannot be measured in a way which does not disturb the system.
- There does not exist any sensor for measuring it, or the potential existing sensors do not fit the specifications of the system.
- There are too many points of interest to realistically measure them all.

The *state estimation problem* then consists in reconstructing the system state without directly measuring it. To do so, one can only use the *accessible knowledge*, which means the model of the system and the values of the known inputs (*prior knowledge*), as well as the measured outputs of the system (*posterior knowledge*). In addition, we do not have access to the exact values of the unknown inputs disturbing in the system.

To solve the state estimation problem, a common solution is to use the accessible knowledge in order to compute an estimate of the system state through an algorithm called a *state estimator*.

The state estimation framework started to be developed in the late 1950s and early 1960s. In the first place, it was developed for linear systems, and in the presence of either no disturbance for the Luenberger observers [Lue64], or Gaussian disturbances for the Kalman Filter [Kal60]. From there, the study of state estimators then grew throughout the years. For instance, we can cite the development of state estimators for nonlinear systems through the Extended Kalman Filter [Chu17]. The question of the robustness of state estimators was also thoroughly explored [Pet99].

Every state estimator is designed to operate in the presence of given types of *disturbances*, which are quantities unknown to the estimator and which disturb the system. This report will focus on state estimation in the presence of *impulsive noises*, *i.e.* noises which most of the time are equal to zero but whose nonzero values can potentially have arbitrarily large magnitudes. Such noises can model a wide range of system events, such as intermittent sensor failures, temporary loss of measurements, or even attacks where an attacker replaces actual measurements with aberrant values.

To design state estimators able to reconstruct the system state despite the presence of impulsive noises, we investigate the *resilience property*, which characterise an estimator whose performances are insensitive to the presence of a given type of disturbances. This topic of research has been gaining more and more interest in the past ten years. This rather recent interest can be explained by the development of *Cyber-physical systems* (CPS), systems operated through a computer network, since the early 2000s. This development has even been encouraged through national [Fou06] and international [EC18] programs.

However, a major vulnerability of this type of system is the risk of cyberattacks, as it was evidenced by an attack launched on an electrical substation of Kiev (Ukraine) in 2016 [Inc17]. During this attack, a malware infected the substation operating network and managed to obtain a direct access to the substation automation system, greatly impacting the electric grid operations as a result. One of the conclusions of the report [Inc17], analysing the capabilities of the malware, is that no passive computer security can prevent such an attack. Consequently, there is a need to provide systems like CPS with estimation processes capable of performing accurate estimation even under attacks, in order to still provide accurate monitoring for the operators as well as protecting critical installations relying on the estimate to operate.

Nevertheless, since they were designed to operate in the presence of dense disturbances like Gaussian noises only, the "classical" state estimators which have been developed for the last sixty years, such as the Kalman Filter [Kal60], perform poorly in the presence of impulsive noises. Consequently, this spurred the need to design *resilient estimation frameworks*, *i.e.* estimation frameworks insensitive to the presence of impulsive disturbances.

This context motivates our work and the present manuscript. Our purpose is to design a family of state estimators and analyse their resilience properties. This work is mainly theoretical, and aim at providing guarantees about the property of resilience of those frameworks. Nevertheless, a part of this manuscript is also devoted to cover more practical aspects of resilient state estimation, such as the derivation of recursive resilient state estimators, or a review of some possible use cases of resilient estimators.

Structure of the document & Contributions

The present manuscript designs and studies analysis tools to assess the resilience of different class of optimisation-based estimators. The following outline underlines the structure of the document as well as summarises the several points of contribution of our work:

Chapter 1. In this chapter, we review all the already-existing analysis tools which will be necessary for the subsequent chapters. The most notable concepts introduced in this chapter are:

- the considered class of systems, the Linear Time-Varying Discrete-time state-space representations.
- the optimal estimation framework through which every studied state estimator will be defined. Indeed, every optimal state estimator will be defined as the set-valued map which associates every set of measurement to the most likely state trajectories with respect to a given *performance index function* composed of smaller objective functions called the *loss functions*.
- the specifications of the resilient estimation setting and of *arbitrary noises*, which are the disturbances that resilient estimators must face in our framework.

Most of the results presented in this chapter are taken from the estimation literature, and every borrowed result is duly referenced. In particular, a review of the state of the art of resilient state estimation will be presented. This review is structured around two families of resilient approaches. Those two approaches were developed independently but share the same core structure and ideas which make them suited to tackle the resilient estimation problem. Consequently, we structured our analysis in order to properly explore those two types of resilient estimation frameworks, yielding Chapters 2 and 3.

Chapter 2. This chapter, constituting the first part of our analysis, is focused on the study of the resilience property for a class of optimisation-based state estimators. This class of estimators is meant as a generalisation of the resilient state estimators derived from the compressed sensing theory [Faw14; Paj17; Cha18]. We define these optimal estimators through a class of performance index functions which are defined by their properties rather than by a closed-form expression. This allows a more general analysis as well as helps us understand which properties induce the resilience of an estimator.

All the developments presented in this chapter are novel. The main result of the chapter is the derivation of an upper bound on the estimation error which, under the right circumstances, is independent from the greater values of the disturbances: this ensure the resilience of the class of estimators, *i.e.* the insensitivity to the extreme values of arbitrary noises. In order for this property to hold, the system whose state

is to be estimated must be observable enough with respect to a custom quantitative measure which will be introduced. Moreover, the derived bound, despite not being easily computable in practice, is linked to the properties of the estimator and of the system. This provides qualitative hindsight on which parameters play a role in the quality of the estimation and to what extent.

Several other developments and discussions are provided in this chapter. Among them, we discuss the exact recoverability, which is the case where the estimator yields exactly the real state trajectory, in the case where there is no process noise. We will also deal with how we can derive heuristic recursive estimation algorithms from the studied estimators. Finally, we will provide some simulations in order to numerically assess some of theoretical developments presented in the chapter.

Chapter 3. This chapter, in the continuity of Chapter 2, proposes an analysis of resilience for *another* class of optimisation-based state estimators. In this chapter, the loss functions are still defined through their properties, but they are wrapped in a decreasing exponential function in order to induce a saturation in the resulting performance index functions defining the state estimators. Those saturated performance index functions are meant as a way to generalise the Maximum Correntropy Criterion (MCC)-based state estimators [Iza16; Che17a; Liu17].

If the core idea of the analysis is inspired by [Bak18], the novelty resides in its extension to the LTV Discrete-time state-space representations. The main result is similar to the one of Chapter 2, and it ensures that the estimation error is bounded by a value which does not depend on the extreme values of the noise if it verifies conditions which are linked with the observability of the system. Once again, the bound itself involves parameters of the estimator and the system, which allows us to qualitatively interpret it.

In this framework, none of the considered performance index functions is convex. A discussion on how to implement them will therefore be provided, leading to the definition of several heuristic batch and recursive algorithms. To complete the chapter, like in Chapter 2, several numerical simulations will be presented in order to illustrate some aspects of the analysis.

Chapter 4. In the last chapter, we propose four use cases of the frameworks studied in Chapters 2 and 3:

- The filtering of measured time series presenting outliers.
- The estimation of the parameter vector of regressive static models in the presence of impulsive noise.
- The estimation of the state of a switching system without any knowledge of the switching signal.
- The online estimation of the position of a drone with temporary loss of measurements.

For every use case, the relevancy of the presented estimators will be argued and then corroborated with simulation results. There will be no additional theoretical contribution in this chapter, its goal being to showcase the variety of engineering problems which can be addressed with resilient state estimation frameworks.

Publications

Accepted peer-reviewed conference papers

Alexandre Kircher, Laurent Bako, Éric Blanco, Mohamed Benallouch, and Anton Korniienko. "Analysis of resilience for a State Estimator for Linear Systems". In: American Control Conference (ACC). July 2020, pp. 1495–1500. URL: https://hal.archives-ouvertes.fr/hal-03181789

Alexandre Kircher, Laurent Bako, Éric Blanco, and Mohamed Benallouch. "On the resilience of a class of correntropy-based state estimators". In: IFAC World Congress (1st IFAC-V). Berlin, Germany, July 2020. URL: https://hal.archives-ouvertes.fr/hal-02903156

Accepted peer-reviewed journal paper

Alexandre Kircher, Laurent Bako, Éric Blanco, and Mohamed Benallouch. "An optimization framework for resilient batch estimation in cyber-physical systems". In: *Transactions on Automatic Control* (2021). (Provisionally accepted). URL: https://arxiv.org/abs/1906.01714

Chapter 1

Overview of optimal state estimation

1.1 Introduction

Before tackling the analysis of the resilience properties of optimisation-based state estimators, a few key concepts must be stated and explained in order to ensure a comprehensive basis on which the further developments will be conducted.

The present chapter is constructed in order to gradually lead to the formulation of the resilient state estimation problem. It starts by presenting the *state estimation problem* (Section 1.2), requiring the introduction of state-space representations and of a key property for estimation called the *Observability*. Luenberger estimators, which constitute a first introductory example to state estimators, will then be presented. First, they will be presented through the scope of their original development. Secondly, we will deal with the $\mathcal{H}_\infty$ approach which is a way to design a Luenberger estimator as the solution of an optimisation problem.

In the second place, we consider *optimisation-based estimators* (Section 1.3), whose structure and parameters are decided through an optimisation process. This optimisation process is performed over a performance index function which discriminates all the potential state trajectories in order to indicate the most plausible ones: we will therefore present this type of functions, and especially the specific structure they will respect throughout this manuscript. We will also introduce the Least Squares Estimator (LSE), which is the optimal estimator in the presence of Gaussian noise sequences. Subsequently, the link between batch and recursive implementation will be explored through the Forward Dynamic Programming (FDP). Both concepts (LSE and FDP) will play a preponderant role in ulterior developments presented in Chapters 2, 3 and 4.

Finally, we will deal with resilience in state estimation. Section 1.4 starts by showing the limits of classical optimal observers, such as the LSE, in the presence of *impulsive noises*, *i.e.* noises which are almost always equal to zero but can potentially take large nonzero values. The rest of the section will then aim at characterising the type of disturbances which are to be handled in a resilient framework. This leads us to present a review of resilient state estimation in the literature (Section 1.5). This review will be articulated around three main points: detection approaches, compressed-sensing inspired methods and Maximum Correntropy Criterion (MCC)-related works. For each point, we will describe existing solutions, if there are potential guarantees about their resilience, and sometimes deal with the question of their implementation. This eventually allows us to better position the contribution of this report, which is in the continuity of the compressed-sensing and MCC-related approaches.

1.2 The framework for state estimation

1.2.1 State-space representations of systems

A system can be viewed as a part of the universe which has been isolated. From the outside, it is mainly characterised by its inputs and its outputs which are what enters and comes out of it (see Figure 1.1). Inputs can be classified into two main categories: known inputs and unknown inputs. Indeed, there are inputs whose values are known at all times, either because they can be measured or they are directly applied by an operator. Some other inputs are unknown, which means that we do not know their value at any time: we may have a model of those signals, but such a model cannot help us assess the real exact value. Most of the time, the known inputs do not pose any particular problem in an estimation process: consequently, from now on, we will consider that systems are only affected by unknown inputs.

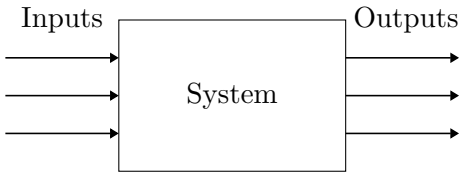

FIGURE 1.1: Schematic principle of a system

Systems obviously also have an internal functioning in order to produce their outputs from their (unknown) inputs, and it is this internal functioning which is at stake when modelling a system. For this work, we will consider *Linear Time-Varying (LTV) Discrete-Time state-space representations* which are models of the form

$$\Sigma : \left\{ \begin{array}{rl} x_{t+1} & = A_t x_t + w_t \\ y_t & = C_t x_t + f_t \end{array} \right. , \tag{1.1}$$

with $x_0 \in \mathbb{R}^n$ the initial state of the system.

For these models, time index t is a natural number. At a given time $t \in \mathbb{N}$, the *unknown input variables* $w_t \in \mathbb{R}^n$, $f_t \in \mathbb{R}^m$ and the *output variables* (or *measurements*) $y_t \in \mathbb{R}^m$ of the model are interconnected through two equations by internal variables, the *states*, which are gathered in the *state vector* $x_t \in \mathbb{R}^n$. The first equation, called the *state equation* (or *dynamic equation*), encapsulates the internal dynamics of the system and how it evolves through time. The second equation is called the *output equation* (or *measurement equation*) and models how the internal dynamics produce the outputs of the system.

Input signals $\{w_t\} \subset \mathbb{R}^n$ and $\{f_t\} \subset \mathbb{R}^m$ will be labelled as *disturbances*: they represent quantities which disturb the two system equations, like sensor noise or small dynamical elements omitted in the model.

The relations between the variables x_t, y_t, w_t, f_t of the system defined in (1.1) are *linear*. More precisely, they are linked by matrices which do not depend on them, namely the *state matrix* $A_t \in \mathbb{R}^{n \times n}$ and the *output matrix* $C_t \in \mathbb{R}^{m \times n}$. Those matrices can still change over time, as indicated by the mention *Time-Varying*. However, we might sometimes consider the Time-Invariant case, *i.e.* state-space representations of the form

$$\Sigma : \left\{ \begin{array}{rl} x_{t+1} & = A x_t + w_t \\ y_t & = C x_t + f_t \end{array} \right. , \tag{1.2}$$

with $x_0 \in \mathbb{R}^n$ the initial state of the system.

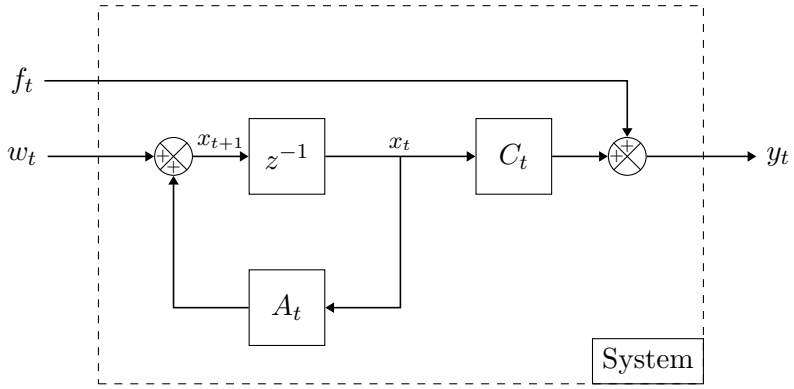

FIGURE 1.2: Block diagram of an LTV Discrete-Time State-Space representation

To help visualising how the components of the model are interconnected, Figure 1.2 presents a block diagram which illustrates how a LTV Discrete-Time state-space representation works: the z^{-1} block is simply a lag block, which represents the fact that after one time iteration, x_{t+1} becomes x_t.

Remark 1.1. *We acknowledge that in practice, a model represents only partially the way a system functions. It will however be assumed that the model is accurate enough for our objectives, which means that we will often use the words "System" and "Model" interchangeably, even though they do not designate the exact same thing.*

The choice to consider Discrete-Time state-space representations was made in order to be able to easily implement the estimation processes on chips, as nowadays, more and more estimation is performed on digital devices. As most engineering systems deal with continuous-time dynamics for which continuous-time state-space representations might be more indicated, there is a need to discretise those models, which can be performed through various methods such as the Euler methods or the Zero-order hold method [Mat].

1.2.2 The state estimation problem

With the class of considered systems defined, we can now characterise the problem of *state estimation*, which is the problem of estimating the inner state of a system modelled through the framework of state-space representations. The estimation process of the state vector x_t can only be performed with the help of matrices A_t, C_t and of the measurements $\{y_t\}$, but without knowing the exact value of disturbances $\{w_t\}$ and $\{f_t\}$. A *state estimator* (or *observer*) is a method implemented in order to solve this issue: it uses all the accessible knowledge, *i.e.* the model of the system and the measurement y_t, to obtain an estimate of the state vector (which will be denoted $\hat{x}_t$) as an output of the estimator. This process is summarised in the block diagram presented in Figure 1.3.

Let T be an integer denoting a time-horizon of interest. For convenience, we define matrices $X_{T-1} \in \mathbb{R}^{n\times T}$, $\hat{X}_{T-1} \in \mathbb{R}^{n\times T}$ and $Y_{T-1} \in \mathbb{R}^{m\times T}$ which are the matrices concatenating respectively the states, the estimated states and the measurement

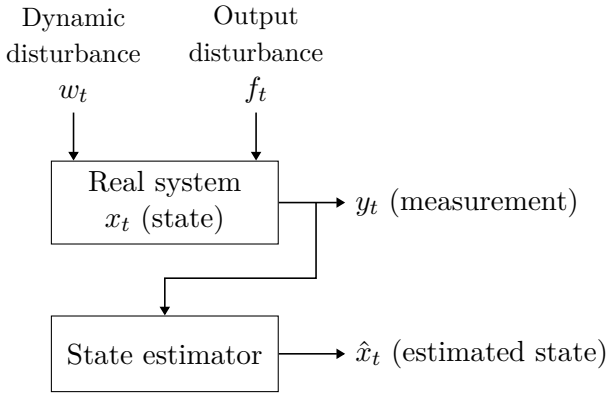

FIGURE 1.3: Block diagram of the principle of state estimation

between $t = 0$ and $t = T - 1$, *i.e.*

$$X_{T-1} = \begin{pmatrix} x_0 & x_1 & \cdots & x_{T-1} \end{pmatrix}, \tag{1.3}$$

$$\hat{X}_{T-1} = \begin{pmatrix} \hat{x}_0 & \hat{x}_1 & \cdots & \hat{x}_{T-1} \end{pmatrix}, \tag{1.4}$$

$$Y_{T-1} = \begin{pmatrix} y_0 & y_1 & \cdots & y_{T-1} \end{pmatrix}. \tag{1.5}$$

X_{T-1} and $\hat{X}_{T-1}$ will be called *state trajectory* and *estimated state trajectory* respectively, while Y_{T-1} will be called the *measurement history*. As $T - 1$ will be the default time horizon used throughout this document (in order to have matrices with T columns), the index will sometimes be omitted, and unless explicitly stated otherwise, X, $\hat{X}$ and Y will respectively refer to the state trajectory, the estimated state trajectory and the measurement history from $t = 0$ to $t = T - 1$.

The problem of estimating the state trajectory X over the time horizon $[0, T-1]$ depends on the range of measurements which are accessible at the time of the estimation. If we assume that the measurements are accessible up to $t = k$, *i.e.* we have access to Y_k, at the time of the estimation $(T - 1)$, the different values that k can take lead to different estimation scenarios according to a standard classification [Jaz07, p.143]:

- **If** $k < T - 1$, we are in the **prediction scenario** where we want to predict the state trajectory which will occur between $k+1$ and $T-1$ without knowing what the output of the system is on that interval.
- **If** $k = T - 1$, it is the **filtering scenario** where we filter the measurement history Y_k to estimate the state trajectory on the same time horizon.
- **If** $k > T - 1$, we are in the **smoothing scenario** where we want to update past estimates with the additional knowledge of measurements which happen afterwards.

To express this nuance, the extent of the knowledge used to obtain an estimated state or trajectory will sometimes be specified through the notations $\hat{x}_{T-1|k}$ and $\hat{X}_{T-1|k}$, which means both were obtained with Y_k, the measurements up to k. However, since this document mainly deals with the filtering and smoothing scenarios, the notations $\hat{x}_t$, $\hat{X}_T$ will implicitly mean that the estimated state/trajectory was obtained thanks to Y_t and Y_T respectively.

1.2.3 On the concept of observability

Before discussing some classical solutions to the state estimation problem, we start by asking whether it is well-posed. In other words, under what condition the state trajectory X of System (1.1) can be inferred uniquely from the measurements? Indeed, some minimal condition needs to be imposed on the model (1.1). To illustrate the necessity for such a condition, consider the example of the autonomous system

$$\Sigma : \left\{ \begin{array}{ll} x_{t+1} & = A_t x_t \\ y_t & = C_t x_t \end{array} \right. \tag{1.6}$$

with

$$\forall t \in \mathbb{N},\ A_t = \begin{pmatrix} 2 & 2 \\ 1 & 1 \end{pmatrix},\ C_t = \begin{pmatrix} 1 & 1 \end{pmatrix}.$$

By considering the two potential initial states $x_0 = (\,1 \quad -1\,)^\top$ and $x_0 = (\,-1 \quad 1\,)^\top$, we realise that for any time t, y_t is equal to zero in both cases. As a result, those two initial states are entirely indistinguishable from each other given that the measurement history Y_T they generate are identical for every $T \in \mathbb{N}^\star$.

This example illustrates the existence of systems for which the state cannot be uniquely recovered from the output. To rule out such pathological cases, the estimation problem is confined to systems having the following property, called *observability*:

Definition 1.1 (Observability of a system [Oga06, p.389])**.** *Let a system Σ be ruled by (1.6). Σ is said to be completely observable if every initial state $x_0 \in \mathbb{R}^n$ can be inferred from the observation of a finite measurement history $Y \in \mathbb{R}^{m \times T}$.*

By this definition, the model presented in the introductory example is not observable as we exhibited two potential initial states for which every measurement history, no matter how large, is identical.

In this manuscript, we will consider LTV systems on a given time horizon of interest. Consequently, we define the concept of *Observability on a given time horizon*:

Definition 1.2 (Observability of an LTV system on a given time horizon)**.** *Let Σ be a system ruled by equations (1.1) and T in $\mathbb{N}_{\neq 0}$. Σ is said to be observable on time-horizon $[0, T-1]$ if the matrix*

$$\mathcal{O}_{T-1} = \begin{pmatrix} C_0^\top & (C_1 A_0)^\top & \cdots & (C_{T-1} A_{T-2} \ldots A_0)^\top \end{pmatrix}^\top \in \mathbb{R}^{(mT) \times n} \tag{1.7}$$

is of full column rank, i.e. of rank n.

The matrix $\mathcal{O}_{T-1}$, called the *Observability matrix*, plays a key role in the assessment of the observability property. To study this a little bit further, if we consider a system ruled by equations (1.6), then every measurement y_t can directly be expressed from the initial state as

$$\forall t \in \mathbb{N},\ y_t = C_t A_t A_{t-1} \ldots A_0 x_0 \tag{1.8}$$

If we gather T measurements of the system, then the vectorization of measurement history matrix Y can be calculated in the matrix form, *i.e.*

$$\text{vec}(Y) = \begin{pmatrix} y_0 \\ y_1 \\ \vdots \\ y_{T-1} \end{pmatrix} = \begin{pmatrix} C_0 \\ C_1 A_0 \\ \vdots \\ C_{T-1} A_{T-2} ... A_0 \end{pmatrix} x_0 \tag{1.9}$$

which entails $\text{vec}(Y) = \mathcal{O}_{T-1} x_0$. If the system is observable on time-horizon $[0, T-1]$, the observability matrix $\mathcal{O}_{T-1}$ is of full column rank, and is therefore injective. As a result, two potential initial states will necessarily generate different measurement history matrix Y.

In the case of a LTI system, it is worth noting that for any $T > n$, the observability of the system on $[0, T-1]$ can be equivalently assessed by studying the rank of $\mathcal{O}_{n-1}$:

Theorem 1.1 (Observability condition for LTI systems [Oga06])**.** *Let Σ be a LTI system ruled by (1.2) and T an integer greater than n. Then the system is observable on time-horizon $[0, T-1]$ if and only if the matrix*

$$\mathcal{O}_{n-1} = \begin{pmatrix} C^\top & (CA)^\top & \cdots & (CA^{n-1})^\top \end{pmatrix}^\top \tag{1.10}$$

is full column rank, i.e. of rank n.

Remark 1.2. *As $\mathcal{O}_{n-1}$ solely involves matrices A and C, the observability of the LTI system can be viewed as a property of the pair (A, C) of its model. Hence we may speak of observability of the pair (A, C).*

Finally, there indeed exist many different notions of observability, which can be stronger, like the *Uniform Complete Observability* (see [Bat17]) or weaker, like the *Detectability* (see [Oga09, Sec. 9-7]), than the one presented here. These various notions of observability can confer different properties to the state estimators.

1.2.4 A first example of a state estimator: the Luenberger observer

In 1964, David Luenberger, an American mathematician at Stanford University, published a paper to address the state estimation problem [Lue64]. If the paper handles continuous-time systems, we will present the extension to Discrete-Time systems which is fairly similar. The point of presenting this first example of state estimation is to have a first discussion about how state estimators can be designed and present some key aspects of state estimation such as *estimation error* or the concept of *recursive estimation*.

We consider the noiseless LTI version of state-space representations (1.2), *i.e.*

$$\Sigma : \begin{cases} x_{t+1} &= Ax_t \\ y_t &= Cx_t \end{cases} \tag{1.11}$$

The principle behind Luenberger's paper is the construction of a second system with the following dynamic equation

$$z_{t+1} = Gz_t + Hy_t, \tag{1.12}$$

with $G \in \mathbb{R}^{n \times n}$ and $H \in \mathbb{R}^{n \times m}$. We notice that y_t plays the role of an input for this system. Moreover, we want to design this second system so that its state vector

$z_t \in \mathbb{R}^n$ is a linear combination of the original state vector x_t, *i.e.* there should exist an injective matrix $F \in \mathbb{R}^{n\times n}$ such that

$$z_t = Fx_t + a_t \tag{1.13}$$

with a_t a quantity which should be as small as possible and tending towards the null vector when t tends to infinity.

The goal of the Luenberger estimator is to design this system, *i.e.* the triplet (G, H, F), such that both (1.12) and (1.13) hold true, and also such that F is invertible. In this case, the estimate $\hat{x}_t$ can be obtained such that

$$\hat{x}_t = F^{-1}z_t. \tag{1.14}$$

Remark 1.3. *If F is assumed to be square in this example, the framework of the Luenberger estimator can be extended to non-square matrices by replacing the inverse of F with the generalised inverse of F [Ber09a, Sec 6.1].*

The following result gives a sufficient condition for the existence of the matrix F, and therefore of the whole estimator:

Theorem 1.2 (Sufficient condition for the existence of F [Lue64])**.** *Let Σ be a system as in (1.11) and consider a system ruled by dynamic equation (1.12). If A and G do not have any eigenvalue in common, then there exists a unique matrix F such that*

$$\begin{cases} \forall t \geq 0, \quad z_t = Fx_t + G^t(z_0 - Fx_0) \\ \qquad\qquad FA - GF = HC \end{cases} \tag{1.15}$$

where G^t designates the matrix G multiplied by itself t times.

Proof. If A and G do not have any eigenvalue in common, then the equation of unknown M

$$MA - GM = HC, \tag{1.16}$$

also known as a Sylvester equation, admits a unique matrix solution [Hor12, Thm 2.4.4.1]. We denote with F this solution, which yields $FA - GF = HC$, the second equation of (1.15).

By replacing y_t by its expression from (1.11) in (1.12), we obtain

$$\begin{aligned} & z_{t+1} = Gz_t + HCx_t \\ \Leftrightarrow \quad & z_{t+1} = Gz_t + (FA - GF)x_t \quad && \text{as } HC = FA - GF \\ \Leftrightarrow \quad & z_{t+1} = Gz_t + Fx_{t+1} - GFx_t \quad && \text{as } x_{t+1} = Ax_t \\ \Leftrightarrow \quad & z_{t+1} - Fx_{t+1} = G(z_t - Fx_t) \end{aligned} \tag{1.17}$$

From this recursive relation, it is then easy to obtain the first equation of (1.15). □

This theorem proves that under the right circumstances, we can design a system ruled by the dynamic equation (1.12) such that its state vector z_t is a linear combination of the state vector of System Σ plus a certain quantity, *i.e.* there exists a matrix F such that $z_t = Fx_t + a_t$ with $a_t = G^t(z_0 - Fx_0)$.

Ideally, a_t should converge towards zero when t grows towards infinity. We observe that for a_t to do so, we must either have $z_0 = Fx_0$ or $\lim_{t\to\infty} G^t = 0$:

- $z_0 = Fx_0$ represents the case where we would be able to initialise system (1.12) with the exact initial state of the system. However, the initial state of system (1.11) is unknown, otherwise the whole state estimation problem would be trivial.
- $\lim_{t\to\infty} G^t = 0$ is true if and only if every (complex) eigenvalue of G is of magnitude strictly smaller than one: this is the case where system (1.12) is designed to be stable, which is a logical design choice to make.

As a result, as long as we make sure that the state estimator is stable, a_t asymptotically converges towards zero which means that z_t gets closer to Fx_t as t grows towards infinity. Nevertheless, even if we ensure this asymptotic convergence, the existence of F is not sufficient to invert it and subsequently obtain the estimate $\hat{x}_t$ through (1.14). Hence we must additionally require that F is invertible, a property which is guaranteed to hold under the conditions stated in Theorem 1.3: its proof can be found in [Lue64].

Theorem 1.3 (Inversibility of matrix F [Lue64])**.** *Let Σ be a system as in (1.11) and $(G, H) \in \mathbb{R}^{n\times n} \times \mathbb{R}^{n\times m}$ two matrices such that A and G do not have any eigenvalue in common. If (A, C) is observable and (G, H) is controllable*[1]*, then the unique matrix F satisfying $FA - GF = HC$ is invertible.*

If (A, C) is observable – which shows the importance of the observability of a system for the existence of a well-defined state estimator – and if (G, H) is controllable and designed such that G is stable and does not have any eigenvalue in common with A, then the Luenberger estimator can be defined as the LTI state-space representation such that

$$\Sigma_{\text{Lue}} : \begin{cases} z_{t+1} &= Gz_t + Hy_t \\ \hat{x}_t &= F^{-1}z_t \end{cases} \tag{1.18}$$

where F is the unique matrix satisfying $FA - GF = HC$.

Recursive estimation. A Luenberger estimator is an *online estimator*, which means it is implemented in order to estimate the state while the system is being operated by being fed with the measurement of the system output in real time.

The formulation of the estimator as a state-space representation can be compacted in order to obtain in one equation the link between two consecutive state estimates, *i.e.* between $\hat{x}_{t+1}$ and $\hat{x}_t$, making the computation of the estimate at each time iteration easier. Given that $\hat{x}_{t+1} = F^{-1}z_{t+1}$ and $z_{t+1} = Gz_t + Hy_t$, we obtain the relation

$$\hat{x}_{t+1} = F^{-1}(GF\hat{x}_t + Hy_t).$$

Thanks to the fact that $FA - GF = HC$ which implies $F^{-1}GF = A - F^{-1}HC$, we can reformulate the latest equation to be

$$\hat{x}_{t+1} = A\hat{x}_t + L(y_t - \hat{y}_t). \tag{1.19}$$

with $\hat{y}_t = C\hat{x}_t$ the estimated output of the system and $L = F^{-1}H$. This relation is called the *recursive form* of the Luenberger estimator, and the corresponding structure is represented as a block diagram in Figure 1.4.

A few observations can be made about this recursive form:

[1] The *controllability* is a dual notion to the observability. It makes sure that the system can reach every state in $\mathbb{R}^n$ in a finite amount of time. For LTI systems, (G, H) is controllable if and only if $(G^\top, H^\top)$ is observable [Oga06, pp. 392–394].

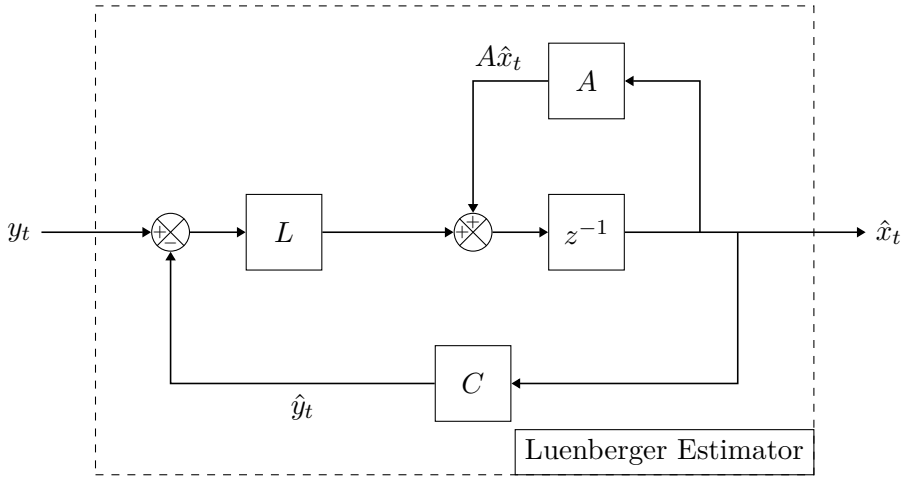

FIGURE 1.4: Block Diagram of the Luenberger estimator in its recursive form

- The term $A\hat{x}_t$ is a *predictive term* which is the most likely prediction of the next state in the absence of new knowledge. Indeed, if $\hat{x}_t$ is the estimate of state x_t with all the accessible knowledge, then one of the most logical choices to make for the prediction is simply to run the state estimate through the dynamics of the system.
- The term $L(y_t - \hat{y}_t)$ is an *innovation term* which corrects the prediction in the light of the new knowledge which is here y_t. The matrix L, often called the *gain matrix of the estimator*, weighs the innovation which is the part that cannot be obtained by prediction, *i.e.* the difference between the real measurement and the predicted measurement.

The recursive approach of the Luenberger estimator shows that to implement it in its form (1.19), we only need to compute L, and therefore do not need to compute H, F and G. Surprisingly enough, this means that we do not need to consider the Sylvester equation, and the assumption that A and G do not share any eigenvalue can be discarded given that we do not compute the latter explicitly anymore.

A common method to design L is through the eigenvalue assignment. The principle of this method is to select the matrix gain L such that the eigenvalues of $A - LC$ correspond to a set of predefined values. This allows control over the dynamics of the closed loop constituting the Luenberger estimator as highlighted by Figure 1.4.

Remark 1.4. *It is worth mentioning that the eigenvalues of $A - LC$ can be chosen over the whole complex plane thanks to the observability property. If the system is only detectable, which is a weaker notion than the observability, a Luenberger estimator can still be designed but the choice for the eigenvalues of $A - LC$ is limited [O'R83].*

Estimation Error. A very important way to assess the performances of an estimator is to have a look at its *estimation error*, which is the gap between the real state and the estimated state. In the case of the Luenberger estimator, this error can be precisely obtained, and for all $t \in \mathbb{N}$,

$$e_t = x_t - \hat{x}_t = x_t - F^{-1}z_t = -F^{-1}G^t(z_0 - Fx_0) = F^{-1}G^tF(x_0 - \hat{x}_0)$$

Given that $A - LC = F^{-1}GF$, we then obtain

$$e_t = (A - LC)^t(x_0 - \hat{x}_0). \tag{1.20}$$

This equation shows that the estimation error dynamics are dictated by those of the closed loop constituting the Luenberger estimator. For instance, the the Schur stability[2] of $A - LC$, and therefore of the estimator, ensures that the estimation error converges towards zero. As a result, we have that the estimate $\hat{x}$ asymptotically converges towards the real state which was the goal of the estimator. However, this observation does not necessarily provide insight on the actual performances of the estimator, as only the asymptotic convergence is ensured and the estimation could converge very slowly towards zero. The speed of convergence will be specified through the choice of the eigenvalues of $A - LC$ which will be set through the eigenvalue assignment method: the smaller the eigenvalues (in magnitude) of the closed loop, the faster it will converge towards zero. This choice must however be performed appropriately, making sure that the estimator is converging in a timely manner, but not too fast, as in the presence of noise, the estimator may be very sensitive to the quick variations induced by it.

Basic Example. To further illustrate the Luenberger estimator, we provide an example of the state trajectory estimation over a time-horizon of length $T = 50$ for an LTI system of the form (1.11) with

$$A = \begin{pmatrix} 0.7 & 0.45 \\ -0.5 & 1 \end{pmatrix}, \quad C = \begin{pmatrix} 1 & 2 \end{pmatrix}, x_0 = \begin{pmatrix} 1 \\ 2 \end{pmatrix}. \tag{1.21}$$

We will use this example for several different simulation tests throughout the thesis. As a result, we will often refer to this specific triplet (A, C, x_0) as System (1.21).

To design a Luenberger estimator, we use the expression `place(A',C',eta)` on MATLAB which returns the estimator gain L such that $A - LC$ has the eigenvalues specified by vector η. Figure 1.5 presents the real state trajectory alongside with the estimated trajectories resulting from two Luenberger estimators, whose gain L respects $\eta = (\,0.4 \quad 0.6\,)$ and $\eta = (\,0.8 \quad 0.9\,)$ respectively. The figure shows how the estimated trajectories converge towards the real trajectory when time grows, since both estimators are stable. Moreover, we see that when the elements of η, *i.e.* the eigenvalues of $A - LC$, are smaller, the estimator converges quicker.

Conclusion. The Luenberger estimator is a powerful solution to the estimation problem as it provides a framework which guarantees that its output will always converge towards the real state with a convergence speed which can be controlled. However, a few limitations can be pointed out, such as the fact that the framework does not explicitly take into account any potential disturbance. There is therefore no theoretical guarantee of being able to maintain a good level of performance in presence of disturbances. Consequently, the eigenvalue assignment method is easy and quick to implement, but apart from the speed of convergence, it does not allow a design of L so as to achieve a performance related to the influence of potential disturbances.

There exist other methods to design the gain matrix L. These methods aim at designing the *best* Luenberger estimator with regards to a criterion which depends on the nature of the disturbances acting on the model. To illustrate this portion of

[2] A square matrix is called *Schur stable* if all its eigenvalues have magnitudes strictly less than 1

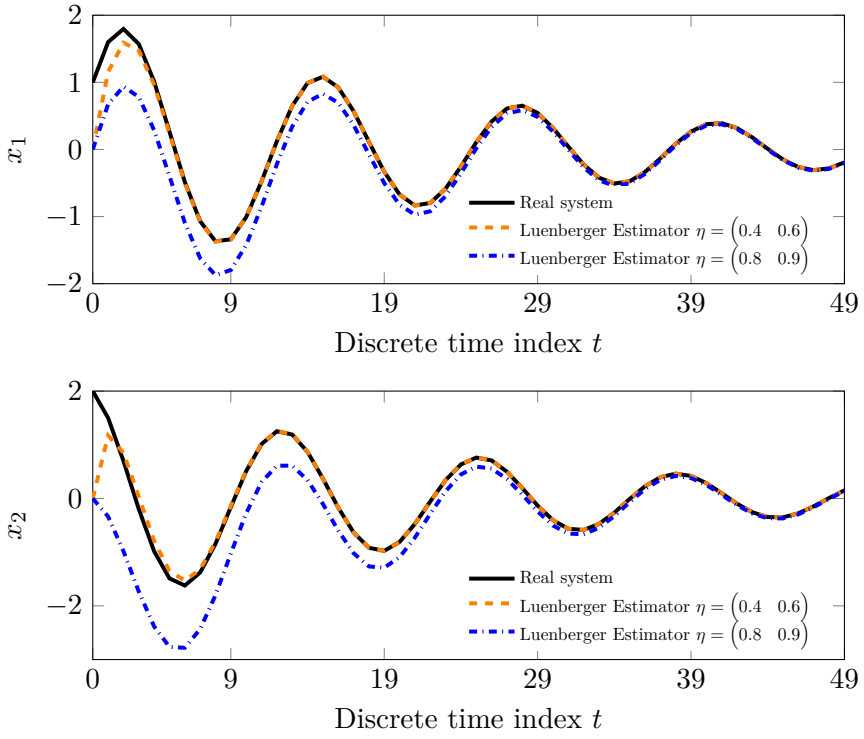

FIGURE 1.5: State trajectories of System (1.21) and estimated state trajectories obtained by a Luenberger estimator

the state estimation literature, we will present the design of a Luenberger estimator through one of those methods, *i.e.* the $\mathcal{H}_\infty$ approach.

1.2.5 $\mathcal{H}_\infty$ approach to the Luenberger estimator gain design

We now consider a general LTI system of the form (1.2) with $\{w_t\}$ and $\{f_t\}$ two noise sequences bounded with respect to the supremum norm. This means that

$$\sup_{(t,i)\in\mathbb{N}\times\mathbb{I}} |w_t[i]| < +\infty \qquad \sup_{(t,j)\in\mathbb{N}\times\mathbb{I}} |f_t[j]| < +\infty,$$

with $w_t[i]$ the i-th component of w_t, $f_t[j]$ the j-th component of f_t, $\mathbb{I} = \{1, ..., n\}$ the set of state indexes and $\mathbb{J} = \{1, ..., m\}$ the set of sensor indexes.

The aim of this new example is to quickly address the point raised in the conclusive remark of the Luenberger estimator example by presenting a method which takes the presence of disturbances into account for the design of the estimator gain L. The development presented below are taken from [Cav19, Sec. 5.2.2] and [Dua13, Sec. 9.2.2.1].

First of all, let us reformulate System Σ such that

$$\Sigma : \begin{cases} x_{t+1} &= Ax_t + Bu_t \\ y_t &= Cx_t + Du_t \end{cases} \tag{1.22}$$

with

$$u_t = \begin{pmatrix} w_t \\ v_t \end{pmatrix}, \; B = \begin{pmatrix} I_n & \mathbb{0}_{m,m} \end{pmatrix}, C = \begin{pmatrix} \mathbb{0}_{n,n} & I_m \end{pmatrix}. \tag{1.23}$$

where $\mathbb{0}_{m,m}$ the zero matrix from $\mathbb{R}^{a\times b}$ and I_a designates the identity matrix from $\mathbb{R}^a$.

In this formulation, the sequence $\{u_t\}$, called the *input vector*, gathers all the disturbances happening in the system. The core idea of the method is to design L so that this input vector u_t has as little influence on the estimation error as possible. To ensure this, we consider the transfer matrix function $T_{u\to e}(z)$ from the input sequence $\{u_t\}$ to the estimation error sequence $\{e_t\}$, and we design L so that the $\mathcal{H}_\infty$ norm of $T_{u\to e}$, *i.e.* the value[3]

$$\|T_{u\to e}\|_\infty = \sup_{u\in\mathcal{L}_2} \frac{\|T_{u\to e}u\|_2}{\|u\|_2}, \tag{1.24}$$

is as small as possible, hence the name of $\mathcal{H}_\infty$ approach. It is worth noting that the supremum in (1.24) exists if $T_{u\to e}$ is stable, given that there would exists $\gamma > 0$ such that $\|T_{u\to e}u\|_2 \leq \gamma\|u\|_2$.

In practice, this is performed by using the Discrete-Time Bounded Real Lemma [Cav19, Sec. 3.2.2] which provides equivalent condition to the boundedness of the $\mathcal{H}_\infty$ norm of $T_{u\to e}$.

It can be shown that in the case of System (1.22), $T_{u\to e}$ can be written

$$T_{u\to e}(z) = (zI - (A - LC))^{-1}(B - LD). \tag{1.25}$$

The Discrete-Time Bounded Real Lemma then states that $\|T_{u\to e}\|_\infty < \gamma$ ($\gamma > 0$) if and only if there exists $P \in \mathcal{S}_n^+(\mathbb{R})$ [4] and $K \in \mathbb{R}^{n\times m}$ which verify $K = PL$ and such that

$$\begin{pmatrix} P & PA-KC & PB-KD & \mathbb{0}_{n\times 1} \\ * & P & \mathbb{0}_{n\times(n+m)} & \mathbb{0}_{n\times 1} \\ * & * & \gamma I_{n+m} & \mathbb{0}_{(n+m)\times 1} \\ * & * & * & \gamma \end{pmatrix} > 0 \tag{1.26}$$

where we recall that the notation $M > 0$ means that the (symmetric) matrix M is definite positive. Moreover, $*$ represents the transposed matrix of the matrix in the opposite corner (to ensure the symmetry of the global matrix). Equation (1.26) is called *Linear Matrix Inequality* (LMI). It can be numerically solved through the convex optimisation framework (see [Boy04, Sec. 4.6.2]).

As a result, designing L so as to minimise the $\mathcal{H}_\infty$ norm of $T_{u\to e}$ boils down to solving the optimisation problem

$$\begin{aligned} \underset{\gamma\in\mathbb{R}_{>0}, P\in\mathbb{R}^{n\times n}, K\in\mathbb{R}^{n\times m}}{\text{minimize}} \quad & \gamma \\ \text{subject to} \quad & P > 0 \\ & \begin{pmatrix} P & PA-KC & PB-KD & \mathbb{0}_{n\times 1} \\ * & P & \mathbb{0}_{n\times(n+m)} & \mathbb{0}_{n\times 1} \\ * & * & \gamma I_{n+m} & \mathbb{0}_{(n+m)\times 1} \\ * & * & * & \gamma \end{pmatrix} > 0 \end{aligned} \tag{1.27}$$

and then posing $L = P^{-1}K$ with P and K the resulting matrices from the optimisation problem. To prevent any conditioning problem, we will rather implement the

[3] By notation abuse, we use $T_{u\to e}$ to designate both the operator (mapping two signal spaces) and the transfer function (which is a function of $\mathbb{C}$).

[4] $\mathcal{S}_n^+(\mathbb{R})$ is the set of definite positives matrices with n rows.

similar optimisation problem

$$\begin{aligned} \underset{\gamma\in\mathbb{R}_{\geq 0}, P\in\mathbb{R}^{n\times n}, K\in\mathbb{R}^{n\times m}}{\text{minimize}} \quad & \gamma \\ \text{subject to} \quad & P \geq \varepsilon I_n \\ & \begin{pmatrix} P & PA-KC & PB-KD & \mathbb{0}_{n\times 1} \\ * & P & \mathbb{0}_{n\times(n+m)} & \mathbb{0}_{n\times 1} \\ * & * & \gamma I_{n+m} & \mathbb{0}_{(n+m)\times 1} \\ * & * & * & \gamma \end{pmatrix} \geq \varepsilon I_{3n+m+1} \end{aligned} \tag{1.28}$$

with $\varepsilon > 0$ a small constant quantity. Contrary to (1.27), (1.28) presents large inequalities, due to the fact that in practice, solvers only handle large inequalities.

Basic Example. We simulate the state estimation of System (1.21) in the presence of uniformly distributed disturbances $\{w_t\}$, $\{v_t\}$ taken independently in $[-0.3, 0.3]$ and $[-0.1, 0.1]$ respectively. To design L, we implemented the optimisation problem (1.28) with $\varepsilon = 0.1$ through the CVX interface [Gra18] in MATLAB.

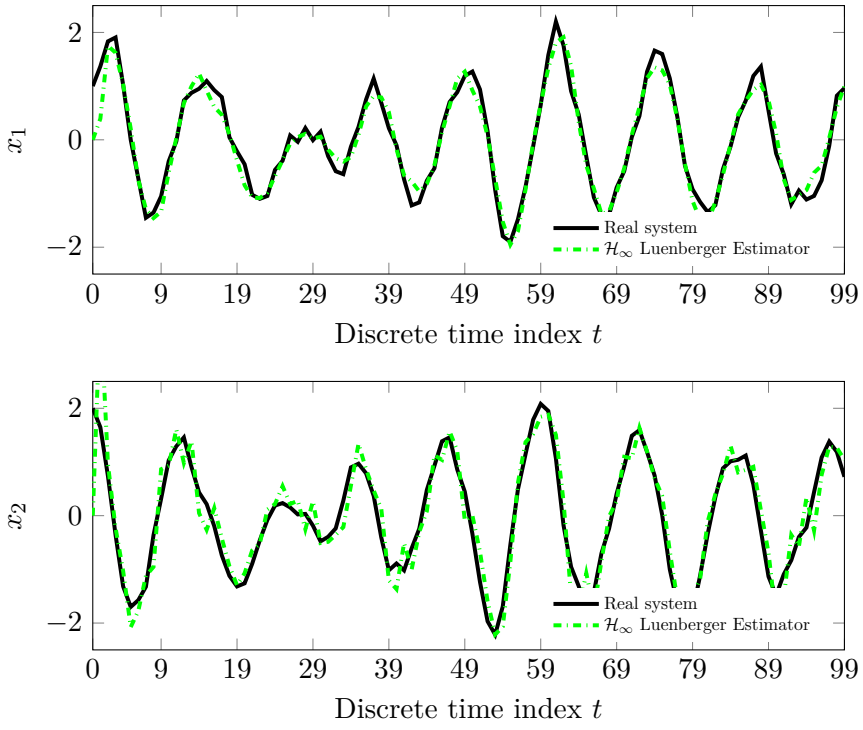

FIGURE 1.6: State trajectories of System (1.21) disturbed by uniformly distributed noises and estimated state trajectories obtained by a $\mathcal{H}_\infty$ Luenberger estimator

In Figure 1.6, we can observe the real state trajectories alongside the estimated state trajectories obtained by the $\mathcal{H}_\infty$ Luenberger estimator, and we can see that the latter seem to be accurate as they fit the original state trajectories. It is also worth noting that the obtained estimator has a fast convergence time, which is corroborated by the fact that the resulting closed loop matrix $A - LC$ has two conjugated eigenvalues of magnitude 0.1076, which is close from zero.

Conclusion. The $\mathcal{H}_\infty$ approach provides a way to design a Luenberger estimator

which is optimal with respect to the $\mathcal{H}_\infty$ norm of the transfer function matrix between the estimation error and the (unknown) input of the system. Other approaches, such as the $\mathcal{H}_2$ approach, are also possible in order to obtain an optimal Luenberger estimator with respect to a given criterion. However, those optimisation-based methods only aim at obtaining the best estimator gain within the Luenberger estimator structure, but they do not modify the structure itself.

To deal with this limitation, throughout the rest of this manuscript, we will consider state estimation through the optimal state estimation framework presented below.

1.3 The optimal estimation framework

Contrary to the Luenberger estimator approaches, the optimal estimation framework aims at providing both the structure of the estimator and its parameters. Moreover, the estimated state is selected to optimize a certain criterion/performance function.

1.3.1 The performance index function

In the first place, we need a way to quantitatively compare trajectories between each other. This is the reason for the introduction of *performance index functions*, also called *cost functions* or *objective functions*, which will assign a value to every hypothetical trajectory that the system can take. Given a system of the form (1.1), we want to consider the estimation of the state trajectory on time-horizon $T-1$, X, for which we have the measurement history matrix Y. The structure of performance index functions to be studied in this thesis is the one such that for all $Z = \begin{pmatrix} z_0 & z_1 & \cdots & z_{T-1} \end{pmatrix}$ in $\mathbb{R}^{n\times T}$,

$$V_{\Sigma,T-1}(Y,Z) = \chi(z_0-\mu_0) + \sum_{t\in\mathbb{T}'} \phi_t(z_{t+1}-A_tz_t) + \sum_{t\in\mathbb{T}} \psi_t(y_t-C_tz_t) \tag{1.29}$$

with $\mathbb{T} = \{0,1,...,T-1\}$, $\mathbb{T}' = \{0,...,T-2\}$, $\mu_0 \in \mathbb{R}^n$, $\chi : \mathbb{R}^n \to \mathbb{R}_{\geq 0}$ a function and $\{\phi_t\}$, $\{\psi_t\}$ two families of functions from $\mathbb{R}^n$ to $\mathbb{R}_{\geq 0}$ and $\mathbb{R}^m$ to $\mathbb{R}_{\geq 0}$ respectively. As it was already stated, $T-1$ will be used as the default time-horizon length throughout this manuscript, which means that the $T-1$ index of $V_{\Sigma,T-1}$ will sometimes be dropped: V_Σ, by default, will designate $V_{\Sigma,T-1}$.

Each term in this performance index function is intended to assess the likelihood of the matrix Z as a potential trajectory of the system:

- The term $\chi(z_0-\mu_0)$ assesses the compliance of the hypothetical initial state z_0 with a prior knowledge μ_0 that we might have on the real initial state of the system.
- The terms of the form $\phi_t(z_{t+1}-A_tz_t)$ assess how the hypothetical estimate comply with the dynamics of the system. Indeed, if it does respect the dynamic equation of (1.1), then for each t in $\mathbb{T}'$, $z_{t+1} \approx A_tz_t + w_t$, which means the argument of each term should be close to w_t.
- The terms of the form $\psi_t(y_t-C_tz_t)$ verify how the measurements which would be obtained from trajectory Z compare to the actual output of the system. If for all t in $\mathbb{T}$, $C_tz_t \approx y_t - f_t$, it means that the trajectory Z simulates an output of the system which is close to the actual one, which means the argument of those terms will also be close to f_t.

Consequently, the more the hypothetical trajectory dictated by matrix Z complies with the system dynamics and provides plausible output when compared to the actual system output, the closer $V_\Sigma(Y, Z)$ should be to $V_\Sigma(Y, X)$ with X the real state trajectory. The *loss functions*, *i.e.* the function χ and the members of the families of function $\{\phi_t\}$ and $\{\psi_t\}$, need to be chosen in order for $V_\Sigma(Y, X)$ to be small.

With this structure, the performance index functions can now provide a value to each trajectory in order to specify how likely it is. The goal of the optimal state estimation framework is then to consider the most likely trajectories with respect to V_Σ, which are the matrices Z which minimise the performance index function. An *optimal estimator* Ψ will therefore be defined as the mapping from $\mathbb{R}^{m\times T}$ to $\mathcal{P}(\mathbb{R}^{n\times T})$ such that for all $Y \in \mathbb{R}^{m\times T}$,

$$\Psi(Y) = \underset{Z\in\mathbb{R}^{n\times T}}{\arg\min}\, V_\Sigma(Y, Z) \tag{1.30}$$

If the loss functions are well designed, then $V_\Sigma(Y, X)$ is small, which entails that minimising $V_\Sigma(Y, Z)$ with respect to Z yields estimated trajectories which are close from the real state trajectory.

The optimal state estimation framework will now be presented through the example of an LTV Discrete-Time state-space representation disturbed by Gaussian noises. This case will be addressed by the presentation of one of the most common optimal state estimators, the *Least Squares Estimator*. This will, in the first place, give us the opportunity to deal with several key aspects of optimal estimation such as the well-definedness of an estimator or its batch implementation. Subsequently, to further explore down the notion of implementation, the framework of the Forward Dynamic Programming, which provides a theoretical systematic process to obtain a recursive online estimator, will be introduced.

1.3.2 The Least Squares Estimator

We consider an LTV system Σ defined by (1.1) in the presence of white Gaussian disturbances. This type of noise is one of the most common representations for disturbances which naturally occur in system, like sensor noises for instance. A Gaussian noise is characterised by two constants, which are its mean and its variance.

In this example, $\{w_t\}$ and $\{f_t\}$ are therefore assumed to be two white Gaussian noise sequences with a zero mean and covariance matrices which will be denoted with $\{Q_t\} \in \mathcal{S}_n^+(\mathbb{R})$ and $\{R_t\} \in \mathcal{S}_m^+(\mathbb{R})$ respectively. Moreover, the initial state x_0 is also the realisation of a white Gaussian random variable of covariance $S \in \mathcal{S}_n^+(\mathbb{R})$ and for all $t \in \mathbb{N}$, x_0, w_t and f_t are mutually independent.

In every optimal state estimation approach, there is a need to instantiate the performance index function appropriately with regards to the characteristics of the system whose state is to be estimated. Indeed, if we recall the explanations of the previous section, we need $V_\Sigma(Y, X)$ to be somewhat small.

Using stochastic arguments, and especially the Maximum Likelihood framework (see [Jaz07, p.156-158]), it can be proven that when $\{w_t\}$ and $\{f_t\}$ are white independent Gaussian noise sequences which are also independent from the initial state,

the most suited function is V_Σ such that for all (Y, Z) in $\mathbb{R}^{m\times T} \times \mathbb{R}^{n\times T}$,

$$V_\Sigma(Y,Z) = \frac{1}{2}\|z_0-\mu_0\|^2_{S^{-1}} + \frac{1}{2}\sum_{t\in\mathbb{T}'}\|z_{t+1}-A_tz_t\|^2_{Q_t^{-1}} + \frac{1}{2}\sum_{t\in\mathbb{T}\setminus\{0\}}\|y_t-C_tz_t\|^2_{R_t^{-1}} \quad (1.31)$$

where $\|\cdot\|^2_M$ refers to the quadratic form weighted by the definite positive matrix $M \in \mathcal{S}^+_a(\mathbb{R})$, *i.e.* such that

$$\forall z \in \mathbb{R}^a, \qquad \|z\|^2_M = z^\top Mz. \quad (1.32)$$

The *Least Squares Estimator* is then defined through the minimisation of the cost function V_Σ in (1.31) :

Definition 1.3 (Least Squares Estimator)**.** *Given a system Σ as in (1.1), the Least Squares estimator is defined as the mapping $\mathcal{E}$ from $\mathbb{R}^{m\times T}$ to $\mathcal{P}(\mathbb{R}^{n\times T})$ such that*

$$\mathcal{E}(Y) = \underset{Z\in\mathbb{R}^{n\times T}}{\arg\min}\, V_\Sigma(Y,Z) \quad (1.33)$$

with V_Σ defined as in (1.31).

If we compare V_Σ with its first definition (1.29), we see that the loss functions were chosen as quadratic forms weighted by the covariance matrices of the Gaussian noises w_t and f_t. The role of those weights is to indicate which terms should be minimised the most, as the terms in V_Σ with the most weight are the ones which will be minimised in priority when minimising the performance index function as a whole.

Moreover, the covariance matrix of a Gaussian noise is an indicator of its magnitude: indeed, when the noise varies a lot and takes greater value, the covariance is greater. As a result, the inverse of this matrix acts as a trust index in the corresponding system equation. For example, if Q_t has small coefficients, the noise value w_t is more likely to be small. This means it will barely disturb the dynamic equation at time t, which induces $x_{t+1} \approx A_tx_t$. Consequently, the corresponding term in V_Σ, $z_{t+1} - A_tz_t$, should be minimised in priority, and that is the case since Q_t^{-1} will have great coefficients.

Well-definedness of an estimator. When defining an estimator through the solution of an optimisation problem, the optimisation problem needs to be well-defined in order to always ensure the existence of at least one solution. We therefore say that an optimal state estimator is *well-defined* when for all $Y \in \mathbb{R}^{m\times T}$, there exists at least one element in $\mathcal{E}(Y)$.

In the case of the Least Squares estimator, its well-definedness can be proved thanks to the fact that V_Σ is coercive with respect to Z. The definition of a coercive function we use is the one presented in [Ber09b, p.119] but adapted to functions from $\mathbb{R}^{a\times b}$ to $\mathbb{R}_{\geq 0}$.

Definition 1.4 (Coercive function)**.** *A function ξ from $\mathbb{R}^{a\times b}$ to $\mathbb{R}_{\geq 0}$ is said to be coercive if for every sequence $\{Z_k\}$ such that $\lim_{k\to\infty}\|Z_k\| = +\infty$, $\lim_{k\to\infty}\xi(Z_k) = +\infty$ with $\|\cdot\|$ any norm on $\mathbb{R}^{a\times b}$*

The main interest of the coercivity property is that it is a sufficient condition for the well-definedness of the minimisation problem. It is stated in [Ber09b, Prop.3.2.1], from which we draw the following simplified lemma:

Lemma 1.1 ([Ber09b])**.** *If a continuous function $\xi : \mathbb{R}^{a\times b} \to \mathbb{R}_{\geq 0}$ is coercive, then the set $\arg\min_{Z\in\mathbb{R}^{a\times b}}\xi(Z)$ is nonempty.*

The proof of the coercivity of $V_\Sigma(Y, \cdot)$ as defined in (1.31) can be found in Appendix A.1. The well-definedness of the Least Square Estimator then follows from the application of Lemma 1.1.

Batch implementation of an optimal state estimator. The question of the implementation is indeed central in optimal state estimation: how to obtain the minimising state trajectory – and therefore the state estimate – from the defining optimisation problem?

A *batch implementation* designates an implementation which obtains the whole estimated state trajectory $\hat{X}_T$ as it processes a batch of measurements. In the case of the Least Squares Estimator, there is a closed-form formula which calculates this state trajectory:

Theorem 1.4 (Batch implementation of the Least Squares Estimator)**.** *Let Σ be a system as in (1.1) and $\mathcal{E}$ be a Least Squares Estimator as defined in (1.33). Then, for a given measurement history $Y \in \mathbb{R}^{m\times T}$, $\mathcal{E}(Y)$ contains a unique estimated state trajectory matrix $\hat{X}_T \in \mathbb{R}^{n\times T}$ such that*

$$vec(\hat{X}_T) = (\mathcal{Q} + \mathcal{R})^{-1}\tilde{Y} \tag{1.34}$$

with

$$\mathcal{Q} = \begin{pmatrix} A_0^\top Q_0^{-1} A_0 & -A_0^\top Q_0^{-1} & 0 & \cdots & 0 \\ -Q_0^{-1}A_0 & Q_0^{-1} + A_1^\top Q_1^{-1} A_1 & \ddots & \ddots & \vdots \\ 0 & \ddots & \ddots & \ddots & 0 \\ \vdots & \ddots & \ddots & Q_{T-3}^{-1} + A_{T-2}^\top Q_{T-2}^{-1} A_{T-2} & -A_{T-2}^\top Q_{T-2}^{-1} \\ 0 & \cdots & 0 & Q_{T-2}^{-1} A_{T-2} & Q_{T-2}^{-1} \end{pmatrix} \tag{1.35}$$

$$\mathcal{R} = \begin{pmatrix} S^{-1} & 0 & \cdots & \cdots & 0 \\ 0 & C_1^\top R_1^{-1} C_1 & \ddots & & \vdots \\ \vdots & \ddots & \ddots & \ddots & \vdots \\ \vdots & & \ddots & \ddots & 0 \\ 0 & \cdots & \cdots & 0 & C_{T-1}^\top R_{T-1}^{-1} C_{T-1} \end{pmatrix}, \qquad \tilde{Y} = \begin{pmatrix} S^{-1}\mu_0 \\ C_1^\top R_1^{-1} y_1 \\ \vdots \\ \vdots \\ C_{T-1}^\top R_{T-1}^{-1} y_{T-1} \end{pmatrix} \tag{1.36}$$

Proof. See Appendix A.2. □

Remark 1.5. *We notice that Theorem 1.4 does not require an assumption on the observability of the system. Indeed, Theorem 1.4 gives the value of the estimated trajectory but does not guarantee the quality of the estimation. Using $\mathcal{E}$ to estimate the state of a system which is not observable will therefore probably yield poor results.*

Moreover, the absence of an observability requirement is due to the initial cost $\|z_0 - \mu_0\|^2_{S^{-1}}$ in the performance index function V_Σ considered in (1.31). Given the presence of μ_0 acting like a regularising parameter, this initial cost presents regularising properties, and it makes the observability not necessary.

However, we can consider the Least Squares Estimator defined through the less standard objective function

$$V_\Sigma(Y, Z) = \frac{1}{2}\sum_{t\in\mathbb{T}'} \|z_{t+1} - A_t z_t\|^2_{Q_t^{-1}} + \frac{1}{2}\sum_{t\in\mathbb{T}} \|y_t - C_t z_t\|^2_{R_t^{-1}}. \tag{1.37}$$

with an initial cost $\|y_0 - C_t z_0\|^2_{R_0^{-1}}$ *using a first system measurement* y_0.

Theorem 1.4 is still applicable, by replacing $S^{-1}\mu_0$ *by* $C_0^\top R_0^{-1} y_0$ *in* $\tilde{Y}$ *and* S^{-1} *by* $C_0^\top R_0^{-1} C_0$ *in* $\mathcal{R}$*, but also requires the system to be observable over time-horizon* $[0, T-1]$.

Indeed, if we conduct the proof carried in Appendix A.2 for the optimal estimator defined through the minimisation of V_Σ *in (1.37), we notice that (A.10) is written*

$$\tilde{Z}^\top (\mathcal{Q} + \mathcal{R}) \tilde{Z} = \sum_{t \in \mathbb{T}'} \|z_{t+1} - A_t z_t\|^2_{Q_t^{-1}} + \sum_{t \in \mathbb{T}} \|C_t z_t\|^2_{R_t^{-1}} \geq 0.$$

$\mathcal{Q}+\mathcal{R}$ *is therefore positive semidefinite, but to prove that* $\tilde{Z}^\top(\mathcal{Q}+\mathcal{R})\tilde{Z}$ *implies* $\tilde{Z} = 0$ *and obtain the invertibility of* $\mathcal{Q} + \mathcal{R}$*, we need the observability of the system over* $[0, T-1]$.

The key property to obtain the batch implementation of the Least Squares Estimator is that the loss functions composing the cost function V_Σ are all differentiable with respect to Z. However, this is not an assumption made on the loss functions in the general case. Consequently, an optimal state estimate cannot be systematically obtained in closed form as in Theorem 1.4.

In the general case, one might want to directly solve the optimisation problem underlying the definition of the state estimator. A very common assumption to make this efficient is to assume that the loss functions are *convex functions*.

Definition 1.5 (Convex function [Roc70])**.** *Let* ξ *be a function from* $\mathbb{R}^{a \times b}$ *to* $\mathbb{R}_{\geq 0}$. *Such a function is said to be* convex *if for any* Z_1,Z_2 *in* $\mathbb{R}^{a \times b}$,

$$\forall \lambda \in [0,1],\ \xi(\lambda Z_1 + (1-\lambda) Z_2) \leq \lambda \xi(Z_1) + (1-\lambda)\xi(Z_2) \tag{1.38}$$

If the inequality is strict for λ *in* $]0,1[$*, then the function is said to be* strictly *convex.*

When all the loss functions are convex, the performance index function is itself convex, which makes the use of convex optimisation methods possible. Indeed, the Least Squares performance index V_Σ in (1.31) is convex.

Nevertheless, the batch implementation shows its limits when the length of the time-horizon over which we want to perform the estimation process grows towards infinity, as the size of the defining optimisation problem grows accordingly. Even in the case where there is a direct formula to obtain the estimated state trajectory, like (1.34) for the Least Squares Estimator, the involved matrices will grow in size as well. In both cases, the amount of resources needed in order to compute the estimate grows, which can be problematic when the operator only has access to limited resources or if the computing needs to be performed in a given amount of time, typically in an online setting. On the other hand, a recursive approach, which allows to obtain the estimate at a given time from the previous estimate, does not grow in size as the time-horizon grows, which makes it more suited for an online setting. The following section introduces the Forward Dynamic Programming framework as a way to conduct such a recursive approach.

1.3.3 The Forward Dynamic Programming (FDP) framework

In this section, we will investigate recursive implementation of optimal state estimation. The goal is therefore to obtain $\hat{x}_T$, the last state of the estimated trajectory $\hat{X}_T$

which would be obtained through the optimisation of objective function $V_{\Sigma,T}$ when T potentially grows towards infinity.

The *Forward Dynamic Programming* framework, introduced by Richard Bellman [Bel54] in the 1950s, proposes a method to break down an optimisation problem into smaller optimisation problems of lesser complexity. We will first introduce the main ideas of this framework before applying it to the Least Squares Estimator and obtain a recursive implementation of it.

Given a performance index function $V_{\Sigma,T} : \mathbb{R}^{m\times(T+1)} \times \mathbb{R}^{n\times(T+1)} \to \mathbb{R}_{\geq 0}$, let us define a new performance index, called the *optimal objective function* (or *value function*) $V^\star_{\Sigma,T} : \mathbb{R}^{m\times(T+1)} \times \mathbb{R}^n \to \mathbb{R}_{\geq 0}$ such that

$$V^\star_{\Sigma,T}(Y_T, z) = \min_{Z_T \in \mathbb{R}^{n\times(T+1)}} \{V_{\Sigma,T}(Y_T, Z_T) \ : \ z_T = z\}. \tag{1.39}$$

For a given $Y_T \in \mathbb{R}^{m\times(T+1)}$, $V^\star_{\Sigma,T}(Y_T, z)$ is the smallest value of $V_{\Sigma,T}(Y_T, Z_T)$ which can be obtained by a hypothetical matrix Z whose last column is z. This means that z would be the hypothetical state at time $t = T$. In other words, $V^\star_{\Sigma,T}(Y_T, z)$ is an image of how likely the vector z is to be the state estimate at time T with respect to $V_{\Sigma,T}$.

To further explore this idea, when considering the minimisation of the optimal objective function $V^\star_{\Sigma,T}$, we can interchange the order of minimisation (see [Roc98, Prop 1.35]) which yields

$$\min_{z\in\mathbb{R}^n} V^\star_{\Sigma,T}(Y_T, z) = \min_{z\in\mathbb{R}^n} \left\{ \min_{\substack{Z_T\in\mathbb{R}^{n\times T} \\ z_T = z}} V_{\Sigma,T}(Y_T, Z_T) \right\} = \min_{Z_T\in\mathbb{R}^{n\times T}} V_{\Sigma,T}(Y_T, Z_T). \tag{1.40}$$

This means that both the original objective function and the optimal objective function share the same minimum value, and the vectors minimising $V^\star_{\Sigma,T}$ are necessarily the last column of a matrix minimising $V_{\Sigma,T}$. As a result, the last estimated state vectors $\hat{x}_T$ of the estimated trajectories $\hat{X}_T$ can be theoretically obtained through the minimisation of $V^\star_{\Sigma,T}(Y_T, z)$, *i.e.*

$$\hat{x}_T \in \arg\min_{z\in\mathbb{R}^n} V^\star_{\Sigma,T}(Y_T, z). \tag{1.41}$$

One of the advantages of the FDP framework, in the case where $V_{\Sigma,T}$ is in the form (1.29), is how the relationship between $V^\star_{\Sigma,T+1}$ and $V^\star_{\Sigma,T}$ can be expressed through what is called the *Bellman Equation*:

Theorem 1.5 (Bellman equation)**.** *Let $V_{\Sigma,T}$ be a performance index function as defined in (1.29) and $V^\star_{\Sigma,T}$ be the optimal objective function associated with $V_{\Sigma,T}$ as defined in (1.39). Then, for all $T \in \mathbb{N}_{\neq 0}$ and all z in $\mathbb{R}^n$,*

$$V^\star_{\Sigma,T}(Y_T, z) = \min_{s\in\mathbb{R}^n} \left\{ V^\star_{\Sigma,T-1}(Y_{T-1}, s) + \phi_{T-1}(z - A_{T-1}s) \right\} + \psi_T(y_T - C_T z), \tag{1.42}$$

with $Y_T = \begin{pmatrix} Y_{T-1} & y_T \end{pmatrix}$ ($Y_{T-1} \in \mathbb{R}^{m\times T}$ and $y_T \in \mathbb{R}^m$).

Proof. See Appendix A.3. □

Even when T becomes large, it is theoretically possible, through the Bellman equation, to obtain the value $V^\star_{\Sigma,T}(Y_T, z)$ without solving the optimisation problem

with $(n-1)T$ unknowns which composes $V^\star_{\Sigma,T}$ as defined in (1.39). Assuming we have access to the value of $V^\star_{\Sigma,T-1}(Y_{T-1}, s)$ for every $s \in \mathbb{R}^n$, obtaining the value $V^\star_{\Sigma,T}(Y_T, z)$ would require solving one optimisation problem with n unknowns.

However, the main issue remains to have this knowledge of the value $V^\star_{\Sigma,T-1}(s)$ for every $s \in \mathbb{R}^n$ without having to solve the underlying optimisation problem. In practice, to compute $\hat{x}_t$ the estimate of the current state vector, we need a closed-form expression of $V^\star_{\Sigma,T}(z)$, and the Bellman equation allows us to recursively build one. Theorem 1.6 presents a way to derive a recursive implementation of the Least Squares Estimator thanks to the Bellman Equation.

Theorem 1.6 (Forward Dynamic implementation of the Least Squares Estimator)**.** *Let Σ be a system as in (1.1) and $V_{\Sigma,T}$ be the performance index function defined in (1.31) for a given $T \in \mathbb{N}$.*

(i) the optimal cost function $V^\star_{\Sigma,T}$, defined in (1.39), is such that for all z in $\mathbb{R}^n$,

$$V^\star_{\Sigma,T}(Y_T, z) = \frac{1}{2}(z - \hat{x}_T)^\top P_T^{-1}(z - \hat{x}_T) + r_T \tag{1.43}$$

with r_T a known quantity which is independent from z. $\hat{x}_T \in \mathbb{R}^n$ and $P_T \in \mathbb{R}^{n\times n}$ are recursively built such that $\hat{x}_0 = \mu_0$, $P_0 = S$, and

$$\hat{x}_T = A_{T-1}\hat{x}_{T-1} + P_T C_T^\top R_T^{-1}(y_T - C_T A_{T-1}\hat{x}_{T-1}) \tag{1.44}$$

$$P_T = \left((Q_{T-1} + A_{T-1}P_{T-1}A_{T-1}^\top)^{-1} + C_T^\top R_T^{-1} C_T\right)^{-1} \tag{1.45}$$

(ii) $\hat{x}_T$ is the unique solution of (1.41), which means that $\hat{x}_T$ is the estimated state at time T.

Proof. See Appendix A.4. □

The formulas (1.44)–(1.45) recursively constructing $\hat{x}$ and P_T have the disadvantage of involving many matrix inversions, which are resource-heavy from an implementation point of view. However, these formulas can be reformulated [Rei01, Eq. (22)–(24)], subsequently yielding Algorithm 1.1. It is worth noting that this algorithm could also have been directly derived from the batch formula obtained in Theorem 1.4.

This result is not new, as Algorithm 1.1 is what is commonly known as the *Kalman Filter*. The original development of this state estimator, which can be found in [Kal60], was made in a stochastic framework: in such a framework, all the signals involved (x_t, y_t, w_t, f_t) are assumed to be random, and the estimator is defined through the minimisation of the covariance matrix of the estimation error. When $\{w_t\}$ and $\{f_t\}$ are white independent Gaussian noise sequences which are also independent from the initial state, the Kalman Filter is proven to be the optimal estimator in the sense that it yields the covariance matrix for the estimation error with the smallest trace [5].

Remark 1.6. *The Kalman filter is a recursive implementation of the Least Squares Estimator since it generates a state trajectory which minimizes the cost function $V_{\Sigma,T}$ defined in (1.31). Nevertheless, throughout this document, the term "Least Squares Estimator" will be used when dealing with the batch implementation, while "Kalman Filter" will rather designate the recursive implementation.*

[5] The sum of the diagonal elements of the matrix

Algorithm 1.1 Recursive implementation of the Least Squares Estimator

Inputs: $\{A_T\}$, $\{C_T\}$, $\mu_0 \in \mathbb{R}^n$, $S \in \mathbb{R}^n$, $\{Q_T\}$, $\{R_T\}$, $T_{\max} \in \mathbb{N}$, $Y \in \mathbb{R}^{m \times T_{\max}}$
Initialization:
$T \leftarrow 1$
$\hat{x}_0 \leftarrow \mu_0$
$P_0 \leftarrow S$
End of Initialization.
while $T < T_{\max}$ **do**
  $\hat{x}_{T|T-1} \leftarrow A_{T-1}\hat{x}_{T-1}$
  $P_{T|T-1} \leftarrow A_{T-1}P_{T-1}A_{T-1}^\top + Q_{T-1}$
  $L_T \leftarrow P_{T|T-1}C_T^\top \left(C_T P_{T|T-1} C_T^\top + R_T\right)^{-1}$
  $\hat{x}_T \leftarrow \hat{x}_{T|T-1} + L_T(y_T - C_T\hat{x}_{T|T-1})$
  $P_T \leftarrow (I_n - L_T C_T)P_{T|T-1}$
  $T \leftarrow T + 1$
end while

The method we used to derive Algorithm 1.1 solely relies on a deterministic framework. However, it can be observed that the matrices P_T as defined in (1.45), correspond to the covariance matrices of the estimation error $e_T = \hat{x}_T - x_T$ in a stochastic framework. As a result, for the sake of simplicity, we will sometimes refer to P_T as the covariance matrix of the estimation error, even outside of any stochastic consideration. Even in a deterministic framework, P_T is still an image of the magnitude of the estimation error.

Remark 1.7. *From Equation (A.14) presented in the proof of Theorem 1.6, we notice that $V^\star_{\Sigma,T+1}$ can be written*

$$\forall z \in \mathbb{R}^n,\ V^\star_{\Sigma,T}(Y_T, z) = \frac{1}{2}(z - \hat{x}_{T|T-1})^\top P^{-1}_{T|T-1}(z - \hat{x}_{T|T-1}) + \frac{1}{2}(y_T - Cz)^\top R_T^{-1}(y_T - Cz) + r_T \quad (1.46)$$

with

$$\hat{x}_{T|T-1} = A_{T-1}\hat{x}_{T-1},$$
$$P_{T|T-1} = Q_{T-1} + A_{T-1}P_{T-1}A_{T-1}^\top.$$

Indeed, $A_{T-1}\hat{x}_{T-1}$ is the best mean square prediction of the state at time T which can be obtained from the knowledge of measurements up to y_{T-1}. $P_{T|T-1}$ is the best mean square prediction of the covariance matrix of the estimation error if there were no new measurement. We then note that $\hat{x}_T$ and P_T can then be written

$$\hat{x}_T = \hat{x}_{T|T-1} + P_T C_T^\top R_T^{-1}(y_T - C_T\hat{x}_{T|T-1}), \quad (1.47)$$
$$P_T = \left(P^{-1}_{T|T-1} + C_T^\top R_T^{-1} C_T\right)^{-1}, \quad (1.48)$$

which shows that in both cases, the estimated state and the covariance matrix of the estimation error at time T are built from the addition of a prediction term which is a simulation of the system obtained from the estimate at time $T-1$, and a correction term which updates the estimate and the covariance matrix of the estimation error by taking into account the new knowledge at time T.

By posing $L_T = P_T C_T^\top R_T^{-1}$, we observe that the Kalman filter has the same structure as the Luenberger observer discussed earlier (see Eq. (1.19)). The main difference lies in the fact that the Luenberger estimator has a static gain matrix while the Kalman Filter has a time-varying gain matrix.

Basic Example. Similarly to the case of the Luenberger estimator, we illustrate the performances of the Least Squares Estimator by simulating the estimation of the state of System (1.21) in the presence of Gaussian disturbances $\{w_t\}$, $\{f_t\}$ of constant covariances $0.1I_2$ and 0.1 respectively. To implement the LSE, we implemented Algorithm 1.1 with $\mu_0 = \mathbb{0}_{2,1}$, $S = I_2$, $Q_T = I_2$ and $R_T = 1$ for all $T \in \mathbb{N}$, and $T_{\max} = 100$.

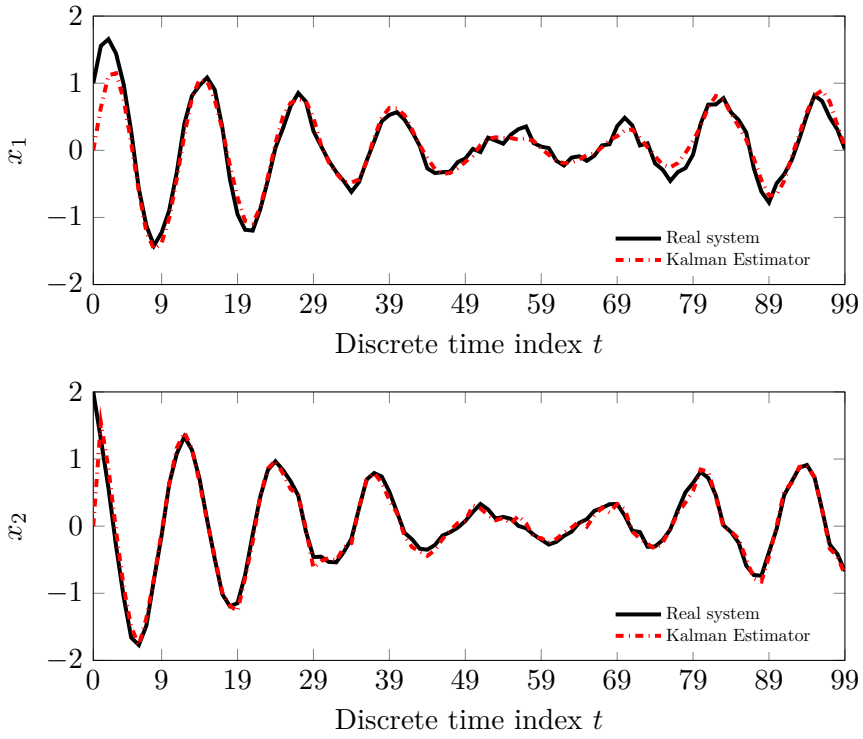

FIGURE 1.7: State trajectories of System (1.21) disturbed by Gaussian noises and estimated state trajectories obtained by a Least Squares Estimator

Figure 1.7 presents the two real state trajectories as well as the estimated state trajectories obtained by the Least Squares Estimator. We can see that the LSE is able to accurately track the real state trajectories despite the presence of the Gaussian disturbances $\{w_t\}$ and $\{f_t\}$.

Conclusion. Similarly to the batch implementation which was studied in the previous section, the recursive implementation of $V_{\Sigma,T}$ through Theorem 1.6 is mainly made possible due to its differentiability, a feature which ultimately allows $s \mapsto V^\star_{\Sigma,T}(Y_T, s) + \lambda\phi_T(z - A_T s)$ to be differentiable and to obtain its minimising argument explicitly. In the case where this function is not differentiable with respect to s or if the minimising argument $s_{\min}$ cannot be computed explicitly, such an approach is logically harder to conduct. The FDP framework therefore proposes a theoretical recursive estimation framework for any performance index function $V_{\Sigma,T}$ as defined

in (1.29), but this recursive framework results in a closed-form implementable structure only for a few cases, such as when the loss functions are all quadratic functions. This particular case will be useful in the subsequent chapters.

1.4 Introduction to Resilient Estimation

The Least Squares Estimator is an optimal estimator which was designed to deal with the estimation problem in the presence of Gaussian white noises. This kind of noise occurs in about every system, as the output, which is in practice measured by real sensors, always presents small variations around the theoretical value. Such noises occur at all times. However, systems can sometimes also be disturbed by extreme values of noise: these disturbances, sometimes labelled as *impulsive noises*, would not occur at all time but would present values which are potentially large when they do occur. What happens when a Least Squares Estimator tries to estimate the state trajectory of a system disturbed by impulsive noise?

1.4.1 The limits of the LSE in the presence of noise of large amplitude

To show the behaviour of the Least Squares Estimator in this case, we consider the simulation over the time-horizon $[0, 99]$ of System (1.21) without any dynamic disturbance $\{w_t\}$ but with $\{f_t\}$ a disturbance such that $f_{15k} = 100$ with $k \in \{1, 2, 3, ..., 6\}$ and $f_t = 0$ otherwise.

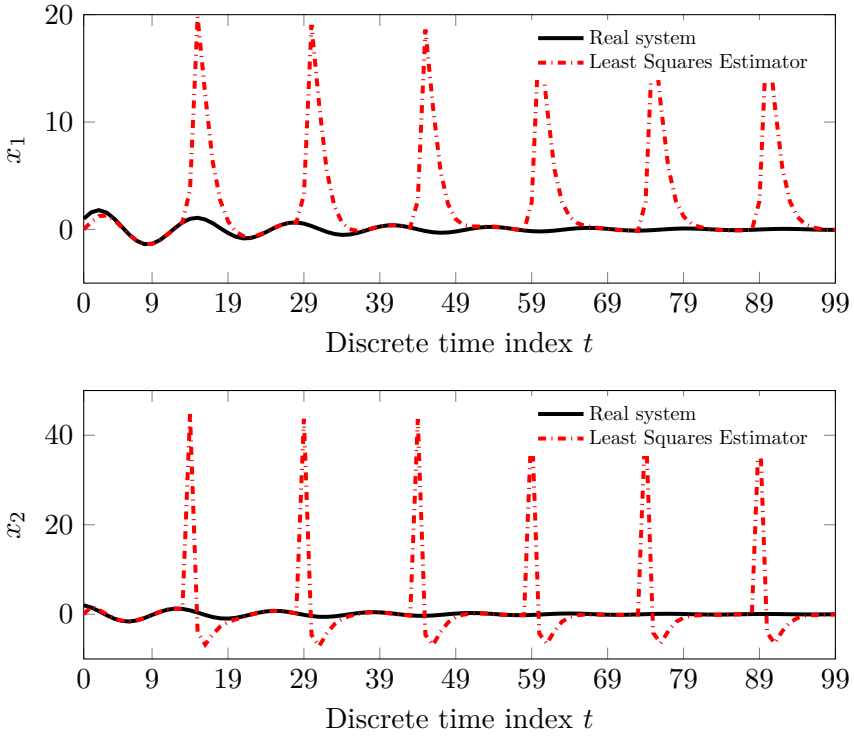

FIGURE 1.8: Example of state trajectories of a system disturbed by non-Gaussian measurement noise and its estimation by a Least Squares Estimator

Figure 1.8 presents the trajectories of the two states of the system as well as the trajectories of the estimated states obtained by a Kalman Filter implemented with

Algorithm 1.1 with $\mu_0 = (0 \quad 0)^\top$, $S = I_2$ and for all $t \in \mathbb{N}$, $Q_t = I_2$ and $R_t = 1$. As it can be observed, the Least Squares estimator fails to retrieve the right state trajectories in the presence of f, and we also notice that the estimated states present peaks which are concomitant with the non-zero entries of f.

To provide some informal explanation about this phenomenon, we need to look at the residuals $\hat{f}_t = y_t - C_t\hat{x}_t$. The residuals $\{\hat{f}_t\}$ are the reconstructed values of the output disturbance corresponding to the estimated trajectory $\hat{X}$. To maximise the chances of the estimate to be accurate, the performance index function V_Σ must logically encourage $\{\hat{f}_t\}$ to have the same structure as $\{f_t\}$. In the case where $\{f_t\}$ is a Gaussian noise sequence, as stated in Section 1.3.2, a quadratic function is the most suited loss function in order for $\{\hat{f}_t\}$ to have the same structure as $\{f_t\}$. However, this is not the case when $\{f_t\}$ is sparse, as a Gaussian-like structure and a sparse one are fairly different.

This explains the bad performances of the Least Square Estimator, since the quadratic functions constituting V_Σ encourage $\{\hat{f}_t\}$ to have a Gaussian-like structure despite $\{f_t\}$ having a sparse structure. Given that $\hat{f}_t = y_t - C\hat{x}_t$ for all t in $\mathbb{T}$, V_Σ subsequently forces the estimated output $C\hat{X}$ to fit the measurement trajectory Y, which explains why the estimate features the same peaks as the measurement.

In conclusion, the Least Squares Estimator does not provide satisfactory results in the presence of noises of large amplitude, which is mainly explained by the choice of the loss functions composing its defining performance index function. In the next section, we will discuss estimation methods that are more robust to measurement noises of impulsive nature. In particular, we will show (see, *e.g.*, Chapter 2) that the estimation error can be made completely insensitive to sparse noise sequences $\{f_t\}$ provided that the number of nonzero instances they contain is small enough. This property of robustness is termed *resilience*.

1.4.2 Arbitrary disturbances and the concept of resilience

First of all, the characteristics of the disturbances to be taken into account within resilient estimation will be discussed: among other topics, the question of their physical origin and of their model will be addressed. Subsequently, a discussion about the term *resilient* will be provided.

From a physical point of view, we can divide disturbances into two groups depending on when they occur:

- On the one hand, we consider **dense noises**, which occur at all times within the system. This is the most classic type of disturbances, which has been considered so far and include "classic" noises such as sensor noises.
- On the other hand, there are **sparse noises**, also known as *impulsive noises*, which are intermittent and *do not* occur at all time within the system. They model a wide range of disturbances which greatly shift the behaviour of the system when they happen, and are not taken into account by classical estimators such as the Least Squares Estimator.

Sparse noises are mainly consequences of failures or attacks on the system. Failures are most of the time due to a component of the system which is either broken or on the verge of breaking: for instance, a failing sensor can produce sparse noise in the measurement, while a broken actuator can lead to the presence of sparse noise within

the dynamic equation of the system. Attacks are actions performed by an adversary on the system in order to purposefully damage it or hide its true state. For example, the General Introduction took the example of the *Cyber-Physical Systems* [Car08], whose measurements are gathered through a communication network in order to feed an external processing unit which performs the process of estimating the system. Such systems are prone to cyber-attacks where the processing unit is fed with aberrant measurements in order to derail the estimation process, which has been proved doable by already existing malwares [Inc17].

However, it is worth noting that the presence of impulsive noises within the system is not necessarily the sign of an attack or a failure: for instance, in telecommunication networks, short voltage outbursts, caused by the normal behaviours of various sources present in the network, can occur [Pri93].

Being able to successfully estimate the state of a system under such circumstances is essential for several reasons:

- In the case where the sparse noise is a constraint of the system itself and not a consequence of an attack or a failure, there is still a need to provide accurate estimation.
- In the case of a sparse noise induced by a failure, successfully estimating the state even in its presence can help detecting the failure itself: for example, it can help detect a sensor which is failing and needs to be replaced.
- Several crucial processes, such as the control of the system, might rely on the estimation to operate. If the estimates starts diverging, there is a risk that those processes diverge as well, which can potentially cause damage to the system.

In the context of LTV Discrete-Time systems as in (1.1), we now introduce *arbitrary noises*, which can present the behaviours of *both* dense noises and sparse noises. For the sake of simplicity, only the measurement disturbance $\{f_t\}$ will be considered an arbitrary disturbance unless explicitly stated otherwise.

The hypothesis surrounding the arbitrary noises will be kept to a minimum. In particular, no assumption will be made on the probabilistic distribution of its values. Nevertheless, analysis tools will be used in order to describe the behaviour of the arbitrary noise $\{f_t\}$: those tools will be sets of the form

$$\mathbb{T}_\varepsilon = \{t \in \mathbb{T} : \gamma_t(f_t) \leq \varepsilon\},$$

$$\mathbb{T}_\varepsilon^c = \mathbb{T} \setminus \mathbb{T}_\varepsilon = \{t \in \mathbb{T} : \gamma_t(f_t) > \varepsilon\},$$

where γ_t is a function from $\mathbb{R}^m$ to $\mathbb{R}_{\geq 0}$, $\mathbb{T} = \{0, 1, ..., T-1\}$ and $\varepsilon > 0$ an analysis parameter. γ_t serves to measure of the magnitude of f_t and the intervals $\mathbb{T}_\varepsilon$ and $\mathbb{T}_\varepsilon^c$ divide the indexes t into two groups, depending on whether the magnitude of f_t is smaller or greater than ε.

The decomposition obtained by the introduction of sets $\mathbb{T}_\varepsilon$ and $\mathbb{T}_\varepsilon^c$ therefore splits f_t into two categories: the occurrences of f_t which are "*reasonable*" with respect to ε, and its *outliers*. However, it is important to understand that ε is not a bound assumed on the arbitrary noise sequence, $\{f_t\}$, but can vary and subsequently provide different decompositions of f_t depending on its value (see Figure 1.9 for an example of how different values of ε lead to different composition of $\mathbb{T}_\varepsilon$ and $\mathbb{T}_\varepsilon^c$ when the number m of outputs is equal to 1 and $\gamma_t = |\cdot|$).

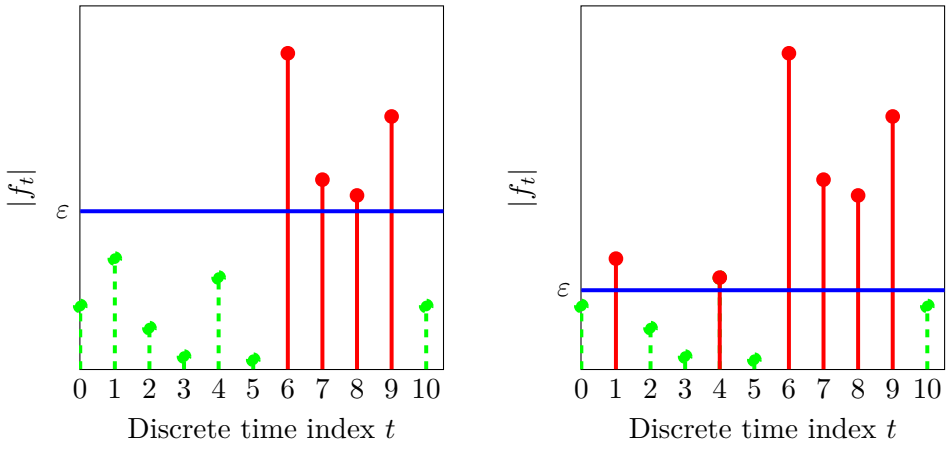

FIGURE 1.9: Examples of the decomposition of $\{f_t\}$ ($\mathbb{T}_\varepsilon$ are the time indexes for which f_t is dashed green, $\mathbb{T}_\varepsilon^c$ those for which f_t is red) for different values of ε

Any noise sequence can be formally decomposed under the form

$$f_t = v_t + s_t \tag{1.49}$$

where $\{v_t\}$ is a bounded noise sequence while $\{s_t\}$ is a *sparse* noise sequence. When we assume such a decomposition (*e.g.* when we simulate f_t), v_t will be often referred to as the *dense component* of f_t, while s_t will be labelled as the *sparse component* of f_t.

Remark 1.8. *We did not assume any probability distribution for the arbitrary noises. Nevertheless, it would be possible to consider this type of noise in a stochastic framework. For instance, one can model an arbitrary disturbance as a Laplacian noise [Sha10], or any heavy-tailed noise in general [Aga12]. The principle of heavy-tailed noises is that their associated probability distribution presents a heavy tail, meaning that these noises are more likely to take higher values than Gaussian noises.*

We will distinguish between two types of sparsity for the sequence $\{s_t\}$: *componentwise sparsity* and *timewise block sparsity*. Componentwise sparsity implies that for every t, s_t is a sparse vector of $\mathbb{R}^m$, while timewise block sparsity means that most s_t vectors are zero but non-zero vectors s_t can be full vectors.

To illustrate this concept, if we denote with $S \in \mathbb{R}^{m\times T}$ the sparse noise matrix formed from the sequence $\{s_t : t \in \mathbb{T}\}$, consider the two following sparse noise configurations for $m = 4$ and $T = 5$:

$$S_1 = \begin{pmatrix} 0 & 0 & 0 & 12 & 0 \\ 3 & 0 & 14 & 0 & 0 \\ 0 & 0 & 0 & 0 & 20 \\ 0 & 15 & 0 & 5 & 5 \end{pmatrix} \text{ and } S_2 = \begin{pmatrix} 0 & 3 & 0 & 0 & 10 \\ 0 & 15 & 0 & 0 & 9 \\ 0 & 17 & 0 & 0 & 17 \\ 0 & 11 & 0 & 0 & 0 \end{pmatrix}. \tag{1.50}$$

The k-th row corresponds to the noise sequence affecting sensor k over $\mathbb{T}$, while the column l is simply the value of the sparse noise sequence at time l: in that context, to determine if a sparse noise is either *componentwise sparse* or *timewise block sparse*, we need to study the sparsity of the columns of S.

The two sparse noise matrices defined above share the same number of non-zero elements: however, their structures are completely different. The columns of S_1 are

clearly all sparse, while the columns of S_2 are not, given that its non zero elements are all gathered in two columns (2 and 5). As a result, S_1 is componentwise sparse, but S_2 is timewise block sparse.

The term *resilience*. Throughout the thesis, we will use the term *resilience* to describe a specific robustness property of a state estimator to a class of uncertainties[6]. More specifically, we say that a state estimator is *resilient* to a given class $\mathcal{F}$ of disturbances (uncertainties, *e.g.* the noise sequence $\{f_t\}$) if it induces an estimation error which is completely insensitive to that class of disturbances. That is, the associated estimation error is zero so long as the disturbance affecting the system (whose state is being estimated) lies in $\mathcal{F}$.

We will also make use of the *approximate resilience*, which designates a weaker version of resilience, where the estimator is not insensitive to a given class $\mathcal{F}$ of disturbances, but the impact of this class is bounded given that the number of the outliers is below some threshold.

For a more formal definition of the resilience and the approximate resilience properties, you can refer to Section 2.3.1.

Remark 1.9. *The distinction between the concepts of* resilience *and* approximate resilience *resembles the difference between the properties of "outlier rejection" and "outlier attenuation" which can be found in the literature, such as in [Ale16].*

1.5 State of the art of Resilient estimation

The goal of this section is to provide a coherent view of what has been done in the domain of resilient estimation.

We will focus our review on three aspects of the resilient estimation literature:

- An intuitive type of approach which consists in separating the fault/attacks detection and the estimation process.
- Methods deriving from the compressed-sensing theory and which define optimal estimators through performance index functions with sparsity inducing properties.
- The Maximum Correntropy Criterion framework, which defines optimal estimators with saturated performance index functions.

Although resilient estimation is a quite recent topic in a formal sense, the related literature has grown rapidly. Our classification above emphasizes only those methods which are conceptually close to the treatment made of this problem in the current thesis. Nevertheless, we do acknowledge the existence of other works, such as the ones studying the performance limits of classical optimal state estimators in the presence of sparse noise [Sin04; Nie14; Mo15; Ren20], the ones proposing heuristics modifications of the Kalman Filter to make it more resilient [Aga11; Tin07a; Tin07b], or the ones developing resilient Luenberger-based estimators [Sho16; Ast21; Jeo16].

1.5.1 Detection approaches

Since the measurements are assumed to be affected by a sequence of outliers which is sparse in time, a natural scheme of solution to the state estimation problem may be to

[6] For an informal discussion about the link between resilience and robustness, [Arg16] deals with those concepts in the scope of power networks.

first process the data so as to detect the occurrences of the nonzero instances of that sparse noise, remove the corrupted data and then proceed with classical estimation methods such as the Kalman filter or the Luenberger estimator which we already presented:

- In [Mis17], the principle is to find a subset of sane sensors, *i.e.* unaffected by sparse noise. To do so, they compute a Kalman Filter estimate for a given subset of sensors and then compute the residuals $\hat{f}_t$ to verify if they respect a given criterion. If they do, the sensor subset is said to be *attack-free*.

  The first algorithm derived in the paper then consisted in exhaustively testing all the sensor subsets possible, but such an approach is combinatorial. Consequently, Mishra et al. also explore algorithms which prune out bad sensor subsets without actually testing them through a boolean-based weighting system. The problem with such an approach is that it does not necessarily yield an algorithm with predictable complexity.

- In [Pas13], the focus is put on *monitors* which are deterministic algorithms returning whether the system is attacked (attack detection) and what is the subset of attacked sensors (attack identification). They design such algorithms as closed-loop system filters and specify under which conditions they are able to detect or identify attacks based on a characterisation of detectable and identifiable attacks. However, this solution is also very combinatorial, as the number of filters they need to construct in order to successfully perform the identification process grows dramatically with the number of attacked sensors: if there are k attacked sensors in the system with n states, about n^k filters needs to be constructed.

.

This detection approach is reasonable, and allows to rely on the extensive literature of optimal state estimation. However, the main challenge remains to achieve an efficient detection and isolation of the outliers, and this can be at the cost of a loss of information. It is therefore needed to study the interaction between the fault detection scheme and the estimation process, which can sometimes be a hard task (addressed for instance by Theorem 3 of [Mis17]). Moreover, identifying the subset of attacked sensors poses an algorithmic challenge as it is NP-complex [Pas13, Cor.4.5].

Finally, the detection approach does not make the handling of outliers within the dynamics of the system possible through a non-resilient optimal state estimator. Indeed, it possible to identify faulty sensors prior to the estimation in order to ignore them, but faulty actuators cannot be ignored, since they still impact the system dynamics.

An alternative to the detection-isolation approaches may be to design optimal estimators which would be robust to impulsive noise by construction. As it will be discussed in the next section, such robustness properties depend on the loss functions defining the to-be-minimized performance index function. Hence, a question of interest is: how can we design the loss functions so that the estimator is more likely to present resilience properties?

1.5.2 Compressed-sensing inspired methods

In Section 1.4.1, it was stated that the quadratic functions involved in the defining cost function of the Least Squares estimator were not encouraging a sparse structure on the residuals $\hat{f}_t = y_t - C_t\hat{x}_t$.

To promote a residual sequence which is sparse, we need to construct the estimator on the basis of sparsity-inducing loss functions. A very intuitive choice of loss function would be the pseudo-norm ℓ_0 which is defined such that for all z in $\mathbb{R}^a$ with $a \in \mathbb{N}$,

$$\|z\|_0 = |\{k \in \{1, ..., a\} \ : \ z[k] \neq 0\}| \tag{1.51}$$

with $z[k]$ designating the k-th component of z. The ℓ_0-norm of a vector is therefore equal to the number of nonzero elements within z, meaning that the minimising argument of such a norm has to be sparse, given that it will have as many zero entries as possible. As a result, using it in Equation (1.29) for all ψ_t for $t \in \mathbb{T}$ would make the residual terms $\hat{f}_t$ sparse, which is exactly what is needed in the case where the measurement equation is disturbed by sparse noises.

However, the ℓ_0-norm presents two problems. First of all, it would impose strict sparsity on the residuals. It is problematic for state estimation in the presence of arbitrary noise as they present both a dense and a sparse behaviours. Secondly, the ℓ_0-norm is not convex, and this is a problem for the implementation of the resulting optimal state estimator. Indeed, in general, minimising the ℓ_0-norm is a hard combinatorial problem.

The second point was already addressed by the compressive sampling framework, which aims at reconstructing a sparse vector from a limited amount of measurements [Can08a; Fou13]. In this framework, the solution chosen was to relax the ℓ_0-norm by replacing it with the ℓ_1-norm, *i.e.* the norm such that for all z in $\mathbb{R}^a$ with $a \in \mathbb{N}$,

$$\|z\|_1 = \sum_{k=1}^{a} |z[k]|, \tag{1.52}$$

known for its sparsity-inducing properties. Moreover, the ℓ_1-norm does not induce strict sparsity, so it seems like a more suitable way to deal with arbitrary noises.

This compressive sampling-inspired approach was introduced to the scope of resilient estimation in [Faw14]. In this paper, the case of the attack of an LTI system without any dense noise is considered. Moreover, it is assumed that only a fixed number of sensors are subject to attacks (sparse over time but otherwise arbitrary disturbances). The challenge then resides in the fact that at each time instant, one does not know which sensor is compromised. To tackle this challenge and recover the initial state (which is enough to reconstruct the whole trajectory when there is no dense noise within the system), Fawzi *et al.* introduce the performance index functions V_Σ such that for all $Y \in \mathbb{R}^n$, $z \in \mathbb{R}^n$,

$$V_\Sigma(Y, z) = \sum_{t \in \mathbb{T}} \|y_t - CA^t z\|_p \tag{1.53}$$

where $\|\cdot\|_p$ designates the the ℓ_p-norm, *i.e.* the norm such that for all z in $\mathbb{R}^a$,

$$\|z\|_p = \left(\sum_{k=1}^{a} z[k]^p \right)^{\frac{1}{p}}. \tag{1.54}$$

This class of loss functions comes from the block-sparsity compressed sensing literature, and especially [Eld09] where the ℓ_2-norm is used in order to estimate a signal which presents a structure similar to what we designate as *timewise block sparsity*.

Contrary to the detection approach, the one presented in [Faw14] can tackle the

case where there is a impulsive noise in the dynamic equation of the system, by considering a similar performance index function to V_Σ such that for all $Y \in \mathbb{R}^n$, $z \in \mathbb{R}^n$,

$$V_\Sigma(Y, Z) = \sum_{t \in \mathbb{T}'} \|z_{t+1} - Az_t\|_p + \sum_{t \in \mathbb{T}} \|y_t - Cz_t\|_p. \tag{1.55}$$

Finally, [Faw14] also present results to characterise if the state of a given system can be accurately estimated when a certain amount of its sensors are attacked. This basically consists in having a condition on the richness of the measurements that the system can provide.

After the publication of [Faw14], many papers were published in order to extend and complete its analysis. We will cite two analysis extensions:

- [Paj17] studies how the presence of dense noise within the system can degrade the performances of the resilient optimal state estimator defined by the performance index functions V_Σ as defined in (1.53) for $p = 1$. In the case where the system is observable enough, Pajic *et al.* are able to derive an upper bound on the estimation error of the initial state. The interest of this bound is that it is linear with the magnitude of the dense noises present in the system, even though it is conservative.
- In [Cha18], the assumption of a fixed number of attacked sensors is relaxed. This is achieved by establishing conditions on the time-horizon over which the estimation process is performed: if the length of the time-horizon is chosen greater than a value linked with the parameters of the system, then the results of [Faw14] can be reformulated in the case where every sensor can be disturbed.

Finally, the more recent paper [Han19] proposes a unified framework for analysing resilience capabilities of most of convex optimisation-based estimators,, similarly to what we intend to do in Chapter 2. Although a bound on the estimation error was derived in this paper, it is not quantitatively related to the properties (e.g., observability) of the dynamic system being observed. The state estimation problem treated there is rather viewed as a linear regression problem similarly to [Bak17; Can08b].

As a conclusion, compressed-sensing inspired methods constitute a very interesting way to tackle the resilient state estimation problem. A lot of results ensuring the resilience of state estimators were already obtained in the domain and the experiments presented in all the papers mentioned above show promising results. It is however worth noting that most of those estimators are designed without taking into account the presence of dense process noise. The works considering a non-zero dense $\{w_t\}$ (such as [Paj17]) simply quantify the degradation of the performances of the defined estimators in the presence of such noises. Moreover, to the best of our knowledge, the design of recursive estimator based on compressed-sensing inspired methods has yet to be explored.

1.5.3 The Maximum Correntropy Criterion (MCC) Framework

Another possible choice of loss functions would be functions which present a saturation when the magnitude of their argument tends towards infinity. We recall that the terms in a cost function which weigh the most are minimised in priority, and this is a

problem with the arbitrarily large magnitudes of the outliers. Having saturated loss functions is therefore a way to prevent this issue.

The *Maximum Correntropy Criterion (MCC)* framework was developed in order to improve the performances of the Kalman Filter in the presence of non-Gaussian noise by replacing the quadratic forms by functions presenting a saturation. For instance, the *Maximum Correntropy Criterion Kalman Filter* (MCCKF), as stated in [Iza16], is an optimal recursive state estimator $\mathcal{E}_{\text{MCC}}$ defined such that

$$\mathcal{E}_{\text{MCC}} = \arg\max_{z\in\mathbb{R}^n} V_{\Sigma,T}(y_T, z) \tag{1.56}$$

with $V_{\Sigma,T}$ the performance index function such that for all (y_T, z) in $\mathbb{R}^m \times \mathbb{R}^n$,

$$V_{\Sigma,T}(y_T, z) = \exp\left(-\frac{\|z - A_{T-1}\hat{x}_{T-1}\|^2_{P^{-1}_{T|T-1}}}{\sigma^2}\right) + \exp\left(-\frac{\|y_T - C_T z\|^2_{R_T^{-1}}}{\sigma^2}\right) \tag{1.57}$$

where $\sigma > 0$ and $P_{T|T-1}$ is as defined in (1.47). The parallel between the MCCKF and the Kalman Filter (see Eq. (1.46)) is clear: the quadratic forms were wrapped in a decreasing exponential which tends towards zero when its arguments tends towards infinity. Consequently, the presence of large outliers in the measurements y_t should have a lesser impact in the MCC Kalman Filter than in the original Kalman Filter.

Remark 1.10. *$\mathcal{E}_{MCC}$ is defined as the maximisation of cost function $V_{\Sigma,T}$ which is different from the framework we presented in 1.3.1. However, we can always consider the function $(y_T, z) \mapsto 2 - V_{\Sigma,T}(y_T, z)$ which is nonnegative and increasing.*

The MCC approach is based on the *correntropy*, which is a measure of similarity between two random variables. If we have two scalar random variables $\mathcal{X}_1$ and $\mathcal{X}_2$ then the correntropy between those two variables is defined as [Pri10, Eq. (10.1)]

$$V(\mathcal{X}_1, \mathcal{X}_2) = \int_{\mathbb{R}^2} \kappa(x_1, x_2)\mathrm{d}F_{\mathcal{X}_1\mathcal{X}_2}(x_1, x_2), \tag{1.58}$$

where $F_{\mathcal{X}_1\mathcal{X}_2}$ is the joint probability density function of $\mathcal{X}_1$ and $\mathcal{X}_2$ and κ a mapping from $\mathbb{R}\times\mathbb{R}$ to $\mathbb{R}_{\geq 0}$ called a *kernel* (for more information on the mathematical definition of a kernel, please refer to [Thi19]).

However, since the joint probability density function is unknown in most cases and the number of data is limited, correntropy measures are in practice performed using the empirical correntropy defined such that [Pri10, Eq. (10.3)]

$$\hat{V}(\mathcal{X}_1, \mathcal{X}_2) = \frac{1}{N}\sum_{k=1}^{N} \kappa(x_{1,k}, x_{2,k}) \tag{1.59}$$

where $\{(x_{1,k}, x_{2,k})\}$ is a sequence of N independent samples of $(\mathcal{X}_1, \mathcal{X}_2)$.

The kernel is a similarity measure between $\mathcal{X}_1$ and $\mathcal{X}_2$. The more similar $x_{1,k}$ of $\mathcal{X}_1$ and $x_{2,k}$ of $\mathcal{X}_2$ are, the bigger $\kappa(x_{1,k}, x_{2,k})$ will be. A common way to design a kernel is to define a new univariate function $\xi : \mathbb{R} \to \mathbb{R}_{\geq 0}$, called a *kernel function*, such that

$$\forall (x_1, x_2) \in \mathbb{R}^2,\ \kappa(x_1, x_2) = \xi(x_1 - x_2). \tag{1.60}$$

One of the most commonly used kernel functions is the Gaussian kernel function, *i.e.*

$$\forall a \in \mathbb{R},\ \xi(a) = e^{-\frac{a^2}{2\sigma^2}}$$

with $\sigma \in \mathbb{R}$ the width of the kernel. This is the kernel function used in the MCCKF mentioned earlier, but it is also employed in [Che17a; Liu17] which derive fixed-point algorithms for state estimators inspired by MCC.

The MCC framework regroups a wide variety of possible performance index functions with different kernel functions, such as the exponential absolute value kernel functions, *i.e.*

$$\forall a \in \mathbb{R},\ \xi(a) = e^{-\frac{|a|}{2\sigma}},$$

which are studied in [Che17b].

In the MCC-related works, a prominent place is given to the derivation of recursive estimators: we already cited [Che17a; Liu17; Che17b], but we can also mention [Kul17] in which an estimator defined by an MCC-based performance function is implemented in the form of a Kalman Filter with approximated weights based on the prior estimation at each step. However, one of the main issues of the MCC approach is that it is based on the solving of non-convex optimisation problems.

In conclusion, the MCC is another possible framework to provide state estimators which yield good performances in the presence of arbitrary noises. However, contrary to the literature dealing with compressed-sensing inspired methods, the literature surrounding MCC methods has been primarily focused on the design of recursive estimators. On the one hand, it yielded successful implementation for engineering problems, such as in machine learning with robust facial recognition [He11] or in robust channel estimation for wireless communications [Ma15]. On the other hand, the question of the analytical proof of resilience for the MCC-based estimators is a more open question. It is worth noting that this question raises more and more interest: in particular, [Bak18] and [Che19] propose an analysis of the resilience of MCC-based estimators under the scope of regression problems.

1.5.4 The behaviour of resilience-inducing loss functions

The starting point of our reflection is the desire to explore what makes a loss function actually induce resilience in a state estimator. Indeed, the two types of frameworks presented in the last two sections were developed independently and the loss functions involved in the performance index functions of their respective state estimators are fairly different. However, they both yield interesting results in resilient state estimation. What is the common point between those two approaches, and especially between the loss functions involved in the resilient optimal state estimators they produce?

To provide some preliminary elements to this reflection, Figure 1.10 presents several graphs of possible loss functions when the argument is a scalar:

- the square loss function $\psi : a \mapsto a^2$, typical from the Least Squares Estimator.
- the absolute value loss function $\psi : a \mapsto |a|$, the scalar equivalent of a norm which is at the core of the compressed sensing-inspired methods.
- a saturated exponential loss function $\psi : a \mapsto 3(1 - e^{-\lambda|a|})$ instantiated with $\lambda = 1$, which is similar to the ones used in the MCC framework.

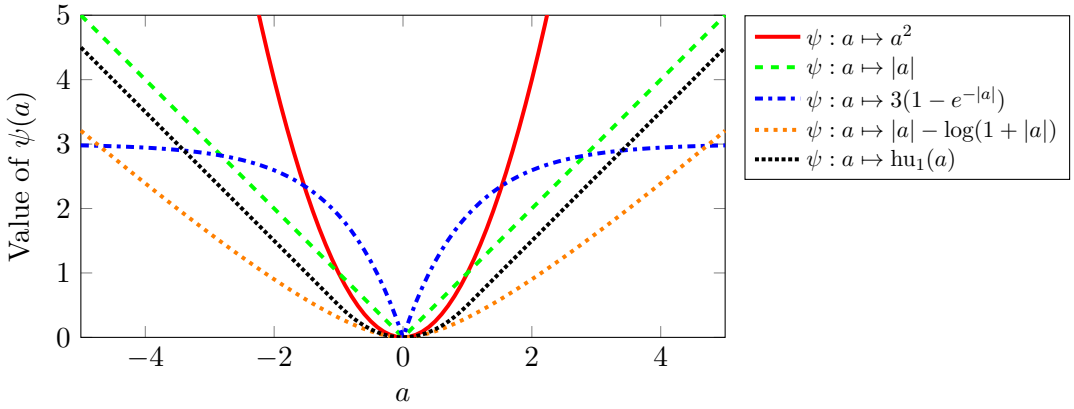

FIGURE 1.10: Example of different loss functions ψ

- the logarithmic loss function $\psi : a \mapsto |a| - \frac{1}{\lambda}\log(1+\lambda|a|)$ instantiated for $\lambda = 1$, presented in [Say14, Eq. (1)] as another robustness-inducing function.
- the Huber loss function $\psi : a \mapsto \mathrm{hu}_\lambda(a)$ such that

$$\forall a \in \mathbb{R}, \quad \mathrm{hu}_\lambda(a) = \begin{cases} \dfrac{1}{2}a^2 & \text{if } |a| < \lambda \\ \lambda\left(|a| - \dfrac{1}{2}\lambda\right) & \text{else} \end{cases}, \tag{1.61}$$

  instantiated for $\lambda = 1$. This loss function, originating from the robust regression framework, has been studied for its resilient properties in [Han19].

The common point between all the resilience-inducing loss functions is that contrary to the square function, their behaviour remains "reasonable" when their argument tends towards infinity. In the most extreme case, the saturated loss function tends towards 3 when its argument tends toward infinity, but in the case of the absolute value loss function, the size of $\psi(a)$ grows linearly with the size of a.

This plays a huge role in the behaviour of the resulting performance index functions. We already stated that the minimisation of the performance index functions prioritises the minimisation of the terms which weigh more. A loss function is a way to tune this prioritisation with respect to the magnitude of its argument. The prioritisation scheme of a given loss function is dictated by its growth when the argument tends towards infinity: for instance, the growth of the saturated exponential loss function tends towards zero when the argument tends towards infinity, which means it does not give more priority to the minimisation of its argument passed a certain threshold. All the sparsity inducing loss functions have a growth which is linear at best, which means it gives, at most, the same priority regardless of the magnitude of the argument. On the other hand, the square function (or quadratic function in the vector case) gives more priority to greater terms, as it squares them: this behaviour is another intuitive explanation as to why the Least Squares Estimator behaves poorly in the presence of impulsive noises, which present really large magnitudes.

1.5.5 Our contributions

Taking into account the intuitions we have about what makes a loss function induce resilience, the goal of our work is to design and analyse optimal state estimators able to estimate, on a given time horizon $[0, T-1]$, the state trajectory of a system whose output equation is disturbed by the presence of an arbitrary noise. This arbitrary

noise can present both dense and impulsive behaviours, and we assume that it can happen on every sensor at every time. This relaxes the frequent hypothesis, made in [Faw14; Paj17] for instance, that the arbitrary noises only disturb a fixed set of sensors in the system. Moreover, the system also presents a bounded noise in its dynamic equation.

Our contributions address three main questions:

How to design estimators which are either resilient or approximately resilient?

In Section 1.5.4, we exhibited several loss functions which have been involved in interesting approaches tackling the state estimation problem in the presence of arbitrary noises. Our approach now consists in defining classes of performance index functions constituted by loss functions (*i.e.* χ and the elements of families $\{\phi_t\}$ and $\{\psi_t\}$ in (1.29)) which share properties with the aforementioned functions. In particular, these classes will be defined solely through their properties, and not through a given closed-form expression.

Two classes of optimal state estimators will be studied in this report. The first one, $\mathcal{E}$, is studied in Chapter 2, and aims at generalising the properties of loss functions in compressed sensing-inspired methods. Subsequently, the loss functions constituting the performance index functions of class $\mathcal{E}$ will have properties generalising norm properties. This includes a generalized homogeneity property and a generalized triangle inequality. Considered in Chapter 3, the second class of estimators, $\mathcal{E}^{\exp}$, contains estimators defined by performance index functions resembling those involved in MCC approaches. This means that the loss functions constituting them will be of the form $\psi_t : z \mapsto 1 - \exp(-\lambda\psi(z))$, inducing a saturation when the size of their argument increases. It is worth noting that the argument function ψ will be defined through its properties, in order to consider a large class of estimators.

By defining loss functions through their properties rather than through a specific closed-form expression, we aim at having a better understanding about which exact properties are ultimately giving the resilience (or approximate resilience) property to the corresponding optimal state estimator. At the same time, this also allows us to consider a whole class of state estimators and not only one, which gives a wider reach to our analysis.

What are the theoretical guarantees of the performances of (approximately) resilient state estimators?

Some papers mentioned in the previous sections, such as [Han19] or [Bak17], already present an analysis of the resilience of classes of optimal state estimators. However, both papers present an analysis for linear regressions, system models which do not explicitly take into the account the dynamical behaviour of a system.

We conduct our analysis in the scope of state-space representations, and we also take into account the presence of dynamic disturbances in the design of the estimators themselves, as indicated by the defining equation (1.29) of V_Σ. The main theoretical contributions of our work are:

- The definition of new quantitative characterisations of the observability, adapted to the class of estimators we consider and to the estimation setting.
- The derivation of bounds on the estimation error for the considered classes of estimators. Most of the time, the existence of these bounds will be guaranteed if a condition, linked with the observability of the considered system, holds. The extreme values of the arbitrary noise have either no impact or a small impact

on these bounds, which will prove the resilience or the approximate resilience of the studied estimators.

- A qualitative interpretation of these derived bounds. Indeed, the bounds on the estimation error are expressed explicitly through the parameters of the system and of the estimators. Consequently, we provide a discussion about how these parameters impact the quality of the estimation, and what key parameters need to be taken into account when considering a resilient state estimation approach.

How to implement (approximately) resilient state estimators?

Finally, the present report will deal with the batch and recursive implementations of the considered classes of estimators. Indeed, being able to implement the resilient (or approximately resilient) estimators which were theoretically analysed is a crucial step towards the implementation on real systems. Moreover, these implementations need to be numerically tested.

We defined the considered optimal estimators in batch, given that they are defined through the minimisation of a performance index function over a given time-horizon of length $T-1$. Consequently, since some estimators from class $\mathcal{E}$ are defined by convex cost functions, implementing them in batch by directly solving the underlying optimisation problem is a viable solution, given that we can use efficient convex optimisation algorithms. However, estimators from $\mathcal{E}^{\text{exp}}$ are defined by nonconvex cost functions, which makes the direct solving of their defining optimisation problem harder. Consequently, we derived an Iteratively Reweighted Least Squares Algorithm in order to approximately implement this class of estimators.

To derive recursive algorithms, we made use of the Forward Dynamic Programming introduced in Section 1.3.3. This allowed us to approximately implement both classes $\mathcal{E}$ and $\mathcal{E}^{\text{exp}}$ through Kalman-like algorithms.

We also numerically assessed the performances of the derived algorithms. This was done in various different settings, for instance with different ratios of nonzero entries of outliers or with different Signal-to-Noise ratios for the dense noises. All the implemented algorithms displayed promising results, with good performances even in the presence of outliers with extreme values.

1.6 Conclusion

The resilient state estimation framework results from a need to be able to estimate the inner state of a system despite the presence of arbitrary disturbances, which can have both a dense behaviour, *i.e.* it happens at all times but with a moderate amplitude, and a sparse behaviour, which presents rare occurrences but with potentially large amplitudes. There are many potential ways to design such a framework, but we put our focus on methods making use of the optimal state estimation framework, a framework which designs estimators through the minimisation of a performance index function discriminating every potential state trajectory in order to obtain the most likely state trajectories.

Many resilient estimators have already been proposed and their resilient properties successfully assessed, but the next chapters aim at proposing an analysis covering many different resilient estimators by defining performance index functions through the properties verified by the loss functions composing them rather than by closed-form expressions. This analysis will be decomposed into two main parts, and therefore two chapters, depending on whether we consider non-saturated or saturated loss functions.

Chapter 2

Resilient estimators based on non-saturated objective functions

2.1 Introduction

To address the Resilient Estimation problem stated in Section 1.2.2, this chapter will be focused on a specific class of optimal estimators. For this purpose, we introduce a family of to-be-minimised performance functions of the form (1.29) where the loss functions ϕ and ψ are required to obey a set of properties. Our goal in so doing is to try to characterise jointly the minimal properties of the system (whose state is being estimated) and those of the loss functions (entering the construction of the performance index) which are necessary to ensure the resilience of a state estimator. The behaviour of the loss functions involved in the performance index function will be similar to norms and/or quadratic functions which grow towards infinity when their argument grows, hence the term "non-saturated". Some elements of this newly defined class of estimators can present saturated performance indexes, but Chapter 3 will study a class of estimators designed to have saturated performance indexes, in order to provide a more thorough study.

First, we will define the class of estimators in Section 2.2.1, and then discuss a few basic properties of the loss functions involved in the performance index in Section 2.2.2. The analysis of resilience of this class (Section 2.3) will then be presented, and structured around two cases depending on the structure of the objective function.

Section 2.4 will deal with a reformulation of the class of estimators in the case where every dense component of both disturbances is equal to zero. A few results on the exact recoverability of the initial state, *i.e* when the estimator returns the exact value of the initial state, can be obtained in that setting.

The rest of the chapter will be centred about numerical considerations and estimator implementation. Section 2.5 is about how to numerically assess some key resilience parameters from the system, and Section 2.6 presents a way of implementing this class of estimators with a recursive algorithm. Finally, Section 2.7 will provide simulation results in order to give insight on the influence of system and estimator parameters on the quality of the estimation.

2.2 Optimal estimators based on norm-like loss functions

2.2.1 Definition of the class of estimators

In this section we present an optimization-based framework for solving the state estimation problem defined in Chapter 1, and consider the LTV system of the form (1.1)

$$\begin{cases} x_{t+1} &= A_t x_t + w_t \\ y_t &= C_t x_t + f_t \end{cases}$$

with $x_0 \in \mathbb{R}^n$ its initial state, $\{w_t\}$ a dense noise sequence (unless explicitly stated otherwise) and $\{f_t\}$ an arbitrary noise sequence.

To define formally the proposed state estimators, let us first introduce the to-be-minimized objective function. Given the matrices $\{(A_t, C_t)\}$ of the system and T output measurements $Y = (\, y_0 \quad \cdots \quad y_{T-1} \,)$, we consider a performance function (or performance index) $V_\Sigma : \mathbb{R}^{m\times T} \times \mathbb{R}^{n\times T} \to \mathbb{R}_{\geq 0}$ defined by

$$V_\Sigma(Y, Z) = \lambda \sum_{t\in\mathbb{T}'} \phi_t(z_{t+1} - A_t z_t) + \sum_{t\in\mathbb{T}} \psi_t(y_t - C_t z_t) \tag{2.1}$$

where $Z = (\, z_0 \quad \cdots \quad z_{T-1} \,) \in \mathbb{R}^{n\times T}$ is a hypothetical state trajectory matrix with z_i denoting the i-th column of Z; $\lambda > 0$ is a user-defined parameter which aims at balancing the contributions of the two terms involved in the expression of the performance index $V_\Sigma(Y, Z)$. $\{\phi_t\}$ and $\{\psi_t\}$ are two families of nonnegative functions (called here loss functions) defined on $\mathbb{R}^n$ and $\mathbb{R}^m$ respectively. For the sake of simplicity, we will assume throughout the paper that for all t in $\mathbb{T}$, ϕ_t and ψ_t can be expressed by

$$\phi_t(z) = \phi(W_t z) \quad \forall z \in \mathbb{R}^n \tag{2.2}$$
$$\psi_t(z) = \psi(V_t z) \quad \forall z \in \mathbb{R}^m, \tag{2.3}$$

where $\phi : \mathbb{R}^n \to \mathbb{R}_{\geq 0}$ and $\psi : \mathbb{R}^m \to \mathbb{R}_{\geq 0}$ are two fixed loss functions and $\{W_t\}$ and $\{V_t\}$ are two families of *nonsingular* weighting matrices with appropriate dimensions.

We then define the class of estimators studied in this chapter:

Definition 2.1. *Given a system Σ such as the one in (1.1) and given an output measurement matrix $Y \in \mathbb{R}^{m\times T}$, we define the studied state estimator to be the set-valued map $\mathcal{E} : \mathbb{R}^{m\times T} \to \mathcal{P}(\mathbb{R}^{n\times T})$ such that*

$$\mathcal{E}(Y) = \operatorname*{arg\,min}_{Z\in\mathbb{R}^{n\times T}} V_\Sigma(Y, Z) \tag{2.4}$$

where V_Σ is a function defined as in (2.1).

Remark 2.1. *With this definition of an estimator, once the loss functions are set, the tuning parameter is λ, and its tuning may not be trivial. An alternative formulation of the solution would be to consider an estimator $\mathcal{E}_\varepsilon$ such that for all Y in $\mathbb{R}^{m\times T}$,*

$$\mathcal{E}_\varepsilon(Y) = \operatorname*{arg\,min}_{Z\in\mathbb{R}^{n\times T}} \sum_{t\in\mathbb{T}} \psi_t(y_t - C_t z_t) \quad \text{subject to} \quad \phi_t(z_{t+1} - A_t z_t) \leq \varepsilon \qquad \forall t \in \mathbb{T}'. \tag{2.5}$$

Now the tuning parameter is the variable ε, given that it dictates how tight the adequacy with the dynamics of the system the returned estimated trajectory needs to be. How to select this value remains difficult, but if we knew the upper bound to the bounded noise sequence $\{w_t\}$, then a very intuitive way would be to select ε equal to this upper bound. However, this value is not accessible in most cases but can sometimes be inferred or approached.

Defined as such, the estimator $\mathcal{E}$ is well-defined if for any fixed Y, $V_\Sigma(Y,Z)$ admits a non empty minimising set, that is, if there exists at least one $Z^\star$ such that $V_\Sigma(Y,Z) \geq V_\Sigma(Y,Z^\star)$ for all $Z \in \mathbb{R}^{n\times T}$. To ensure this property we will need to put an observability assumption on the system whose state is being estimated and require some further properties on the loss functions ϕ and ψ entering in the definition of the objective function V_Σ.

2.2.2 Well-definedness of the estimator: basic properties of the loss functions

Let us start by stating the properties required for the loss functions involved in the definition of V_Σ. Due to the multiple usages that will be made of these properties, it is convenient to state them for a generic loss function defined on a set of matrices (of which vectors constitute a special case). Throughout this chapter, a loss function is a positive function $\xi : \mathbb{R}^{a\times b} \to \mathbb{R}_{\geq 0}$ which will be required to satisfy a subset (depending of the specific usage) of the following properties:

(P2.1) **Positive definiteness:** $\xi(0) = 0$ and $\xi(Z) > 0$ for all $Z \neq 0$

(P2.2) **Continuity:** ξ is continuous

(P2.3) **Symmetry:** $\xi(-Z) = \xi(Z)$ for all $Z \in \mathbb{R}^{a\times b}$

(P2.4) **Generalized Homogeneity (GH):** There exists a $\mathcal{K}_\infty$ function $q : \mathbb{R}_{\geq 0} \to \mathbb{R}_{\geq 0}$ such that for all nonzero $\lambda \in \mathbb{R}$ and for all $Z \in \mathbb{R}^{a\times b}$,

$$\xi(Z) \geq q\left(\frac{1}{|\lambda|}\right)\xi(\lambda Z). \tag{2.6}$$

(P2.5) **Generalized Triangle Inequality (GTI):** There exists a positive real number γ_ξ such that for all Z_1, Z_2 in $\mathbb{R}^{a\times b}$

$$\xi(Z_1 - Z_2) \geq \gamma_\xi \xi(Z_1) - \xi(Z_2). \tag{2.7}$$

It can be usefully observed, for the future developments, that (2.7) can be equivalently written as $\xi(Z_1 + Z_2) \leq \gamma_\xi^{-1}\xi(Z_1) + \gamma_\xi^{-1}\xi(Z_2)$.

Examples of loss functions. Note that norms on $\mathbb{R}^{a\times b}$ satisfy naturally the properties (P2.1)–(P2.5) with $q : \lambda \mapsto \lambda$ and $\gamma_\xi = 1$, hence yielding the classic homogeneity property and triangle inequality. It can also be checked that functions ξ of the form $\xi(Z) = \|Z\|^p$ with $p > 0$, fully qualify as loss functions in the sense that they fulfill all the properties (P2.1)–(P2.5). In this case, γ_ξ in (2.7) can be taken equal to $2^{1-1/p}$ if $0 < p \leq 1$ and 2^{1-p} otherwise. Lastly, we note that if $\ell : \mathbb{R}^{a\times b} \to \mathbb{R}_{\geq 0}$ satisfies (P2.1)–(P2.3) and (P2.5), then so does the function ξ defined by $\xi(Z) = 1 - e^{-\ell(Z)}$ (see Lemma B.4 in the Appendix). Similarly, saturated functions of the form $\xi(Z) = \min(\ell(Z), R_0)$ for some $R_0 > 0$ satisfy (P2.1)–(P2.3) and (P2.5). In the case of convex functions, a link can be established between (P2.4) and (P2.5).

Lemma 2.1. *If $\xi : \mathbb{R}^{a\times b} \to \mathbb{R}_{\geq 0}$ is convex and satisfies property (P2.4) with a $\mathcal{K}_\infty$ function q, then it also satisfies (P2.5) with $\gamma_\xi = 2q(1/2)$.*

Proof. Let Z_1 and Z_2 be given matrices of $\mathbb{R}^{a\times b}$. As ξ is convex, $\xi(\lambda\zeta_1 + (1-\lambda)\zeta_2) \leq \lambda\xi(\zeta_1) + (1-\lambda)\xi(\zeta_2)$ for all λ in $[0,1]$ and ζ_1, ζ_2 in $\mathbb{R}^{a\times b}$. For $\lambda = 1/2$, $\zeta_1 = Z_1 - Z_2$

and $\zeta_2 = Z_2$, this yields

$$\xi\left(\frac{Z_1}{2}\right) \leq \frac{\xi(Z_1 - Z_2) + \xi(Z_2)}{2} \tag{2.8}$$

Moreover, as ξ verifies (P2.4) for $\mathcal{K}_\infty$ function q, then

$$\xi\left(\frac{Z_1}{2}\right) \geq q\left(\frac{1}{2}\right)\xi(Z_1) \tag{2.9}$$

By combining (2.8) and (2.9), we finally obtain

$$\xi(Z_1 - Z_2) \geq 2q\left(\frac{1}{2}\right)\xi(Z_1) - \xi(Z_2) \tag{2.10}$$

This reasoning holds for any Z_1, Z_2 in $\mathbb{R}^{a\times b}$. Therefore, ξ satisfies (P2.5) with $\gamma = 2q(1/2)$. □

Observe that quadratic functions $\xi : \mathbb{R}^{a\times b} \to \mathbb{R}_{\geq 0}$ of the form $\xi(Z) = \mathrm{Tr}(Z^\top Q Z)$ with $Q \in \mathbb{R}^{a\times a}$ being a positive definite matrix and Tr referring to the trace of a matrix, satisfy properties (P2.1)–(P2.4) with a $\mathcal{K}_\infty$ function $q : \lambda \mapsto \lambda^2$. Since such functions are convex, it follows from Lemma 2.1 above that they also verify (P2.5) for $\gamma_\xi = 2q(1/2) = 1/2$.

Remark 2.2. *In virtue of* (2.2)-(2.3)*, the families* $\{\phi_t\}$ *and* $\{\psi_t\}$ *satisfy (P2.1)–(P2.5) if* ϕ *and* ψ *satisfy the same properties.*

We now recall a Lemma from [Kir20b] which will play a fundamental role in analysing the properties of the estimator (2.4). In particular, our proof of well-definedness relies on this lemma.

Lemma 2.2 (Lower Bound of a loss function)**.** *Let* $\xi : \mathbb{R}^{a\times b} \to \mathbb{R}_{\geq 0}$ *be a function which has properties (P2.1)–(P2.2) and (P2.4) with a* $\mathcal{K}_\infty$ *function* q*. Then, for all norm* $\|\cdot\|$ *on* $\mathbb{R}^{a\times b}$*,*

$$\xi(Z) \geq Dq(\|Z\|) \quad \forall Z \in \mathbb{R}^{a\times b} \tag{2.11}$$

where

$$D = \min_{\|Z\|=1} \xi(Z) > 0. \tag{2.12}$$

Proof. We start by observing that the unit hypersphere $\mathcal{S} = \left\{Z \in \mathbb{R}^{a\times b} : \|Z\| = 1\right\}$ is a compact set in the topology induced by the norm $\|\cdot\|$. By the extreme value theorem (see [Rud76, Thm 4.16], ξ being continuous, admits necessarily a minimum value on $\mathcal{S}$, i.e., there is $Z^\star \in \mathcal{S}$ such that $\xi(Z) \geq D \triangleq \xi(Z^\star) > 0$ for all $Z \in \mathcal{S}$. For any nonzero $Z \in \mathbb{R}^{a\times b}$, $\dfrac{Z}{\|Z\|} \in \mathcal{S}$ so that $\xi\left(\frac{Z}{\|Z\|}\right) \geq D$. On the other hand, by the relaxed homogeneity of ξ,

$$\xi(Z) \geq q(\|Z\|)\xi\left(\frac{Z}{\|Z\|}\right) \geq Dq(\|Z\|).$$

Moreover, this inequality holds for $Z = 0$. It therefore holds true for any $Z \in \mathbb{R}^{a\times b}$. □

Proposition 2.1 (Well-definedness of the estimator)**.** *Let the loss functions* ϕ *and* ψ *in* (2.2)-(2.3) *satisfy properties (P2.1)–(P2.5).*

If the LTV system (1.1) is observable on time-horizon $[0, T-1]$ (see Definition 1.2), then the estimator (2.4) is well-defined, i.e., the objective function $V_\Sigma(Y, \cdot)$ attains its minimum for any fixed Y.

Hence the condition of the proposition guarantees that $\mathcal{E}(Y)$ is non empty for all $Y \in \mathbb{R}^{m\times T}$. Before proving this result, we first make the following observation.

Lemma 2.3 (Equivalent condition of Observability)**.** *Consider the objective function V_Σ defined in (2.1) where $\{(\phi_t, \psi_t)\}$ are defined as in (2.2)-(2.3) with ϕ and ψ satisfying (P2.1)–(P2.4). Then the following two statements are equivalent:*

(i) The system is observable on the time-horizon $[0, T-1]$.

(ii) There exists a $\mathcal{K}_\infty$ function q such that for all $Z = \begin{pmatrix} z_0 & z_1 & \cdots & z_{T-1} \end{pmatrix}$ in $\mathbb{R}^{n\times T}$,

$$V_\Sigma(0, Z) \geq q(\|z_0\|) \tag{2.13}$$

Proof. (i) $\Rightarrow$ (ii): Assuming that the system is observable on the interval $[0, T-1]$, we need to prove that there exists a $\mathcal{K}_\infty$ function q which verifies (2.13). The idea of the proof is to apply Lemma B.1 to the function F of $\mathbb{R}^{n\times T}$ defined by $F(Z) = V_\Sigma(0, Z)$ with V_Σ defined as in (2.1). To begin with, we note that F can be decomposed as $F = \xi \circ \ell$ where $\xi : \mathbb{R}^{n\times(T-1)} \times \mathbb{R}^{n\times T} \to \mathbb{R}_{\geq 0}$ is a loss function such that for $Z = \begin{pmatrix} z_0 & \cdots & z_{T-2} \end{pmatrix}$ in $\mathbb{R}^{n\times(T-1)}$, $Y = \begin{pmatrix} y_0 & \cdots & y_{T-1} \end{pmatrix}$ in $\mathbb{R}^{n_y\times T}$,

$$\xi(Z, Y) = \sum_{t=0}^{T-2} \phi_t(z_t) + \sum_{t=0}^{T-1} \psi_t(y_t)$$

and $\ell : \mathbb{R}^{n\times T} \to \mathbb{R}^{n\times(T-1)} \times \mathbb{R}^{n\times T}$ a linear mapping such that for all $Z = \begin{pmatrix} z_0 & \cdots & z_{T-1} \end{pmatrix}$ in $\mathbb{R}^{n\times T}$,

$$\ell(Z) = \Big(\begin{pmatrix} z_1 - A_0 z_0 & \cdots & z_{T-1} - A_{T-2} z_{T-2} \end{pmatrix}, \begin{pmatrix} C_0 z_0 & \cdots & C_{T-1} z_{T-1} \end{pmatrix} \Big). \tag{2.14}$$

To apply Lemma B.1 to F, we need to check that F fulfills the properties (P2.1)–(P2.3). In virtue of the assumptions on ϕ_t and ψ_t agreed in the statement of the lemma, the first two properties are obviously satisfied. The third will be satisfied if ℓ is injective, a propriety which we now check. Let Z be such that $\ell(Z) = 0$. Then

$$\forall t \in \{0, \ldots, T-2\}, \qquad z_{t+1} - A_t z_t = 0 \tag{2.15}$$

$$\forall t \in \{0, \ldots, T-1\}, \qquad C_t z_t = 0 \tag{2.16}$$

An immediate consequence of (2.15)–(2.16) is that $\mathcal{O}_{0,T-1} z_0 = 0$ which yields $z_0 = 0$ because the system is observable on $[0, T-1]$. Therefore, thanks to the recursive relation (2.15), we can conclude that $Z = 0$, and so, the linear mapping ℓ is injective. We can therefore apply Lemma B.1 to conclude that F satisfy indeed (P2.1)–(P2.4). Now, consider a matrix norm $\|\cdot\|_{\text{ind}}$ on $\mathbb{R}^{n\times T}$ induced by two vector norms $\|\cdot\|_T$ and $\|\cdot\|$ defined respectively on $\mathbb{R}^T$ and $\mathbb{R}^n$ in the sense that

$$\|Z\|_{\text{ind}} = \sup_{\substack{\eta\in\mathbb{R}^T \\ \eta\neq 0}} \frac{\|Z\eta\|}{\|\eta\|_T}$$

Applying Lemma 2.2 to F with the so-defined induced norm, we infer that there exists $D > 0$ defined as in (2.12) and a $\mathcal{K}_\infty$ function q', such that for all Z in $\mathbb{R}^{n\times T}$,

$$F(Z) \geq D q'(\|Z\|_{\text{ind}}) \tag{2.17}$$

If we denote with e_1 the canonical vector of $\mathbb{R}^T$ with all entries equal to zero except the first one which is equal to 1, then $Ze_1 = z_0$. However, by definition of the induced norm, we know that $\|Ze_1\|/\|e_1\|_T \leq \|Z\|_{\text{ind}}$. Therefore, as q' is an increasing function, we get that $q'(\|z_0\|/\|e_1\|_T) \leq q'(\|Z\|_{\text{ind}})$. By posing $q : \lambda \mapsto Dq'(\lambda/\|e_1\|_T)$, it is easy to see that q is a $\mathcal{K}_\infty$ function so that for all Z in $\mathbb{R}^{n\times T}$, $V(0, Z) = F(Z) \geq q(\|z_0\|)$. (ii) $\Rightarrow$ (i): Assume that there exists q in $\mathcal{K}_\infty$ such that for all $Z = \begin{pmatrix} z_0 & z_1 & z_{T-1} \end{pmatrix}$ in $\mathbb{R}^{n\times T}$ such that (2.13) holds. We want to prove that the matrix $\mathcal{O}_{T-1}$ defined in (1.7) is of full column rank, which is equivalent to showing that for z in $\mathbb{R}^n$, $\mathcal{O}_{0,T-1}z = 0$ implies $z = 0$. For all $z \in \mathbb{R}^n$, construct a sequence $Z^* = \begin{pmatrix} z_0^* & \cdots & z_{T-1}^* \end{pmatrix}$ as follows: $z_0^* = z$ and $z_{t+1}^* = A_t z_t^*$ for all $t \in \{0, \dots, T-2\}$. Since the inequality (2.13) is supposed to be true for any sequence, so it is for the particular sequence $\{z_t^*\}$ defined above. Applying this inequality to Z^* yields

$$V(0, Z^*) = \sum_{t=0}^{T-1} \psi_t(C_t z_t^*) \geq q(\|z_0^*\|) \tag{2.18}$$

Now, observe that if $\mathcal{O}_{0,T-1}z = 0$, then it follows from the recursive relation $z_{t+1}^* = A_t z_t^*$ that for all t in $\{0, \dots, T-1\}$, $C_t z_t^* = 0$. Injecting this in (2.18) imposes that $q(\|z_0^*\|) \leq 0$ which necessarily implies that $z = 0$ as q is a $\mathcal{K}_\infty$ function. Therefore, the matrix $\mathcal{O}_{0,T-1}$ is injective and the system is observable on the interval $[0, T-1]$. □

The function q can be interpreted here as a gain function which measures how much the system is observable with regards to the two families $\{\phi_t\}$ and $\{\psi_t\}$: the more the system is observable, the more q amplifies its argument magnitude, making different trajectories more discernible.

Proof of Proposition 2.1: The idea of the proof is to show that $V_\Sigma(Y, \cdot)$ is *coercive* (*i.e.* continuous and radially unbounded) for any given Y and then apply a result[1] in [Roc98, Thm 1.9] to conclude on the attainability of the infimum (which certainly exists since $V_\Sigma(Y, \cdot)$ is a positive function). Clearly, $V_\Sigma(Y, \cdot)$ is continuous as a consequence of ϕ and ψ being continuous by assumption (see property (P2.2)). We then just need to prove the radial unboundedness of $V_\Sigma(Y, \cdot)$, *i.e.*, $\lim_{\|Z\|\to+\infty} V_\Sigma(Y, Z) = +\infty$ for an arbitrary norm $\|\cdot\|$ on the Z-space and for all fixed Y. Since ψ satisfies property (P2.5), there exists a constant $\gamma_\psi > 0$ such that $\psi_t(y_t - C_t z_t) \geq \gamma_\psi \psi_t(C_t z_t) - \psi_t(y_t)$. Applying this property leads naturally to

$$V_\Sigma(Y, Z) \geq F(Z) - \sum_{t\in\mathbb{T}} \psi_t(y_t),$$

where

$$F(Z) = \lambda \sum_{t\in\mathbb{T}'} \phi_t(z_{t+1} - A_t z_t) + \gamma_\psi \sum_{t\in\mathbb{T}} \psi_t(C_t z_t). \tag{2.19}$$

It can then be shown (following a similar reasoning as in the proof of Lemma 2.3), under the observability assumption, that F satisfies the conditions of Lemma 2.2. It follows that for any norm $\|\cdot\|$ on $\mathbb{R}^{n\times T}$, there exists a $\mathcal{K}_\infty$ function q such that

$$F(Z) \geq q(\|Z\|).$$

[1] Note that radial unboundedness is equivalent to level-boundedness in the terminology of [Roc98].

Combining this with the inequality above, we obtain that

$$V_\Sigma(Y,Z) \geq q(\|Z\|) - \sum_{t\in\mathbb{T}} \psi_t(y_t)$$

which implies the radial unboundedness of $V_\Sigma(Y,\cdot)$ for any fixed Y. Hence the estimator (2.4) is well-defined as stated. □

As it turns out from Proposition 2.1, observability of system (1.1) and properties (P2.1)–(P2.4) imposed on ϕ and ψ ensure that $\mathcal{E}(Y)$ is a non empty set for any given Y. We then call any member $\hat{X} = (\,\hat{x}_0 \quad \hat{x}_1 \quad \dots \quad \hat{x}_{T-1}\,)$ of $\mathcal{E}(Y)$, an estimate of the state trajectory of system (1.1) on the time interval $\mathbb{T}$. In particular, $\hat{x}_t$ is called an estimate of the state x_t at time $t \in \mathbb{T}$.

To conclude this section, note that the definition of the estimator in (2.4) does not require any convexity assumption on the objective function V_Σ. Hence the theoretical analysis to be presented in the next sections does not make use of convexity either. However, we may prefer in practice to select convex loss functions ϕ and ψ. In effect, the elements of $\mathcal{E}(Y)$ are not necessarily expressible through an explicit formula. So, in practice one would resort instead to numerical solvers to approach the solution of the underlying optimization problem. And the numerical search process is more efficient when $V_\Sigma(Y,Z)$ is a convex function of Z [Boy04; Gra18].

2.3 The resilience property of the proposed class of estimators

In this section, we prove that the state estimator proposed in (2.4) possesses the resilience property under some conditions.

2.3.1 Definition of the resilience of an estimator

Let us start with a formal definition of the resilience property for a state estimator of the form (2.4). For this purpose, let

$$Y^\star = (\,y_0^\star \quad \dots \quad y_{T-1}^\star\,) \tag{2.20}$$

denote the noise-free output matrix of (1.1), i.e., the output defined by $y_t^\star = C_t x_t^\star$, $t \in \mathbb{T}$, with $x_{t+1}^\star = A_t x_t^\star$ and $x_0^\star = x_0$ (x_0 being the true initial state of (1.1)). Let $\mathcal{F}_r$, a subset of $\mathbb{R}^{m\times T}$ containing 0, denote a set of measurement noise components.

Definition 2.2 (Resilience of an estimator)**.** *The set-valued estimator $\mathcal{E}$ defined in (2.4) is called resilient against the set $\mathcal{F}_r$ of measurement noise if there exists a $\mathcal{K}_\infty$ function g such that, when the process noise $\{w_t\}$ is zero, it holds that for any measurement noise matrix $F \in \mathbb{R}^{n_y\times T}$,*

$$\|\hat{X} - X\| \leq g\big(\inf_{\Omega\in\mathcal{F}_r} d(F-\Omega)\big) \quad \forall \hat{X} \in \mathcal{E}(Y^\star + F) \tag{2.21}$$

with $\|\cdot\|$ denoting some norm, $Y^\star$ as defined in (2.20) and $d : \mathbb{R}^{m\times T} \to \mathbb{R}_{\geq 0}$ being a function subject to (P2.1)-(P2.5). Hence $\inf_{\Omega\in\mathcal{F}_r} d(F-\Omega)$ denotes some pseudo-distance from F to the set $\mathcal{F}_r$.

Since $0 \in \mathcal{F}_r$, a consequence of property (2.21) is that $\mathcal{E}(Y^\star) = \{X\}$, which follows from (2.21) for $F = 0$. This fact expresses correctness of the estimator in a nominal situation, i.e., its ability to recover the true state matrix X in the absence of any

uncertainty in the a priori known model. Indeed this condition is guaranteed to hold if the system Σ is observable over the considered observation time horizon T. Another key implication of condition (2.21) is that the estimation error associated with a resilient estimator is totally insensitive to any measurement noise matrix F which lies in $\mathcal{F}_r$, that is, $\mathcal{E}(Y^\star + F) = \{X\}$ for all measurement noise $F \in \mathcal{F}_r$. Throughout this paper, we consider a set $\mathcal{F}_r$ defined as follows. For $F = (\, f_0 \quad \cdots \quad f_{T-1}\,) \in \mathbb{R}^{m\times T}$, let $\mathbb{T}_0^c(F) = \{t \in \mathbb{T} : \psi_t(f_t) > 0\}$ and $\mathbb{T}_0(F) = \{t \in \mathbb{T} : \psi_t(f_t) = 0\}$. For r a positive integer, define $\mathcal{F}_r$ to be the set of matrices in $\mathbb{R}^{m\times T}$ having at most r nonzero columns, i.e.,

$$\mathcal{F}_r = \{F : |\mathbb{T}_0^c(F)| \leq r\}\,. \tag{2.22}$$

For the need of making explicit the resilience property (in the results to be presented) with respect to the set $\mathcal{F}_r$, we will need the following lemma.

Lemma 2.4. *Consider the set $\mathcal{F}_r$ of measurement noise matrix defined in (2.22) and select a (pseudo distance) function $d : \mathbb{R}^{m\times T} \to \mathbb{R}_{\geq 0}$ defined by $d(F) = \sum_{t\in\mathbb{T}} \psi_t(f_t)$ with ψ_t a function defined as in (2.3) and having the properties (P2.1)-(P2.5). Then $\inf_{\Omega\in\mathcal{F}_r} d(F-\Omega)$ is equal to the sum of the $T-r$ smallest terms in $\{\psi_t(f_t) : t \in \mathbb{T}\}$.*

Proof. Let $I_r^c(F)$ denote the index set of the r largest entries of the vector

$$\Big(\psi_0(f_0) \quad \ldots \quad \psi_{T-1}(f_{T-1})\Big)$$

and $I_r(F)$ denote the index set of its $T-r$ smallest entries. Then, with the notation $\Omega = (\,\omega_0 \quad \cdots \quad \omega_{T-1}\,)$,

$$\begin{aligned}
\inf_{\Omega\in\mathcal{F}_r} d(F-\Omega) &= \inf_{\Omega\in\mathcal{F}_r} \sum_{t\in\mathbb{T}} \psi_t(\omega_t - f_t) \\
&= \inf_{\Omega\in\mathcal{F}_r} \Big[\sum_{t\in I_r(F)} \psi_t(\omega_t - f_t) + \sum_{t\in I_r^c(F)} \psi_t(\omega_t - f_t) \Big] \\
&= \inf_{\substack{\Omega\in\mathcal{F}_r \\ \mathbb{T}_0(\Omega)=I_r(F)}} \Big[\sum_{t\in I_r(F)} \psi_t(f_t) + \sum_{t\in I_r^c(F)} \psi_t(\omega_t - f_t) \Big] \\
&= \sum_{t\in I_r(F)} \psi_t(f_t)
\end{aligned}$$

where the notation $\mathbb{T}_0(\Omega)$ is defined in the lines preceding Eq. (2.22). The infimum is reached here for $\Omega \in \mathcal{F}_r$ such that $\omega_t = 0\ \forall t \in I_r(F)$ and $\omega_t = f_t\ \forall t \in I_r^c(F)$. Hence $\inf_{\Omega\in\mathcal{F}_r} d(F-\Omega)$ is, as claimed, the sum of the $T-r$ smallest values among $\{\psi_t(f_t) : t \in \mathbb{T}\}$. □

We will also introduce in the sequel a notion of *approximate resilience* of $\mathcal{E}$. This terminology refers to Definition 2.2 when the right hand side of (2.21) is modified as $g\big(\inf_{\Omega\in\mathcal{F}_r} d(F-\Omega) + \delta\big)$ with δ some nonnegative real number.

More specifically, our main result states that the estimation error, *i.e.* the difference between the real state trajectory and the estimated one, is upper bounded by a bound which does not depend on the amplitude of the outliers contained in $\{f_t\}$ provided that the number of such outliers is below some threshold.

2.3.2 Some notational conventions for the analysis

For convenience, let us introduce a few more notations. Let $\Phi : \mathbb{R}^{n\times T} \to \mathbb{R}_{\geq 0}$ and $\Psi_{\mathbb{T}} : \mathbb{R}^{n\times T} \to \mathbb{R}_{\geq 0}$ be defined by

$$\Phi(Z) = \sum_{t\in\mathbb{T}'} \phi_t(z_{t+1} - A_t z_t) \tag{2.23}$$

$$\Psi_{\mathbb{T}}(Z) = \sum_{t\in\mathbb{T}} \psi_t(C_t z_t) \tag{2.24}$$

We also introduce the partial cost function $\Psi_{\mathcal{T}}$ defined for any $\mathcal{T} \subset \mathbb{T}$ by $\Psi_{\mathcal{T}}(Z) = \sum_{t\in\mathcal{T}} \psi_t(C_t z_t)$. We will assume throughout the paper that the loss functions ϕ and ψ satisfy a subset of the properties (P2.1)–(P2.5) and in particular, when they are required to satisfy the GTI (P2.5), we will denote the associated positive constants with γ_ϕ and γ_ψ respectively. Finally, let us pose

$$H_\Sigma(Z) = \lambda\gamma_\phi \Phi(Z) + \gamma_\psi \Psi_{\mathbb{T}}(Z). \tag{2.25}$$

We will now organize the resilience analysis for the estimator (2.4) along two cases. In the first one, it will be assumed to be block-sparse in time, while in the second one, the arbitrary noise sequence will be assumed to be sparse both temporally and componentwise. Indeed, it was explained in Section 1.4.2 that if you concatenate each value of the sparse component of $\{f_t\}$ through time, the resulting matrix could be sparse along his rows and/or its columns. The loss functions involved in the performance function V_Σ can be chosen in order to reflect this assumption, which leads to the consideration of those two cases. It can be noted that the two cases coincide when the system of interest is single-input single-output (SISO).

For further discussions, a third case dealing with an additional arbitrary noise sequence disturbing the dynamic equation of the system will be presented in Appendix B.4. We will develop the case where this noise as well as the arbitrary one disturbing the measurement equation are assumed to be both componentwise and temporally sparse, even though it would be possible to apply a similar framework as the one used in the first case onto this third case.

2.3.3 Resilience to intermittent timewise block-sparse errors

We start by introducing the concept of r-Resilience index of an estimator such as the one in (2.4), a measure which depends of the system matrices, the structure of the performance function V_Σ and on the loss functions ϕ and ψ.

Definition 2.3. *Let r be a nonnegative integer. Assume that the system Σ in (1.1) is observable on $[0, T-1]$. We then define the r-Resilience index of the estimator $\mathcal{E}$ in (2.4) (when applied to Σ) to be the real number p_r given by*

$$p_r = \sup_{\substack{Z\in\mathbb{R}^{n\times T}\\ Z\neq 0}} \sup_{\substack{\mathcal{T}\subset\mathbb{T}\\ |\mathcal{T}|=r}} \frac{\Psi_{\mathcal{T}}(Z)}{H_\Sigma(Z)} \tag{2.26}$$

where H_Σ is as defined in (2.25). The supremum is taken here over all nonzero Z in $\mathbb{R}^{n\times T}$ and over all subsets $\mathcal{T}$ of $\mathbb{T}$ with cardinality equal to r.

The index p_r can be interpreted as a quantitative measure of the observability of the system Σ. The observability is needed here to ensure that the denominator $H_\Sigma(Z)$ of (2.26) is different from zero whenever $Z \neq 0$. Furthermore, it should be

remarked that $\Psi_{\mathcal{T}}(Z) \leq H_\Sigma(Z)$ for any $\mathcal{T} \subset \mathbb{T}$, which implies that the defining suprema of p_r are well-defined. Note that p_r is an non-decreasing function of r and satisfies $p_0 = 0$ and $p_T = 1$. More discussions on the numerical evaluation of p_r are deferred to Section 2.5.

In order to state the resilience result for the estimator (2.4) when applied to system Σ, let us introduce a last notation to be used in the analysis. Let $\varepsilon \geq 0$ be a given number. For any admissible sequence $\{f_t\}_{t\in\mathbb{T}}$ in (1.1), we can split the time index set $\mathbb{T}$ into two disjoint label sets,

$$\mathbb{T}_\varepsilon = \{t \in \mathbb{T} : \psi_t(f_t) \leq \varepsilon\}, \tag{2.27}$$

indexing those f_t which are upper bounded by ε and $\mathbb{T}_\varepsilon^c = \{t \in \mathbb{T} : \psi_t(f_t) > \varepsilon\}$ indexing those f_t which are possibly unbounded. It is important to keep in mind that ε is just a parameter for decomposing the noise sequence in two parts in view of the analysis (and not necessarily a bound on elements of the sequence $\{\psi(f_t)\}$). For example, taking $\varepsilon = 0$ would be appropriate for analysing the properties of the estimator when f_t is strictly sparse and each of its nonzero elements is treated as an outlier.

Theorem 2.1 (Upper bound on the estimation error)**.** *Consider the system Σ defined by (1.1) with output Y together with the state estimator (2.4) in which the loss functions ϕ and ψ are assumed to obey (P2.1)–(P2.5). Denote with γ_ϕ and γ_ψ the constants associated with the GTI (P2.5) and q_ϕ and q_ψ the $\mathcal{K}_\infty$ functions associated with the GH (P2.4) for ϕ and ψ respectively. Let $\varepsilon \geq 0$ and set $r = |\mathbb{T}_\varepsilon^c|$.*
If the system is observable on $[0, T-1]$ and $p_r < 1/(1+\gamma_\psi)$, then for any norm $\|\cdot\|$ on $\mathbb{R}^{n\times T}$,

$$\|\hat{X} - X\| \leq h\left(\frac{2\beta_\Sigma(\varepsilon)}{D[1-(1+\gamma_\psi)p_r]} + \delta(\varepsilon)\right) \quad \forall \hat{X} \in \mathcal{E}(Y) \tag{2.28}$$

with X denoting the true state matrix from (1.1), $D = \min_{\|Z\|=1} H_\Sigma(Z) > 0$ and $\beta_\Sigma(\varepsilon)$, $\delta(\varepsilon)$ and h being defined by

$$\beta_\Sigma(\varepsilon) = \lambda \sum_{t\in\mathbb{T}'} \phi_t(w_t) + \sum_{t\in\mathbb{T}_\varepsilon} \psi_t(f_t), \tag{2.29}$$

$$\delta(\varepsilon) = \frac{1-\gamma_\psi}{D[1-(1+\gamma_\psi)p_r]} \sum_{t\in\mathbb{T}_\varepsilon^c} \psi_t(f_t) \tag{2.30}$$

$$h(\alpha) = \max\left\{q_\phi^{-1}(\alpha), q_\psi^{-1}(\alpha)\right\}, \alpha \in \mathbb{R}_{\geq 0} \tag{2.31}$$

Proof. Let $\hat{X}$ in $\mathcal{E}(Y)$. By definition of $\mathcal{E}$ in (2.4), we have $V_\Sigma(Y, \hat{X}) \leq V_\Sigma(Y, X)$, which gives explicitly

$$\lambda \sum_{t\in\mathbb{T}'} \phi_t(\hat{x}_{t+1} - A_t\hat{x}_t) + \sum_{t\in\mathbb{T}} \psi_t(y_t - C_t\hat{x}_t) \leq \lambda \sum_{t\in\mathbb{T}'} \phi_t(w_t) + \sum_{t\in\mathbb{T}} \psi_t(f_t) \tag{2.32}$$

Using the fact that $x_{t+1} = A_t x_t + w_t$ from (1.1) and applying the GTI and the symmetry properties of ϕ_t, we can write

$$\begin{aligned}\phi_t(\hat{x}_{t+1} - A_t\hat{x}_t) &= \phi_t(\hat{x}_{t+1} - x_{t+1} - A_t(\hat{x}_t - x_t) + w_t) \\ &\geq \gamma_\phi \phi_t(e_{t+1} - A_t e_t) - \phi_t(w_t)\end{aligned}$$

with $e_t = \hat{x}_t - x_t$. It follows that the first term on the left hand side of (2.32) is lower bounded as follows

$$\lambda \sum_{t\in\mathbb{T}'} [\gamma_\phi \phi_t(e_{t+1} - A_t e_t) - \phi_t(w_t)] \leq \lambda \sum_{t\in\mathbb{T}'} \phi_t(\hat{x}_{t+1} - A_t \hat{x}_t). \tag{2.33}$$

Similarly, by making use of (1.1), observe that $\psi_t(y_t - C_t\hat{x}_t) = \psi_t(f_t - C_t e_t)$. We now apply the GTI and symmetry of ψ_t in two different ways depending on whether t belongs to $\mathbb{T}_\varepsilon$ or $\mathbb{T}_\varepsilon^c$:

$$\begin{aligned} &\forall t \in \mathbb{T}_\varepsilon, && \psi_t(y_t - C_t\hat{x}_t) \geq \gamma_\psi \psi_t(C_t e_t) - \psi_t(f_t) \\ &\forall t \in \mathbb{T}_\varepsilon^c, && \psi_t(y_t - C_t\hat{x}_t) \geq \gamma_\psi \psi_t(f_t) - \psi_t(C_t e_t) \end{aligned}$$

These inequalities imply that the second term on the left hand side of (2.32) is lower bounded as follows

$$\sum_{t\in\mathbb{T}_\varepsilon} [\gamma_\psi \psi_t(C_t e_t) - \psi_t(f_t)] + \sum_{t\in\mathbb{T}_\varepsilon^c} [\gamma_\psi \psi_t(f_t) - \psi_t(C_t e_t)] \leq \sum_{t\in\mathbb{T}} \psi_t(y_t - C_t\hat{x}_t) \tag{2.34}$$

Combining (2.32), (2.33) and (2.34) gives

$$\begin{aligned} \lambda\gamma_\phi \sum_{t\in\mathbb{T}'} \phi_t(e_{t+1} - A_t e_t) + \gamma_\psi \sum_{t\in\mathbb{T}} \psi_t(C_t e_t) - (1+\gamma_\psi) \sum_{t\in\mathbb{T}_\varepsilon^c} \psi_t(C_t e_t) \\ \leq 2\Big(\lambda \sum_{t\in\mathbb{T}'} \phi_t(w_t) + \sum_{t\in\mathbb{T}_\varepsilon} \psi_t(f_t)\Big) + \sum_{t\in\mathbb{T}_\varepsilon^c} (1-\gamma_\psi)\psi_t(f_t) \end{aligned} \tag{2.35}$$

which, by using (2.24), (2.25), (2.29), can be written as

$$H_\Sigma(E) - (1+\gamma_\psi)\Psi_{\mathbb{T}_\varepsilon^c}(E) \leq 2\beta_\Sigma(\varepsilon) + \sum_{t\in\mathbb{T}_\varepsilon^c} (1-\gamma_\psi)\psi_t(f_t)$$

with $E = \begin{pmatrix} e_0 & e_1 & \cdots & e_{T-1} \end{pmatrix}$. As $\mathbb{T}_\varepsilon^c$ has r elements, applying the definition of p_r gives

$$\Psi_{\mathbb{T}_\varepsilon^c}(E) \leq p_r H_\Sigma(E) \tag{2.36}$$

By the assumption that $p_r < 1/(1+\gamma_\psi)$ we have that $1 - (1+\gamma_\psi)p_r > 0$, and consequently, that

$$H_\Sigma(E) \leq \frac{1}{1-(1+\gamma_\psi)p_r} \Big[2\beta_\Sigma(\varepsilon) + (1-\gamma_\psi) \sum_{t\in\mathbb{T}_\varepsilon^c} \psi_t(f_t)\Big] \tag{2.37}$$

Given that the system is observable on $[0, T-1]$, it can be shown, thanks to Lemma B.1 in the Appendix, that H_Σ satisfies properties (P2.1)–(P2.4) (the proof of this is quite similar that of Lemma 2.3). We can therefore apply Lemma 2.2 to conclude that for any norm $\|\cdot\|$, there exists a $\mathcal{K}_\infty$ function q' such that

$$H_\Sigma(E) \geq D q'(\|E\|) \tag{2.38}$$

with D defined by $D = \min_{\|Z\|=1} H_\Sigma(Z)$. Finally, the result follows by selecting h to be $h = q'^{-1}$ with q'^{-1} denoting the inverse of q', which can be simplified to match its definition in (2.31) through Lemma B.3 presented in Appendix B.2. □

Strict resilience. Now we state our (strict) resilience result as a consequence of Theorem 2.1 when the output error-measuring loss function ψ satisfies the triangle

inequality.

Corollary 2.1.1 (Resilience property)**.** *Let the conditions of Theorem 2.1 hold with the additional requirement that* $\gamma_\psi = 1$*. Then*

$$\|\hat{X} - X\| \leq h\Big(\frac{2\beta_\Sigma(\varepsilon)}{D(1-2p_r)}\Big) \quad \forall \hat{X} \in \mathcal{E}(Y). \tag{2.39}$$

Proof. The proof is immediate by considering the bound in (2.28) and observing that $\delta(\varepsilon)$ expressed in (2.30) vanishes when $\gamma_\psi = 1$, hence eliminating completely the contribution of the extreme values of $\{f_t\}$ to the error bound. This gives immediately (2.39). It remains now to make clear that (2.39) is consistent with the requirement (2.21) of Definition 2.2. For this purpose note that the bound in (2.39) can be written as $g(\beta_\Sigma(\varepsilon))$ with $g \in \mathcal{K}_\infty$ defined by $g(\alpha) = h(2\alpha/(D(1-2p_r)))$. Moreover, $\beta_\Sigma(\varepsilon)$ reduces to $\sum_{t\in\mathbb{T}_\varepsilon} \psi_t(f_t) = \inf_{\Omega\in\mathcal{F}_r} d(F-\Omega)$ when the process noise is zero (see (2.29) and Lemma 2.4). Hence, $\mathcal{E}$ qualifies, in the sense of Definition 2.2, as an estimator which is resilient to the set $\mathcal{F}_r$ of measurement noise defined in (2.22). □

The resilience property of the estimator (2.4) lies here in the fact that, under the conditions of Theorem 2.1 and Corollary 2.1.1, the bound in (2.39) on the estimation error does not depend on the magnitudes of the extreme values of the noise sequence $\{f_t\}_{t\in\mathbb{T}}$. Considering in particular the function $\beta_\Sigma(\varepsilon)$, we remark that it can be overestimated as follows

$$\beta_\Sigma(\varepsilon) \leq \lambda \sum_{t\in\mathbb{T}'} \phi_t(w_t) + |\mathbb{T}_\varepsilon|\varepsilon. \tag{2.40}$$

The first term on the left hand side of (2.40) represents the uncertainty brought by $\{w_t\}$ over the whole state trajectory. It is bounded since $\{w_t\}$ is bounded by assumption (see the description of the system at the beginning of Section 2.2.1). The second term is a bound on the sum of those instances of f_t whose magnitude is smaller that ε.

Because β_Σ is a function of ε, the bound in (2.39) represents indeed a family of bounds parameterised by ε. Since ε is a mere analysis device, a question would be how to select it for the analysis to achieve the smallest bound. Such favorable values, say $\varepsilon^\star$, satisfy

$$\varepsilon^\star \in \arg\min_{\varepsilon\geq 0} \left\{ h\Big(\frac{2\beta_\Sigma(\varepsilon)}{D(1-2p_r)}\Big) : r = |\mathbb{T}_\varepsilon^c|,\ p_r < 1/2 \right\}.$$

Another interesting point is that the inequality stated by Theorem 2.1 holds for any norm $\|\cdot\|$ on $\mathbb{R}^{n\times T}$. Note though that the value of the bound depends (through the parameter D) on the specific norm used to measure the estimation error. Moreover, different choices of the performance-measuring norm will result in different geometric forms for the uncertain set, that is, the ball (in the chosen norm) centred at the true state with radius equal to the upper bound displayed in (2.39).

We also observe that the smaller the parameter p_r is, the tighter the error bound will be, which suggests that the estimator is more resilient when p_r is lower. A similar reasoning applies to the number D which is desired to be large here. These two parameters (i.e., p_r and D) reflect properties of the system whose state is being estimated. They can be interpreted, to some extent, as measures of the degree of observability of the system. In conclusion, the estimator inherits partially its resilience property from characteristics of the system being observed. This is consistent with the well-known fact that the more observable a system is, the more robustly its state can be estimated from output measurements.

It can be noted that the condition $p_r < 1/2$ sets for a theoretical maximum number of corrupted measures r that system Σ can handle according to Theorem 2.1: as a result, we will defined $r_{\max}$ this maximum number of corrupted measures such that

$$r_{\max} = \max_{r \in \mathbb{N}} r \quad \text{subject to} \quad p_r < \frac{1}{2} \tag{2.41}$$

Approximate resilience. As discussed above, the triangle inequality property of the loss function ψ is fundamental for achieving strict resilience. When ψ does not satisfy this property (i.e., when $\gamma_\psi \neq 1$), the term $\delta(\varepsilon)$ in (2.28) is unlikely to vanish completely. However we can prevent it from growing excessively by an appropriate choice of ψ in (2.3). To see this, assume for example that ψ is defined by $\psi(y) = 1 - e^{-\ell(y)}$. Then since $\psi(y) \leq 1$ for all y, $\delta(\varepsilon)$ saturates to a constant value regardless of how large the f_t are for $t \in \mathbb{T}_\varepsilon^c$. On the other hand, this choice introduces a new technical challenge related to the fact that the function q' in (2.38) is no longer a $\mathcal{K}_\infty$ function but a bounded (saturated) function. Handling this situation will require some additional condition on the upper bound in (2.37). To sum up, by selecting a saturated loss function for ψ, we obtain the following *approximate resilience* result.

Corollary 2.1.2 (Case where $\gamma_\psi \neq 1$)**.** *Let the conditions of Theorem 2.1 hold. Assume further that the loss function ψ in (2.3) is defined by $\psi(y) = 1 - e^{-\ell(y)}$ where $\ell : \mathbb{R}^m \to \mathbb{R}_{\geq 0}$ satisfies (P2.1)–(P2.5). In particular, assume that property (P2.4) is satisfied by ℓ with a $\mathcal{K}_\infty$ function q such that (2.6) is an equality relation. Also, let $\varepsilon \geq 0$ be such that*

$$b(\varepsilon) \triangleq \frac{2\beta_\Sigma(\varepsilon) + r(1-\gamma_\psi) r^o(\varepsilon)}{D\,[1 - (1+\gamma_\psi)p_r]} < 1, \tag{2.42}$$

where $r = r(\varepsilon) = |\mathbb{T}_\varepsilon^c|$ and $r^o(\varepsilon) = \max_{t \in \mathbb{T}_\varepsilon^c} \psi_t(f_t) \leq 1$. Then there exists a continuous and strictly increasing function $h_{\text{sat}} : [0,1] \to [0,1]$ (obeying $h_{\text{sat}}(0) = 0$ and $h_{\text{sat}}(1) = 1$) such that for any norm $\|\cdot\|$ on $\mathbb{R}^{n \times T}$,

$$\|\hat{X} - X\| \leq h_{\text{sat}}^{-1}(b(\varepsilon)) \quad \forall \hat{X} \in \mathcal{E}(Y). \tag{2.43}$$

with D in (2.42) defined as in the proof of Theorem 2.1 using the norm $\|\cdot\|$.

Proof. That the particular function ψ specified in the statement of the corollary satisfies the properties (P2.1)–(P2.3) and (P2.5) is a question which is fully answered by Lemma B.4 in Section B.3 of the appendix. Consequently, let us observe that the inequality (2.37) arising in the proof of Theorem 2.1 still holds true here. As to (2.38), it also holds as well but with the slight difference that q' is just a saturated function in $\mathcal{K}_{\text{sat},1}$ (as defined in the notation section) with bounded range $[0,1]$. This results in fact from Lemma B.4 and the proof of Lemma 2.2. We can therefore write

$$\begin{aligned} q'(\|E\|) &\leq \frac{1}{D\,(1-(1+\gamma_\psi)p_r)} \Big[2\beta_\Sigma(\varepsilon) + (1-\gamma_\psi) \sum_{t \in \mathbb{T}_\varepsilon^c} \psi_t(f_t) \Big] \\ &\leq b(\varepsilon) < 1 \end{aligned}$$

with $q' \in \mathcal{K}_{\text{sat},1}$. Note from the definition of the class $\mathcal{K}_{\text{sat},1}$, that $q'(\|E\|) < 1$ implies that $\|E\| < 1$ (since otherwise we would have $q'(\|E\|) = 1$). Letting h_{sat} be the restriction of such a function q' on $[0,1]$, we have $q'(\|E\|) = h_{\text{sat}}(\|E\|) \leq b(\varepsilon)$ with h_{sat} being invertible. We can now apply h_{sat}^{-1} to each member of this inequality to reach the desired result since $b(\varepsilon)$ lies in the range of h_{sat}. □

2.3.4 Resilience to attacks on the individual sensors

We now consider the situation where the matrix $S \in \mathbb{R}^{m\times T}$ formed from $\{s_t\}$ in (1.49) may be sparse componentwise. This case is relevant when any individual sensor may be faulty (or compromised by an attacker) at any time. To address the resilient state estimation problem in this scenario, we select the loss functions ψ_t to have a separable structure. To be more specific, let ψ_t be such that for any $z \in \mathbb{R}^m$

$$\psi_t(e) = \sum_{j\in\mathbb{J}} \psi_{t,j}(z[j]) \tag{2.44}$$

where, consistently with (2.3), $\psi_{t,j}(z[j]) = \psi_j^\circ(V_{t,j}z[j])$ with $V_{t,j} \in \mathbb{R}_{>0}$ and $\psi_j^\circ : \mathbb{R} \to \mathbb{R}_{\geq 0}$, $j = 1, \ldots, m$, being some loss functions on $\mathbb{R}$ enjoying the properties (P2.1)–(P2.5). As in the statement of Corollary 2.1.1, we shall require that $\gamma_{\psi_{t,j}^\circ} = 1$. It follows that one can set ψ_j° to be the absolute value without loss of generality. Let therefore set $\psi_j^\circ(z[j]) = |z[j]|$ so that $\psi_{t,j}(z[j]) = |V_{t,j}z[j]|$ and

$$\psi_t(z) = \|V_t z\|_1 \tag{2.45}$$

with $V_t = \mathrm{diag}(V_{t,j})$.

To state the resilience property in this particular setting, we partition the index set $\mathbb{T}\times\mathbb{J}$ of the entries of S as

$$\begin{aligned} \Lambda_\varepsilon &= \{(t,j) \in \mathbb{T}\times\mathbb{J} \,:\, \psi_{t,j}(f_t[j]) \leq \varepsilon\} \\ \Lambda_\varepsilon^c &= \{(t,j) \in \mathbb{T}\times\mathbb{J} \,:\, \psi_{t,j}(f_t[j]) > \varepsilon\} \end{aligned} \tag{2.46}$$

with $f_{t[j]}$ denoting the j-th entry of the vector $f_t \in \mathbb{R}^m$. Also, in order to account for the specificity of the new scenario, let us refine slightly the r-Resilience index (2.26) to be

$$\tilde{p}_r = \sup_{\substack{Z\in\mathbb{R}^{n\times T}\\ Z\neq 0}} \sup_{\substack{\mathcal{T}\subset\mathbb{T}\times\mathbb{J}\\ |\mathbb{J}|=r}} \frac{\sum_{(t,j)\in\mathcal{T}} \psi_{t,j}(c_{t,j}^\top z_t)}{H_\Sigma(Z)} \tag{2.47}$$

where H_Σ is defined as in (2.25) from ψ_t in (2.44) and $c_{t,j}^\top$ is j-th row of the measurement matrix C_t. The difference between p_r in (2.26) and $\tilde{p}_r$ in (2.47) resides in the index sets for counting possible error occurrences which are $\mathbb{T}$ and $\mathbb{T}\times\mathbb{J}$, respectively.

With these notations, we can provide the following theorem which is the analog of Corollary 2.1.1 in the case where the disturbance matrix S (see Eq. (1.49)) is entrywise sparse.

Theorem 2.2 (Upper bound on the estimation error: Separable case)**.** *Consider the system Σ defined by (1.1) with output Y together with the state estimator (2.4) in which ϕ is assumed to obey (P2.1)–(P2.5) and ψ is defined as in (2.45). Let $\varepsilon \geq 0$ and set $r = |\Lambda_\varepsilon^c|$ with Λ_ε^c defined in (2.46).*
If the system is observable on $[0, T-1]$ and if $\tilde{p}_r < 1/2$, then there exists a $\mathcal{K}_\infty$ function $\tilde{h}$ such that for all norm $\|\cdot\|$ on $\mathbb{R}^{n\times T}$,

$$\|\hat{X} - X\| \leq \tilde{h}\left(\frac{2\tilde{\beta}_\Sigma(\varepsilon)}{\tilde{D}(1-2\tilde{p}_r)}\right) \quad \forall \hat{X} \in \mathcal{E}(Y) \tag{2.48}$$

with X denoting the true state matrix from (1.1) and $\tilde{\beta}_\Sigma(\varepsilon)$ defined by

$$\tilde{\beta}_\Sigma(\varepsilon) = \lambda \sum_{t\in\mathbb{T}'} \phi_t(w_t) + \sum_{(t,j)\in\Lambda_\varepsilon} \psi_{t,j}(f_t[j])$$

$\tilde{D}$ and $\tilde{h}$ are defined as in the statement of Theorem 2.1 with H_Σ being constructed from ψ in (2.45).

To some extent, Theorem 2.2 can be viewed as a special case of Theorem 2.1 in which the function ψ is taken to be the ℓ_1-norm and the data set is modified to be $\mathbb{T} \times \mathbb{J}$. Hence the proof follows a similar line of arguments as that of Theorem 2.2. Again it is not hard to see that the result of Theorem 2.2 implies the property of resilience with respect to the set $\mathcal{F}_r$ in (2.22) of measurement noise in the sense of Definition 2.2 (see the proof of Corollary 2.1.1).

An interesting property of the estimator can be stated in the absence of dense noise, i.e., when only the sparse noise is active:

Corollary 2.2.1. *Consider the system Σ defined by (1.1) and let $r = |\Lambda_0^c|$ (which means that we consider every nonzero occurrence of f_{it} as an outlier by taking $\varepsilon = 0$ in (2.46)). If the conditions of Theorem 2.2 and $\tilde{p}_r < 1/2$, and if $w_t = 0$ in (1.1) for all t, then the estimator defined by (2.4) retrieves exactly the state trajectory of the system, i.e., $\mathcal{E}(Y) = \{X\}$.*

Proof. This follows directly from the fact that $\tilde{\beta}_\Sigma(0) = 0$ in the case where there is no dense noise w_t and $\varepsilon = 0$. □

Therefore, the estimator (2.4) has the exact recoverability property, that is, it is able to recover exactly the true state of the system (1.1) when only the sparse noise is active in the measurement equation provided that the number $r = |\Lambda_0^c|$ of nonzero in the sequence $\{f_t[j]\}_{(t,j)\in\mathbb{T}\times\mathbb{J}}$ is small enough for $\tilde{p}_r$ to be less than $1/2$. According to our analysis, the number of outliers that can be handled by the estimator in this case can be underestimated by

$$\max\{r : \tilde{p}_r < 1/2\}. \tag{2.49}$$

2.4 Further discussions on the exact recoverability property of the estimator

In this section, we consider a constrained reformulation of the estimator $\mathcal{E}$ defined in (2.4). As will be shown shortly, this reformulation also enjoys the resilience property but under a condition which is more easily verifiable from a numerical perspective.

We start by considering the simple scenario where the process noise w_t in (1.1) is identically equal to zero and the sequence $\{f_t\}$ is sparse in the sense that its dense component v_t displayed in (1.49) does not exist. In this setting we can obtain a more resilient (to sparse noise in the measurement) estimator than (2.4) by making it aware of the absence of dense process noise. This can be achieved by contraining the searched state matrix to be in the set $\mathcal{Z}_\Sigma \subset \mathbb{R}^{n\times T}$ defined by

$$\mathcal{Z}_\Sigma = \left\{ Z = \begin{pmatrix} z_0 & A_0 z_0 & \cdots & A_{T-1}\cdots A_1 A_0 z_0 \end{pmatrix} : z_0 \in \mathbb{R}^n \right\} \tag{2.50}$$

of possible trajectories starting in any initial state $z_0 \in \mathbb{R}^n$. Following this idea, we consider the estimator $\mathcal{E}^\circ$ defined by

$$\mathcal{E}^\circ(Y) = \underset{Z\in\mathcal{Z}_\Sigma}{\arg\min}\, V_\Sigma(Y, Z).$$

Then $\mathcal{E}^\circ(Y)$ can be rewritten more simply in the form

$$\mathcal{E}^\circ(Y) = \left\{ Z = \begin{pmatrix} z_0 & A_0 z_0 & \cdots & A_{T-1}\cdots A_1 A_0 z_0 \end{pmatrix} : z_0 \in \underset{z\in\mathbb{R}^n}{\arg\min}\, V_\Sigma^\circ(Y, z) \right\} \tag{2.51}$$

where

$$V_\Sigma^\circ(Y,z)=\sum_{t\in\mathbb{T}}\psi_t(y_t-M_tz) \tag{2.52}$$

with

$$M_t=C_tA_{t-1}\cdots A_1A_0 \tag{2.53}$$

for all $t\geq 1$ and $M_0=C_0$. Hence the estimation of the state trajectory reduces to estimating the initial state x_0. This can be viewed as a robust regression problem, like the ones discussed in [Han19; Bak17]. Generalizing a result in [Bak17], we derive next a necessary and sufficient condition for exact recovery of the true state, which holds if and only if $\arg\min_{z\in\mathbb{R}^n} V_\Sigma^\circ(Y,z)=\{x_0\}$ with x_0 being the exact initial state of the system Σ. To this end, we first introduce the concept of concentration ratio of a collection of matrices with respect to a loss function. A notational convention will be necessary for the statement of this property: for any subset $\mathcal{T}$ of $\mathbb{T}$, let

$$\Psi_\mathcal{T}^\circ(z)=\sum_{t\in\mathcal{T}}\psi_t(M_tz). \tag{2.54}$$

Definition 2.4 (r-th concentration ratio)**.** *Let $\{\psi_t\}$ be a family of loss functions defined by (2.3) in which ψ is assumed to satisfy (P2.1), (P2.3) and (P2.5) with constant $\gamma_\psi=1$. Let $M=\{M_t\}_{t\in\mathbb{T}}$ be a sequence of matrices such that the function $\Psi_\mathbb{T}^\circ$, defined in (2.54) with $\mathcal{T}=\mathbb{T}$, is positive definite. We call r-th concentration ratio of M, the number defined by*

$$\nu_r(M)=\sup_{\substack{z\in\mathbb{R}^n\\ z\neq 0}}\sup_{\substack{\mathcal{T}\subset\mathbb{T}\\ |\mathcal{T}|=r}}\frac{\Psi_\mathcal{T}^\circ(z)}{\Psi_\mathbb{T}^\circ(z)} \tag{2.55}$$

At a fixed r, $\nu_r(M)$ quantifies a genericity property for the sequence $M=\{M_t\}_{t\in\mathbb{T}}$. In view of the particular structure of the collection M in (2.53), note that $\Psi_\mathbb{T}^\circ$ is positive definite whenever the system Σ is observable on $\mathbb{T}$. Furthermore, $\nu_r(M)$ can be interpreted to some extent, as a quantitative measure of observability. It is indeed all the smaller as the system is strongly observable. To see this, recall from Lemma 2.3 that if the system is observable on $[0,T-1]$, then for all $Z\in\mathcal{Z}_\Sigma$ initiated at z in $\mathbb{R}^n$, we have $V_\Sigma(0,Z)=\Psi_\mathbb{T}^\circ(z)\geq q(\|z\|)$ for some $\mathcal{K}_\infty$ function q. It follows that

$$\nu_r(M)\leq\sup_{\substack{z\in\mathbb{R}^n\\ z\neq 0}}\sup_{\substack{\mathcal{T}\subset\mathbb{T}\\ |\mathcal{T}|=r}}\frac{\Psi_\mathcal{T}^\circ(z)}{q(\|z\|)} \tag{2.56}$$

Hence the more observable (i.e., the larger the gain function q), the smaller $\nu_r(M)$.

For all $(Y,z_0)\in\mathbb{R}^{m\times T}\times\mathbb{R}^n$ with Y expressed columnwise in the form $Y=\begin{pmatrix}y_0 & \cdots & y_{T-1}\end{pmatrix}$, consider now the following notations:

$$\mathcal{I}^0(Y,z_0)=\{t\in\mathbb{T}\ :\ y_t-M_tz_0=0\}$$
$$\mathcal{I}^c(Y,z_0)=\{t\in\mathbb{T}\ :\ y_t-M_tz_0\neq 0\}.$$

Theorem 2.3 (Exact Recoverability Condition)**.** *Consider the cost function (2.52) where $M=\{M_t\}$ is assumed to have been constructed as in (2.53) from the matrices of system (1.1). Assume that the loss functions $\{\psi_t\}$ involved in (2.52) are defined by (2.3) in which ψ is assumed to satisfy (P2.1), (P2.3) and (P2.5) with constant $\gamma_\psi=1$. Let r be a positive integer. If the system (1.1) is observable on $[0,T-1]$, then the two following propositions are equivalent:*

(i) *For all* Y *in* $\mathbb{R}^{m\times T}$ *and all* z_0 *in* $\mathbb{R}^n$,

$$|\mathcal{I}^c(Y,z_0)|\leq r \;\Rightarrow\; \arg\min_{z\in\mathbb{R}^n} V_\Sigma^\circ(Y,z)=\{z_0\} \tag{2.57}$$

(ii) *The index* $\nu_r(M)$ *satisfies*

$$\nu_r(M)<1/2 \tag{2.58}$$

Proof. (i) $\Rightarrow$ (ii): Assume that (i) holds. Consider an arbitrary subset $\mathcal{T}$ of $\mathbb{T}$ such that $|\mathcal{T}|\leq r$. Let $z_0\neq 0$ be a vector in $\mathbb{R}^n$. Construct a sequence Y in $\mathbb{R}^{m\times T}$ such that $y_t=0$ if $t\in\mathcal{T}$ and $y_t=M_tz_0$ otherwise. Then $\mathcal{I}^c(Y,z_0)\subset$ $mathcalT$, so that $|\mathcal{I}^c(Y,z_0)|\leq r$. It then follows from (i) that $\arg\min_{z\in\mathbb{R}^n} V_\Sigma^\circ(Y,z)=\{z_0\}$ which means that $V_\Sigma^\circ(Y,z_0)<V_\Sigma^\circ(Y,z)$ for all $z\in\mathbb{R}^n$, $z\neq z_0$. In particular, $V_\Sigma^\circ(Y,z_0)<V_\Sigma^\circ(Y,0)$ which, by taking into account the definition of Y, gives

$$\Psi_{\mathcal{T}}^\circ(z_0)<\Psi_{\mathcal{T}^c}^\circ(z_0),$$

where $\mathcal{T}^c=\mathcal{T}\setminus\mathcal{T}$. Since $\Psi_{\mathbb{T}}^\circ(z_0)=\Psi_{\mathcal{T}}^\circ(z_0)+\Psi_{\mathcal{T}^c}^\circ(z_0)$, we see that

$$\frac{\Psi_{\mathcal{T}}^\circ(z_0)}{\Psi_{\mathbb{T}}^\circ(z_0)}<1/2$$

This reasoning works for every nonzero z_0 and for every subset $\mathcal{T}$ of $\mathbb{T}$. We can hence conclude that $\nu_r(M)<1/2$.

(ii) $\Rightarrow$ (i): Assume that (ii) holds. Let $(Y,z_0)\in\mathbb{R}^{m\times T}\times\mathbb{R}^n$ be such that $|\mathcal{I}^c(Y,z_0)|\leq r$. We then need to prove that $\arg\min_{z\in\mathbb{R}^n} V_\Sigma^\circ(Y,z)=\{z_0\}$. Since the assertion (ii) is assumed true, it follows from (2.55) and (2.58) that

$$2\Psi_{\mathcal{T}^c}^\circ(z_0')<\Psi_{\mathbb{T}}^\circ(z_0')\quad\forall z_0'\in\mathbb{R}^n,\ z_0'\neq 0 \tag{2.59}$$

where, for simplicity, we have posed $\mathcal{T}^c=\mathcal{I}^c(Y,z_0)$. In the derivation of (2.59), we have used the obvious fact that $r_1\leq r_2\Rightarrow\nu_{r_1}(M)\leq\nu_{r_2}(M)$. If we pose $\mathcal{T}=\mathcal{I}^0(Y,z_0)=\mathbb{T}\setminus\mathcal{T}^c$, then the inequality (2.59) is equivalent to

$$\sum_{t\in\mathcal{T}^c}\psi_t(M_tz_0')<\sum_{t\in\mathcal{T}}\psi_t(M_tz_0') \tag{2.60}$$

Now we observe that for all t in $\mathcal{T}=\mathcal{T}^0(Y,z_0)$, $y_t=M_tz_0$, so that $\psi_t(M_tz_0')=\psi_t(y_t-M_t(z_0+z_0'))$. On the other hand, for $t\in\mathcal{T}^c=\mathcal{I}^c(Y,z_0)$, if we apply the GTI (2.7) with $\gamma_\psi=1$, we obtain

$$\begin{aligned}\psi_t(M_tz_0')&=\psi_t(y_t-M_tz_0-(y_t-M_t(z_0+z_0'))\\&\geq\psi_t(y_t-M_tz_0)-\psi_t(y_t-M_t(z_0+z_0'))\end{aligned}$$

Combining all these remarks with (2.60) yields

$$\sum_{t\in\mathcal{T}^c}[\psi_t(y_t-M_tz_0)-\psi_t(y_t-M_t(z_0+z_0')]<\sum_{t\in\mathcal{T}}\psi_t(y_t-M_t(z_0+z_0'))$$

Rearranging this gives $V_\Sigma^\circ(Y,z_0)<V_\Sigma^\circ(Y,z_0+z_0')$ for all $z_0'\in\mathbb{R}^n$ with $z_0'\neq z_0$. This is equivalent to $\arg\min_{z\in\mathbb{R}^n} V_\Sigma^\circ(Y,z)=\{z_0\}$. Hence (ii) holds as claimed. □

From the statement of Theorem 2.3, we infer that under the assumption that only the sparse noise $\{s_t\}$ is active (i.e., there is no dense noise (w_t, v_t)) in the system equations (1.1), $\mathcal{E}^\circ(Y) = \{X\}$ whenever $\nu_r(M) < 1/2$, i.e, the estimator $\mathcal{E}^\circ$ returns exactly the true state. For a given system, if one can evaluate numerically the index $\nu_r(M)$, then it becomes possible to assess the number $r_{\max} \triangleq \max\{r : \nu_r(M) < 1/2\}$ of gross errors that can be corrected by the estimator when applied to that system. We will get back to the computational matter in Section 2.5.

It is also worth noting that this theorem can be interpreted as a generalisation of Proposition 6 from [Faw14], which is focused on ℓ_p-norms, to a wider class of loss functions ψ_t.

2.4.1 Special case of ℓ_0-norm loss based estimator

Consider the special case where the loss functions $\{\psi_t\}$ are defined, for all $t \in \mathbb{T}$, by

$$\forall z \in \mathbb{R}^m, \quad \psi_t(z) = \begin{cases} 1 & \text{if } z \neq 0 \\ 0 & \text{otherwise} \end{cases} \tag{2.61}$$

This corresponds to the block ℓ_0-norm. Note that such functions satisfy the assumptions (P2.1), (P2.3) and (P2.5) requested in the definition 2.4 of $\nu_r(M)$ and in the statement of Theorem 2.3. Hence $\nu_r(M)$ is well-defined in this case.

Corollary 2.3.1. *Consider system (1.1) under the assumption that $w_t = 0$ for all t. Assume observability of the system on $[0, T-1]$. Consider the estimator (2.51) in which the cost V_Σ° is defined from the family of loss functions $\{\psi_t\}$ expressed in (2.61). Then for all $(Y, z_0) \in \mathbb{R}^{m\times T} \times \mathbb{R}^n$,*

$$|\mathcal{I}^c(Y, z_0)| < \frac{T - \mu(M) + 1}{2} \;\Rightarrow\; \mathcal{E}^\circ(Y) = \{X\},$$

where $\mu(M)$ defined by

$$\mu(M) = \min\left\{k : \forall J \subset \mathbb{T}, \Big(|J| = k \;\Rightarrow\; \operatorname{rank}(M_J) = n\Big)\right\} \tag{2.62}$$

is the minimum number k such that any matrix $M_J \in \mathbb{R}^{|J|m\times n}$ formed by stacking vertically the matrices of the collection $\{M_t : t \in J\}$ indexed by $J \subset \mathbb{T}$ with $|J| = k$, has full column rank.

Proof. Let us start by observing that with the particular loss functions invoked in the statement of the corollary, $\Psi_{\mathbb{T}}^\circ(z)$ denotes the number of $t \in \mathbb{T}$ for which $\psi_t(M_t z) \neq 0$. It follows from the definition of $\mu(M)$ that $\Psi_{\mathbb{T}}^\circ(z) \geq T - \mu(M) + 1$ for all $z \neq 0$. The reason for this is that if $\psi_t(M_t z)$ was to be equal to zero more than $\mu(M) - 1$ times, then z would be necessarily equal to zero. As a result we get

$$\nu_r(M) \leq \frac{r}{T - \mu(M) + 1}$$

Hence by applying Theorem 2.3, $|\mathcal{I}^c(Y, z_0)|/(T - \mu(M) + 1) < 1/2$ is a sufficient condition for exact recovery by the ℓ_0-norm based estimator. □

Remark 2.3. *Assume that ψ_t is defined to be the counting norm, i.e.*

$$\psi_t(z) = \|z\|_0 \tag{2.63}$$

Then ψ_t has a separable structure as illustrated in (2.44). Consider then defining, still under the observability assumption, an entrywise version of the concentration ratio by

$$\tilde{\nu}_r(M) = \sup_{\substack{z\in\mathbb{R}^n \\ z\neq 0}} \sup_{\substack{\mathcal{T}\subset\mathbb{T}\times\mathbb{J} \\ |\mathcal{T}|=r}} \frac{\sum_{(t,j)\in\mathcal{T}} \|M_{t,j}z\|_0}{\Psi^\circ_{\mathbb{T}}(z)} \tag{2.64}$$

where $M_{t,j}$ refers to the j-th row of M_t. Further, let

$$\tilde{\mu}(M) = \min\Big\{k : \forall J \subset \mathbb{T}\times\mathbb{J}, \Big(|I| = k \;\Rightarrow\; \operatorname{rank}(\tilde{M}_J) = n\Big)\Big\}$$

with $\tilde{M}_J \in \mathbb{R}^{|J|\times n}$ denoting the matrix obtained by stacking the row vectors $\{M_{t,j} : (t,j)\in J\}$. Then a result similar to Corollary 2.3.1 is obtainable: if the number the measurements corrupted by a nonzero error (among the mT available) is strictly less than $(mT - \tilde{\mu}(M) + 1)/2$, then the estimator $\mathcal{E}^\circ$ (2.51) (with ψ_t being the ℓ_0 norm as in (2.63)) recovers exactly the true state.

Remark 2.4. *Under the condition of Remark 2.3, if we consider the scenario where only a set of $k < m$ sensors may be compromised by attackers, then exact recovery is achieved if*

$$k < \frac{m}{2} - \frac{\tilde{\mu}(M) - 1}{2T}. \tag{2.65}$$

Taking into consideration the fact that $\tilde{\mu}(M) - 1 < T$, it can then be seen that (2.65) is equivalent to $k \le \lceil m/2 - 1\rceil$ where the notation $\lceil r\rceil$, for $r\in\mathbb{R}$, refers to the smallest integer larger or equal to r. To sum up, when the ψ_t are defined as in (2.63), the estimator (2.51) is able to return the true state matrix even when $\lceil m/2 - 1\rceil$ sensors get faulty over the entire observation horizon. This is reminiscent of another result stated in [Faw14] which therefore appears to be a consequence of Theorem 2.3.

2.4.2 Stability of the class of estimators $\mathcal{E}^\circ$ with respect to dense noise

We have argued that the class of estimators $\mathcal{E}^\circ$ in (2.51) is able to obtain exactly the true state matrix when there is no dense noises (w_t, v_t) in the system equations and only the sparse noise $\{s_t\}$ is active. The question we ask now is whether this set of estimators can, in addition to sparse noise, handle dense process and output noises and to what extent this is possible. The starting point of our reflection is the observation that the dynamical system defined by

$$\begin{aligned} \tilde{x}_{t+1} &= A_t\tilde{x}_t, \quad \tilde{x}_0 = x_0 \\ y_t &= C_t\tilde{x}_t + s_t + (v_t + \tilde{v}_t), \end{aligned} \tag{2.66}$$

produces the same output as system (1.1). Here, $\tilde{v}_t = \sum_{k=0}^{t-1} C_tA_{t-1}\cdots A_{k+1}w_k$, with the convention that the product $A_{t-1}\cdots A_{k+1} = I$ if $k = t-1$. Then the idea is to apply the estimator $\mathcal{E}^\circ$ to (2.66) by neglecting the dense component $(v_t + \tilde{v}_t)$ of the output equation. To state the resilience result for $\mathcal{E}^\circ$, consider for a given $\varepsilon \ge 0$, a partition $(\tilde{\mathbb{T}}_\varepsilon, \tilde{\mathbb{T}}^c_\varepsilon)$ of $\mathbb{T}$ defined as in (2.27) with f_t replaced by $\tilde{f}_t \triangleq s_t + (v_t + \tilde{v}_t) = f_t + \tilde{v}_t$.

Theorem 2.4. *Consider the estimator (2.51) for the system (1.1). Assume that the loss functions $\{\psi_t\}$ involved in (2.52) are defined by (2.3) in which ψ is assumed to satisfy (P2.1)–(P2.5) with constant $\gamma_\psi = 1$. Let $\varepsilon \ge 0$ and set $r = |\tilde{\mathbb{T}}^c_\varepsilon|$. Denote*

with $\mathfrak{N}$ a norm on $\mathbb{R}^{n\times T}$ defined by $\mathfrak{N}(Z) = \max_{t=0,\dots,T-1} \|z_t\|$ with z_t being the t-th column of Z and $\|\cdot\|$ being a norm on $\mathbb{R}^n$.
If the system (1.1) is observable on $[0, T-1]$ and $\nu_r(M) < 1/2$, then there exists a $\mathcal{K}_\infty$ function α such that for all norm $\|\cdot\|$ on $\mathbb{R}^{n\times T}$,

$$\mathfrak{N}(\hat{X} - X) \leq R_\Sigma \alpha^{-1}(\rho) + \max_{t\in\mathbb{T}} \|\tilde{w}_t\| \quad \forall \hat{X} \in \mathcal{E}^\circ(Y), \tag{2.67}$$

where R_Σ is some constant depending on the system Σ and

$$\rho = \frac{2}{D_1(1 - 2\nu_r(M))} \sum_{t\in\tilde{\mathbb{T}}_\varepsilon} \psi_t(\tilde{f}_t)$$

with $\tilde{f}_t = f_t + \tilde{v}_t$, and $D_1 = \min_{\|z\|=1} \Psi^\circ_{\mathbb{T}}(z)$.

Proof. Let $\hat{x}_0 \in \arg\min_{z\in\mathbb{R}^n} V^\circ_\Sigma(Y, z)$. We first provide a bound on the error $e_0 = \hat{x}_0 - x_0$ with x_0 denoting the true initial state of system (1.1). By exploiting the fact that $V^\circ_\Sigma(Y, \hat{x}_0) \leq V^\circ_\Sigma(Y, x_0)$ and noting that $y_t = M_t x_0 + \tilde{f}_t$, we reach the inequality

$$\sum_{t\in\mathbb{T}} \psi_t(\tilde{f}_t - M_t e_0) \leq \sum_{t\in\mathbb{T}} \psi_t(\tilde{f}_t).$$

By then reasoning quite similarly as in the proof of Theorem 2.1, we get

$$\Psi^\circ_{\mathbb{T}}(e_0) - 2\Psi^\circ_{\mathbb{T}^c_\varepsilon}(e_0) \leq \sum_{t\in\tilde{\mathbb{T}}_\varepsilon} \psi_t(\tilde{f}_t)$$

which, by exploiting (2.55) and the assumption that $\nu_r(M) < 1/2$, leads to

$$\Psi^\circ_{\mathbb{T}}(e_0) \leq \frac{2}{1 - 2\nu_r(M)} \sum_{t\in\tilde{\mathbb{T}}_\varepsilon} \psi_t(\tilde{f}_t)$$

Applying now Lemma 2.2, we conclude that for any norm $\|\cdot\|$ on $\mathbb{R}^n$, there exists a $\mathcal{K}_\infty$ function α such that $\|e_0\| \leq \alpha^{-1}(\rho)$. Now by observing that for any $\hat{X} \in \mathcal{E}^\circ(Y)$,

$$\hat{X} - X = \begin{pmatrix} e_0 & A_0 e_0 & \cdots & A_{T-1}\cdots A_0 e_0 \end{pmatrix} - \begin{pmatrix} 0 & \tilde{w}_0 & \cdots & \tilde{w}_{T-1} \end{pmatrix}$$

with $\tilde{w}_t = \sum_{k=0}^{t-1} A_{t-1}\cdots A_{k+1} w_k$, the result follows by posing[2]

$$R_\Sigma = \max_{t\in\mathbb{T}} \|A_{t-1}\cdots A_0\|_{\text{ind}}$$

with $\|\cdot\|_{\text{ind}}$ being the matrix norm induced by the vector norm $\|\cdot\|$ on $\mathbb{R}^n$. □

The interest in Theorem 2.4 is that it provides a condition of resilience for the estimator $\mathcal{E}^\circ$ which can be checked numerically as will be discussed in the next section.

2.5 On the numerical evaluation of the resilience conditions

The analysis results presented in Sections 2.3 and 2.4 rely on some functions (resilience index, concentration ratio,...) which characterize quantitatively some properties of the system being observed. A question we ask now is whether it would be possible

[2] We use here the convention that $A_{t-1}\cdots A_0 = I$ if $t = 0$.

to evaluate numerically these measures. Indeed, computing the r-resilience index in (2.26) would help testing for example the resilience condition in Theorem 2.1. Similarly, evaluating the concentration ratio $\nu_r(M)$ introduced in (2.55) is the way to assess whether a given estimator is able to return the true state of a given system if we make an hypothesis on the number of potential nonzero errors in the measurements.

Numerically obtaining the numbers p_r or ν_r can be challenging, as it requires solving some hard nonconvex and combinatorial optimization problems. This is indeed a common characteristic of the concepts which are usually used to assess resilience; for example, the popular Restricted Isometry Property (RIP) constant [Can08a] is comparatively as hard to evaluate. In this section, we will provide elements in order to address the challenge of computing p_r (Section 2.5.1) and ν_r (Section 2.5.2).

2.5.1 The r-Resilience indexes p_r, $\tilde{p}_r$

In order to discuss the calculability of the r-Resilience indexes p_r and $\tilde{p}_r$, we recall their definitions

$$p_r = \sup_{\substack{Z\in\mathbb{R}^{n\times T}\\ Z\neq 0}} \sup_{\substack{\mathcal{T}\subset\mathbb{T}\\ |\mathcal{T}|=r}} \frac{\sum_{t\in\mathcal{T}} \psi_t(C_t z_t)}{H_\Sigma(Z)} \quad \text{and} \quad \tilde{p}_r = \sup_{\substack{Z\in\mathbb{R}^{n\times T}\\ Z\neq 0}} \sup_{\substack{\mathcal{T}\subset\mathbb{T}\times\mathbb{J}\\ |\mathbb{J}|=r}} \frac{\sum_{(t,j)\in\mathcal{T}} \psi_{t,j}(c_{t,j}^\top z_t)}{H_\Sigma(Z)}$$

As mentioned earlier, calculating those parameters requires solving two connected optimisation problems, a non-convex one and a combinatorial one. The present section aims at providing an overestimation of p_r and $\tilde{p}_r$ relying on the fact that for every r in $\mathbb{N}_{\neq 0}$,

$$p_r \leq r p_1 \quad \text{and} \quad \tilde{p}_r \leq r\tilde{p}_1 \tag{2.68}$$

The following lemma provides a way of calculating $\tilde{p}_r$ when $\{\phi_t\}$ is a family of norms and ψ_t is the ℓ_1-norm for all $t \in \mathbb{T}$:

Lemma 2.5 (An estimate of the r-Resilience index $\tilde{p}_r$)**.** *Consider the resilience parameter $\tilde{p}_r$ defined in (2.47) where we assume that $\psi_{t,j}(e) = |e|$ for all $(t,j,e) \in \mathbb{T}\times\mathbb{J}\times\mathbb{R}$ and ϕ_t is an arbitrary norm. Then*

$$\tilde{p}_r \leq \frac{r}{b_1} \tag{2.69}$$

where

$$b_1 = \inf_{(t,j)\in\mathbb{T}\times\mathbb{J}} \inf_{Z\in\mathbb{R}^{n\times T}} \left\{ H_\Sigma(Z) : c_{t,j}^\top z_\tau = 1 \right\} = \frac{1}{\tilde{p}_1}. \tag{2.70}$$

Proof. As mentioned earlier, the starting point of the proof is the observation that for every integer r in $\{1,\dots,T\}$, $\tilde{p}_r \leq r\tilde{p}_1$. Hence it suffices to show that $\tilde{p}_1 = 1/b_1$ and is as expressed in (2.70). Recall that by definition,

$$\tilde{p}_1 = \sup_{(t,j)\in\mathbb{T}\times\mathbb{J}} \sup_{\substack{Z\in\mathbb{R}^{n\times T}\\ Z\neq 0}} \frac{|c_{t,j}^\top z_t|}{H_\Sigma(Z)}. \tag{2.71}$$

Without loss of generality, assume that $c_{t,j}^\top \neq 0$ for all $(t,j) \in \mathbb{T}\times\mathbb{J}$. Then, for any (t,j),

$$\sup_{\substack{Z\in\mathbb{R}^{n\times T}\\ Z\neq 0}} \frac{|c_{t,j}^\top z_t|}{H_\Sigma(Z)} = \sup_{\substack{Z\in\mathbb{R}^{n\times T}\\ Z\neq 0}} \left\{ \frac{|c_{t,j}^\top z_t|}{H_\Sigma(Z)} : c_{t,j}^\top z_t \neq 0 \right\} \triangleq \frac{1}{\beta_{t,j}}$$

where

$$\begin{aligned}\beta_{t,j} &= \inf_{\substack{Z\in\mathbb{R}^{n\times T}\\ Z\neq 0}} \left\{ \frac{H_\Sigma(Z)}{|c_{t,j}^\top z_t|} : c_{t,j}^\top z_t \neq 0 \right\} \\ &= \inf_{\substack{Z\in\mathbb{R}^{n\times T}\\ Z\neq 0}} \left\{ H_\Sigma(Z) : |c_{t,j}^\top z_t| = 1 \right\} \\ &= \inf_{\substack{Z\in\mathbb{R}^{n\times T}\\ Z\neq 0}} \left\{ H_\Sigma(Z) : c_{t,j}^\top z_t = 1 \right\}\end{aligned}$$

Recalling that $H_\Sigma(Z)$ is a norm under the conditions of the lemma, the second equality in the expression of $\beta_{t,j}$ above follows from the (strict) homogeneity property of norms. As to the last equality, it follows from the fact that $c_{t,j}^\top z_t$ is a scalar which induces the possibility to replace the constraint $|c_{t,j}^\top z_t| = 1$ indifferently either by $c_{t,j}^\top z_t = 1$ or by $c_{t,j}^\top z_t = -1$.
Now by invoking the definition of $\tilde{p}_1$, it can be seen that

$$\tilde{p}_1 = \sup_{(t,j)\in\mathbb{T}\times\mathbb{J}} \frac{1}{\beta_{t,j}} = \frac{1}{\inf_{(t,j)\in\mathbb{T}\times\mathbb{J}} \beta_{t,j}} = \frac{1}{b_1}.$$

□

Remark 2.5. *This lemma can indeed be extended to any family of cost functions* $\{\psi_t\}$ *which has a separable structure as defined in* (2.44)*. The overestimation is then*

$$\tilde{p}_r \leq \frac{r}{b_1'},$$

with

$$b_1 = \inf_{(t,j)\in\mathbb{T}\times\mathbb{J}} \inf_{Z\in\mathbb{R}^{n\times T}} \left\{ \frac{H_\Sigma(Z)}{\psi_{t,j}(1)} : c_{t,j}^\top z_\tau = 1 \right\}.$$

Note, under the assumptions of Lemma 2.5, that $\inf_{Z\in\mathbb{R}^{n\times T}} \left\{ H_\Sigma(Z) : c_{t,j}^\top z_\tau = 1 \right\}$ is a convex optimization problem for any given (t, j). Hence, solving for b_1 in (2.70) requires solving mT convex problems and picking the smallest value among all. The interest of the lemma is that it provides an overestimate of $\tilde{p}_r$ which is numerically computable. Based on the so obtained overestimate of $\tilde{p}_r$, we see from Theorem 2.1 that the estimator (2.4) is resilient to r outliers if $r < b_1/2$. Moreover, we can deduce an underestimate of the maximum number of outliers $r_{\max}$ (see Eq. (2.41)) that the estimator (2.4) is able to handle as

$$\tilde{r}_{\max} = \max \left\{ r : r < \frac{b_1}{2} \right\} \tag{2.72}$$

Remark 2.6. *We observe that Lemma 2.5 is also applicable to overestimate* p_r *defined in* (2.26) *in the case of a single-output system, i.e. when* $m = 1$*, given that* $p_r = \tilde{p}_r$ *for all* $r \in \mathbb{T}$ *in this case.*

2.5.2 The concentration ratio ν_r

When the dimension of the state is small enough, $\nu_r(M)$ can be exactly computed by taking inspiration from a method presented in [Sha09] even though at the price of a huge computational cost. Alternatively, a cheaper overestimation can be obtained by means of convex optimization as suggested in [Bak17]. The next lemma provides such an overestimate for $\nu_r(M)$.

Lemma 2.6. *Assuming all quantities are well-defined (see the conditions in Definitions 2.3 and 2.4), the following statements hold:*

(a) $\nu_r \leq p_r$

(b) If $\mu(M) \leq T-1$ *then*

$$\nu_r(M) \leq \frac{r\nu^o}{1+\nu^o}, \tag{2.73}$$

where

$$\nu^o = \max_{t\in\mathbb{T}} \min_{\lambda_t\in\mathbb{R}^T} \left\{ \|\lambda_t\|_\infty : V_t M_t = \sum_{k\in\mathbb{T}} \lambda_t[k] V_k M_k, \lambda_t[t] = 0 \right\} \tag{2.74}$$

In (2.74), the $\lambda_t[k]$ *denote the entries of the vector* $\lambda_t \in \mathbb{R}^T$ *and* $\{V_t\}$ *refers to the sequence of nonsingular weighting matrices involved in (2.3).*

The proof of statement (a) is straightforward by noticing that (2.55) follows from (2.26) by constraining the variable Z to be in $\mathcal{Z}_\Sigma$. As to the proof of statement (b), it follows a similar reasoning as the proof of Theorem 2 in [Bak17].
The interest of this lemma is twofold. First it suggests that the resilience condition of $\mathcal{E}^\circ$ is weaker (in the sense that it is easier to achieve) than that of $\mathcal{E}$. Second, it provides an upper bound on $\nu_r(M)$ which can be computed by solving a convex optimization problem (see Eqs (2.73)-(2.74)). More specifically, given ν^o in (2.74), checking numerically whether $|\mathbb{T}_\varepsilon^c| < 1/2(1+1/\nu^o)$ provides a sufficient condition for $\nu_r(M) < 1/2$ and so, for the resilience of the estimator (2.51).

2.6 An approximate recursive implementation

The estimators studied in this chapter are defined as the solutions of an optimisation problem over the whole time-horizon $[0, T-1]$. The most direct approach to implement them is to directly solve the defining optimisation problem, which yields an estimate of the whole trajectory and is therefore a *batch implementation*. However, as it was discussed in Section 1.3.2, batch implementations have limits, especially in online settings where the length of the time-horizon grows towards infinity.

As a result, in this section, we will discuss a recursive, though approximate, implementation of a particular instance of the family of estimators defined in (2.4). We will consider the estimator $\mathcal{E}$ such that for all $t \in \mathbb{N}$, $\phi_t = \|\cdot\|_{Q_t}^2$ with $\{Q_t\}$ being a sequence of positive definite matrices, and $\psi_t = \|\cdot\|_1$.

To be consistent with the previously defined notations, the goal of the recursive estimator is to estimate the final state of the time-horizon T which is not fixed anymore and can grow towards infinity. To do so, we will make use of the *Forward Dynamic Programming* framework already presented in Section 1.3.3. We recall that the Forward Dynamic Programming framework is a way to define a recursive performance index function based on a batch performance index function. Indeed, based on the performance index V_Σ defining the class of estimators $\mathcal{E}$ through Equation (2.4), we can define the cost function $V_{\Sigma,T}^\star$ such that for all $T \in \mathbb{N}$,

$$\forall (Y, z) \in \mathbb{R}^{m\times T} \times \mathbb{R}^n,\ V_{\Sigma,T}^\star(Y, z) = \min_{\substack{Z\in\mathbb{R}^{n\times T} \\ z_T = z}} V_\Sigma(Y, Z).$$

It is worth noting that V_Σ, Y and Z implicitly depend on T as they were all defined over the time-horizon T. We then consider the estimators $\mathcal{E}_{\text{online}}$ such that

$$\mathcal{E}_{\text{online}}(Y,T) = \underset{z\in\mathbb{R}^n}{\arg\min}\, V^\star_{\Sigma,T}(Y,z). \tag{2.75}$$

Moreover, given the structure of V_Σ, the Bellman Equation (1.42) also provides a recursive relationship between $V^\star_{\Sigma,T+1}$ and $V^\star_{\Sigma,T}$, stating that

$$V^\star_{\Sigma,T+1}(Y,z) = \min_{s\in\mathbb{R}^n}\left\{V^\star_{\Sigma,T}(Y,s) + \lambda\|z - A_T s\|^2_{Q_T}\right\} + \|y_{T+1} - C_{T+1}z\|_1. \tag{2.76}$$

Directly implementing this recursive formula is impossible since it would require an analytical algebraic formula of $\min_{s\in\mathbb{R}^n}\left\{V^\star_{\Sigma,T}(Y,s) + \lambda\|z - A_T s\|^2_{Q_T}\right\}$ with respect to z and the system variables. This seems hard to obtain due to the presence of $\psi_T = \|\cdot\|_1$, a non-differentiable loss function, in $V^\star_{\Sigma,T}(Y,s)$.

However, if we were able to approximate the absolute value with a quadratic function, it would then be possible to obtain an analytical formula of $V^\star_{\Sigma,T+1}$ by applying Theorem 1.6. Indeed, the value of the ℓ_1-norm can be locally approached by a quadratic function, due to the fact that for any nonzero a in $\mathbb{R}$,

$$|a| = \frac{a^2}{|a|}.$$

The idea is to estimate the value of $|a|$ in the right-hand side in order to approach its real value through the previous equality, yielding

$$|a| \approx \frac{a^2}{|a|_{\text{pred}}},$$

where $|a|_{\text{pred}}$ is a prediction of the value a.

In the present context, at time T, the absolute values to estimate are $|y_T[j] - c_{t,T}^\top z|$ for j in $\mathbb{J}$. We want to approach this absolute value for the estimated state $\hat{x}_T$, so the prediction we can use is $\hat{x}_{T|T-1} = A_{T-1}\hat{x}_{T-1}$. Consequently, we define an approximated loss function $\psi_{T,\text{approx}}$ such that for all z in $\mathbb{R}^m$,

$$\psi_{T,\text{approx}}(z) = z^\top(\text{diag}(\gamma)R_T + \epsilon I_m)^{-1}z \tag{2.77}$$

with $\gamma \in \mathbb{R}^m$ a vector of positive weights, $\epsilon > 0$, and R_T a matrix of $\mathbb{R}^{m\times m}$ designed such that

$$R_T = \text{diag}(|y_T[1] - c_{T,1}^\top\hat{x}_{T|T-1}|, ..., |y_T[m] - c_{T,m}^\top\hat{x}_{T|T-1}|). \tag{2.78}$$

γ is introduced as a vector of tuning parameters which tunes the influence of each component $(y_T[j] - c_{T,j}^\top z)^2$ in $\psi_{T,\text{approx}}$. ϵ was added in order to avoid numerical issues when the difference $y_T - C_T\hat{x}_{T|T-1}$ is close from 0.

Overall, the definition (2.77) of $\psi_{T,\text{approx}}(z)$ gives, for all z in $\mathbb{R}^n$,

$$\psi_{T,\text{approx}}(y_T - C_T z) = \sum_{j=1}^{m}\frac{(y_T[j] - c_{T,j}^\top z)^2}{\gamma[j]\,|y_T[j] - c_{T,j}^\top\hat{x}_{T|T-1}| + \epsilon},$$

which should locally approach the ℓ_1-norm of $y_T - C_T\hat{x}_T$.

If we replace the ℓ_1-norm by $\psi_{T,\text{appprox}}$ in the Bellman equation (2.76), $V^\star_{\Sigma,T}$ is then recursively constructed with quadratic functions only. We can therefore apply Theorem 1.6, and the returned estimated state $\hat{x}_T$ can be obtained algebraically through the same formulas as a Least Square Estimator.

Consequently, we can derive a Kalman-like algorithm in order to minimise the optimal recursive performance index $V^{\star}_{\Sigma,T}$, and therefore implement the estimator $\mathcal{E}_{\text{online}}$ defined in (2.75). The resulting algorithm is presented in Algoritm 2.1. We note the input $T_{\max}$ is just an arbitrary number defined in order to give a maximum number of iterations to the loop within the algorithm, but this loop can be iterated as many times as needed.

Algorithm 2.1 Kalman-like Algorithm to approximately implement $\mathcal{E}_{\text{online}}$ (2.75)

Inputs: $\{A_T\}$, $\{C_T\}$, $\lambda \in \mathbb{R}_{>0}$, $\gamma \in \mathbb{R}^m_{>0}$, $\epsilon \in \mathbb{R}_{>0}$, $\hat{x}_0 \in \mathbb{R}^n$, $\{Q_T\}$, $P_0 \in \mathcal{S}^+_n(\mathbb{R})$, $T_{\max} \in \mathbb{N}$, $Y \in \mathbb{R}^{m \times T_{\max}}$
Initialization:
$T \leftarrow 0$
End of Initialization.
while $T < T_{\max}$ **do**
  $\hat{x}_{T|T-1} \leftarrow A_{T-1}\hat{x}_{T-1}$
  $R_T \leftarrow \text{diag}(|y_T[1] - c_{T,1}^\top \hat{x}_{T|T-1}|, ..., |y_T[m] - c_{T,m}^\top \hat{x}_{T|T-1}|)$
  $P_{T|T-1} \leftarrow A_{T-1}P_{T-1}A_{T-1}^\top + Q_{T-1}$
  $L_T \leftarrow P_{T|T-1}C_T^\top \left(C_T P_{T|T-1} C_T^\top + \text{diag}(\gamma)R_T + \epsilon I_m\right)^{-1}$
  $\hat{x}_T \leftarrow \hat{x}_{T|T-1} + L_T(y_T - C_T\hat{x}_{T|T-1})$
  $P_T \leftarrow (I_n - L_T C_T)P_{T|T-1}$
  $T \leftarrow T + 1$
end while

The performances of this algorithm and how it compares with the performances of the batch implementation will be discussed in Section 2.7.3.

Remark 2.7. *The whole process described above can also be conducted in the case where $\psi_t = \|\cdot\|_2$, given that for all z in $\mathbb{R}^m_{\neq 0}$,*

$$\|z\|_2 = \frac{z^\top z}{\sqrt{z^\top z}} \approx \frac{z^\top z}{\sqrt{z_{pred}^\top z_{pred}}}$$

2.7 Simulation Results

In this section, we will illustrate numerically the resilience properties of the proposed class of estimators. For this purpose, we will simulate System (1.21), *i.e.* the LTI system of the form (1.2) such that

$$\forall t \in \mathbb{N},\ A_t = A = \begin{pmatrix} 0.7 & 0.45 \\ -0.5 & 1 \end{pmatrix}, \quad C_t = C = \begin{pmatrix} 1 & 2 \end{pmatrix}, x_0 = \begin{pmatrix} 1 \\ 2 \end{pmatrix},$$

on a time horizon of length $T = 100$. For each test, the studied estimators will be specified in terms of functions ϕ and ψ as defined in (2.2)–(2.3) as well as the parameter λ defined in (2.1). For all t, the weighting matrices W_t and V_t defined in (2.2)–(2.3) will be assumed equal to the identity matrix unless stated otherwise.

Unless explicitly stated otherwise, every estimator presented in this section is implemented in batch mode by directly solving their defining optimisation problems. Indeed, in the case where there are defined by convex functions, we can use efficient convex optimisation algorithms to compute the estimate. This was performed through the CVX interface [Gra18] in MATLAB.

2.7.1 Numerical certificate of exact recoverability

Suppose in this section that the process noise w_t and the dense component v_t of f_t (see Eq. (1.49)) are both identically equal to zero. We then focus on testing the exact recoverability property of $\mathcal{E}^\circ$, the estimator defined in (2.51) for ψ equal to the ℓ_1-norm, in the presence of only the sparse noise $\{s_t\}$. The times of occurrence of the nonzeros values in the sequence $\{s_t\}$ are picked at random. As to its values, they are also randomly generated from a zero-mean normal distribution with variance 100^2. Given $T = 100$ output measurements and the system matrices in (1.21), the estimator $\mathcal{E}^\circ$ is implemented by directly solving the optimisation problem defined in (2.51). Note that the implementation of the estimator (2.51)-(2.52) requires computing the matrices M_t expressed in (2.53), which take the form CA^t in the LTI case. A problem that may occur however is that if A is Schur stable as is the case here (or unstable), taking successive powers of A produces matrices M_t which might not be of the same order of magnitude. To preserve the contribution of each term of (2.52), we redefine the weighting matrices $\{V_t\}$ (in the loss functions ψ_t according to (2.3)) to normalize the rows of these matrices so that they all have unit 2-norm. V_t is therefore selected to be a diagonal matrix of the form $V_t = \mathrm{diag}(\nu_t[1], \cdots, \nu_t[m])$, where

$$\nu_t[j] = \begin{cases} 1/\left\|c_j^\top A^t\right\|_2 & \text{if } c_j^\top A^t \neq 0 \\ 1 & \text{otherwise} \end{cases}, \tag{2.79}$$

with $c_j^\top$ ($j \in \mathbb{J}$) representing the rows of C. Indeed the effect of the weighting function in (2.52) is equivalent to changing y_t and M_t respectively to $\tilde{y}_t = V_t y_t$ and $\tilde{M}_t = V_t C A^t$. Posing $M = \{\tilde{M}_t\}$, it can be checked using the methods discussed in Section 2.5 that $r_{\max} = 30$ erroneous data (out of $T = 100$ measurements) can be accommodated by the estimator while still returning exactly the true state.

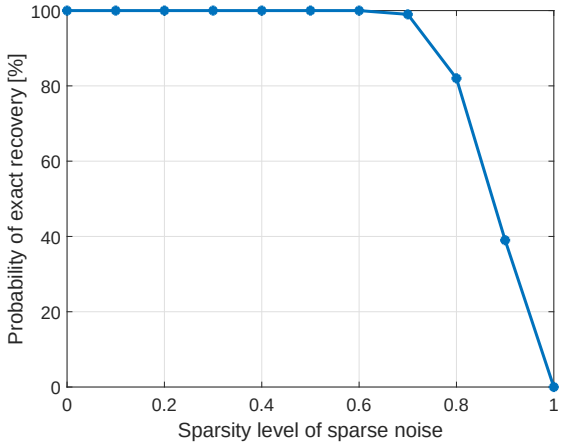

FIGURE 2.1: Probability of exact recovery (expressed in percentage) by the estimator (2.51) in the presence of only sparse measurement noise $\{s_t\}$. The level of sparsity of the noise is expressed in terms of a fraction of nonzero values in the sequence $\{s_t : t \in \mathbb{T}\}$ with $|\mathbb{T}| = T = 100$.

To investigate empirical performance, we consider different ratios $|\Lambda_0^c|/T$ of nonzero values in the sequence $\{s_t\}$. For each fixed proportion of nonzero values, we run the estimator over 100 different realizations of the output measurements. The results depicted in Figure 2.1 tend to show that the estimator can still find the true state even for proportions of gross errors as large as 60%.

2.7.2 Simulation studies of the r-Resilience index p_r

Following the discussion in Section 2.5.1 where we presented a way to overestimate the r-Resilience index $\tilde{p}_r$, we perform a few studies on this index to see how it is influenced by different parameters of the estimation problem. Moreover, we will restrict the case study to single-output system, *i.e.* $m = 1$. Consequently, we will rather talk about p_1 and p_r, given that for all r in $\mathbb{T}$, $p_r = \tilde{p}_r$ in this case.

Lemma 2.5, used to perform this overestimation, is stated in scenarios where $\{\phi_t\}$ are norms and $\psi_t = \|\cdot\|_1$ at all time. Consequently, throughout this section, we will consider $\mathcal{E}_{\ell_1,\ell_1}$ the state estimator from $\mathcal{E}$ defined by (2.4) with $\phi = \|\cdot\|_1$ and $\psi = \|\cdot\|_1$. The tests were performed for $\lambda = 100$ and $T = 100$ unless specifically stated otherwise.

Statistical properties of the 1-Resilience Index p_1

The first test we perform aims at checking how the estimator $\mathcal{E}_{\ell_1,\ell_1}$ is likely to be resilient to at least one corrupted measurement. This means that we check if $p_1 < 1/2$. We will also check the number of outliers that $\mathcal{E}_{\ell_1,\ell_1}$ is guaranteed to handle. This consists in computing $\tilde{r}_{\max} = 1/(2p_1)$. $\tilde{r}_{\max}$ is merely an underestimation of the actual number of outliers the estimator is able to handle, but gives a good idea of what we can expect from the estimator.

To perform this test, p_1 and $\tilde{r}_{\max}$ were computed for a hundred completely random stable systems generated through the `drss` function in MATLAB with $n = 2$ and $m = 1$. The results of this first test are presented in Figure 2.2.

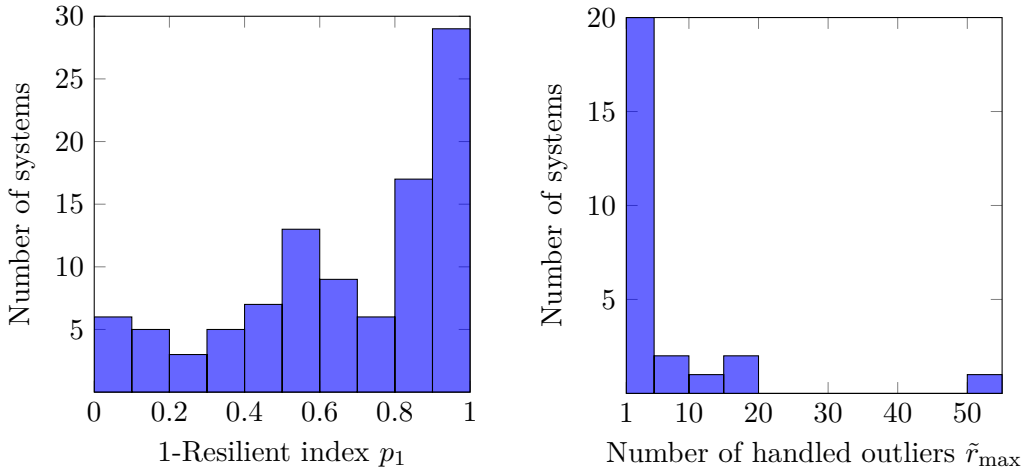

(A) (B)

FIGURE 2.2: Repartition of p_1 (A) and of $\tilde{r}_{\max}$ (B) among 100 randomly generated stable systems

A few observations can be drawn from those results. First of all, by looking at the repartition of p_1 among the generated systems (Figure 2.2a), there do exist systems for which p_1 is smaller than $1/2$, meaning that the class of systems to which Theorem 2.1 applies is not empty. However, most of the generated systems, namely 74% of them, have a $p_r \geq 1/2$.

If we omit the 76% of systems for which $\mathcal{E}_{\ell_1,\ell_1}$ is not resilient, we can have a look into the guaranteed number of outliers $\tilde{r}_{\max}$ that $\mathcal{E}_{\ell_1,\ell_1}$ can handle, yielding Figure 2.2b. Most of them, namely 20%, can handle between 1 and 5 outliers. We also notice that there is a system for which $\mathcal{E}_{\ell_1,\ell_1}$ is able to handle about 50 of

outliers, representing half of the potential entries of f_t given that $T = 100$. However, this system is such that $A = I_2$, making it a very particular case.

A first conclusion to this study is that a randomly generated system is not very likely to favour resilience properties in the estimator. This is due to the fact that its properties are probably not suited for resilient estimation. For instance, it can be too weakly observable.

A system can also present arbitrarily fast dynamics. $\mathcal{E}_{\ell_1,\ell_1}$ is less likely to be resilient for a system with fast dynamics given that the state can greatly vary throughout time. The dynamics of a discrete system are dictated by the modulus of the eigenvalues of A. The smaller the modulus, the faster the dynamics. As a result, assuming that the eigenvalues have a modulus greater than a given threshold is not an uncommon hypothesis. We therefore reiterated the aforementioned test and calculated p_1 for 100 randomly generated stable systems, with the condition that the smallest eigenvalue in modulus is bigger than 0.8: the results of this test were then presented in Figure 2.3.

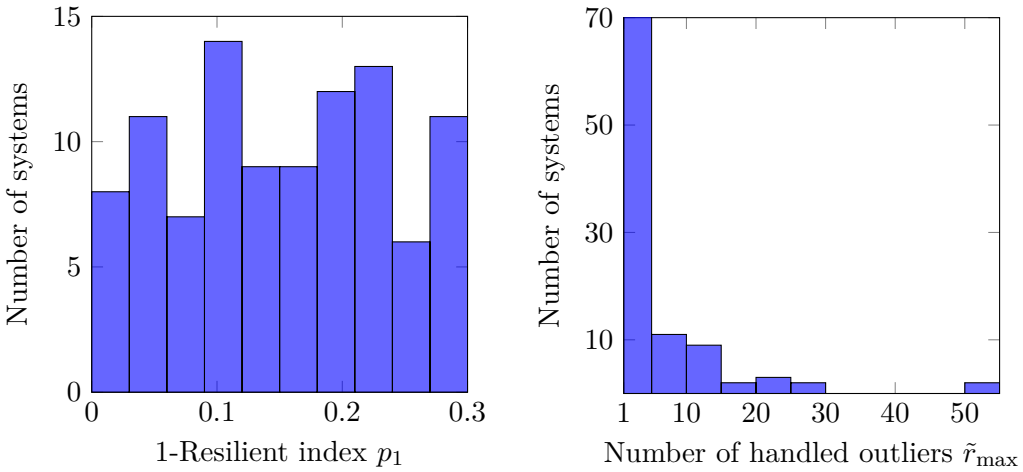

(A) (B)

FIGURE 2.3: Repartition of p_1 (A) and of $\tilde{r}_{\max}$ (B) among 100 randomly generated stable systems with a minimum eigenvalue modulus of 0.8

Contrary to the previous experiment, we see that $\mathcal{E}_{\ell_1,\ell_1}$ is resilient for every tested system, given that all the calculated p_1 were smaller than 0.3 (and therefore smaller than 1/2), as displayed in Figure 2.3a. This shows how the eigenvalues of the state matrix play a role in the resilience properties of the estimator when applied to a given system. If we consider the guaranteed number of handled outliers $\tilde{r}_{\max}$ (Figure 2.3b), we see that the values are distributed similarly to Test 1. For instance, the proportion of systems for which $\mathcal{E}_{\ell_1,\ell_1}$ can handle between 1 and 5 outliers represents 20 systems, so about 70% of them. This is roughly the same ratio obtained in Test 1 among the system for which $\mathcal{E}_{\ell_1,\ell_1}$ was resilient.

Role of λ in the value of p_1

The second test we conducted aimed at highlighting how the value of λ influences the value of p_1. This test consisted in calculating the 1-Resilient index p_1 of system (1.21)

for different values of λ from 10^{-3} to $5 \cdot 10^3$. The obtained results can be found in Figure 2.4.

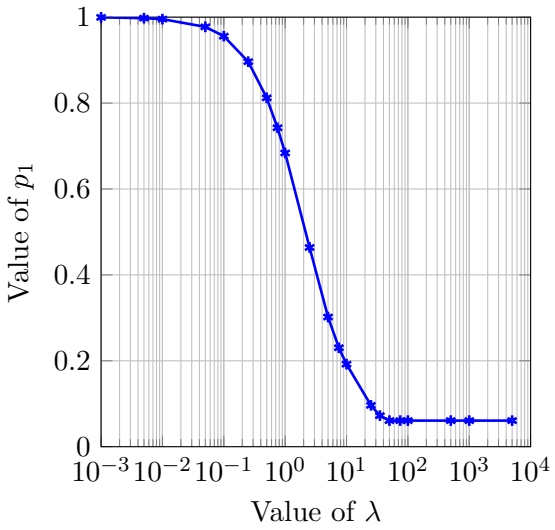

FIGURE 2.4: Value of the 1-Resilient index Parameter p_1 in function of λ for System (1.21)

Figure 2.4 shows that λ does indeed play a role in the value p_1. p_1 is decreasing when λ grows, meaning that the number of outliers the estimator is able to handle grows with λ. To further discuss this, we recall the expression of p_1 for $\mathcal{E}_{\ell_1,\ell_1}$ applied to System (1.21):

$$p_1 = \sup_{\substack{Z \in \mathbb{R}^{n \times T} \\ Z \neq 0}} \max_{\tau \in \mathbb{T}} \frac{|Cz_\tau|}{\lambda \sum_{t \in \mathbb{T}'} \|z_{t+1} - Az_t\|_1 + \sum_{t \in \mathbb{T}} |Cz_t|}.$$

In p_1, λ weights the sum representing the contribution of the system dynamics. When λ tends to 0, the limit of p_1 is 1. This result shows that we are not able to handle any outlier at all when we completely ignore the state evolution model or the system dynamics. On the other hand, when λ grows towards infinity, p_1 seems to converge towards a value, which is equal to 0.0607 in this case. Nevertheless, it is worth noting that a smaller p_1 only guarantees that the estimator will be able to handle more outliers, but does not prefigure a small estimation error, as it will be discussed later on.

The influence of the time-horizon T on p_1

For this test, we calculated several values of p_1 for different values of the time-horizon T ranging from 10 to 1000. The goal is to see if the value of p_1 will change, but also look at the ratio of corrupted measurements that the estimator can handle over the time horizon, namely $\tilde{r}_{\max}/T$. The results of this test are presented in Figure 2.5.

If we consider Figure 2.5a, we can see that p_1 indeed decreases when the time horizon increases. This confirms the intuition that an estimator is more likely to be able to handle one outlier corrupting a measurement if it is compensated by many sane measurements. However, p_1 seems to be converging towards 0.0595 when T grows. As a result, the ratio of guaranteed outliers that $\mathcal{E}_{\ell_1,\ell_1}$ can handle in System (1.21) plunges towards zero when the time horizon increases (Figure 2.5b). The best ratios are achieved for the smallest time-horizon tested, namely $T = 10$ and $T = 25$.

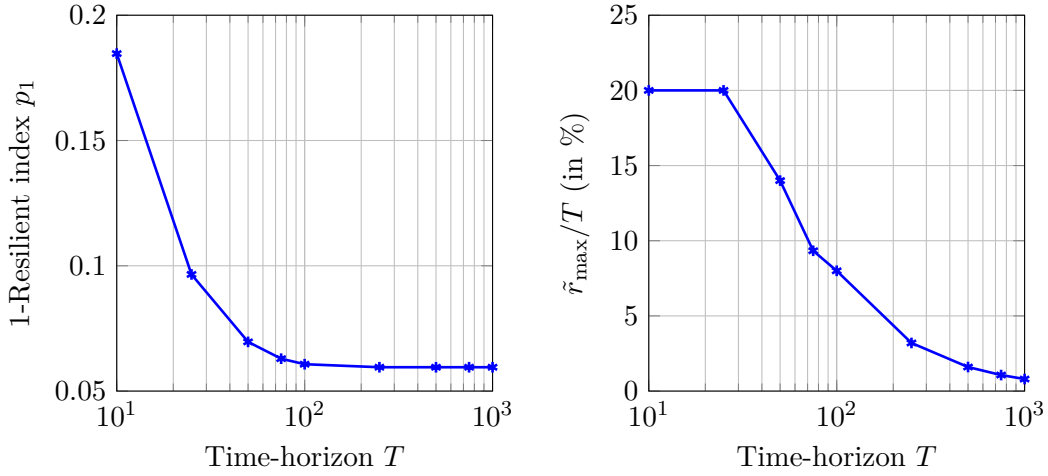

(A) (B)

FIGURE 2.5: 1-Resilient index p_1 (A) and tolerated outlier ratio $\tilde{r}_{\max}/T$ (B) in function of the time-horizon T of the state estimation for System (1.21)

There seems to be a limit to how many additional sane measurements help the estimator to handle one outlier. This phenomenon is similar to the one observed in the exact recoverability test (see Section 2.7.1). When A is Schur stable and T grows, the terms CA^t get smaller when t increases. Consequently, less and less information is brought by additional rows in the observability matrix, which, in the context of the calculation of p_1, means that the terms in $H_\Sigma(Z)$ can have different orders of magnitude[3].

To preserve the contribution of each term in $H_\Sigma(Z)$, we redefine both families of weighting matrices $\{W_t\}$ and $\{V_t\}$ (defined in (2.2)–(2.3)). For all t in $\mathbb{T}$, $V_t = \nu_t[1]$ is a sclar as specified by (2.79). For all t in $\mathbb{T}'$, W_t, which is a matrix from $\mathbb{R}^{2\times 2}$, is defined such that $W_t = \mathrm{diag}(\nu_t[1], \nu_t[1])$. Each term is then expected to share the same order of magnitude. It is also worth noting that as T can be a large time window, the values $1/\|c_j^\top A^t\|_2$ grows to be really large which can cause conditioning problems in the calculation process: therefore, a threshold is applied in order to saturate the weighting coefficient at 1000. p_1 was then calculated for different values of T between 10 and 1000, and the obtained results can be found in Figure 2.6.

As we can see in Figure 2.6a, with normalised terms in H_Σ, p_1 seems to converge towards zero, which subsequently makes the ratio of outliers tolerated by $\mathcal{E}_{\ell_1,\ell_1}$ converge towards 50% after a dent at $T = 250$. This is a first improvement compared to the first case presented in Figure 2.5.

Another improvement is the fact that the normalisation made p_1 much smaller, and therefore made $\tilde{r}_{\max}/T$ much greater. According to Figure 2.6b, the estimator should even be able to handle 100% of outliers for $T = 10$ and $T = 25$. According to Theorem 2.1, even if all the available measurements are corrupted, the estimation error should still be bounded in theory. This means that the estimator does not rely on the available measurements at all, but solely on the information brought by the state model of the system. A possibility is that for small time-horizons, λ, weighing the terms assessing the compliance with the state model in V_Σ (2.1), needs to be

[3] $H_\Sigma(Z)$ is involved in the computation of p_1, see Eq. (2.25).

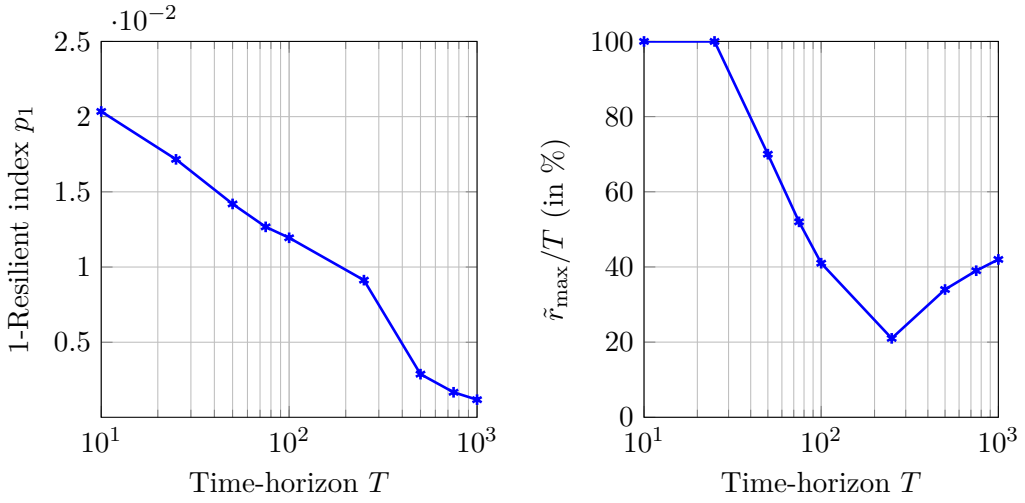

(A) (B)

FIGURE 2.6: 1-Resilient index p_1 (A) and tolerated outlier ratio $\tilde{r}_{\max}/T$ (B) in function of the time-horizon T of the state estimation for System (1.21) with normalised terms in H_Σ

chosen smaller than with longer time-horizons. The bound on the estimation error is likely to be loose, which is not contradictory with the value of p_1 as already stated (a small p_1 does not prefigure a tight bound on the estimation error).

For larger time windows, p_1 guarantees the resilience of the estimator for ratios of corrupted measurements smaller than 100%, but they are still higher than the one obtained without the normalization for the same time horizon. This is partly due to the fact that the underestimation $\tilde{r}_{\max}$ of $r_{\max}$ provided by p_1 is more accurate than in the case without normalisation: as every term in V_Σ is now of the same order of magnitude, so are the terms in the numerator of p_r (see Eq. (2.26)). Each term representing a corrupted measurement in the numerator of p_r should therefore have a similar value, which makes the overestimation of p_r as rp_1 more relevant.

Conclusion to this study

The major conclusion from the study of the r-Resilience index p_r is that there exist systems for which it is smaller than $1/2$, meaning that the class of estimators to which the framework developed in this chapter applies is non-empty. The value of p_1, and subsequently the value of p_r, is influenced by the studied system: for instance, the greater the eigenvalues of A (in modulus), the more likely p_1 is to be smaller than $1/2$, and even small enough to allow outliers. In the case where the to-be-observed system has fast dynamics, meaning the modulus of its eigenvalues are small, and resampling the system is impossible, one can shift the position of the eigenvalue through output injection, also known as *feedback*, given that the system is observable. More precisely, we can apply the estimation method to the system

$$\begin{cases} x_{t+1} &= (A - LC)x_t + Ly_t + Lf_t + w_t \\ y_t &= Cx_t + f_t \end{cases}$$

given that we can place the eigenvalues of $(A-LC)$ wherever we want on the complex plane under the observability assumption. However, it is worth noting that this method brings sparse noise in the state equation, which is still within the estimator scope of application.

p_r also depends on the parameters of the estimator, such as λ, which lowers p_1 when it grows larger, or the horizon over which the estimation process takes place which lowers p_1 to some extent when it grows but ultimately worsen the ratio of tolerated corrupted measurements over the whole set of measurements.

To mitigate this issue, one can perform different things: for instance, we can decide to use the estimator as sliding-horizon estimator, splitting the time window into smaller ones and then estimate the state trajectory on each small window. One can also normalise the contributions of each term in the performance index V_Σ and therefore in $H_\Sigma(Z)$ which is used to compute p_1 (see Eq. (2.70)). This results in the ratio of tolerated corrupted measurements not converging towards zero when the time horizon T grows towards infinity. However, the parameter λ also needs to be re-evaluated to prevent the estimator from not relying on the available measurements.

All the aforementioned improvements were proposed in order to have a guaranteed number of tolerated corrupted measurements $\tilde{r}_{\max}$ as large as possible. As mentioned several times during the experiment, this value, and p_1 value as well, only indicates that the estimation error will be bounded in presence of the according number of outliers (which are virtually unbounded). To actually assess the performances, *i.e.* how small the estimation error is, we decided on simulating the estimation process given that the upper bound derived in Theorem 2.1 is not easily computable in practice.

2.7.3 Performances of the estimators in the presence of dense noise

In the previous section, we considered the case of the exact recoverability (*i.e.* in the absence of dense noise) and the theoretical prospect of the number of corrupted measurements that one instance of the class $\mathcal{E}$ (namely $\mathcal{E}_{\ell_1,\ell_1}$) can handle based on the calculation of the 1-Resilience index. We consider now the more practical scenario where we look at the estimation error of several instances of the class $\mathcal{E}$ when applied to System (1.21) in the case were both $\{w_t\}$ and the dense component of the measurement noise $\{v_t\}$ (see Eq. (1.49)) are nonzero. We further assume them to be bounded, white and uniformly distributed. For the numerical experiments these signals are uniformly sampled from an interval of the form $[-a, a]$.

To conduct the performance tests, we implemented the following estimators:

- The estimator $\mathcal{E}^\circ$ which instantiates the one defined in (2.51) for $\phi = \|\cdot\|_1$ (already studied in Section 2.7.1).
- The estimator $\mathcal{E}_{\ell_2^2,\ell_1}$ which instantiates estimator $\mathcal{E}$ defined in (2.4) for $\phi = \|\cdot\|_2^2$, $\psi = \|\cdot\|_1$ and $\lambda = 1000$.
- The estimator $\mathcal{E}_{\ell_1,\ell_1}$ which instantiates estimator $\mathcal{E}$ defined in (2.4) for $\phi = \|\cdot\|_1$, $\psi = \|\cdot\|_1$ and $\lambda = 10$ (already studied in Section 2.7.2).

To provide comparison, we will also consider Oracle estimators: the term "Oracle" indicates estimators will work with the unaltered output of the system $\tilde{y}_t = y - s_t$ with s_t being the arbitrary component of f_t (see Eq (1.49)). Indeed, Oracle $\mathcal{E}_{\ell_2^2,\ell_1}$ was considered. Moreover, as a way to provide a lower limit of the performances which can be expected, an Oracle Least Squares (OLS), also called Oracle $\mathcal{E}_{\ell_2^2,\ell_2^2}$, will also be implemented: it was chosen as a reference for comparison given that it is the best estimator with regards to the covariance of the estimation error in presence of Gaussian noises [Gee05, p. 1041] and should therefore provide good results with bounded noises.

The performance indicator we choose is the Relative Estimation Error (REE), i.e.

$$\text{REE} = \frac{\|\hat{X} - X\|_2}{\|X\|_2} \tag{2.80}$$

where X is the real trajectory of the system and $\hat{X}$ is the estimated trajectory obtained from the estimator. For every setting, a hundred realisations with different noise values were performed, and the REE was subsequently averaged over those realisations in order to be plotted.

Experiment 1: Sparsity test

Keeping the level of both dense noises (i.e., w_t and v_t) fixed with amplitude $a = 0.03$ for the entries of the former and $a = 0.1$ for the latter (yielding a Signal to Noise Ratio (SNR) of about 30 dB in each case), we apply the estimators defined above to 100 different realizations of the output data and we compute the average of the corresponding REE. This process is repeated for different fractions of nonzeros in the sparse noise $\{s_t\}$ ranging from 0 to 1. The estimates obtained by these estimators are displayed in Figure 2.7a in log scale. The results tend to show that the estimator (2.4) remains stable until the (empirical) resilience condition is violated (an event that happens when the sparsity level for the sparse noise is around 60%). This is consistent with the resilience property characterized in Theorem 2.1 and the empirical observations made in Section 2.7.1 according to which the estimator is insensitive to the sparse noise sequence $\{s_t\}$ as long as the number of nonzero values in it (whose magnitudes are possibly arbitrarily large) is less than a certain threshold determined by the properties of the system.

While Lemma 2.5 provides an underestimate of the number of correctable outliers as $r_{\max} = 8$ (out of 100), in the current example, we can observe that the empirical breakpoint, *i.e.* the sparsity level over which the average REE starts diverging, seems to be indeed around 40%. The discrepancy between the two values is partly explained by the pessimism of the upper bound of p_r proposed in Lemma 2.5.

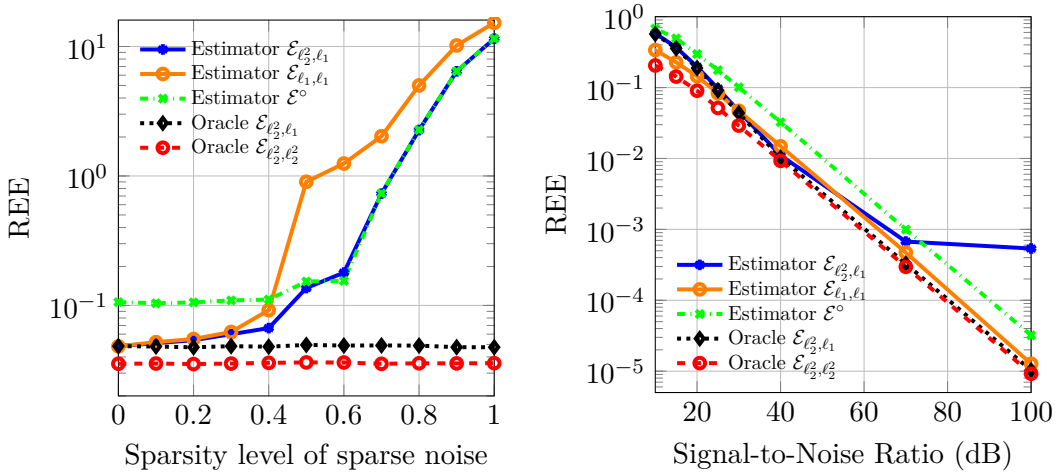

(A) Sparsity test (B) SNR test

FIGURE 2.7: Average relative estimation error (in logarithm scale) induced by different estimators versus sparsity level of the sparse noise $\{s_t\}$ (left) and for different levels of both dense noises w_t and v_t (right)

Experiment 2: SNR test. Now, we fix the sparsity level of the time sequence $\{s_t\}$ to 0.2 and let the powers of the dense noise $\{(w_t, v_t)\}$ vary jointly from 5 dB to 100 dB in term of SNR. The results obtained for the implemented estimators are displayed in Figure 2.7b.

What this illustrates is that, whenever the number of faulty data is reasonable (here 20% of the available measurements), the estimator discussed in this section behaves almost in the same way as when there is no faulty data at all.

Experiment 3: Study of the influence of λ

In this study, we fixed both the amplitude of the dense noises (to their level in the first test, *i.e.* with an SNR of 30dB, and the ratio of nonzero entries of $\{s_t\}$ (to 30%) in order to assess the influence of λ on the performances of $\mathcal{E}_{\ell_2^2,\ell_1}$ and $\mathcal{E}_{\ell_1,\ell_1}$. To do so, for several values of λ, we performed a hundred realisations with system (1.21) and different noise configurations to obtain the averaged Relative Estimation Error (REE). The results of this test are presented in Figure 2.8.

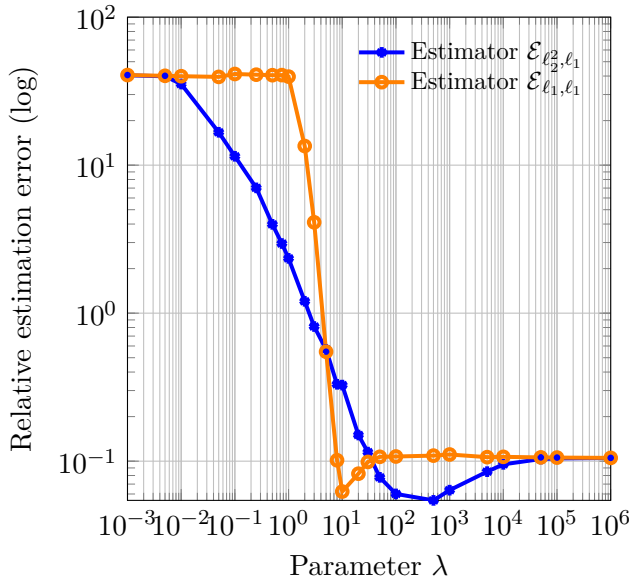

FIGURE 2.8: Averaged REE induced by $\mathcal{E}_{\ell_2^2,\ell_1}$ and $\mathcal{E}_{\ell_1,\ell_1}$ for System (1.21), SNR= 30dB and 30% of non-zero entries in $\{s_t\}$ for different values of the regularisation parameter λ

In Figure 2.8, we can observe that lower values of λ yield very poor results. This is due to the fact that λ is the parameter weighing the terms assessing the compliance of the potential state trajectory with the system dynamics in the definition of the performance index V_Σ (see Eq. (2.1). A low λ means that the terms assessing the adequacy of the estimate with the dynamics of the system is completely outweighed by the terms fitting the estimation to the available measurements. As a result, when some of these measurements are corrupted, the estimation is likely to try to fit them and therefore yields poor results. Conversely, when λ tends towards infinity, both estimators' performances converge towards the same value, namely 10^{-1}. This is the invert phenomenon which is at stake here, as a very high λ puts so much emphasis on the terms assessing the dynamics of the system that the obtained estimated trajectory is structured with the state matrix, i.e. $\hat{x}_{t+1} \approx A\hat{x}_t$ for $t \in \mathbb{T}'$. As a corroborating observation to back this idea up, the value towards which the performances of the

estimator converge is the actual value obtained for $\mathcal{E}^\circ$ in *Experiment 1* in the exact same configuration (SNR= 30dB and 30% of non-zero entries in $\{s_t\}$).

Moreover, it can be noted that between those two extremes, there exists a value for λ, called $\lambda_{\min}$, such that the average REE is minimal: this value is different for both estimators, and is equal to $\lambda_{\min} = 750$ for $\mathcal{E}_{\ell_2^2,\ell_1}$ and $\lambda_{\min} = 1$ for $\mathcal{E}_{\ell_1,\ell_1}$. In both cases, $\lambda_{\min}$ was not used to implement the estimators since it depends on the sparsity ratio studied (30% here): the values used are of a similar order of magnitude ($\lambda = 1000$ for $\mathcal{E}_{\ell_2^2,\ell_1}$ and $\lambda = 10$ for $\mathcal{E}_{\ell_1,\ell_1}$).

If we recall the test assessing the influence of λ in the value of p_1 for $\mathcal{E}_{\ell_1,\ell_1}$ (see Fig. 2.4), the values for which the REE is the lowest is not a value for which p_1 is the lowest. Indeed, the value of p_r is involved in the bound on the estimation error (2.28) expressed in Theorem 2.1, and as it gets lower, the bound should be tighter. However, λ is also involved in other quantities in the bound, namely $\beta_\Sigma(\varepsilon)$ and D, making its influence on the bound nontrivial to assess. As a result, the low value of p_1 is only a way to assess how many corrupted measurements the estimator would be able to handle, but it does not guarantee a small bound.

Experiment 4: Impact of the normalisation in the performances of $\mathcal{E}_{\ell_1,\ell_1}$

In the conclusion of the tests performed in Section 2.7.2, one advice to guarantee as many tolerated corrupted measurements as possible was to normalise the contribution of each term composing V_Σ defined in (2.1) in order to compensate the decrease (in norm) of the rows of the observability matrix. To assess the influence of the normalisation on the performances of the estimator, *i.e.* on the estimation error, we conducted the test performed in *Experiment 1* on a normalised version of $\mathcal{E}_{\ell_1,\ell_1}$. The results obtained by both the regular $\mathcal{E}_{\ell_1,\ell_1}$ and normalised $\mathcal{E}_{\ell_1,\ell_1}$ are presented in Figure 2.9 for $\lambda = 10$ and $\lambda = 100$, for a total of four instances of $\mathcal{E}$ presented.

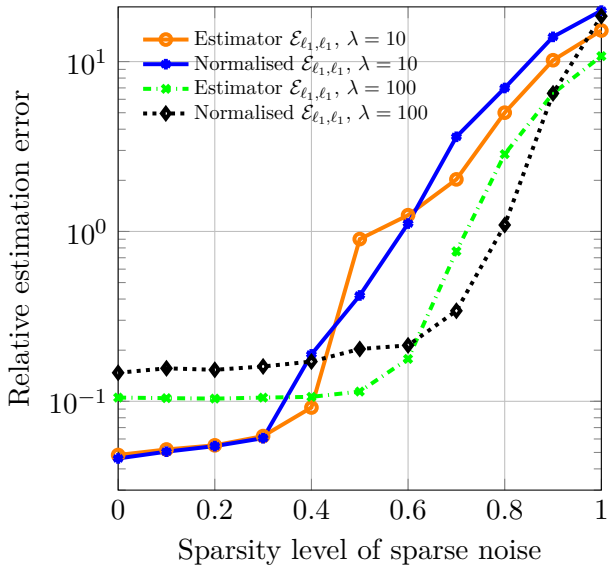

FIGURE 2.9: Averaged REE for System (1.21) , SNR= 30dB and 30% of non-zero entries in $\{s_t\}$ in function of λ

For $\lambda = 100$, the normalised $\mathcal{E}_{\ell_1,\ell_1}$ seems to have a larger breakpoint compared to regular $\mathcal{E}_{\ell_1,\ell_1}$, namely 60% instead of 50%. This is consistent with the intuition that normalising helps make the most out of every measurement available.

Regarding the actual value of the averaged REE, comparing $\mathcal{E}_{\ell_1,\ell_1}$ and Normalised $\mathcal{E}_{\ell_1,\ell_1}$ for the same value of λ reveals two different behaviours: for $\lambda = 10$, the two estimators return very similar results until the breakpoint of $\mathcal{E}_{\ell_1,\ell_1}$. However, for $\lambda = 100$, the relative estimation error of the normalised version of $\mathcal{E}_{\ell_1,\ell_1}$ is significantly larger than the one of the regular $\mathcal{E}_{\ell_1,\ell_1}$. Therefore, the normalisation does not necessarily comes with a deterioration in the estimator performances, but there is potentially a need to tune λ differently in order for the terms assessing the compliance of the trajectory with the state model to not outweigh the other terms in V_Σ.

It is also worth noting that for $T = 100$, the guaranteed ratio of corrupted measurements $\tilde{r}_{\max}/T$ that Normalised $\mathcal{E}_{\ell_1,\ell_1}$ is able to handle is 17% for $\lambda = 10$ and 41% for $\lambda = 100$, which highlights the fact that $\tilde{r}_{\max}$ is an underestimation of the actual maximum number of corrupted measurements that the estimator can handle, since the effective breakpoint ratios seems to be larger. The fact that the instances of sparse noise generated do not account for all the possible configurations of the sparse noise can also explain why the estimator is resilient to larger ratios of corrupted measurements than the study of $\tilde{r}_{\max}$ would have suggested.

Experiment 5: Comparison with the recursive algorithm

In order to study the performance of the recursive implementation discussed in Section 2.6, we implemented the recursive estimator $\mathcal{E}_{\text{online}}$ through Algorithm 2.1 with the values $\gamma = 0.05$, $\mu = 5$, $\varepsilon = 10^{-5}$, $P_0 = I_2$ and $\hat{x}_0$ a random vector whose entries are uniformly chosen between 0 and 1. We then performed the same test described in *Experiment 1*. The results are presented in Figure 2.10 and as a mean of comparison, the results of the $\mathcal{E}_{\ell_2^2,\ell_1}$ and the Oracle $\mathcal{E}_{\ell_2^2,\ell_2^2}$ are provided.

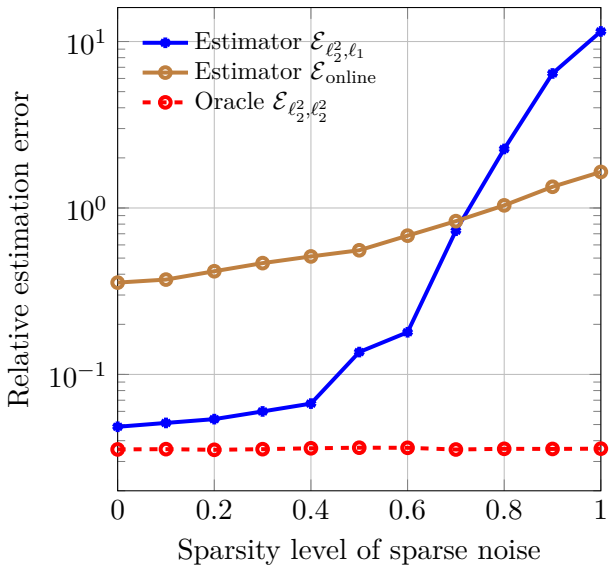

FIGURE 2.10: Averaged REE of batch and recursive estimators for System (1.21)

The first observation which can be made is that contrary to the batch algorithm, the performances of $\mathcal{E}_{\text{online}}$ vary way less as the ratio in non-zero entries of $\{s_t\}$ increases, with the value of the average REE going from 0.36 for a ratio of 0% to 1.65 for 100%. This can be explained by the fact that a resilient recursive estimator is not affected by the overall ratio of outliers across the whole time-horizon the same way as a batch estimator. Indeed, if the recursive estimator is able to recover between

two non-zero occurrences of s_t, then the second outlier would be considered as the first encountered by the estimator. As a result, a recursive estimator is probably more affected by the average time between two outliers than their overall number of occurrences.

This being said, it can be noted that the average estimation error of the recursive estimator is way higher than the one of $\mathcal{E}_{\ell_2^2,\ell_1}$ for ratios up to 70%, and is, logically, far from the limit of performances indicated by Oracle $\mathcal{E}_{\ell_2^2,\ell_2^2}$. How to explain this behaviour?

To further investigate this topic, we simulated the state trajectories of System (1.21) with a given noise configuration (SNR= 20dB for $\{w_t\}$, SNR= 30dB for $\{v_t\}$, 30% of non-zero entries in $\{s_t\}$). The evolution of the sparse noise $\{s_t\}$ through time as well as the statistical repartition of the gap lengths between two consecutive non-zero entries of s_t[4] can be found in Figure 2.11.

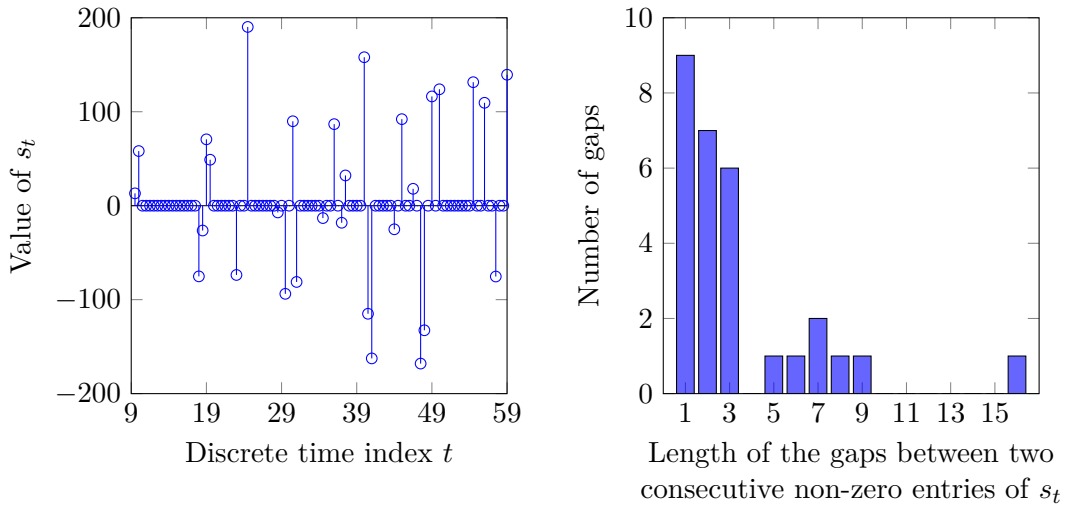

(A) Value of s_t through time

(B) Repartition of gaps between two consecutive non-zero entries of s_t by gap length

FIGURE 2.11: Evolution of s_t through time and repartition of the gaps between consecutive non-zero entries

We then estimated this trajectory with estimators $\mathcal{E}_{\text{online}}$ and $\mathcal{E}_{\ell_2^2,\ell_1}$, and every trajectories are represented in Figure 2.12. We can notice that as every recursive estimator, Algorithm 2.1 presents a transient before converging towards the real state due to the fact that the initial state is set *a priori* without any knowledge about the actual initial state of the system in our implementation. On the contrary, the batch estimator estimates every early values with regards to posterior measurements as well, which makes it fit the real state trajectory better in the early samples.

However, once it has converged, $\mathcal{E}_{\text{online}}$ returns a state trajectory which is on par with the one returned by $\mathcal{E}_{\ell_2^2,\ell_1}$. It is even able to locally estimate the trajectory better, such as on the segment $[89, 100]$ for both states. As the performance indicator we chose, the REE, is computed over the whole trajectory, it will be inherently greater for the recursive estimator because of this transient.

Nevertheless, the presence of the transient does not single-handedly explain the gap in REE, so it is important to put the performances of $\mathcal{E}_{\text{online}}$ into perspective, as

[4] A gap is an interval of the form $[t_1, t_2]$ where t_1, t_2 in $\mathbb{N}$ are such that $t_1 < t_2$, $s_{t_1-1} \neq 0$, $s_{t_2+1} \neq 0$ and $s_t = 0$ for $t \in [t_1, t_2]$.

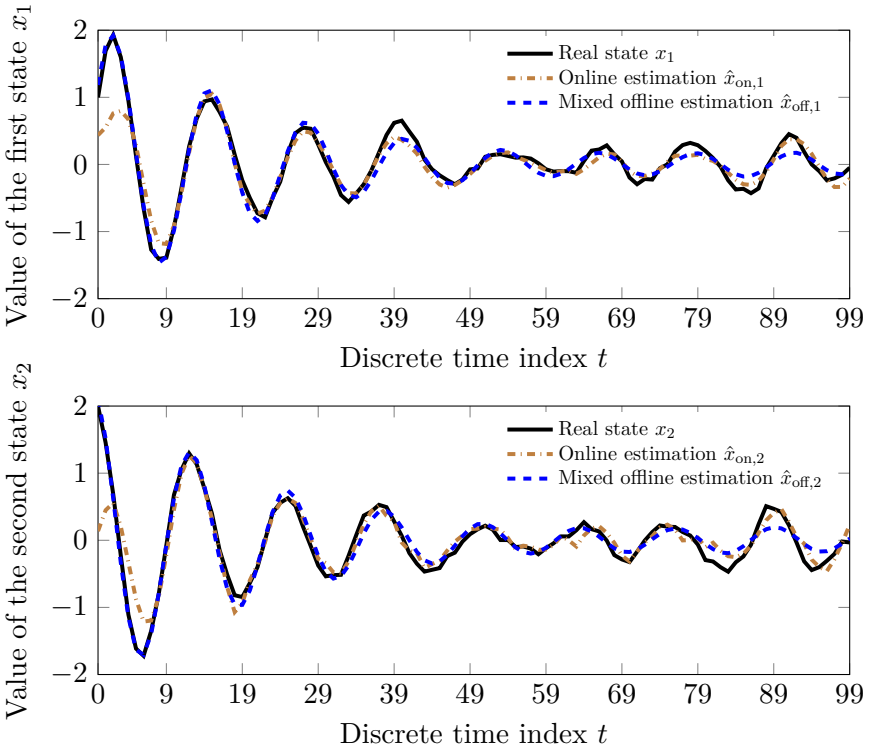

FIGURE 2.12: Trajectory of the states of System (1.21) with a given configuration of noises and the estimated state trajectories returned by $\mathcal{E}_{\text{online}}$ and $\mathcal{E}_{\ell_2^2,\ell_1}$

it is an approximative recursive implementation of the class $\mathcal{E}$. It is therefore normal to obtain worse performances than for $\mathcal{E}_{\ell_2^2,\ell_1}$ which directly solves the optimisation problem defining the estimator.

We note also that this difference in performances comes with a difference in computational complexity: indeed, on one hand, Algorithm 2.1 has the same structure as a Kalman Filter, *i.e.* solely composed of matrix formulas, while on the other hand, $\mathcal{E}_{\ell_2^2,\ell_1}$ estimation is obtained through a "primal-dual interior-point algorithm that uses the path-following paradigm" [Tü03] implemented in the SDPT3 Solver used by CVX. This algorithm is way more complex than the Kalman Filter one, which subsequently provides drastically different computation times: on average, estimating the whole trajectory over a time-horizon of 100 samples takes 7ms for $\mathcal{E}_{\text{online}}$ compared to 1.2s for $\mathcal{E}_{\ell_2^2,\ell_1}$.

To conclude this study, both the batch and the recursive implementations have their advantages: the estimators in batch will provide an overall better estimated trajectory, even for the first samples on the time horizon, but at the cost of a complex implementation necessitating convex optimization methods. The recursive estimator will need a few samples in order to converge towards the real state, but once it has been able to converge, it will yield similar results to the batch estimators, and with a lighter complexity.

2.8 Conclusion

In this chapter, to solve the estimation problem stated at the end of Chapter 1, we studied a class of estimators based on the resolution of a family of parametrisable

optimisation problems. The discussed family is rich enough to include optimisation-based estimators based on various loss functions which may be convex (e.g., ℓ_p-norms) or nonconvex (e.g., ℓ_p quasi-norms or saturated functions), smooth or nonsmooth. In particular, we have proved a resilience property for the proposed class of state estimators, that is, the resulting estimation error is bounded by a bound which is independent of the extreme values of the measurement noise provided that the number of occurrences (over time and over the whole set of sensors) of such extreme values is limited. Note however that the estimators studied here operate in batch mode, that is, they apply to a finite collection of measurements. That is why we proposed an approximate recursive implementation of this class of estimators thanks to the Forward Dynamic Programming, which resulted in an algorithm resembling a Kalman Filter algorithm.

To corroborate the theoretical results obtained for this class of estimators, we performed three main simulation tests:

- Assessing the exact recoverability property of the estimator $\mathcal{E}^\circ$.
- Studying the r-Resilience index p_r in a case where it can be approached and the underlying parameters influencing its value.
- Studying the performances, *i.e.* the estimation error, for different instances of the class.

The obtained results showed that there are instances of the considered class of estimators which present the resilience property, and that the guaranteed number of corrupted measurements that an estimator is able to handle can be improved thanks to relevant choices of λ and the weighting matrices $\{W_t\}$ and $\{V_t\}$. However, there is a balance to find between the number of tolerated corrupted measurements and the quality of the bound on the estimation error, as privileging one of the two can deteriorate the other.

Finally, there are several approaches which could be done in order to complete or improve this framework, such as:

- Widening the considered class of estimators by either changing the structure of V_Σ or generalizing the properties that the loss functions have to verify.
- Finding a less conservative condition in order for more estimators from this class to present the resilience property.
- Develop ways to be able to approach more accurately p_r. In particular, in Section 2.7.2, it was observed that the 1-Resilience index p_1, most of the time, represented the case where the outlier is placed at $t = 0$. Investigating this phenomenon could lead to interesting developments, potentially making the computation of p_r easier.
- Reformulate the r-Resilience index in order to potentially take into account additional characteristics of the sparse noise disturbing the system.

Chapter 3

Approximately resilient estimators based on saturated objective functions

3.1 Introduction

If we recall what has been explained in Section 1.5.3, using saturated performance index functions to deal with disturbances of arbitrary magnitudes is intuitively a good idea given that the impact of large arguments saturates past a certain threshold. To tackle the resilient state estimation problem, the present chapter therefore studies an estimation framework based on the minimisation of performance index functions with saturated exponential losses.

Estimators derived from performance index functions with saturated exponential losses are already included in the class $\mathcal{E}$ studied in Chapter 2. In particular, Corollary 2.1.2 deals with the approximate resilience of estimators with exponential losses. However, this result only applies to a restricted set of estimators with exponential losses from $\mathcal{E}$. The current chapter aims at finding new theoretical results covering more estimators with exponential lossess, as well as addressing the problem of their implementation, a problem which was not tackled in Chapter 2.

First of all, the class of saturated performance index functions used in Chapter 3 will be defined (Section 3.2). Similarly to Chapter 2, those functions are defined through loss functions, which assess the compliance of every hypothetical state trajectory matrix with the dynamics of the system as well as with the measurement history. Those loss functions are defined through their properties, and present an exponential term which induces saturation when the magnitude of their argument tends towards infinity.

Subsequently, some theoretical results on the performances of the estimator will be provided (Section 3.3). The obtained provide insight on the interaction between the different parameters of the system and the performances of the estimator.

A reformulation of the class of estimators in the absence of dynamic dense noise will then be studied in Section 3.4. In this setting, we are able to derive an upper bound on the estimation error which shows the approximate resilience of the estimators when a condition linked to the observability of the system is met. A result on the robustness of the estimator to bounded dynamic dense noise (Section 3.4.3), as well as a numerical study on the condition for approximate resilience (Section 3.4.4), will also be provided.

Contrary to the estimation framework studied in Chapter 2, the framework studied in the present chapter only includes non-convex performance index functions. We

therefore discuss how to implement this class of estimators in Section 3.5, which results in several batch and recursive algorithms.

Finally, Section 3.6 focuses on the numerical assessment of the performances of the newly-derived algorithms. This includes an empirical study on the convergence of the algorithms, a study on the estimation error when the ratio of outliers and the SNR of the dense noises vary, and a study on the tuning of regularisation parameters in the estimators.

3.2 Optimal estimators based on exponential loss functions

3.2.1 Definition of the class of estimators

For the sake of simplicity, this chapter will be presented in the scope of LTI systems, *i.e.* systems of the form (1.2)

$$\begin{cases} x_{t+1} &= Ax_t + w_t \\ y_t &= Cx_t + f_t \end{cases}$$

with $x_0 \in \mathbb{R}^n$ the initial state of the system, and $\{w_t\}$, $\{f_t\}$ two arbitrary noise sequences. However, the developments can be extended easily to the LTV case.

To address the resilient estimation problem stated in Chapter 1 and estimate the state of an LTI Discrete-time system of the form (1.2), we propose another solution based on the optimisation of a performance function of the form

$$V_\Sigma^{\exp}(Y,Z) = \sum_{(t,i)\in\mathbb{T}'\times\mathbb{I}} \left(1 - e^{-\lambda_\phi \phi(z_{t+1}[i] - a_i^\top z_t)}\right) + \sum_{(t,j)\in\mathbb{T}\times\mathbb{J}} \left(1 - e^{-\lambda_\psi \psi(y_t[j] - c_j^\top z_t)}\right) \tag{3.1}$$

with $\lambda_\phi \in \mathbb{R}_{>0}$ and $\lambda_\psi \in \mathbb{R}_{>0}$ two user-defined parameters, $Z \in \mathbb{R}^{n\times T}$ the optimisation variable representing the hypothetical trajectory, and $\mathbb{I} = \{1,...,n\}$, $\mathbb{J} = \{1,...,m\}$ the index sets for the states and the outputs respectively. $\{a_i\}$, $\{c_j\}$ are two families of column vectors from $\mathbb{R}^n$ such that

$$A = \begin{pmatrix} a_1 & \cdots & a_n \end{pmatrix}^\top$$

$$C = \begin{pmatrix} c_1 & \cdots & c_m \end{pmatrix}^\top.$$

With $\mathbb{T}' = \{1,..,T-2\}$ and $\mathbb{T} = \{1,..,T-1\}$, there is a total of $|\mathbb{I}||\mathbb{T}'| + |\mathbb{J}||\mathbb{T}| = n(T-1) + mT$ terms within $V_\Sigma^{\exp}$: for convenience, we pose $N = n(T-1) + mT$, and sometimes, $V_\Sigma^{\exp}$ will be alternatively written such as

$$\forall Z \in \mathbb{R}^{n\times T},\ V_\Sigma^{\exp}(Y,Z) = N - \sum_{(t,i)\in\mathbb{T}'\times\mathbb{I}} e^{-\lambda_\phi \phi(z_{t+1}[i] - a_i^\top z_t)} - \sum_{(t,j)\in\mathbb{T}\times\mathbb{J}} e^{-\lambda_\psi \psi(y_t[j] - c_j^\top z_t)}.$$

The functions ϕ and ψ are defined from $\mathbb{R}$ to $\mathbb{R}_{\geq 0}$ and their properties will be discussed in the next section. If we compare $V_\Sigma^{\exp}$ defined in (3.1) with Equation (1.29) defining the general performance index function, we observe that the general families

of loss functions $\{\phi_t\}$ and $\{\psi_t\}$ correspond, in the present chapter, to

$$\phi_t(z) = \sum_{i\in\mathbb{I}} \left(1 - e^{-\lambda_\phi \phi(z[i])}\right) \quad \forall z \in \mathbb{R}^n, \tag{3.2}$$

$$\psi_t(z) = \sum_{j\in\mathbb{J}} \left(1 - e^{-\lambda_\psi \psi(z[j])}\right) \quad \forall z \in \mathbb{R}^m. \tag{3.3}$$

We are therefore in a case similar to the one presented in Section 2.3.4 (and Appendix B.4) where we dealt with attacks on individual sensors and actuators.

Remark 3.1. *For notational simplicity we consider here loss functions ϕ and ψ which are independent on time. The results presented in the current chapter can be extended to time-dependent ϕ_t and ψ_t. For instance, $\{\phi_t\}$ and $\{\psi_t\}$ could have a structure similar to the one in Chapter 2, i.e.*

$$\phi_t(z) = \sum_{i\in\mathbb{I}} \left(1 - e^{-\lambda_\phi \phi(W_{t,i} z[i])}\right) \quad \forall z \in \mathbb{R}^n,$$

$$\psi_t(z) = \sum_{j\in\mathbb{J}} \left(1 - e^{-\lambda_\psi \psi(V_{t,j} z[j])}\right) \quad \forall z \in \mathbb{R}^m,$$

where for all $t \in \mathbb{T}$, $i \in \mathbb{I}$, $j \in \mathbb{J}$, $W_{t,i}$ and $V_{t,j}$ are positive scalars.

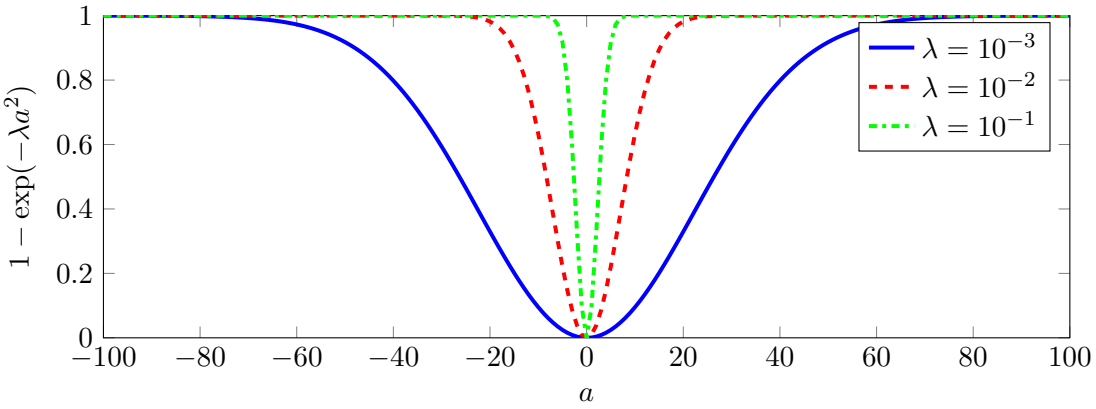

FIGURE 3.1: Plot of function $a \mapsto 1 - \exp(-\lambda a^2)$ for $\lambda \in \{10^{-1}, 10^{-2}, 10^{-3}\}$ over $[-100, 100]$

It is worth noting that the two user-defined parameters λ_ϕ and λ_ψ involved in the exponential terms in (3.1), play a different role than the user-defined parameter λ in the performance functions V_Σ defined in (2.1). In both definitions ((2.1) and (3.1)), the two sums involved in V_Σ and $V_\Sigma^{\exp}$ assess two different things: the left-hand sum assess the compliance of the hypothetical state trajectory with the dynamics of the system and the right-hand assesses the compliance of the trajectory with the obtained output of the system. Subsequently, in Chapter 2, the parameter λ was used in order to balance the contribution of those sums since their orders of magnitude could be different. However, in the present chapter, it does not appear necessary to introduce a balancing weight in (3.1) because each term in $V_\Sigma^{\exp}$ is between 0 and 1.

A new problem which arises is the sensitivity of each exponential term. Indeed, the point of exponential terms is that their value converges towards zero when the magnitude of their argument grows, but the speed at which the terms converge towards zero is something that needs to be tuned. As a mean of illustration, Figure 3.1

provides the plot of function $a \mapsto 1-\exp(-\lambda a^2)$ for three different values of λ. When the tuning parameter gets smaller, the curves gets flatter, and higher values of the argument have a non-zero image through the exponential. The two user-defined parameters λ_ϕ and λ_ψ entering the definition of $V_\Sigma^{\exp}$ are therefore used as a way to define a threshold for values to saturate.

Given the performance index function $V_\Sigma^{\exp}$ defined in (3.1), we define the estimator $\mathcal{E}^{\exp} : \mathbb{R}^{m\times T} \to \mathcal{P}(\mathbb{R}^{n\times T})$ by

$$\mathcal{E}^{\exp}(Y) = \underset{Z\in\mathbb{R}^{n\times T}}{\arg\min}\, V_\Sigma^{\exp}(Y,Z). \tag{3.4}$$

3.2.2 Basic properties verified by the loss functions

The properties which will be used to characterise the loss functions in this chapter are very similar to the one presented in Chapter 2. For the sake of clarity, they will be restated. Throughout this chapter, the term *loss functions* involved in the performance function $V_\Sigma^{\exp}$ defined in (3.1) will therefore describe functions from $\mathbb{R}$ to $\mathbb{R}_{\geq 0}$ which will respect following properties:

(P3.1) **Positive definiteness:** $\psi(0) = 0$ and $\psi(a) > 0$ for all non-zero real a.

(P3.2) **Symmetry:** $\psi(-a) = \psi(a)$ for all $a \in \mathbb{R}$.

(P3.3) **Non-decreasingness:** for any a_1, a_2 in $\mathbb{R}$, $|a_1| < |a_2|$ implies $\psi(a_1) \leq \psi(a_2)$.

(P3.4) **Generalized Triangle Inequality (GTI):** there exists $\gamma \in \mathbb{R}_{>0}$ such that for all a_1, a_2 in $\mathbb{R}$,

$$\psi(a_1 - a_2) \geq \gamma\psi(a_1) - \psi(a_2). \tag{3.5}$$

In the context of the exponential terms constituting the sums involved in $V_\Sigma^{\exp}$ (3.1), those properties aim at generalizing the approach used in the Maximum Correntropy Criterion (MCC) framework. As it was presented in Section 1.5.3, this approach is based on the information-theoretic concept of correntropy which is defined as a similarity measure between two random variables.

The point of defining loss functions through their properties is that class $\mathcal{E}^{\exp}$ includes kernel functions studied in the state estimation literature (see [Che17a] for the Gaussian kernel function and [Che17b] for the absolute value kernel function), but it also includes optimal state estimators which have not been studied yet. For example, class $\mathcal{E}^{\exp}$ includes absolute value power functions, *i.e.*

$$\forall a \in \mathbb{R},\ \xi(a) = e^{-\frac{|a|^p}{2\sigma^p}}$$

with $p \leq 1$ (see [Bak18] for the proof that the functions of the form $a \mapsto |a|^p$ verify properties (P3.1)–(P2.3)).

3.3 Analysis of the resilience

The point of this section is to provide a few analysis elements on the estimators $\mathcal{E}^{\exp}$ in the case where both $\{w_t\}$ and $\{f_t\}$ present outliers. The main result obtained in this section is an upper bound on an image of the estimation error. This result does not allow us to conclude on the resilience or the approximate resilience of $\mathcal{E}^{\exp}$, but it still enables a discussion about the impact of the different parameters of the system

on the estimation. Moreover, it helps proving a few properties of class $\mathcal{E}^{\exp}$, such as its correctness, *i.e.* the fact that it returns the true state when the system is noiseless.

3.3.1 Notational convention for the analysis

Before properly conducting the analysis, we pose a few conventions. First of all, for this section, we note

$$\mathbb{S}_1 = \mathbb{I} \times \mathbb{T}' \qquad \mathbb{S}_2 = \mathbb{J} \times \mathbb{T}. \tag{3.6}$$

Moreover, ϕ and ψ will be assumed to verify properties (P3.1)–(P3.4), and the constants with which they respect (P3.4) are noted γ_ϕ and γ_ψ respectively.

Finally, for $\mathcal{S}_1 \subseteq \mathbb{S}_1$ and $\mathcal{S}_2 \subseteq \mathbb{S}_2$, we define $\Phi_{\mathcal{S}_1} : \mathbb{R}^{n\times T} \to \mathbb{R}_{\geq 0}$ and $\Psi_{\mathcal{S}_1} : \mathbb{R}^{n\times T} \to \mathbb{R}_{\geq 0}$ the two following sums such that for all $Z \in \mathbb{R}^{n\times T}$,

$$\Phi_{\mathcal{S}_1}(Z) = \sum_{(i,t)\in\mathcal{S}_1} \left(1 - e^{-\gamma_\phi \lambda_\phi \phi(z_{t+1}[i] - a_i^\top z_t)}\right) \tag{3.7}$$

$$\Psi_{\mathcal{S}_2}(Z) = \sum_{(j,t)\in\mathcal{S}_2} \left(1 - e^{-\gamma_\psi \lambda_\psi \psi(c_j^\top z_t)}\right) \tag{3.8}$$

3.3.2 Elements of analysis

First of all, we define the following parameter, which is the counterpart of the r-Resilience index parameter p_r introduced in Chapter 2:

Definition 3.1. *Let r, r' be two nonnegative integers. Assume that the system Σ in (1.2) is observable on $[0, T-1]$. We then define the (r, r')-Resilience index of the estimator $\mathcal{E}^{\exp}$ in (3.4) (when applied to Σ) to be the real number $p^{\exp}_{r,r'}$ given by*

$$p^{\exp}_{r,r'} = \sup_{\substack{Z\in\mathbb{R}^{n\times T}\\ Z\neq 0}} \sup_{\substack{\mathcal{S}_1\times\mathcal{S}_2\subset\mathbb{S}_1\times\mathbb{S}_1\\ |\mathcal{S}_2|=r\\ |\mathcal{S}_2|=r'}} \frac{\Phi_{\mathcal{S}_1}(Z) + \Psi_{\mathcal{S}_2}(Z)}{\Phi_{\mathbb{S}_1}(Z) + \Psi_{\mathbb{S}_2}(Z)} \tag{3.9}$$

where Φ and Ψ are as defined in (3.7)–(3.8).

Similarly to its counterpart in Chapter 2, $p^{\exp}_{r,r'}$ can be interpreted as a quantitative measure of how much System Σ is observable. Its structure is fairly similar to the one of $\tilde{p}_{r,r'}$ presented in Appendix B.4 (see Eq. (B.14)), where the system was assumed to be operated in the presence of arbitrary noises in both the state equation and the measurement equation. The main difference lies in the way γ_ϕ and γ_ψ intervene in $p^{\exp}_{r,r'}$, as they are involved within the exponential terms due to the structure of the loss functions in the current chapter.

Moreover, we also need to partition the sets $\mathbb{S}_1$ and $\mathbb{S}_2$. More precisely, we consider the following subsets:

$$\Pi_\varepsilon = \{(t,i) \in \mathbb{S}_1 \ : \ \phi(w_t[i]) \leq \varepsilon\} \tag{3.10}$$

$$\Pi^c_\varepsilon = \{(t,i) \in \mathbb{S}_1 \ : \ \phi(w_t[i]) > \varepsilon\} \tag{3.11}$$

$$\Lambda_{\varepsilon'} = \{(t,j) \in \mathbb{S}_2 \ : \ \psi(f_t[j]) \leq \varepsilon'\} \tag{3.12}$$

$$\Lambda^c_{\varepsilon'} = \{(t,j) \in \mathbb{S}_2 \ : \ \psi(f_t[j]) > \varepsilon'\} \tag{3.13}$$

with $\varepsilon \geq 0$ and $\varepsilon' \geq 0$. Those sets allow us to partition $\mathbb{S}_1$ and $\mathbb{S}_2$ with respect to the reasonable values and the outliers in $\{w_t\}$ and $\{f_t\}$. The thresholds ε and ε', which are analysis tools, set the limit between reasonable and unreasonable values.

For the sake of simplicity, we can assume that the two thresholds verify $\lambda_\phi \varepsilon = \lambda_\psi \varepsilon'$. The analysis can be easily extended to the case where this assumption is not true, by redefining $p_{r,r'}$ to take ε and ε' into account.

Proposition 3.1. *Consider the system Σ defined by (1.2) with output Y together with the state estimator (3.4) in which the loss functions ϕ and ψ are assumed to obey (P3.1)–(P3.4). Denote with γ_ϕ and γ_ψ the constants associated with the GTI (P3.4). Let $\varepsilon \geq 0$ and $\varepsilon' \geq 0$ be such that $\lambda_\phi \varepsilon = \lambda_\psi \varepsilon'$ and set $r = |\Pi_\varepsilon^c|$ as well as $r' = |\Lambda_{\varepsilon'}^c|$. If the system is observable on $[0, T-1]$ and $p_{r,r'}^{\exp} < 1$, then for every $\hat{X} \in \mathcal{E}^{\exp}(Y)$,*

$$\frac{1}{N}\left(\Phi_{\mathbb{S}_1}(\hat{X} - X) + \Psi_{\mathbb{S}_2}(\hat{X} - X)\right) \leq \frac{1}{1 - p_{r,r'}^{\exp}}\left[e^{-\lambda_\phi \varepsilon} - \left(1 - \frac{r + r'}{N}\right)\left(e^{-2\lambda_\phi \varepsilon} + e^{-\lambda_\phi \varepsilon} - 1\right)\right] \tag{3.14}$$

with X the true state trajectory matrix and $N = n(T-1) + mT$.

Proof. Every $\hat{X} \in \mathcal{E}^{\exp}(Y)$ minimises the objective function $V_\Sigma^{\exp}$ in (3.1), which implies that

$$V_\Sigma^{\exp}(Y, \hat{X}) \leq V_\Sigma^{\exp}(Y, X)$$

with X being the true state trajectory matrix. More explicitly, this reads as

$$\sum_{(t,i)\in\mathbb{S}_1}\left(1 - e^{-\lambda_\phi \phi(\hat{x}_{t+1}[i] - a_i^\top \hat{x}_t)}\right) + \sum_{(t,j)\in\mathbb{S}_2}\left(1 - e^{-\lambda_\psi \psi(y_t[j] - c_j^\top \hat{x}_t)}\right) \leq \sum_{(t,i)\in\mathbb{S}_1}\left(1 - e^{-\lambda_\phi \phi(w_t[i])}\right) + \sum_{(t,j)\in\mathbb{S}_2}\left(1 - e^{-\lambda_\psi \psi(f_t[j])}\right)$$

By letting $e_t = \hat{x}_t - x_t$, it is easy to see that $\hat{x}_{t+1} - A\hat{x}_t = e_{t+1} - Ae_t + w_t$ and $y_t - C\hat{x}_t = f_t - Ce_t$. Plugging this in the above inequality gives

$$N - \sum_{(t,i)\in\mathbb{S}_1} e^{-\lambda_\phi \phi(e_{t+1}[i] - a_i^\top e_t + w_t[i])} - \sum_{(t,j)\in\mathbb{S}_2} e^{-\lambda_\psi \psi(f_t[j] - c_j^\top e_t)} \leq N - \sum_{(t,i)\in\mathbb{S}_1} e^{-\lambda_\phi \phi(w_t[i])} - \sum_{(t,j)\in\mathbb{S}_2} e^{-\lambda_\psi \psi(f_t[j])}$$

We now partition the terms in the Left-Hand Side (LHS) sums along the index sets Π_ε, Π_ε^c, $\Lambda_{\varepsilon'}$, $\Lambda_{\varepsilon'}^c$. This gives, through the GTI property,

$$\begin{aligned}
\forall (t,i) \in \Pi_\varepsilon, \quad & e^{-\lambda_\phi \phi(e_{t+1}[i] - a_i^\top e_t + w_t[i])} \leq e^{\lambda_\phi \phi(w_t[i])} e^{-\lambda_\phi \gamma_\phi \phi(e_{t+1}[i] - a_i^\top e_t)} \\
\forall (t,i) \in \Pi_\varepsilon^c, \quad & e^{-\lambda_\phi \phi(e_{t+1}[i] - a_i^\top e_t + w_t[i])} \leq 1 \\
\forall (t,j) \in \Lambda_{\varepsilon'}, \quad & e^{-\lambda_\psi \psi(f_t[j] - c_j^\top e_t)} \leq e^{\lambda_\psi \psi(f_t[j])} e^{-\lambda_\psi \gamma_\psi \psi(c_j^\top e_t)} \\
\forall (t,j) \in \Lambda_{\varepsilon'}^c, \quad & e^{-\lambda_\psi \psi(f_t[j] - c_j^\top e_t)} \leq 1
\end{aligned}$$

Knowing that for all (t,i) in Π_ε, $\phi(w_t[i]) \leq \varepsilon$, for all (t,j) in $\Lambda_{\varepsilon'}$, $\psi(f_t[j]) \leq \varepsilon'$ and given that $\lambda_\phi \varepsilon = \lambda_\psi \varepsilon'$, we obtain

$$|\Pi_\varepsilon| + |\Lambda_{\varepsilon'}| - e^{\lambda_\phi \varepsilon}\left[\sum_{(t,i)\in\Pi_\varepsilon} e^{-\lambda_\phi \gamma_\phi \phi(e_{t+1}[i]-a_i^\top e_t)} + \sum_{(t,j)\in\Lambda_{\varepsilon'}} e^{-\lambda_\psi \gamma_\psi \psi(c_j^\top e_t)}\right]$$
$$\leq N - (|\Pi_\varepsilon| + |\Lambda_{\varepsilon'}|)e^{-\lambda_\phi \varepsilon} - \sum_{(t,i)\in\Pi_\varepsilon^c} e^{-\lambda_\phi \phi(w_t[i])} - \sum_{(t,j)\in(t,j)\in\Lambda_{\varepsilon'}^c} e^{-\lambda_\psi \psi(f_t[j])}$$

By getting rid of the last two sums in the Right-Hand Side (RHS), and knowing that $|\Pi_\varepsilon| + |\Lambda_{\varepsilon'}| = N - (r + r')$, the previous inequality implies

$$\sum_{(t,i)\in\Pi_\varepsilon}\left(1 - e^{-\lambda_\phi \gamma_\phi \phi(e_{t+1}[i]-a_i^\top e_t)}\right) + \sum_{(t,j)\in\Lambda_{\varepsilon'}}\left(1 - e^{-\lambda_\psi \gamma_\psi \psi(c_j^\top e_t)}\right)$$
$$\leq Ne^{-\lambda_\phi \varepsilon} - \left(N - (r + r')\right)\left(e^{-2\lambda_\phi \varepsilon} + e^{-\lambda_\phi \varepsilon} - 1\right)$$

The LHS can be identified as $\Phi_{\Pi_\varepsilon}(E) + \Psi_{\Lambda_\varepsilon}(E)$ with $E = \hat{X} - X$. By dividing both sides by N, this eventually yields

$$\frac{1}{N}\left(\Phi_{\Pi_\varepsilon}(E) + \Psi_{\Lambda_\varepsilon}(E)\right) \leq e^{-\lambda_\phi \varepsilon} - \left(1 - \frac{r + r'}{N}\right)\left(e^{-2\lambda_\phi \varepsilon} + e^{-\lambda_\phi \varepsilon} - 1\right) \tag{3.15}$$

By definitions (3.7) and (3.8) of Φ and Ψ, we have

$$\Phi_{\Pi_\varepsilon}(E) + \Psi_{\Lambda_\varepsilon}(E) = \Phi_{\mathbb{S}_1}(E) + \Psi_{\mathbb{S}_2}(E) - \Phi_{\Pi_\varepsilon^c}(E) + \Psi_{\Lambda_\varepsilon^c}(E)$$

which, given that $|\Pi_\varepsilon^c| = r$ and $|\Lambda_{\varepsilon'}^c| = r'$, entails

$$\Phi_{\Pi_\varepsilon}(E) + \Psi_{\Lambda_\varepsilon}(E) \geq (1 - p_{r,r'}^{\exp})\left(\Phi_{\mathbb{S}_1}(E) + \Psi_{\mathbb{S}_2}(E)\right),$$

by definition (3.9) of $p_{r,r'}^{\exp}$.

Given that $p_{r,r'}^{\exp} < 1$, plugging the last inequality into (3.15) provides

$$\frac{1}{N}\left(\Phi_{\mathbb{S}_1}(E) + \Psi_{\mathbb{S}_2}(E)\right) \leq \frac{1}{1 - p_{r,r'}^{\exp}}\left[e^{-\lambda_\phi \varepsilon} - \left(1 - \frac{r + r'}{N}\right)\left(e^{-2\lambda_\phi \varepsilon} + e^{-\lambda_\phi \varepsilon} - 1\right)\right]$$

which is the desired result. □

This proposition shows that akin to Chapter 2, we can express a quantity measuring the estimation error which is bounded by a value which does not depend on the extreme values of the noise sequences $\{w_t\}$ and $\{f_t\}$. However, in the case of upper bound (3.14), this quantity, *i.e.* $\frac{1}{N}\left(\Phi_{\mathbb{S}_1}(E) + \Psi_{\mathbb{S}_2}(E)\right)$ is not radially unbounded but is always between zero and one, by definition.

This entails that the inequality in (3.14) only matters when its RHS is smaller than 1. As a result, this imposes an additional constraint on the (r, r')-Resilience index $p_{r,r'}^{\exp}$, which subsequently must verify

$$p_{r,r'}^{\exp} \leq 1 - e^{-\lambda_\phi \varepsilon} + \left(1 - \frac{r + r'}{N}\right)\left(e^{-2\lambda_\phi \varepsilon} + e^{-\lambda_\phi \varepsilon} - 1\right). \tag{3.16}$$

By posing

$$r_\varepsilon = \frac{r + r'}{N},$$

which is the ratio of outliers among all the entries of $\{w_t\}$ and $\{f_t\}$ with respect to ε, the condition (3.16) can be rewritten as

$$p_{r,r'}^{\exp} \leq (1 - r_\varepsilon)\, e^{-2\lambda_\phi \varepsilon} - r_\varepsilon e^{-\lambda_\phi \varepsilon} + r_\varepsilon. \tag{3.17}$$

We therefore have two requirements for $p_{r,r'}^{\exp}$:

- $p_{r,r'}^{\exp} < 1$ in order for (3.14) to hold.
- $p_{r,r'}^{\exp}$ must verify (3.17) so that the RHS of (3.14) is smaller than 1.

We just need the strongest of the conditions to hold, meaning that we need

$$p_{r,r'}^{\exp} < \min\left(1, (1 - r_\varepsilon)\, e^{-2\lambda_\phi \varepsilon} - r_\varepsilon e^{-\lambda_\phi \varepsilon} + r_\varepsilon\right)$$

The following lemma details when condition (3.17) is the stronger condition:

Lemma 3.1. *Let the conditions of Proposition 3.1 hold. Then, if* $(r + r')/N = r_\varepsilon < 4/5$, *we have for all* $\varepsilon \geq 0$,

$$0 \leq r_\varepsilon \left[\left(\frac{1}{r_\varepsilon} - 1\right) e^{-2\lambda_\phi \varepsilon} - e^{-\lambda_\phi \varepsilon} + 1\right] \leq 1 \tag{3.18}$$

Proof. See Appendix C.1. □

Lemma 3.1 shows that if the outliers in the noise sequences $\{w_t\}$ and $\{f_t\}$ represent less than 80% of their overall entries, the stronger condition which $p_{r,r'}^{\exp}$ must verify is condition (3.17). If the outlier ratio is greater than that, this condition can also have sense but only for restricted values of ε. However, it is worth noting that outliers are unlikely to exceed this bound, otherwise they would probably not be considered outliers anymore.

In most cases, the result of Proposition 3.1 does not allow us to infer on the value of the estimation error, as we do not have a direct link between the norm of the estimation error and the value $\frac{1}{N}\left(\Phi_{\mathbb{S}_1}(E) + \Psi_{\mathbb{S}_2}(E)\right)$. However, $\frac{1}{N}\left(\Phi_{\mathbb{S}_1}(E) + \Psi_{\mathbb{S}_2}(E)\right)$ is still an image of the estimation error, and it is likely to be big if the estimation error is great. There are three interesting cases which are worth mentioning:

- **No dense noise in the system:** in this case, we can take $\varepsilon = \varepsilon' = 0$. This means that the noise sequences $w_t[i]$ and $f_t[j]$ are strictly sparse or that any nonzero noise instance is viewed as an outlier. If the conditions of Proposition 3.1 hold, it entails

$$\frac{1}{N}\left(\Phi_{\mathbb{S}_1}(\hat{X} - X) + \Psi_{\mathbb{S}_2}(\hat{X} - X)\right) \leq \frac{r_\varepsilon}{1 - p_{r,r'}^{\exp}}.$$

  In this configuration, we notice that the bound is not equal to zero, which means that the outliers have a nonzero, but bounded impact on the bound. This therefore seems to corroborate the result about the approximate resilience of $\mathcal{E}^{\exp}$ in Chapter 2 (See Corollary 2.1.2).

- **No outlier in the system:** in this case, we have $r_\varepsilon = r = r' = 0$. We have only dense noise and all noise sequences are bounded in the sense that $\phi_t(w_t[i]) \leq \varepsilon$ and $\psi_t(f_t[j]) \leq \varepsilon'$ for all $(t, i, j) \in \mathbb{T} \times \mathbb{I} \times \mathbb{J}$. By definition, $p_{0,0}^{\exp} = 0$, so the

conditions of Proposition 3.1 hold, and we have

$$\frac{1}{N}\left(\Phi_{\mathbb{S}_1}(\hat{X}-X)+\Psi_{\mathbb{S}_2}(\hat{X}-X)\right) \leq 1-e^{-2\lambda_\phi \varepsilon}.$$

The smaller the threshold ε is, the tighter the upper bound will be.

- **No dense noise and no outlier in the system:** this case combines the two cases stated earlier, *i.e.* $r_\varepsilon = 0$ and $\varepsilon = 0$. It is then straightforward to notice that the RHS of (3.14) is equal to zero, which yields

$$\frac{1}{N}\left(\Phi_{\mathbb{S}_1}(\hat{X}-X)+\Psi_{\mathbb{S}_2}(\hat{X}-X)\right) = 0.$$

We now observe that for $\Phi_{\mathbb{S}_1}(E)+\Psi_{\mathbb{S}_2}(E)$ to be equal to zero, all the exponential terms composing the expression (see (3.7)–(3.8)) must be equal to one. This induces

$$\begin{aligned} &\forall (t,i) \in \mathbb{S}_1, && e_{t+1}[i] - a_i^\top e_t = 0 \\ &\forall (t,j) \in \mathbb{S}_2, && c_j^\top e_t = 0, \end{aligned}$$

which implies $E = 0$, given that the system is observable on time-horizon $[0, T-1]$. In conclusion, when there is no noise and no outlier in the system, if the conditions of Proposition 3.1 holds, estimator $\mathcal{E}^{\text{exp}}$ returns the true state of the system, which proves the correctness of the class of estimators.

3.4 Special case where the process noise is zero

In this section, we discuss how the class of estimators $\mathcal{E}^{\text{exp}}$ can be specialised to handle the case where the process noise $\{w_t\}$ is equal to zero at all time, and present a result on the resilience of this specialised estimator.

In this setting, we can translate the knowledge about the absence of process noise by constraining the estimated state trajectories to be within set $\mathcal{Z}_\Sigma$ defined in (2.50). As a reminder, this set contains all the trajectory matrices which exactly respect the dynamics of the system, *i.e.* for every t in $\mathbb{T}'$, $z_{t+1} = A_t z_t$. As a result, we define estimator $\mathcal{E}^{\circ,\text{exp}}$, minimising V_Σ^{exp} as defined in (3.1) over the set $\mathcal{Z}_\Sigma$, *i.e.*

$$\mathcal{E}^{\circ,\text{exp}}(Y) = \underset{Z \in \mathcal{Z}_\Sigma}{\arg\min}\, V_\Sigma^{\text{exp}}(Y,Z). \tag{3.19}$$

This knowledge also allows us to get rid of the left sum in V_Σ^{exp} defined in (3.1) as it will be equal to 0 for every Z in $\mathcal{Z}_\Sigma$. $\mathcal{E}^{\circ,\text{exp}}(Y)$ can then be rewritten more simply in the form

$$\mathcal{E}^{\circ,\text{exp}}(Y) = \left\{\hat{X} = \begin{pmatrix}\hat{x}_0 & A\hat{x}_0 & \cdots & A^{T-1}\hat{x}_0\end{pmatrix} : \hat{x}_0 \in \underset{z\in\mathbb{R}^n}{\arg\min}\, V_\Sigma^{\circ,\text{exp}}(Y,z)\right\} \tag{3.20}$$

where

$$V_\Sigma^{\circ,\text{exp}}(Y,z_0) = \sum_{(t,j)\in\mathbb{T}\times\mathbb{J}} \left(1 - e^{-\lambda_\psi \psi(y_t[j]-\theta_{t,j}^\top z_0)}\right) \tag{3.21}$$

where $\theta_{t,j}^\top$ are rows of the observability matrix defined such that $\theta_{t,j}^\top = c_j^\top A^{t-1}$.

Hence, the estimation of the state trajectory can be also reduced to estimating the initial state x_0 for saturated performance functions in this setting. Adapting the result in [Bak18] to the state estimation framework, we study the resilience property

of this new class of estimators. First, we need to state a few preliminary results before stating the main theorem. Subsequently, a discussion will be provided about the stability of the newly defined class of estimators $\mathcal{E}^{\circ,\exp}$ with respect to dense noise in the dynamic equation.

3.4.1 Preliminaries

Before stating our main theoretical result, we will first introduce a few notations. For convenience, and without any loss of generality, we can assume that there is no (t, j) in $\mathbb{T} \times \mathbb{J}$ such that $\|\theta_{t,j}\|_2 = 0$.[1] We then define the following variable:

$$\sigma_\Sigma = \min_{(t,j)\in\mathbb{T}\times\mathbb{J}} \|\theta_{t,j}\|_2 > 0 \tag{3.22}$$

Moreover, given ρ in $[0, 1]$ and $z_0 \in \mathbb{R}^n$, we also define the following set of indexes (t, j):

$$\mathcal{J}_\Sigma(z_0, \rho) = \{(t, j) \in \mathbb{T} \times \mathbb{J} \ : \ |\theta_{t,j}^\top z_0| \geq \rho\|\theta_{t,j}\|_2\|z_0\|_2\} \tag{3.23}$$

This set selects the rows in the observability matrix which are almost in the same direction as z_0. (t, j) is in $\mathcal{J}_\Sigma(z_0, \rho)$ if and only if the vector $\theta_{t,j}$ is within the cone of direction z_0 and of half-top angle $\arccos(\rho)$. If $\rho = 1$, then $\mathcal{J}_\Sigma(z_0, \rho)$ collects all the $\theta_{t,j}$ which are colinear to z_0. In the other extreme case where $\rho = 0$, $\mathcal{J}_\Sigma(z_0, \rho)$ contains all the rows of $\mathcal{O}_{T-1}$, *i.e.* $\mathcal{J}_\Sigma(z_0, \rho) = \mathbb{T} \times \mathbb{J}$. As it will be shown in Lemma 3.2 below, the cardinality $\mathcal{J}_\Sigma(z_0, \rho)$ can be considered as a local observability measure with regards to z_0 given that it represents how many $\theta_{t,j}$ are almost in the same direction as z_0 with a tolerance ρ. Following this idea, Figure 3.2 proposes a visual interpretation of $\mathcal{J}_\Sigma(z_0, \rho)$.

What is desired is that all the vectors $\theta_{t,j}$ finely cover all the directions in $\mathbb{R}^n$ so that $\mathcal{J}_\Sigma(z_0, \rho)$ is as large as possible for all z_0. However, we do acknowledge that this property may be strong. In system identification, for instance, the data matrix of interest for this kind of analysis can, in principle, be made rich enough by generating it with an appropriate input signal. In contrast, the properties of the Observability matrix $\mathcal{O}_{T-1}$ are much less controllable given that it is structured by the pair (A, C).

We also define a global observability parameter:

$$R_\Sigma(\rho) = \frac{1}{mT} \inf_{z_0\in\mathbb{R}^n} |\mathcal{J}_\Sigma(z_0, \rho)|. \tag{3.24}$$

R_Σ is a ratio, given that for any ρ in $[0, 1]$, $\mathcal{J}_\Sigma(z_0, \rho) \subseteq \mathbb{T} \times \mathbb{J}$ and $|\mathbb{T} \times \mathbb{J}| = mT$. Consequently, R_Σ is always between 0 and 1. Moreover, R_Σ is decreasing with regards to ρ: in particular, if $\rho = 0$, then $R_\Sigma(\rho) = 1$. The closer $R_\Sigma(\rho)$ is to 1 for high values of ρ, the more the system will be considered observable.

The following lemma provides more context about the link between $R_\Sigma(\rho)$ and the observability of the system:

Lemma 3.2. *Consider the system Σ defined in (1.1). The two following statements are equivalent:*

(i) The system is observable, i.e. $\text{rank}(\mathcal{O}_T) = n$.[2]

[1] If the observability matrix $\mathcal{O}_{T-1}$ (see Eq. (1.10)) contains null rows, the following analysis can still be conducted with a matrix collecting all the non-zero rows of $\mathcal{O}_{T-1}$.

[2] In the case of LTI systems, the observability is rather stated with $\mathcal{O}_n$ (see Theorem 1.1) but stating it with $\mathcal{O}_{T-1}$ is more convenient for the proof and $(\text{rank}(\mathcal{O}_{T-1}) = n) \Leftrightarrow (\text{rank}(\mathcal{O}_n) = n)$.

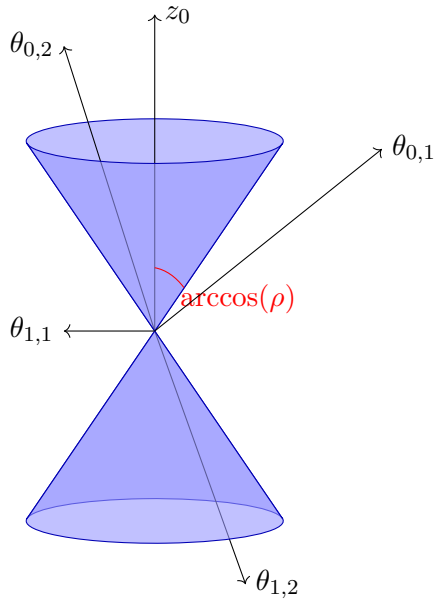

FIGURE 3.2: Visual interpretation of $\mathcal{J}_\Sigma(z_0, \rho)$: the set collects all indexes (t, j) such that $\theta_{t,j}$ is within the blue cone

(ii) There exists $\rho \in]0, 1]$ *such that* $R_\Sigma(\rho) \neq 0$.

Proof. $(i) \Rightarrow (ii)$: if the system is observable, assume that for all ρ in $]0, 1]$, $R_\Sigma(\rho) = 0$. As the set $\{|\mathcal{J}_\Sigma(z_0, \rho)|\}_{z_0 \in \mathbb{R}^n}$ is a subset of $\mathbb{N}$, for any $\rho \in]0, 1]$, its infimum is necessarily attained, which entails that there exists a $z_\rho \in \mathbb{R}^n$ such that $\mathcal{J}_\Sigma(z_\rho, \rho) = \emptyset$. z_ρ is necessarily different from zero given that for every ρ, $\mathcal{J}_\Sigma(0, \rho) = \mathbb{T} \times \mathbb{J}$.

For a fixed ρ, $\mathcal{J}_\Sigma(z_\rho, \rho) = \emptyset$ implies that for all (t, j) in $\mathbb{T}\times\mathbb{J}$, $|\theta_{t,j}^\top z_\rho| < \rho \|\theta_{t,j}\|_2 \|z_\rho\|_2$. By squaring the two sides of the inequalities, we obtain mT inequalities of the form

$$z_\rho^\top \theta_{t,j} \theta_{t,j}^\top z_\rho \leq \rho^2 ||z_\rho||_2^2 ||\theta_{t,j}||_2^2.$$

By adding those inequalities side by side, this leads to

$$z_\rho^\top \mathcal{O}_{T-1}^\top \mathcal{O}_{T-1} z_\rho < \rho^2 \|z_\rho\|_2^2 \sum_{(t,j)\in\mathbb{T}\times\mathbb{J}} \|\theta_{t,j}\|_2^2. \tag{3.25}$$

From [Ber09a, Corollary 8.4.2], $z_\rho^\top \mathcal{O}_{T-1}^\top \mathcal{O}_{T-1} z_\rho \geq \sigma_{\min} z_\rho^\top z_\rho$ where $\sigma_{\min}$ designates the smallest eigenvalue of $\mathcal{O}_{T-1}^\top \mathcal{O}_{T-1}$. Since the system is observable, $\mathcal{O}_{T-1}^\top \mathcal{O}_{T-1}$ is positive definite which yields $\sigma_{\min} > 0$. As a result, (3.25) implies $\rho > \rho_e$ where

$$\rho_e = \sqrt{\frac{\sigma_{\min}}{\sum_{(t,j)\in\mathbb{T}\times\mathbb{J}} \|\theta_{t,j}\|_2^2}} > 0.$$

For any ρ in $]0, \rho_e[\cap]0, 1]$, ρ needs to be both strictly smaller and greater than ρ_e at the same time, which is impossible. This proves that the observability of the system induces the existence of at least one ρ in $]0, 1]$ such that $R_\Sigma(\rho) \neq 0$.

$(ii) \Rightarrow (i)$: by contraposition, if the system is not observable, then there exists some nonzero $z \in \mathbb{R}^n$ such that $\mathcal{O}_{T-1} z = 0$. Given that

$$\mathcal{O}_{T-1} z = \begin{pmatrix} \theta_{0,1}^\top z & \cdots & \theta_{0,m}^\top z & \theta_{1,1}^\top z & \cdots & \theta_{T-1,m}^\top z \end{pmatrix}^\top,$$

we have for every (t,j) in $\mathbb{T}\times\mathbb{J}$, $\theta_{t,j}^\top z = 0$. As a result, for any $\rho\in]0,1]$, $\mathcal{J}_\Sigma(z,\rho)=\emptyset$ since $|\theta_{t,j}^\top z| = 0$ cannot be greater than $\rho\|\theta_{t,j}\|_2\|z\|_2$ given that $\theta_{t,j}\neq 0$ and $\|z\|\neq 0$. This leads to $R_\Sigma(\rho)=0$ for any $\rho\in]0,1]$, which proves the implication. □

This lemma shows that the observability is an equivalent condition to the existence of a $\rho\in]0,1]$ such that $R_\Sigma(\rho)\neq 0$. Σ will thus be supposed to be observable from now on.

Finally, we need to define a last notation. Given ε a positive real number, for any noise sequence $\{f_t[j]\}$, it is possible to split the set $\mathbb{T}\times\mathbb{J}$ into two disjoint subsets,

$$\mathcal{I}_\varepsilon = \{(t,j)\in\mathbb{T}\times\mathbb{J} \,:\, |f_t[j]|\leq\varepsilon\}, \tag{3.26}$$

which gathers the indexes of $f_t[j]$ such that their absolute value is smaller than ε, and

$$\mathcal{I}_\varepsilon^c = \{(t,j)\in\mathbb{T}\times\mathbb{J} \,:\, |f_t[j]|>\varepsilon\}, \tag{3.27}$$

which consists of the indexes of "outliers" in $\{f_t[j]\}$ with regards to ε. ε is therefore a threshold we can choose and tune in order to conduct our analysis.

3.4.2 Boundedness of the estimation error

In the following theorem, we are going to express under which circumstances the norm of the estimation error on the initial state, *i.e.* $e_0=\hat{x}_0-x_0$, and consequently the estimation error over the whole trajectory $E=\hat{X}-X$, can be bounded by a value which does not depend on the largest values of f_t:

Theorem 3.1. *Consider the state estimator (3.20)–(3.21) for system (1.1) with ψ verifying properties (P3.1)–(P3.3) and (P3.4) for a given $\gamma_\psi>0$. Let $\varepsilon\geq 0$. For any noise sequence $\{f_t\}$ and initial state x_0 in (1.1), generating a measurement matrix Y, such that*

$$\frac{1}{1+e^{-\lambda_\psi\psi(\varepsilon)}}R_\Sigma(\rho)+e^{-\lambda_\psi\psi(\varepsilon)}\frac{|\mathcal{I}_\varepsilon|}{mT}>1, \tag{3.28}$$

is verified for some ρ in $]0,1]$, the following holds true :

$$\forall\hat{X}\in\mathcal{E}^{\circ,\exp}(Y),\ \psi(\rho\sigma_\Sigma\|e_0\|_2)\leq\frac{1}{\lambda_\psi\gamma_\psi}\ln(1/\mu) \tag{3.29}$$

with $e_0=\hat{x}_0-x_0$ and

$$\mu=\frac{1+e^{-\lambda_\psi\psi(\varepsilon)}}{\frac{|\mathcal{I}_\varepsilon|}{mT}+R_\Sigma(\rho)-1}\left[\frac{1}{1+e^{-\lambda_\psi\psi(\varepsilon)}}R_\Sigma(\rho)+e^{-\lambda_\psi\psi(\varepsilon)}\frac{|\mathcal{I}_\varepsilon|}{mT}-1\right] \tag{3.30}$$

Moreover, if ψ is (strictly) increasing on $\mathbb{R}_{\geq 0}$, then

$$\mathfrak{N}(\hat{X}-X)\leq\frac{M_\Sigma}{\rho\sigma_\Sigma}\psi^{-1}\left(\frac{1}{\lambda_\psi\gamma_\psi}\ln(1/\mu)\right) \tag{3.31}$$

with $\hat{X}$ in $\mathcal{E}^{\circ,\exp}(Y)$, $\mathfrak{N}(\hat{X}-X)=\max_{t\in\mathbb{T}}\|\hat{x}_t-x_t\|_2$ and M_Σ a constant depending on the system dynamics.

Proof. By the definition (3.20) of the estimator $\mathcal{E}^{\circ,\exp}$, for any measurement matrix Y in $\mathbb{R}^{m\times T}$, we have

$$V_\Sigma^{\circ,\exp}(Y,\hat{x}_0)\leq V_\Sigma^{\circ,\exp}(Y,x_0), \tag{3.32}$$

for every $\hat{x}_0$ in $\mathcal{E}^{\circ,\exp}(Y)$. Replacing the two sides by their definition yields

$$\sum_{(t,j)\in\mathbb{T}\times\mathbb{J}} \left(1 - e^{-\lambda_\psi \psi(y_t[j]-\theta_{t,j}^\top \hat{x}_0)}\right) \leq \sum_{(t,j)\in\mathbb{T}\times\mathbb{J}} \left(1 - e^{-\lambda_\psi \psi(f_t[j])}\right), \tag{3.33}$$

which is equivalent to

$$\sum_{(t,j)\in\mathbb{T}\times\mathbb{J}} e^{-\lambda_\psi \psi(f_t[j])} \leq \sum_{(t,j)\in\mathbb{T}\times\mathbb{J}} e^{-\lambda_\psi \psi(y_t[j]-\theta_{t,j}^\top \hat{x}_0)}. \tag{3.34}$$

The idea is now to underestimate the left sum while overestimating the right sum. To do so, we underestimate each term of the left sum in (3.34) depending on whether they belong to $\mathcal{I}_\varepsilon$ or to $\mathcal{I}_\varepsilon^c$ given that $\mathbb{T}\times\mathbb{J} = \mathcal{I}_\varepsilon \cup \mathcal{I}_\varepsilon^c$:

$$\begin{aligned}
&\forall (t,j) \in \mathcal{I}_\varepsilon, \quad (|f_t[j]| < \varepsilon) \Rightarrow \left(e^{-\lambda_\psi \psi(\varepsilon)} \leq e^{-\lambda_\psi \psi(f_t[j])}\right) \\
&\forall (t,j) \in \mathcal{I}_\varepsilon^c, \quad 0 \leq e^{-\lambda_\psi \psi(f_t[j])}
\end{aligned}$$

Plugging those underestimates in (3.34) entails

$$|\mathcal{I}_\varepsilon| e^{-\lambda_\psi \psi(\varepsilon)} \leq \sum_{(t,j)\in\mathbb{T}\times\mathbb{J}} e^{-\lambda_\psi \psi(y_t[j]-\theta_{t,j}^\top \hat{x}_0)} \tag{3.35}$$

We now apply the same kind of logic to the right sum. First of all, we recall that

$$\psi(y_t[j] - \theta_{t,j}^\top \hat{x}_0) = \psi(\theta_{t,j}^\top x_0 + f_t[j] - \theta_{t,j}^\top \hat{x}_0) = \psi(f_t[j] - \theta_{t,j}^\top e_0),$$

with $e_0 = \hat{x}_0 - x_0$. Then we overestimate the right-side terms based on $\mathcal{I}_\varepsilon$, $\mathcal{I}_\varepsilon^c$ by making use of the GTI (3.5):

$$\begin{aligned}
&\forall (t,j) \in \mathcal{I}_\varepsilon, \quad e^{-\lambda_\psi \psi(f_t[j]-\theta_{t,j}^\top e_0)} \leq e^{\lambda_\psi \psi(f_t[j])} e^{-\lambda_\psi \gamma_\psi \psi(\theta_{t,j}^\top e_0)} \\
&\forall (t,j) \in \mathcal{I}_\varepsilon^c, \quad e^{-\lambda_\psi \psi(f_t[j]-\theta_{t,j}^\top e_0)} \leq 1
\end{aligned}$$

We then plug these overestimates in (3.35) which yields

$$|\mathcal{I}_\varepsilon| e^{-\lambda_\psi \psi(\varepsilon)} \leq \sum_{(t,j)\in\mathcal{I}_\varepsilon} e^{\lambda_\psi \psi(f_t[j])} e^{-\lambda_\psi \gamma_\psi \psi(\theta_{t,j}^\top e_0)} + |\mathcal{I}_\varepsilon^c|$$

Knowing that $|\mathcal{I}_\varepsilon^c| = mT - |\mathcal{I}_\varepsilon|$ and that for all $(t,j) \in \mathcal{I}_\varepsilon$, $e^{\lambda_\psi \psi(f_t[j])} < e^{\lambda_\psi \psi(\varepsilon)}$, the previous equation implies

$$e^{-\lambda_\psi \psi(\varepsilon)} \left[|\mathcal{I}_\varepsilon|(1 + e^{-\lambda_\psi \psi(\varepsilon)}) - mT\right] \leq \sum_{(t,j)\in\mathcal{I}_\varepsilon} e^{-\lambda_\psi \gamma_\psi \psi(\theta_{t,j}^\top e_0)} \tag{3.36}$$

We now consider ρ the value in $]0,1]$ such that (3.28) holds, and decompose the right sum of (3.36) depending on whether (t,j) belongs to $\mathcal{J}_\Sigma(e_0,\rho)$ or not:

- If (t,j) is in $\mathcal{I}_\varepsilon \cap \mathcal{J}_\Sigma(e_0,\rho)$, by the definition (3.23) of $\mathcal{J}_\Sigma(e_0,\rho)$,

$$e^{-\lambda_\phi \gamma_\phi \psi(\theta_{t,j}^\top e_0)} \leq e^{-\lambda_\phi \gamma_\phi \psi(\rho \|\sigma_\Sigma\|_2 \|e_0\|_2)},$$

  given that ψ verifies (P3.3) and that $a \mapsto e^{-\lambda_\phi \gamma_\phi a}$ is decreasing.

- If (t,j) is in $\mathcal{I}_\varepsilon \cap \mathcal{J}_\Sigma^c(e_0,\rho)$, we simply overestimate $e^{-\lambda_\phi\gamma_\phi\psi(\theta_{t,j}^\top e_0)}$ by 1, *i.e.*

$$e^{-\lambda_\phi\gamma_\phi\psi(\theta_{t,j}^\top e_0)} \leq 1$$

Plugging these overestimates in (3.36), we obtain

$$\begin{aligned} e^{-\lambda_\psi\psi(\varepsilon)}\left[|\mathcal{I}_\varepsilon|(1+e^{-\lambda_\psi\psi(\varepsilon)}) - mT\right] &\leq \sum_{(t,j)\in\mathcal{I}_\varepsilon\cap\mathcal{J}_\Sigma(e_0,\rho)} e^{-\lambda_\psi\gamma_\psi\psi(\rho\sigma_\Sigma\|e_0\|_2)} + |\mathcal{I}_\varepsilon\cap\mathcal{J}_\Sigma^c(e_0,\rho)| \\ &\leq |\mathcal{I}_\varepsilon\cap\mathcal{J}_\Sigma(e_0,\rho)|e^{-\lambda_\psi\gamma_\psi\psi(\rho\sigma_\Sigma\|e_0\|_2)} + |\mathcal{I}_\varepsilon\cap\mathcal{J}_\Sigma^c(e_0,\rho)| \\ &\leq |\mathcal{I}_\varepsilon\cap\mathcal{J}_\Sigma(e_0,\rho)|\left[e^{-\lambda_\psi\gamma_\psi\psi(\rho\sigma_\Sigma\|e_0\|_2)} - 1\right] + |\mathcal{I}_\varepsilon| \end{aligned} \tag{3.37}$$

as $|\mathcal{I}_\varepsilon\cap\mathcal{J}_\Sigma^c(e_0,\rho)| = |\mathcal{I}_\varepsilon| - |\mathcal{I}_\varepsilon\cap\mathcal{J}_\Sigma(e_0,\rho)|$.

We now find an overestimation of the term $|\mathcal{I}_\varepsilon\cap\mathcal{J}_\Sigma(e_0,\rho)|\left[e^{-\lambda_\psi\gamma_\psi\psi(\rho\sigma_\Sigma\|e_0\|_2)} - 1\right]$:

$$|\mathcal{I}_\varepsilon\cap\mathcal{J}_\Sigma(e_0,\rho)| = |\mathcal{I}_\varepsilon| + |\mathcal{J}_\Sigma(e_0,\rho)| - |\mathcal{I}_\varepsilon\cup\mathcal{J}_\Sigma(e_0,\rho)| \tag{3.38}$$

$$\geq mT\left(\frac{|\mathcal{I}_\varepsilon|}{mT} + R_\Sigma(\rho) - 1\right) \tag{3.39}$$

since by the definition (3.24) of $R_\Sigma(\rho)$, $mTR_\Sigma(\rho) \leq |\mathcal{J}_\Sigma(e_0,\rho)|$, and $|\mathcal{I}_\varepsilon\cup\mathcal{J}_\Sigma(e_0,\rho)| \leq |\mathbb{T}\times\mathbb{J}|$. Given that the term $e^{-\lambda_\psi\psi(\rho\sigma_\Sigma\|e_0\|_2)} - 1$ is nonpositive, multiplying both sides of (3.39) yields

$$|\mathcal{I}_\varepsilon\cap\mathcal{J}_\Sigma(e_0,\rho)|\left[e^{-\lambda_\psi\psi(\rho\sigma_\Sigma\|e_0\|_2)} - 1\right] \leq mT\left(\frac{|\mathcal{I}_\varepsilon|}{mT} + R_\Sigma(\rho) - 1\right)\left[e^{-\lambda_\psi\psi(\rho\sigma_\Sigma\|e_0\|_2)} - 1\right]$$

Injecting the last inequality into (3.37) and dividing both sides by mT gives us

$$\begin{aligned} e^{-\lambda_\psi\psi(\varepsilon)}\left[\frac{|\mathcal{I}_\varepsilon|}{mT}(1+e^{-\psi(\varepsilon)}) - 1\right] - \frac{|\mathcal{I}_\varepsilon|}{mT} \\ \leq \left(\frac{|\mathcal{I}_\varepsilon|}{mT} + R_\Sigma(\rho) - 1\right)\left[e^{-\lambda_\psi\gamma_\psi\psi(\rho\sigma_\Sigma\|e_0\|_2)} - 1\right]. \end{aligned} \tag{3.40}$$

ρ is such that Condition (3.28) is met, which entails that the term $|\mathcal{I}_\varepsilon|/(mT)+R_\Sigma(\rho)-1$ is positive given that

$$\frac{|\mathcal{I}_\varepsilon|}{mT} + R_\Sigma(\rho) \geq e^{-\lambda_\psi\psi(\varepsilon)}\frac{|\mathcal{I}_\varepsilon|}{mT} + \frac{1}{1+e^{-\lambda_\psi\psi(\varepsilon)}}R_\Sigma(\rho) > 1. \tag{3.41}$$

Consequently, dividing both sides of (3.40) by $|\mathcal{I}_\varepsilon|/(mT) + R_\Sigma(\rho) - 1$ does not change the sense of the inequality, and this, after simplifying the left hand side of (3.40), eventually gives us

$$\mu \leq e^{-\lambda_\psi\gamma_\psi\psi(\rho\sigma_\Sigma\|e_0\|_2)} \tag{3.42}$$

with μ as defined in (3.30). When Condition (3.28) is met, μ is positive, so we can apply ln to both sides, yielding

$$\psi(\rho\sigma_\Sigma\|e_0\|_2) \leq \frac{1}{\lambda_\psi\gamma_\psi}\ln(1/\mu) \tag{3.43}$$

If ψ is increasing on $\mathbb{R}_{\geq 0}$, then it is obviously invertible on that interval, which entails

$$\|e_0\|_2 \leq \frac{1}{\rho\sigma_\Sigma}\psi^{-1}\left(\frac{1}{\lambda_\psi\gamma_\psi}\ln(1/\mu)\right) \tag{3.44}$$

Finally, with $\hat{X}$ in $\mathcal{E}^{\circ,\exp}(Y)$, $\hat{x}_t = A^t\hat{x}_0$ and $x_t = A^t x_0$, so we have $\hat{x}_t - x_t = A^t e_0$ for all $t \in \mathbb{T}$. Consequently, $\mathfrak{N}(\hat{X} - X) = \max_{t\in\mathbb{T}}\|A^t e_0\|_2 \leq \left(\max_{t\in\mathbb{T}}\|A^t\|_2\right)\|e_0\|_2$. This eventually yields

$$\mathfrak{N}(\hat{X} - X) \leq \frac{\max_{t\in\mathbb{T}}\|A^t\|_2}{\rho\sigma_\Sigma}\psi^{-1}\left(\frac{1}{\lambda_\psi\gamma_\psi}\ln(1/\mu)\right) \tag{3.45}$$

which is the desired result with $M_\Sigma = \max_{t\in\mathbb{T}}\|A^t\|_2$. □

What this theorem states is that the estimator $\mathcal{E}^{\circ,\exp}$ yields estimates which are bounded despite the presence of an arbitrary noise which can potentially take any value. Unfortunately, condition (3.28) cannot be easily computed due to the fact that computing $R_\Sigma(\rho)$ is a combinatorial problem and that having access to $|\mathcal{I}_\varepsilon|$ requires knowing the proportion of outliers in $\{f_t[j]\}$ with regards to ε. Nevertheless, it gives us some relevant information about what is important to make sure the estimator is approximately resilient. Indeed, the inequality is composed of three terms: on the left hand side, there are two terms, one which depends on the observability of the system through $R_\Sigma(\rho)$, one which depends on the number of reasonable measurements *with regards to* ε. On the right-hand side there is a constant term which is equal to the total number of measurements on the time horizon. To promote this condition, there are therefore two important things to ensure:

- We need the observability criteria $R_\Sigma(\rho)$ to be as close from 1 as possible for a relatively large ρ.
- The number of outliers must be somehow limited, that is, $|\mathcal{I}_\varepsilon^c|$ must be small.

The interpretation of condition (3.28) is that the estimation error is bounded if the system is observable enough, and the more it is observable, the more outliers the estimator is able to handle.

In addition, the bound itself in (3.31) gives information on what impacts the quality of the estimation: besides the conclusions obtained through the study of condition (3.28), we can see that the actual values of ρ and ε play a role in the quality of the bound. Indeed, if we do not consider their impact on $\mathcal{I}_\varepsilon$ and $R_\Sigma(\rho)$, then the bound tightens when ρ is growing larger and/or ε gets smaller. As a result, given that the bound exists for any (ρ, ε) which verify condition (3.28), the best bound among different values of which can be obtained through Theorem 3.1 with respect to (ρ, ε) would be

$$\mathfrak{N}(E) \leq M_\Sigma \min_{\substack{(\rho,\varepsilon)\\ \mu>0}}\left[\frac{1}{\rho\sigma_\Sigma}\psi^{-1}\left(\frac{1}{\lambda_\psi\gamma_\psi}\ln(1/\mu)\right)\right] \tag{3.46}$$

However, this bound is still likely to be very conservative due to the use of several underestimations and overestimations throughout its derivation. Consequently, its main interest does not lie in its exact value but rather in the way the parameters of the system and of the estimator interact with it. These interactions then provide insight on what are the key elements which have an impact on the performances of the estimator.

3.4.3 Case of systems with bounded process noise

We now consider that the dense component in the process noise w_t defined in (1.2) is no longer equal to zero at all time. Even though estimator $\mathcal{E}^{\circ,\exp}$ is not designed for such a system in the first place, it can still be applied to Σ in this configuration. With a similar idea to Section 2.4.2 from Chapter 2, we notice that for every system Σ, there exists a system $\tilde{\Sigma}$ such that

$$\tilde{\Sigma} : \begin{cases} \tilde{x}_{t+1} = A\tilde{x}_t \\ y_t = C\tilde{x}_t + \tilde{f}_t \end{cases} \tag{3.47}$$

with $\tilde{x}_0 = x_0$, $\tilde{f}_t = C\tilde{w}_t + f_t$ and $\tilde{w}_t = \sum_{k=0}^{t-1} A^k w_k$. This new system verifies the structure defined in (1.2) and gives the exact same output as Σ but without any process noise. In addition, the gap between x_t and $\tilde{x}_t$ can be quantified, and is equal to $x_t - \tilde{x}_t = A^t x_0 + \tilde{w}_t - A^t x_0 = \tilde{w}_t$. As a result, we can draw the following corollary from Theorem 3.1:

Corollary 3.1.1. *Consider the state estimator (3.20)–(3.21) for system (1.2) with ψ an invertible function verifying properties (P3.1)–(P3.4). Let $\varepsilon \geq 0$. For any noise sequences $\{w_t\}$ and $\{f_t\}$ and initial state x_0 in (1.2), generating a measurement matrix Y, such that (3.28) is verified for some ρ in $]0,1]$, the following holds true:*

$$\forall \hat{X} \in \mathcal{E}^{\circ,\exp}(Y), \qquad \mathfrak{N}(\hat{X} - X) \leq \frac{M_\Sigma}{\rho\sigma_\Sigma}\psi^{-1}\left(\frac{1}{\lambda_\psi\gamma_\psi}\ln(1/\mu)\right) + \max_{t\in\mathbb{T}}\|\tilde{w}_t\|_2 \tag{3.48}$$

with $\hat{X}$ in $\mathcal{Z}_\Sigma$, $\tilde{w}$ as defined in (3.47) and μ, $\mathfrak{N}$ and M_Σ as defined in Theorem 3.1.

Proof. By applying Theorem 3.1 to system $\tilde{\Sigma}$ defined in (3.47), we obtain that for all $\hat{X}$ in $\mathcal{E}^{\circ,\exp}(Y)$

$$\|e_0\|_2 \leq \frac{1}{\rho\sigma_\Sigma}\psi^{-1}\left(\frac{1}{\lambda_\psi\gamma_\psi}\ln(1/\mu)\right) \tag{3.49}$$

given that $e_0 = \hat{x}_0 - \tilde{x}_0 = \hat{x}_0 - x_0$. Moreover, we have for all $t \in \mathbb{T}$, $e_t = \hat{x}_t - x_t = A^t e_0 - \tilde{w}_t$, so by considering the norm $\mathfrak{N}$, we have

$$\mathfrak{N}(E) \leq M_\Sigma\|e_0\|_2 + \max_{t\in\mathbb{T}}\|\tilde{w}_t\|_2 \tag{3.50}$$

which yields the desired result. □

Similarly to Theorem 2.4 in Chapter 2, this corollary shows that the estimator $\mathcal{E}^{\circ,\exp}$ still displays approximate resilience even in the presence of a dense noise in the dynamics of the system.

3.4.4 Numerical study of Condition (3.28)

In this section, we aim at numerically studying Condition (3.28) from Theorem 3.1. Ideally, we would like to be able to compute it in advance to check whether the estimator will be approximately resilient in a given configuration. However, some values involved in it, such as $R_\Sigma(\rho)$, are non-trivial to compute (for a lead on how to estimate $R_\Sigma(\rho)$, see Proposition 5 in [Bak17]). Moreover, Condition (3.28) was obtained through several underestimations and overestimations, meaning that it is a potentially conservative sufficient condition to the approximative resilience of Estimator $\mathcal{E}^{\circ,\exp}$. Consequently, this study mainly aims at qualitatively interpreting how

the different parameters of the estimation setting interact with Condition (3.28), and what kind of condition they impose on $R_\Sigma(\rho)$.

We recall the expression of Condition (3.28) from Theorem 3.1:

$$\frac{1}{1+e^{-\lambda_\psi \psi(\varepsilon)}} R_\Sigma(\rho) + e^{-\lambda_\psi \psi(\varepsilon)} \frac{|\mathcal{I}_\varepsilon|}{mT} > 1,$$

For convenience, in this section, we denote with $r_\varepsilon = |\mathcal{I}_\varepsilon^c|/(mT)$ the ratio of outliers in $\{f_t\}$ with respect to ε, meaning that Condition (3.28) can be rewritten as

$$R_\Sigma(\rho) \leq \left(1+e^{-\lambda_\psi \psi(\varepsilon)}\right)\left[1-e^{-\lambda_\psi \psi(\varepsilon)}(1-r_\varepsilon)\right]. \tag{3.51}$$

In this inequality, $R_\Sigma(\rho)$ is the parameter linked with the system properties, assessing how much the system is observable for every given $\rho \in [0,1]$. The goal of the test we are conducting is to study the right hand side of (3.51) to know how much observable the system needs to be, *i.e.* how small $R_\Sigma(\rho)$ has to be, for Condition (3.28) to hold.

The RHS of (3.51) contains four variables: λ_ψ, ψ, ε and r_ϵ. Given that we do not consider any noise configuration in particular, r_ε can be studied independently from ε. Moreover, we notice that λ_ψ, ψ, ε have an impact through the exponential term $e^{-\lambda_\psi \psi(\varepsilon)}$ exclusively. Consequently, we replace the argument of the two exponential terms in (3.51) with a global nonnegative parameter, α, designed to represent the global impact of λ_ψ, ψ, ε on the inequality.

Subsequently, we define the function $R_{\min}$ from $\mathbb{R}_{\geq 0} \times [0,1]$ such that for all (α, r_ε) in $\mathbb{R}_{\geq 0} \times [0,1]$,

$$R_{\min}(\alpha, r_\varepsilon) = \min\left(1, \left(1+e^{-\alpha}\right)\left[1-e^{-\alpha}(1-r_\varepsilon)\right]\right), \tag{3.52}$$

where min is the function returning the minimum value between its two arguments. Indeed, we notice that the RHS of (3.51) can take values greater than 1, *e.g.* for $\alpha = r_\varepsilon = 0$. However, $R_\Sigma(\rho)$ is a ratio and therefore lies between 0 and 1. Any value greater or equal to 1 conveys the idea that the approximate resilience of the estimator cannot be assessed through Theorem 3.1 as Condition (3.28) can never hold, hence the presence of the saturation induced by the min function.

Figure 3.3 presents a heat map of $R_{\min}$ over $[0,1] \times [0, 0.5]$. First of all, we notice that $R_{\min}$ increases with both r_ε and α: concerning the former, it is logical that when the ratio of outliers increases, the system has to be more observable in order to still ensure the approximate resilience of the estimator. The influence of α can be linked with the fact that α increases with respect to ε. ε is a threshold value, which separates outliers from reasonable values of $\{f_t\}$ (see Eq. 3.26). Consequently, it bounds the reasonable values of $\{f_t\}$, similarly to a bound on the dense component used to simulate an arbitrary disturbance (see Eq. (1.49)).

The increase of $R_{\min}$ along the two parameters of the study has two consequences. The first one is that there seems to be ratios of outliers r_ε such that Theorem 3.1 can never guarantee the resilience of the estimator. Indeed, we observe that for a ratio greater than 0.5, $R_\Sigma(\rho)$ needs to be strictly greater than 1 no matter the value of α, which is impossible. Nevertheless, it is important to remember that Condition (3.28) is only a sufficient condition, meaning that Estimator $\mathcal{E}^{\exp,\circ}$ can

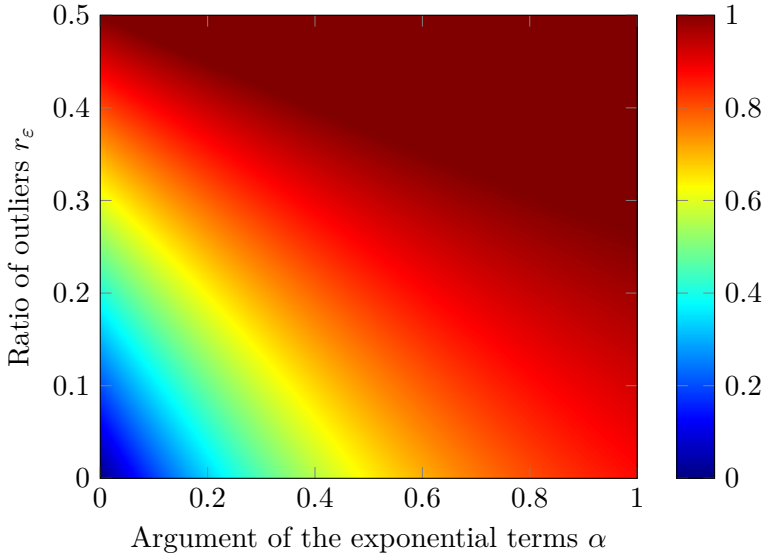

FIGURE 3.3: Heat map of function $R_{\min}$

still provide satisfactory results in the presence of more than 50% of outliers but this cannot be assessed through Theorem 3.1.

The second observation is that the lower α is, the higher ratio of outlier values the estimator will be able to handle according to Theorem 3.1. To illustrate this, if we take $\lambda_\psi = 1$, $\varepsilon = 0.1$ and ψ equal to the square function[3], we have $\alpha = 0.01$. The function $r_\varepsilon \mapsto R_{\min}(\alpha, r_\varepsilon)$ is then represented in Figure 3.4.

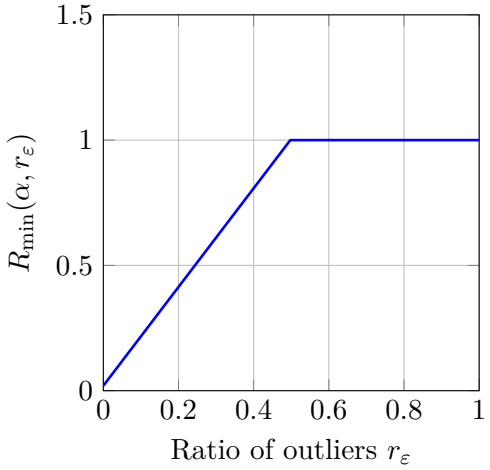

FIGURE 3.4: Value of $R_{\min}(\alpha, r_\varepsilon)$ in function of r_ε for $\alpha = 0.01$

Figure 3.4 shows that it is technically possible for the estimator to handle almost 50% of outliers, but it would require to have $R_\Sigma(\rho) \approx 1$ which is impossible as soon as $\rho \neq 0$. However, for lower ratios of sparse noise, like 10%, we notice that it would only require $R_\Sigma(\rho) \geq 0.25$ which seems more reasonable.

Another way to interpret this is that to ensure that estimator $\mathcal{E}^{\circ,\exp}$ can handle more outliers through Theorem 3.1, α needs to be low. As α is linked with the bound

[3]These choices are consistent with the estimators which are implemented in the simulations of Section 3.6.

on the reasonable values of $\{f_t\}$ as previously explained, it means that $\mathcal{E}^{\circ,\exp}$ is likely to handle more outliers if the arbitrary disturbance $\{f_t\}$ is a pure sparse noise.

To conclude, this test highlights the fact that the number of outliers and the magnitude of the reasonable values in the arbitrary disturbance $\{f_t\}$ noise have a great impact on how much observable the systems needs to be in order to be able to apply Theorem 3.1 to a given estimator. In particular, a greater number of outliers requires a higher degree of observability from the system in order for Condition (3.28) to be verified. In addition, we also saw that for a given ratio of outliers, Estimator $\mathcal{E}^{\circ,\exp}$ is more likely to be approximately resilient if the noise sequence only exhibits a sparse behaviour.

3.5 Discussions on the implementation $\mathcal{E}^{\exp}$ and $\mathcal{E}^{\circ,\exp}$

In the present chapter, contrary to V_Σ in Chapter 2, $V_\Sigma^{\exp}$ (and $V_\Sigma^{\circ,\exp}$) presents a minimum but is not convex. Subsequently, we are not able to directly use the efficient tools of convex optimisation in order to solve the optimisation problems underlying the definition of classes $\mathcal{E}^{\exp}$ and $\mathcal{E}^{\circ,\exp}$.

The current section aims at providing heuristic tools to implement these two classes of estimators in the case where the loss functions ϕ and ψ are both equal to the square function, *i.e.* for all a in $\mathbb{R}$, $\phi(a) = \psi(a) = a^2$.

First of all, we reformulate the search of the minimising arguments of $V_\Sigma^{\exp}$ as a Least Squares optimisation problem. However, this newly defined quadratic optimisation problem relies on pre-emptively setting weights depending on the to-be-obtained minimising argument, which is not implementable as such. The rest of the section will be focused on ways to approximately implement it:

- To derive a batch algorithm, the quadratic optimisation problem will be approximately implemented through an Iteratively Reweighted Least Squares (IRLS) algorithm.
- To derive a recursive implementation, the best *a priori* value of those weights will be used in order to approximately implement this estimator using the Forward Dynamic Programming framework presented in Chapter 1.

3.5.1 Reformulation of the search for the minimising arguments of $V_\Sigma^{\exp}$ and $V_\Sigma^{\circ,\exp}$

In this section, we will show how we want to approach the elements of $\mathcal{E}^{\exp}$ and $\mathcal{E}^{\circ,\exp}$ through a Least Squares optimisation problem. For the sake of simplicity, the reasoning will be conducted for Estimator $\mathcal{E}^{\circ,\exp}$. The results for Estimator $\mathcal{E}^{\exp}$ will be subsequently stated as a remark.

We recall the definition of $V_\Sigma^{\circ,\exp}$,

$$V_\Sigma^{\circ,\exp}(Y,z) = \sum_{(t,j)\in\mathbb{T}\times\mathbb{J}} \left(1 - e^{-\lambda_\psi(y_t[j]-\theta_{t,j}^\top z)^2}\right).$$

$V_\Sigma^{\circ,\exp}$ is differentiable with respect to z, and its gradient $\nabla V_\Sigma^{\circ,\exp}(Y,\cdot) : \mathbb{R}^n \to \mathbb{R}^n$ can be expressed such that for all z in $\mathbb{R}^n$,

$$\nabla V_\Sigma^{\circ,\exp}(Y,z) = -2\lambda_\psi \sum_{(t,j)\in\mathbb{T}\times\mathbb{J}} (y_t[j] - \theta_{t,j}^\top z) e^{-\lambda_\psi \left(y_t[j]-\theta_{t,j}^\top z\right)^2} \theta_{t,j}.$$

For all $\hat{X}$ in $\mathcal{E}^{\circ,\exp}(Y)$, $\hat{x}_0$ is a critical point of $V_\Sigma^{\circ,\exp}$, *i.e.* $\nabla V_\Sigma^{\circ,\exp}(Y,\hat{x}_0) = 0$. Consequently,

$$\sum_{(t,j)\in\mathbb{T}\times\mathbb{J}} (y_t[j] - \theta_{t,j}^\top \hat{x}_0) e^{-\lambda_\psi \left(y_t[j]-\theta_{t,j}^\top \hat{x}_0\right)^2} \theta_{t,j} = 0. \tag{3.53}$$

We observe that the stationary equation (3.53) verified by $\hat{x}_0$ is similar to the one which would be obtained by differentiating the quadratic function V_q° such that for all (Y,z) in $\mathbb{R}^{m\times T} \times \mathbb{R}^n$,

$$V_q^\circ(Y,z) = \sum_{(t,j)\in\mathbb{T}\times\mathbb{J}} \beta_{t,j} \left(y_t[j] - \theta_{t,j}^\top z\right)^2, \tag{3.54}$$

with $\{\beta_{t,j}\}$ a family of appropriately designed real-valued positive weights. Indeed, by posing

$$\forall (t,j) \in \mathbb{T}\times\mathbb{J}, \qquad \beta_{t,j} = \lambda_\psi e^{-\lambda_\psi \left(y_t[j]-\theta_{t,j}^\top \hat{x}_0\right)^2}, \tag{3.55}$$

we notice that $\hat{x}_0$ must be a critical point of V_q° given that it verifies

$$\sum_{(t,j)\in\mathbb{T}\times\mathbb{J}} \beta_{t,j} (y_t[j] - \theta_{t,j}^\top \hat{x}_0) \theta_{t,j} = 0.$$

It is straightforward to prove that if the system is observable, then V_q° presents only one critical point which is its unique global minimum [Boy04, Ex. 4.5]. If we knew the values of $\{\beta_{t,j}\}$ in advance, we could then design V_q° and minimise it in order to obtain $\hat{x}_0$.

However, the main problem which arise when we want to obtain $\hat{x}_0$ through the minimisation of V_q°, is that the values of $\{\beta_{t,j}\}$ *do* depend on the to-be-obtained estimate $\hat{x}_0$. To address this problem, we aim at finding an approximation $\{\hat{\beta}_{t,j}\}$ of family $\{\beta_{t,j}\}$ in order to subsequently solve the optimisation problem

$$\arg\min_{z\in\mathbb{R}^n} \left\{ \sum_{(t,j)\in\mathbb{T}\times\mathbb{J}} \hat{\beta}_{t,j} \left(y_t[j] - \theta_{t,j}^\top z\right)^2 \right\}, \tag{3.56}$$

and obtain an approximation of $\hat{x}_0$.[4] The rest of the section will be focused on providing two different approaches to approximate the values (3.55) of $\{\beta_{t,j}\}$ and solve the minimisation problem (3.56).

[4] As long as the system is observable, and $\{\hat{\alpha}_{t,j}\}$, $\{\hat{\beta}_{t,j}\}$ are families of positive weights, the optimisation problems defined by (3.56) and (3.59) return a singleton. [Boy04, Ex. 4.5]

Remark 3.2. *In the case of the class $\mathcal{E}^{\exp}$ defined in (3.4), the same reasoning can be applied. We define two families of positive weights $\{\alpha_{t,i}\}$ and $\{\beta_{t,j}\}$ such that*

$$\forall (t,i) \in \mathbb{T}' \times \mathbb{I}, \alpha_{t,i} = \lambda_\phi e^{-\lambda_\phi \left(\hat{x}_{t+1}[i] - a_i^\top \hat{x}_t\right)^2} \tag{3.57}$$

$$\forall (t,j) \in \mathbb{T} \times \mathbb{J}, \beta_{t,j} = \lambda_\psi e^{-\lambda_\psi \left(y_t[j] - c_j^\top \hat{x}_t\right)^2}, \tag{3.58}$$

with $\hat{X} = \begin{pmatrix} \hat{x}_0 & \cdots & \hat{x}_{T-1} \end{pmatrix}$ from $\mathcal{E}^{\exp}(Y)$.

The goal of the method is to find two families of approximations $\{\hat{\alpha}_{t,i}\}$ and $\{\hat{\beta}_{t,j}\}$ in order to subsequently solve

$$\underset{Z \in \mathbb{R}^{n \times T}}{\arg\min} \left\{ \sum_{(t,i) \in \mathbb{T}' \times \mathbb{I}} \hat{\alpha}_{t,i} \left(z_{t+1}[i] - a_i^\top z_t \right)^2 + \sum_{(t,j) \in \mathbb{T} \times \mathbb{J}} \hat{\beta}_{t,j} \left(y_t[j] - c_j^\top z_t \right)^2 \right\}, \tag{3.59}$$

and obtain an approximation of $\hat{X}$.[4]

3.5.2 Batch approximative implementation: an Iteratively Reweighted Least Squares Algorithm

In this section, the families $\{\alpha_{t,i}\}$ and $\{\beta_{t,j}\}$ will be approximated through an Iteratively Reweighted Least Squares (IRLS) algorithm [Jor06].

This approach consists in iteratively solving the optimisation problem defined in (3.59) and then updating the weights $\{\alpha_{t,i}\}$ and $\{\beta_{t,j}\}$ with the obtained estimated value. More precisely, at each iteration, we solve the optimisation problem

$$\{\hat{X}^{(k)}\} = \underset{Z \in \mathbb{R}^{n \times T}}{\arg\min}\, V_q^{(k)}(Y, Z), \tag{3.60}$$

with $V_q^{(k)}$ the quadratic function such that for all (Y, Z) in $\mathbb{R}^{m \times T} \times \mathbb{R}^{n \times T}$,

$$V_q^{(k)}(Y,Z) = \sum_{(t,i) \in \mathbb{T}' \times \mathbb{I}} \alpha_{t,i}^{(k)} \left(z_{t+1}[i] - a_i^\top z_t \right)^2 + \sum_{(t,j) \in \mathbb{T} \times \mathbb{J}} \beta_{t,j}^{(k)} \left(y_t[j] - c_j^\top z_t \right)^2. \tag{3.61}$$

$\{\alpha_{t,i}^{(k)}\}$ and $\{\beta_{t,j}^{(k)}\}$ are two families of positive real-valued weights recursively defined so that for all $k \in \mathbb{N}$,

$$\forall (t,i) \in \mathbb{T}' \times \mathbb{I}, \alpha_{t,i}^{(k+1)} = \lambda_\phi e^{-\lambda_\phi \left(\hat{x}_{t+1}^{(k)}[i] - a_i^\top \hat{x}_t^{(k)} \right)^2} \tag{3.62}$$

$$\forall (t,j) \in \mathbb{T} \times \mathbb{J}, \beta_{t,j}^{(k+1)} = \lambda_\psi e^{-\lambda_\psi \left(y_t[j] - c_j^\top \hat{x}_t^{(k)} \right)^2}. \tag{3.63}$$

Finally, to initialise the families $\{\alpha_{t,i}^{(1)}\}$ and $\{\beta_{t,j}^{(1)}\}$, we choose

$$\forall (t,i) \in \mathbb{T}' \times \mathbb{I}, \alpha_{t,i}^{(1)} = \lambda_\phi$$
$$\forall (t,j) \in \mathbb{T} \times \mathbb{J}, \beta_{t,j}^{(1)} = \lambda_\psi e^{-\lambda_\psi y_t[j]^2}.$$

The reasoning behind the choice of $\{\beta_{t,j}^{(1)}\}$ is to regulate the contribution of each term in the right sum of $V_q^{(1)}$ (see Eq. (3.60)). This prevents the terms associated

with a value of $y_t[j]$ greater than others (typically if it presents an outlier) from outweighing the rest of the terms. In the absence of knowledge, every weight $\alpha_{t,i}^{(1)}$ is chosen equal to λ_ϕ in order to weight equally all the terms involved in the left sum of (3.60). The value λ_ϕ also helps maintaining the balance between the left and right sums of $V_q^{(1)}$ which are respectively weighted by λ_ϕ and λ_ψ.

The stopping condition of the algorithm consists in checking if the trajectory $\hat{X}^{(k)}$, obtained at iteration k, is different from $\hat{X}^{(k-1)}$, the estimated state trajectory obtained at the previous iteration: to do so, we compute the *stopping value*

$$\eta^{(k)} = \frac{\|\hat{X}^{(k)} - \hat{X}^{(k-1)}\|_2}{\|\hat{X}^{(k-1)}\|_2}$$

and the algorithm stops once it is smaller than a given quantity $\eta_{\min}$ specified as an input of the algorithm. To make sure that the stopping condition is not verified after only one iteration, we can initialise $\hat{X}^{(0)}$ to be arbitrarily large, for instance $\hat{X}^{(0)} = (\,\hat{x}_0^{(0)} \quad \cdots \quad \hat{x}_{T-1}^{(0)}\,)$ such that for all $(t,i) \in \mathbb{T} \times \mathbb{I}$, $\hat{x}_t^{(0)}[i] = 10^5$.

In addition to the stopping condition, to make sure that the algorithm eventually stops, another stopping condition specifies a maximum number of iterations $k_{\max}$ that it is allowed to perform.

The obtained algorithm is described below as Algorithm 3.1.

Algorithm 3.1 Iterative Reweighted Least Squares (IRLS) Algorithm to approximately implement Problem (3.59)

Inputs: Σ, λ_ϕ, λ_ψ, Y, $k_{\max}$, $\eta_{\min}$
Initialisation:
$k \leftarrow 0$
$\eta^{(0)} \leftarrow 10^8$
$\forall (t,i) \in \mathbb{T} \times \mathbb{I}$, $\hat{x}_t^{(0)}[i] \leftarrow 10^5$
$\forall (t,i) \in \mathbb{T} \times \mathbb{I}$, $\alpha_{t,i}^{(1)} \leftarrow \lambda_\phi$
$\forall (t,j) \in \mathbb{T} \times \mathbb{J}$, $\beta_{t,j}^{(1)} \leftarrow \lambda_\psi e^{-\lambda_\psi y_t[j]^2}$
End of Initialisation.
while $\eta^{(k)} > \eta_{\min}$ **and** $k < k_{\max}$ **do**
  $k \leftarrow k+1$
  $\hat{X}^{(k)} \leftarrow \arg\min_{Z \in \mathbb{R}^{n \times T}} V_q^{(k)}(Y, Z)$
  $\forall (t,i) \in \mathbb{T} \times \mathbb{I}$, $\alpha_{t,i}^{(k+1)} \leftarrow \lambda_\phi e^{-\lambda_\phi (\hat{x}_{t+1}^{(k)}[i] - a_i^\top \hat{x}_t^{(k)})^2}$
  $\forall (t,j) \in \mathbb{T} \times \mathbb{J}$, $\beta_{t,j}^{(k+1)} \leftarrow \lambda_\psi e^{-\lambda_\psi (y_t[j] - c_j^\top \hat{x}_t^{(k)})^2}$
  $\eta^{(k)} \leftarrow \frac{\|\hat{X}^{(k)} - \hat{X}^{(k-1)}\|}{\|\hat{X}^{(k-1)}\|}$
end while
return $\hat{X}^{(k)}$

Remark 3.3. *See Appendix C.2 for the derivation of a batch algorithm for Estimator* $\mathcal{E}^{\circ,\exp}$.

3.5.3 Approximative recursive implementation: application of the Forward Dynamic Programming framework

In this section, similarly to Section 2.6, we will make use of the Forward Dynamic Programming framework in order to recursively implement Problem (3.59) when the time horizon T grows towards infinity.

To proceed, we define the function $V^{\star}_{q,T}$ such that for all $T \in \mathbb{N}$,

$$\forall (Y,z) \in \mathbb{R}^{m\times T} \times \mathbb{R}^n, \qquad V^{\star}_{q,T}(Y,z) = \min_{\substack{Z\in\mathbb{R}^{n\times T}\\ z_T = z}} V_q(Y,Z)$$

Once again, Y, Z and V_q all implicitly depends on T as they were defined on a time-horizon of length T.

The Bellman equation (1.42) gives the relationship between $V^{\star}_{q,T+1}$ and $V^{\star}_{q,T}$ which is such that for all T in $\mathbb{N}$,

$$V^{\star}_{q,T+1}(z) = \min_{s\in\mathbb{R}^n} \left\{ V^{\star}_{q,T}(s) + \sum_{i\in\mathbb{I}} \alpha_{T,i} \left(z[i] - a_i^{\top} s \right)^2 \right\} + \sum_{j\in\mathbb{J}} \beta_{T+1,j} \left(y_{T+1}[j] - c_j^{\top} z \right)^2$$

If we knew coefficients $\{\alpha_{T,i}\}$ and $\{\beta_{T+1,j}\}$ in this relationship, we could apply Theorem 1.6 as we did in the quadratic case. However, those coefficients need the value of $\hat{x}_{T+1}$ in order to be computed. The idea is then to use the *a priori* estimate of $\hat{x}_{T+1}$, which is $\hat{x}_{T+1|T} = A_T \hat{x}_T$, in order to approximate the values of $\{\alpha_{T,i}\}$ and $\{\beta_{T+1,j}\}$.

We therefore define approximated values $\{\hat{\alpha}_{T,i}\}$ and $\{\hat{\beta}_{T+1,j}\}$ as follows for all T in $\mathbb{N}$:

$$\forall i \in \mathbb{I}, \hat{\alpha}_{T,i} = \lambda_\phi e^{-\lambda_\phi \left(\hat{x}_{T+1|T}[i] - a_i^{\top}\hat{x}_T\right)^2} = \lambda_\phi \tag{3.64}$$

$$\forall j \in \mathbb{J}, \hat{\beta}_{T+1,j} = \lambda_\psi e^{-\lambda_\psi \left(y_{T+1}[j] - c_j^{\top}\hat{x}_{T+1|T}\right)^2}. \tag{3.65}$$

Indeed, it is worth noting that with this approximation, the weights $\{\hat{\alpha}_{T,i}\}$ are all equal to λ_ϕ given that $\hat{x}_{T+1|T}[i] = a_i^{\top}\hat{x}_T$ for all (T,i) in $\mathbb{N}\times\mathbb{I}$. This can be interpreted as the fact that the value of the process noise at time T, w_T, cannot be inferred from the estimate of the state at time T alone, and as $\alpha_{T,i}$ is calculated from the deviation from the dynamics induced by A between two consecutive estimates (here $\hat{x}_{T+1}$ and $\hat{x}_T$), we do not have any knowledge about it. This is a common phenomenon when considering exponential terms in the cost function, like in the Correntropy Filter derived in [Iza16, Eq. (17)]. A classic way to solve this issue is to iterate the estimation process of $\hat{x}_T$ in a fixed-point-like approach in order to update weights $\hat{\alpha}_{T,i}$ and $\hat{\beta}_{T+1,j}$ with the *a posteriori* estimates of $\hat{x}_{T+1}$ instead of its *a priori* estimate $A\hat{x}_T$, as in [Che17a].

With the approximations (3.64)–(3.65), we can now apply Theorem 1.6 with the matrices $\{Q_T\}$ and $\{R_T\}$ such that for all T in $\mathbb{N}$,

$$Q_T = \frac{1}{\lambda_\phi} I_n \text{ and } R_T = \text{diag}(1/\hat{\beta}_{T,1}, ..., 1/\hat{\beta}_{T,m})$$

The corresponding algorithm is described as Algorithm 3.2. Its input specifies the initialising values of $\hat{x}_0$ and P_0, as well as a maximum number of time indexes $T_{\max}$. The obtained algorithm resembles the first iteration of the algorithm derived in [Che17a] for the Maximum Correntropy Criterion Kalman Filter (MCCKF). The way their algorithm was derived is slightly different but relies on the same principle, which is to approximate the critical point of an exponential performance index function (see Eq. (1.57)) by differentiating it.

Nevertheless, it is interesting to point out that their algorithm performs several iterations in order to find the estimate as the solution of fixed-point equation. Such

an approach could have also been conducted in our case, and we could have performed steps 6 from 10 in Algorithm 3.2 several times in order to update $\hat{\alpha}_{T,i}$ and $\hat{\beta}_{T+1,j}$ with the knowledge of $\hat{x}_T$.

Algorithm 3.2 Kalman-like Algorithm to approximately implement Problem (3.59)

Inputs: A, C, $\lambda_\phi \in \mathbb{R}_{>0}$, $\lambda_\psi \in \mathbb{R}_{>0}$, $\hat{x}_0 \in \mathbb{R}^n$, $P_0 \in \mathcal{S}_n^+(\mathbb{R})$, $T_{\max} \in \mathbb{N}$, $Y \in \mathbb{R}^{m \times T_{\max}}$
Initialization:
$T \leftarrow 0$
End of Initialization.
while $T < T_{\max}$ **do**
  $\hat{x}_{T|T-1} \leftarrow A\hat{x}_{T-1}$
  $\forall j \in \mathbb{J}$, $\hat{\beta}_{T,j} = \lambda_\psi e^{-\lambda_\psi \left(y_t[j] - c_j^\top \hat{x}_{T|T-1}\right)^2}$
  $R_T \leftarrow \mathrm{diag}(1/\hat{\beta}_{T,1}, ..., 1/\hat{\beta}_{T,m})$
  $P_{T|T-1} \leftarrow AP_{T-1}A^\top + \frac{1}{\lambda_\phi} I_n$
  $L_T \leftarrow P_{T|T-1}C^\top \left(CP_{T|T-1}C^\top + R_T\right)^{-1}$
  $\hat{x}_T \leftarrow \hat{x}_{T|T-1} + L_T(y_T - C\hat{x}_{T|T-1})$
  $P_T \leftarrow (I_n - LC)P_{T|T-1}$
  $T \leftarrow T + 1$
end while

3.6 Simulation results

In this section, we will numerically study the implementation of the class of estimators studied in the present chapter, which will be through the study of the convergence of the derived algorithms as well as a study of their performances on systems in presence of noise.

To do so, we will use the system (1.21) introduced in Chapter 1 with matrices (A, C) defined by

$$A = \begin{pmatrix} 0.7 & 0.45 \\ -0.5 & 1 \end{pmatrix}, \quad C = \begin{pmatrix} 1 & 2 \end{pmatrix}.$$

w_t will be taken as a uniformly distributed white noise with values taken within a segment of the form $[-a, a]$, while f_t is decomposed as in (1.49): v_t will be a uniformly distributed white noise, while s_t will be a sparse vector. It is generated in two steps: (1) the indexes (t, j) for which $s_t[j] \neq 0$ are uniformly selected over $\mathbb{T} \times \mathbb{J}$, and then (2) for each (t, j) such that $s_t[j] \neq 0$, the value of $s_t[j]$ is set as the realization of a Gaussian process of variance 100 and mean 0.

Throughout this section, $\mathcal{E}^{\exp}$ and $\mathcal{E}^{\circ,\exp}$ will designate the algorithms discussed in Section 3.5:

- Estimator $\mathcal{E}^{\exp}$ will designate the algorithms derived in order to solve Problem (3.59), *i.e.* the batch algorithm 3.1 or the recursive algorithm 3.2.
- Estimator $\mathcal{E}^{\circ,\exp}$ will designate the batch algorithm designed to solve Problem (3.56), *i.e.* Algorithm C.1, reported in Appendix C.2.

Moreover, as means of comparison, we will make use of $\mathcal{E}_{\ell_2^2,\ell_1}$ and $\mathcal{E}_{\ell_2^2,\ell_2^2}$ which designate the estimators defined and studied in Section 2.7.

Finally, an *Oracle* estimator will designate an estimator which is aware of the arbitrary component $\{s_t\}$ of $\{f_t\}$, meaning it performs its estimation process on the uncorrupted output $\tilde{y}_t = y_t - s_t$.

The IRLS algorithms described in Section 3.5.2 will be implemented with $\eta_{\min} = 10^{-8}$ and $k_{\max} = 100$ unless explicitly stated otherwise, and the convex optimisation problem occurring at each iteration was directly solved through the CVX interface [Gra18] on MATLAB.

3.6.1 Numerical study of the convergence of the IRLS algorithms

In this section, we will investigate how the Iteratively Reweighted Least Squares (IRLS) algorithms derived in Section 3.5.2 converge, *i.e.* how the stopping value

$$\eta^{(k)} = \|\hat{X}^{(k)} - \hat{X}^{(k-1)}\|/\|\hat{X}^{(k-1)}\|$$

evolves through the iteration process.

To perform this study, we generated 500 different systems with a Signal-to-Noise Ratio (SNR) of 30dB (for w_t and v_t) and 10% of outliers (for s_t). The systems were generated through the `drss` function in MATLAB with the condition that the smallest eigenvalue in modulus is greater than 0.8. We also made sure that the state matrix of the studied systems is never the identity matrix, which is an edge case of stable systems.

For every system, we then implemented the estimation of its state through Algorithm 3.1 for a fixed number of fifty iterations while still calculating the stopping condition $\eta^{(k)}$ at each iteration. Once the estimation process of the 500 system states was performed, for each iteration k, we averaged the value of $\eta^{(k)}$ over all systems, and we picked the maximum value of $\eta^{(k)}$ among all systems. The results of this test can be found in Figure 3.5.

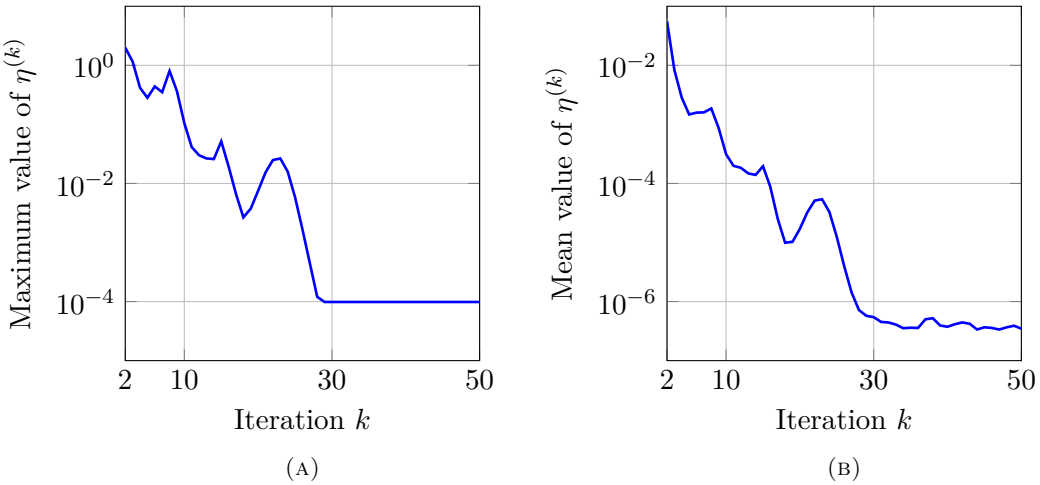

(A) (B)

FIGURE 3.5: Maximum value (A) and mean value (B) of $\eta^{(k)} = \|\hat{X}^{(k)} - \hat{X}^{(k-1)}\|/\|\hat{X}^{(k-1)}\|$ throughout iterations

What can be observed is that across all systems, the stopping value η tends to decrease through the iterations, which means that the estimated trajectory obtained at each iteration tends towards a given trajectory. η as a function of k is not necessarily decreasing over the whole segment $[2, 49]$ (even though it was the case for

several systems), not even non-increasing, as the maximum value registered among all simulated systems indicates a local increase around iteration $k = 25$: however, it seems that $\eta^{(k)}$ converges to a fixed value for iterations higher than $k = 30$. The value towards which it converges however varies from one system to another, and if the limit of the mean value seems slightly smaller than 10^{-6} we can see that there are systems for which η converges towards 10^{-4}.

The conclusion of this study is that the IRLS algorithms derived in Section 3.5.2 seems to be consistently converging, meaning that they reach a fixed point of Problem (3.60). Nevertheless, if $\eta^{(k)}$ seems to converge to a fixed value, this value changes from one system and one noise configuration to another: it is therefore primordial to set the threshold $\eta_{\min}$ so that we make sure that the algorithm can realistically reach it. Another way to proceed is to fix the maximum number of iterations $k_{\max}$ to a reasonable value and then simply make the algorithms perform $k_{\max}$ iterations without taking any $\eta_{\min}$ into account, as this experiment seems to show that the algorithms converges for 30 iterations for most systems.

3.6.2 Performances in the presence of dense noise

If the goal of the previous test was to study the convergence of the IRLS algorithms, it did not provide insight on their actual performances, as it mainly focused on the evolution of the stopping value which merely assess how the returned estimated trajectory $\hat{X}$ varies from one iteration to another.

The performances of the different estimators will be assessed through the same performance indicator used in Section 2.7 in Chapter 2, namely the Relative Estimation Error (REE)

$$\text{REE} = \frac{\|\hat{X} - X\|_2}{\|X\|_2}$$

where X is the real trajectory of the system and $\hat{X}$ is the estimated trajectory obtained from the estimator.

In most tests, a hundred different noise realisations will be generated for each setting, in order to average the REE and make the results more reliable.

It is worth remembering that the results which are going to be presented do not necessarily correspond to those of the theoretical estimators defined at the beginning of the chapter through V_Σ^{exp} or $V_\Sigma^{\circ,\text{exp}}$. Due to the fact that the aforementioned performance index functions are not convex, we are not necessarily able to obtain the true minimizers , and therefore do not know what performances the theoretical estimators would yield. This constitutes a major difference with the estimators resulting from convex performance index functions, as their performances could be assessed through the direct solving of the underlying optimisation problem.

Experiment 1: Sparsity test

For this experiment, we fix the amplitude of w_t to $a = 0.03$ and the amplitude of v_t to $a = 0.1$, yielding a Signal to Noise Ratio (SNR) of about 30 dB for each noise. We then apply the batch estimators defined at the beginning of Section 3.6 to 100 different realisations of the output data and we compute the average of the corresponding REE. This process is repeated for different fractions of nonzero entries in the sparse noise $\{s_t\}$, ranging from 0 to 1. The results from this test are presented in Figure 3.6.

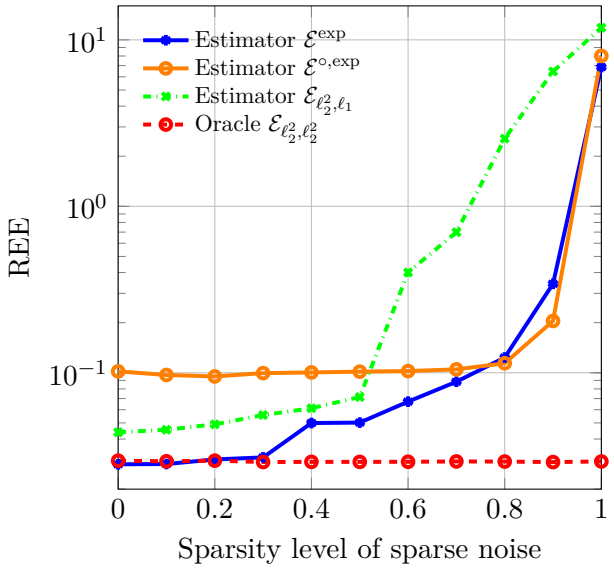

FIGURE 3.6: Average relative estimation error (in logarithm scale) induced by different estimators versus sparsity level of the sparse noise $\{s_t\}$

Considering Figure 3.6, the estimation error of Estimators $\mathcal{E}^{\exp}$ and $\mathcal{E}^{\circ,\exp}$ is stable until the ratio of non-zero elements in s_t is too high, namely 30% for Estimator $\mathcal{E}^{\exp}$ and 80% for Estimator $\mathcal{E}^{\circ,\exp}$. On the range over which its estimation error is stable, Estimator $\mathcal{E}^{\exp}$ actually matches the performances of Oracle $\mathcal{E}_{\ell_2^2,\ell_2^2}$.

$\mathcal{E}^{\exp}$ yields even better results than Estimator $\mathcal{E}_{\ell_2^2,\ell_1}$ for all ratios. The iterative nature of the IRLS algorithm implementing $\mathcal{E}^{\exp}$ (Algorithm 3.1) probably plays a role in these performances, since iterative processes are known to increase the sparsity in estimation results. [Dau10]. Nevertheless, this iterative nature also induce more algorithmic complexity, given that Algorithm 3.1 requires the solving of several convex optimisation problems, while $\mathcal{E}_{\ell_2^2,\ell_1}$ is implemented as the solving of one convex optimisation problem. In addition to that, it is worth noting that $\mathcal{E}^{\exp}$ has a smaller breakpoint, *i.e.* the value of sparsity level such that the estimation error of the estimator starts diverging, than $\mathcal{E}_{\ell_2^2,\ell_1}$.

Finally, regarding Estimator we notice that its breakpoint tends to be much larger than the one of $\mathcal{E}_{\ell_2^2,\ell_1}$ or $\mathcal{E}^{\exp}$ for this example. However, the REE of $\mathcal{E}^{\circ,\exp}$ itself is bigger than for the two other estimators, especially for low sparsity levels of sparse noise.

Experiment 2: SNR test. Now, we fix the sparsity level of the time sequence $\{s_t\}$ to 0.1 and let the powers of the dense noise $\{(w_t, v_t)\}$ vary jointly from 5 dB to 100 dB in term of Signal-to-Noise Ratio (SNR). The results obtained for the implemented estimators are displayed in Figure 3.7.

Figure 3.7 shows that every implemented resilient estimator displays performances which are close from the ones of Oracle $\mathcal{E}_{\ell_2^2,\ell_2^2}$ in terms of averaged REE. For instance, $\mathcal{E}^{\exp}$, $\mathcal{E}_{\ell_2^2,\ell_1}$, and Oracle $\mathcal{E}_{\ell_2^2,\ell_2^2}$ yield the same REE for Signal-to-Noise ratios ranging from 30dB to 50dB. $\mathcal{E}^{\circ,\exp}$ has a REE which is about twice as large on the same range, but it remains between 10^{-1} and 10^{-2} which is acceptable.

However, the performances of the resilient estimators are a lot worse than those of their oracle counterpart for high values of SNR, which correspond to systems which are barely disturbed. In this setting, the gap between the REE of $\mathcal{E}^{\exp}$ or $\mathcal{E}^{\circ,\exp}$ and the REE of $\mathcal{E}_{\ell_2^2,\ell_2^2}$ is much wider than for lower values of SNR. This potentially means

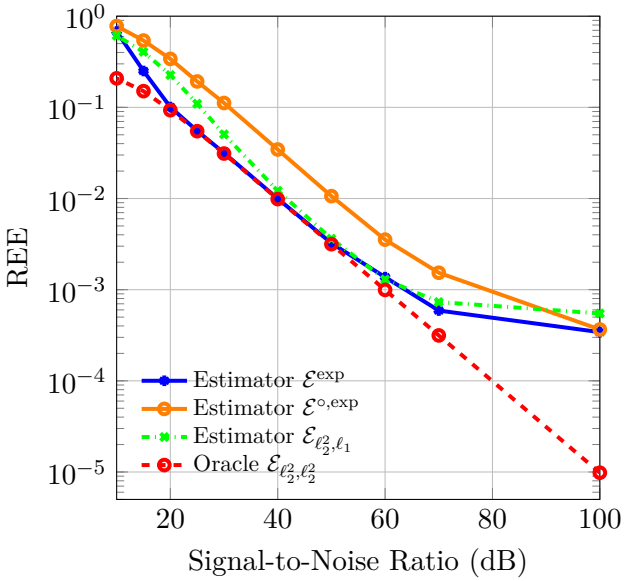

FIGURE 3.7: Average relative estimation error (in logarithm scale) induced by different estimators for different levels of both dense noises w_t and v_t

that resilient estimators, in order to be able to handle outliers, have less sensitivity to the variations of the state, which is especially visible in the case where the dense noises are almost equal to 0.

Experiment 3: Study of the influence of λ_ϕ and λ_ψ

In this study, we fixed both the amplitude of the dense noises (to their level in the first test, *i.e.* with an SNR of 30dB, and the ratio of nonzero entries of $\{s_t\}$ to 30%) in order to assess the influence of λ_ψ and λ_ϕ on the performances of $\mathcal{E}^{\exp}$ and $\mathcal{E}^{\circ,\exp}$. First of all, we performed a test on $\mathcal{E}^{\circ,\exp}$ which only depends on λ_ψ: for several values of λ_ψ, we performed the estimation of the state of System (1.21) under 100 different noise realisations. We then averaged the Relative Estimation Error (REE) obtained for each realisation. The results of this test are presented in Figure 3.8.

We can observe that extreme values of λ_ψ yield rather poor results in terms of average REE. This is due to the fact that λ_ψ tunes the sensitivity of the exponential terms in the performance index function $V_\Sigma^{\circ,\exp}$ (see Eq. (3.21)). If we recall Figure 3.1, the bigger λ_ψ is, the faster function $a \mapsto (1 - \exp(-\lambda_\psi a))$ saturates, *i.e.* is almost equal to 1. Consequently, correctly tuning λ_ψ is a key aspect of the performances of $\mathcal{E}^{\circ,\exp}$. If λ_ψ is too small, $a \mapsto (1 - \exp(-\lambda_\psi a))$ does not saturate even for great arguments, and therefore lets potential outliers disturb the estimation process. Conversely, if λ_ψ is too big, it saturates even for small arguments, which prevents a proper minimisation of the residuals $\hat{f}_t[j] = y_t[j] - c_j^\top \hat{x}_t$, even for reasonable values of f_t.

We then performed a similar test for Estimator $\mathcal{E}^{\exp}$. Compared to the test on $\mathcal{E}^{\circ,\exp}$, there are not one but two tuning parameters in the performance index function $V_\Sigma^{\exp}$, namely λ_ϕ and λ_ψ. For each value of the pair $(\lambda_\phi, \lambda_\psi)$ as specified in Table 3.1, we simulated System (1.21) a hundred times with different noise realisations (30% of non-zero entries in s_t and a SNR of 30dB). The averaged REE for each couple $(\lambda_\phi, \lambda_\psi)$ were then gathered in a heatmap table on Table 3.1.

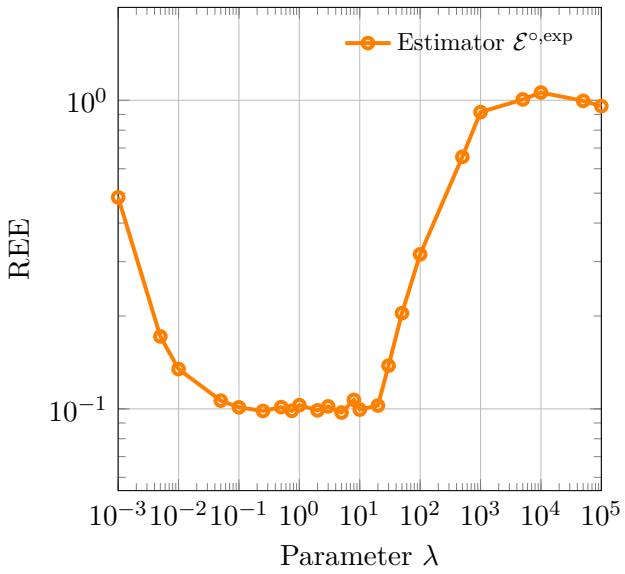

FIGURE 3.8: Average REE of Estimator $\mathcal{E}^{\circ,\exp}$ for different values of λ_ψ in Algorithm C.1

		λ_ψ					
		10^{-2}	10^{-1}	1	10	10^2	10^3
λ_ϕ	10^{-2}	2.01	$4.71 \cdot 10^{-1}$	$1.15 \cdot 10^{-1}$	$6.36 \cdot 10^{-2}$	$3.80 \cdot 10^{-2}$	$1.38 \cdot 10^{-1}$
	10^{-1}	$6.15 \cdot 10^{-1}$	$2.89 \cdot 10^{-1}$	$1.17 \cdot 10^{-1}$	$5.50 \cdot 10^{-1}$	$4.05 \cdot 10^{-2}$	$2.21 \cdot 10^{-1}$
	1	$2.41 \cdot 10^{-1}$	$1.08 \cdot 10^{-1}$	$8.43 \cdot 10^{-2}$	$5.67 \cdot 10^{-2}$	$9.22 \cdot 10^{-2}$	$2.89 \cdot 10^{-1}$
	10	$1.37 \cdot 10^{-1}$	$5.78 \cdot 10^{-2}$	$3.59 \cdot 10^{-2}$	$6.62 \cdot 10^{-2}$	$6.22 \cdot 10^{-2}$	$3.84 \cdot 10^{-1}$
	10^2	$1.23 \cdot 10^{-1}$	$7.63 \cdot 10^{-2}$	$4.17 \cdot 10^{-2}$	$6.61 \cdot 10^{-2}$	$5.71 \cdot 10^{-2}$	$4.84 \cdot 10^{-1}$
	10^3	$1.33 \cdot 10^{-1}$	$9.62 \cdot 10^{-2}$	$7.15 \cdot 10^{-2}$	$4.17 \cdot 10^{-2}$	$5.05 \cdot 10^{-2}$	$7.25 \cdot 10^{-1}$

TABLE 3.1: Averaged REE of Estimator $\mathcal{E}^{\exp}$ in function of the tuning parameters λ_ϕ and λ_ψ in Algorithm 3.1

The results of this test are pretty similar to the ones performed on $\mathcal{E}^{\circ,\exp}$ (Figure 3.8): we observe that for too low or too high values of λ_ϕ and λ_ψ, the averaged REE is higher than for values sitting between 10^{-1} and 10. The smallest averaged REE obtained is for the couple $(\lambda_\phi, \lambda_\psi) = (10, 1)$ which is the couple used for Experiment 1 and 2. It is however worth noting that the exact values of $(\lambda_\phi, \lambda_\psi)$ for which the REE is the smallest indeed varies depending on the characteristics of the noise disturbing the system, and each configuration calls for a different tuning of those parameters.

Experiment 4: Comparison with the recursive algorithm

In this experiment, for one noise realisation, we compare the trajectories estimated by the IRLS (batch) algorithm 3.1 and the recursive algorithm 3.2 to approximately implement Estimator $\mathcal{E}^{\exp}$. To do so, we implemented Algorithm 3.2 for $\lambda_\phi = 10$, $\lambda_\psi = 1$, $\hat{x}_0 = (\,0 \quad 0\,)$, $P_0 = I_2$ and $T_{\max} = 100$.

The noise configuration is as follows: SNR= 20dB for $\{w_t\}$, SNR= 30dB for $\{v_t\}$, 30% of non-zero entries in $\{s_t\}$. Trajectories (real and estimated) are found in Figure 3.10, while the characteristics of the sparse noise s_t can be found in Figure 3.9.

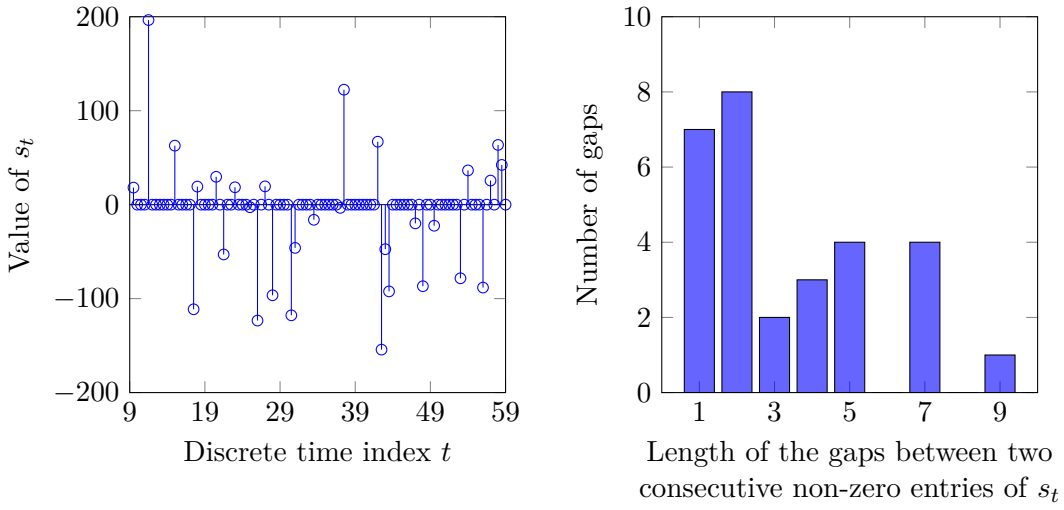

(A) Value of s_t through time

(B) Repartition of gaps between two consecutive non-zero entries of s_t by gap length

FIGURE 3.9: Evolution of s_t through time and repartition of the gaps between consecutive non-zero entries

Similarly to the recursive algorithms of Chapter 2, the recursive implementation of $\mathcal{E}^{\exp}$ presents a transient part at the beginning of the time-horizon where it needs to converge from $\hat{x}_0$. Once it has converged, the trajectory returned by Algorithm 3.2 is on par with the estimation obtained by Algorithm 3.1, which was once again one of the observation of *Experiment 5* in Chapter 2 (see Fig. 2.12).

3.7 Conclusion

In this chapter, to address the resilient state estimation problem stated at the end of Chapter 1, we considered a class of state estimators through a saturated cost function which generalizes the ones used in MCC-based approaches. This class is wide enough

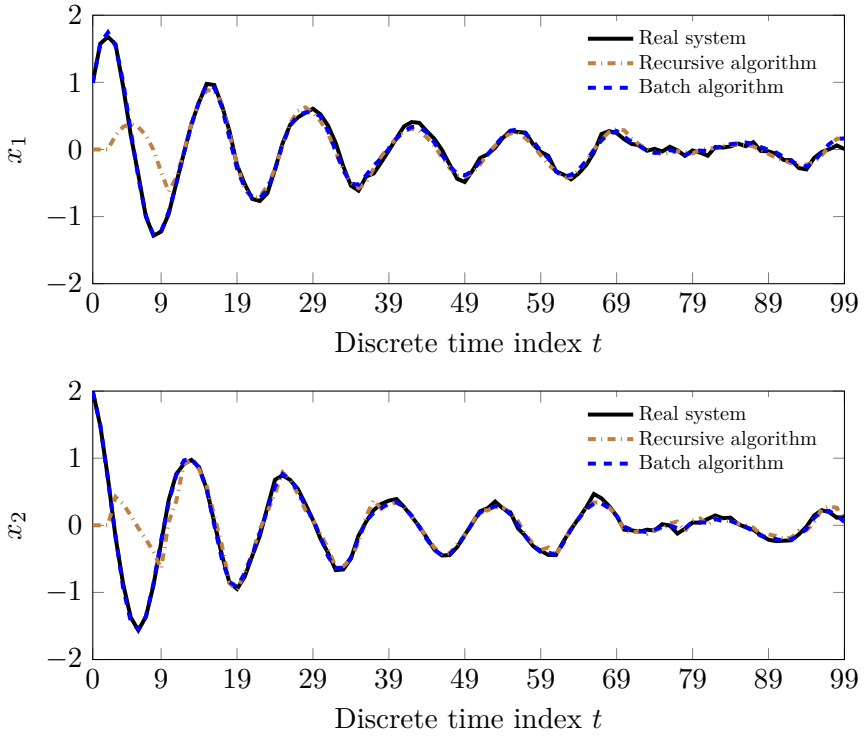

FIGURE 3.10: State trajectories of System (1.21) and estimated state trajectories obtained by recursive algorithm 3.2 and batch algorithm 3.1

to include several MCC estimators which were already studied in the literature, but also gathers estimators which are yet to be studied.

We proposed several theoretical results, which mainly aimed at illustrating how the different parameters and properties of the system, as well as the parameters of the estimators, interact with the parameters of the estimator. In particular, we proved that when the estimator is formulated under a regression-like form, it displays approximate resilience, *i.e.* its estimation error is bounded (but not equal to zero) in the presence of sparse noise, provided that a certain condition linked to the observability of the system and to the ratio of outliers is met. This condition and the upper bound on the estimation error, despite conservative, still did provide insight on a few key elements of resilient estimation. Moreover, the performance index functions defining the studied class of estimators cannot be convex, which required the derivation of heuristics batch and recursive algorithms

To assess the performances of the obtained algorithms, we performed three main simulation tests. They consisted in studying the convergence of the batch algorithm implementing $\mathcal{E}^{\exp}$, assessing the performances of the estimators with varying ratios of outliers and varying Signal-to-Noise Ratios, and studying the impact on the regularisation parameters λ_ϕ and λ_ψ in Algorithms 3.1 and C.1.

Despite not implementing the exact theoretical class of estimators defined in this chapter, the derived algorithms still displayed good performances in the presence of arbitrary noise. Moreover, the performances of the estimators studied in Chapter 3 seemed on par with those of the estimators studied in Chapter 2.

To enhance the analysis and numerical frameworks presented in this chapter, several directions are available. For instance, an upper bound on a norm of the estimation error of $\mathcal{E}^{\exp}$ has yet to be obtained. Indeed, Proposition 3.1 details how an image of the estimation error of $\mathcal{E}^{\exp}$ is upper bounded by a value which does not depend on the values of the outliers present in the system. However, this image is radially bounded, which is not enough to prove the boundedness of the estimation error with respect to a norm.

It would also be possible to analyse the algorithms derived in Section 3.5. For example, one could aim at finding theoretical guarantees on the convergence of Algorithms 3.1, 3.2 or C.1.

Chapter 4

Some case studies

As already pointed out in Chapter 1, state estimation is at the core of many different aspects in engineering, and resilient state estimation is not different in that regard. The goal of this chapter is to present several cases of application for the resilient frameworks developed and studied in Chapters 2 and 3. For each case, we will describe the problem at stake, and explain why the resilient estimation framework can be used to construct a solution. Subsequently, numerical studies will be provided. The exact characteristics of those studies will be stated in each section, but the overall idea is to provide, when possible, simulations which are closer to the reality of modern engineering than the more "virtual" simulations presented in the previous chapters in order to assess the performances of the derived estimators. This will be achieved through using measurements and/or models of real engineering systems as much as possible.

In particular, the present chapter will deal with four different applications:

- The problem of robust *trend filtering*, which consists in filtering a time series disturbed by outliers in order to extract a tendency among its samples (Section 4.1).
- Linear Regression in the presence of sparse noise (Section 4.2).
- The problem of estimating the state of a switched system without knowing its switching signal (Section 4.3).
- The online estimation of the position of a drone with temporary loss of measurements (Section 4.4).

4.1 Robust trend filtering

In this section, we will focus on the problem of *trend filtering* which consists in extracting the trend within a time series (*i.e.* an history of measurement) without any assumption on the actual process producing it. Most of the time, this trend is hidden due to the presence of parasitic variations which one might want to smooth out in order to access it. The trend filtering may concern any time series, which enables many applications in various fields such as Econometrics [Yam18], Astrophysics [Szu09] or Machine Learning [Wan16].

Under the scope of our estimation frameworks, we will investigate trend filtering of time series with outliers. In the first place, we will present how we adapt the resilient estimation framework to the trend filtering paradigm, and then the concept will be illustrated through the filtering of transistor voltage history with outliers.

4.1.1 Adaptation of the estimation framework to trend filtering

First of all, we consider a time series, which is a sequence of numerical values indexed through time: more precisely, in our case, a time series will be a vector $Y = \begin{pmatrix} y_0 & y_1 & \cdots & y_{T-1} \end{pmatrix}$ such that y_t is scalar for every t.[1] This series can represent the evolution of any type of process, from the measurement of a sensor to an economic indicator. The problem of *trend filtering* then consists in finding a *trend* in this evolution, *i.e.* a general tendency in the set of data.

A trend is a vague notion, which depends a lot on the kind of process which generated the time series as well as on how the trend will be used once obtained. To simplify things, the present section will be focused on the cleaning of a set of measured data from a system. In this setting, we do not have a model of this system or a model of the noises disturbing it, but we know that the measurements are disturbed by an undesirable sparse noise. The trend $r = \begin{pmatrix} r_0 & r_1 & \cdots & r_{T-1} \end{pmatrix}$, with r_t scalar for every t, then designates a version of the time series where the outliers are filtered out. The question is: how to filter out the outliers without altering the overall dynamics of the time series?

In our estimation framework, the trend can be modelled by a state-space representation

$$\Sigma_{\text{tf}} : \begin{cases} x_{t+1} &= Ax_t + w_t \\ y_t &= Cx_t + f_t \end{cases} \tag{4.1}$$

such that $C = \begin{pmatrix} 1 & 0 & \cdots & 0 \end{pmatrix}$ (the number of columns of C will be dictated by the size of x). The output y_t of System Σ_{tf} corresponds to samples of the time series Y, and f_t corresponds to the undesirable component of y_t, *i.e.* a part which we do not want to model through the trend.

The first equation in (4.1) must represent the dynamics of the evolution of the trend. A way to impose dynamics onto the trend is by zeroing out its n-th backward differences, *i.e.* the values

$$\Delta_n r(t) = \sum_{k=0}^{n} (-1)^k \binom{n}{k} r_{t-k}, \tag{4.2}$$

with $\binom{n}{k}$ the binomial coefficient

$$\binom{n}{k} = \frac{n!}{k!(n-k)!}.$$

Backward differences come from the finite differences method to calculate derivatives of continuous functions (see [Mat04, Sec. 9.9] for example) and can therefore be loosely interpreted as discrete derivatives. In particular, the first and second backward differences are such that

$$\begin{aligned} \Delta_1 r(t) &= r_t - r_{t-1} \\ \Delta_2 r(t) &= r_t - 2r_{t-1} + r_{t-2}. \end{aligned}$$

Intuitively, by imposing $\Delta_n r(t) = 0$, the trend will present certain dynamics. For instance, for $n = 1$, $\{r_t\}$ will be constant, while for $n = 2$, it will be affine. The order n of the backward difference is therefore an important parameter to choose in

[1] The framework presented in this section could be easily extended to the case where $\{y_t\}$ is a family of vectors.

a trend filtering setting, as it will set the dynamics of the trend, and the operator must decide on it based on their prior knowledge on the evolution of the time series.

To implement this concept of zeroing the n-th backward difference of the trend into System Σ_{tf}, the state x_t of the system will store the value r_t of the trend as well as its $n-1$ previous values, such that

$$x_t = \begin{pmatrix} r_t \\ r_{t-1} \\ r_{t-2} \\ \vdots \\ \vdots \\ r_{t-n+1} \end{pmatrix}, \; A = \begin{pmatrix} \binom{n}{1} & -\binom{n}{2} & \cdots & \cdots & \cdots & (-1)^{n+1}\binom{n}{n} \\ 1 & 0 & \cdots & \cdots & \cdots & 0 \\ 0 & 1 & 0 & \cdots & 0 & \vdots \\ \vdots & 0 & \ddots & \ddots & \vdots & \vdots \\ \vdots & \vdots & \ddots & \ddots & 0 & \vdots \\ 0 & 0 & \cdots & 0 & 1 & 0 \end{pmatrix}, \; w_t = \begin{pmatrix} o_t \\ 0 \\ \vdots \\ 0 \end{pmatrix}, \tag{4.3}$$

where $o_t \in \mathbb{R}$ is a small quantity representing a tolerance on the minimisation of $\Delta_n r(t)$. With these values of x_t, A and w_t, the value of the trend at time $t+1$ r_{t+1} is constructed such that for all t,

$$r_{t+1} = \sum_{k=1}^{n} (-1)^{k+1} \binom{n}{k} r_{t-k+1} + o_t \tag{4.4}$$

and $\Delta_n r(t+1) = o_t$ which is close from zero.

Remark 4.1. *It can be observed that this definition of x_t only makes sense for $t \geq n-1$. The initial state of the system is therefore $x_{n-1} = (\, r_{n-1} \quad \cdots \quad r_0 \,)^\top$.*

We can then estimate the state trajectory of System Σ_{tf} through class $\mathcal{E}$ from Chapter 2 (see (2.4)) or through $\mathcal{E}^{\text{exp}}$ from Chapter 3 (see (3.4)) and retrieve the first row of one of the estimated trajectories $\hat{X}$ as $x_t[1] = r_t$ for all $t \in \mathbb{T}$.

In System Σ_{tf}, $\{f_t\}$ represents a part of the time series Y which we do not want to model through the trend. Consequently, using resilient estimation frameworks allows us to tackle the problem of estimating the trend of a time series in the presence of undesirable outliers, as $\{f_t\}$ will be sparse in this case.

4.1.2 Application to the filtering of data from SiC MOSFET-based Power modules

To illustrate this topic, we will show some examples of robust Trend Filtering on data of Silicon Carbide (SiC) MOSFET[2]-based Power modules. This data was measured at Ampère Laboratory, as part of the PhD work of Malorie Hologne [Hol18], in order to study the failure modes of those power modules. They play a critical role in the development of more reliable power converters, especially in aircraft where there is a trend to replace hydraulic and pneumatic systems by electric actuators (which require power converters). This replacement should lead to a reduction of the cost of maintenance as well as a more efficient fuel consumption.

The data gathered in her experiments partly consisted in measuring drain-to-source voltage/current/resistance in the MOSFET of a power module operated during 15 000 cycles. Those experiments were performed in order to see how the MOSFETs evolve throughout the cycles. The power modules were new at the beginning of the experiment, yet those measurements were disturbed by outliers: those outliers are a

[2]Metal–Oxide–Semiconductor Field-Effect Transistor

common problem in power electronics, because of the high powers involved and the electromagnetic couplings of electrical wires transmitting the measurements. When measuring voltages in power modules, this phenomenon occurs both in experimental settings and in actual implementations. As a result, there is a need to filter out the outliers from the measurements before they can be used for further analysis.

To perform this filtering, we used estimator $\mathcal{E}_{\ell_1,\ell_1}$, studied in Section 2.7, with a regularisation parameter $\lambda = 1$, on Σ_{tf} for $n = 2$, *i.e.* on the system

$$\Sigma_{\text{tf}} : \begin{cases} x_{t+1} &= \begin{pmatrix} 2 & -1 \\ 1 & 0 \end{pmatrix} x_t + w_t \\ y_t &= \begin{pmatrix} 1 & 0 \end{pmatrix} x_t + f_t \end{cases}$$

We then extracted the first row of the obtained estimated state trajectory matrix $\hat{X}_t$ in order to obtain the trend r_t of the time series.

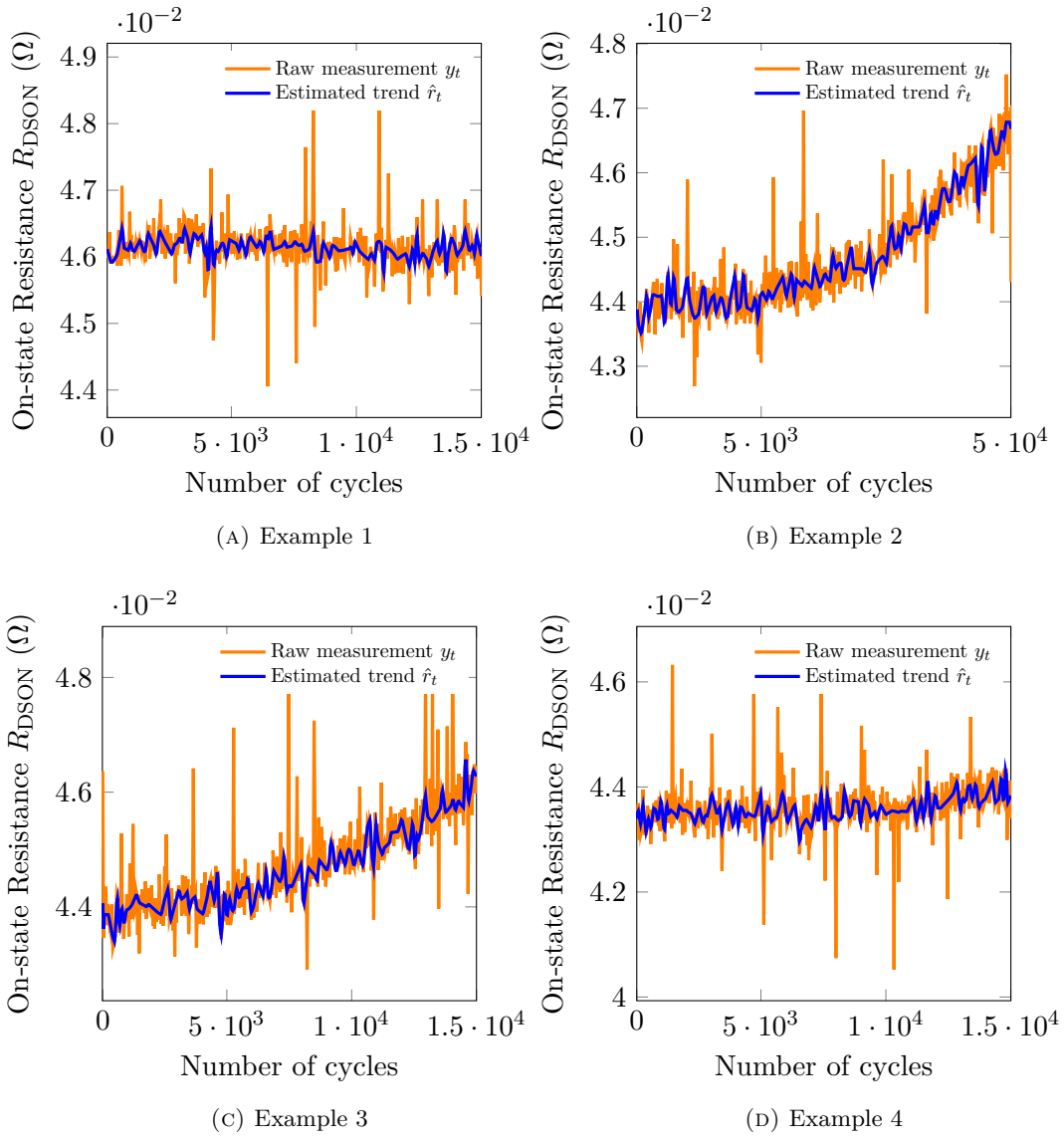

(A) Example 1

(B) Example 2

(C) Example 3

(D) Example 4

FIGURE 4.1: Result of the trend filtering process on the On-State Resistance measurements of four different MOSFETs

Figure 4.1 presents four results of the trend filtering process on on-state drain-to-source resistance R_{DSON} measurements from different MOSFETs. In this figure, we observe that the estimator $\mathcal{E}_{\ell_1,\ell_1}$ is indeed capable of rejecting outliers present in the raw measurements. The regularisation parameter λ is tuned in order to reject the outliers, but it also has an impact on the smoothness of the trend. If we increase λ, the trend gets smoother.

In [Hol18], Hologne used a time-dependent threshold in order to reject any value higher than the threshold and replace it with a default value. This threshold method has the advantage of keeping intact the values which are under the threshold, while our method filters out a little bit the reasonable values. However, the trend filtering method based on our resilient estimation frameworks has two main advantages:

- It does not require the choice of a specific threshold and a specific value to replace the outliers, as they are both implicitly handled by the underlying optimisation problem of the estimator. The only parameter to set is λ, an abstract parameter, weighting the contribution of the trend dynamics.
- The shape of the trend is more flexible. One can modify the hypothesis on the dynamics on the trend, or modify λ in order to modify the trend smoothness, and therefore tune the trend filtering process to their needs.

Conclusion of the study. The resilient estimation frameworks developed in Chapters 2 and 3 are an interesting solution to tackle the problem of estimating the trend in measurements which are disturbed by undesirable outliers. They provide a great flexibility, as the tuning of the regularisation parameters allows to either preserve the small variations of the time series or have a smoother trend.

4.2 Dealing with outliers in Linear Regression Problems

In this section, we will discuss the application of our estimation frameworks to the estimation of a system modelled by a regression model.

A regression model is a model of the form

$$y = Hx + f \tag{4.5}$$

with y and f in $\mathbb{R}^m$, x in $\mathbb{R}^n$ a *vector of parameters* and H, called the *regression matrix*, in $\mathbb{R}^{m\times n}$. In this setting, the estimation problem consists in estimating the parameter vector x from the data y and the regression matrix H, and in the presence of the unknown disturbance f.

Similarly to the state estimation problem in the context of state-space representations, when considering on optimal estimator, the choice of the cost function depends on the assumptions we can make about f.

When f is an arbitrary disturbance, we can adapt the resilient estimation frameworks we studied in Chapters 2 and 3. Indeed, the regression problem can be viewed as a special case of the state estimation problem where the equation related to the dynamics has been removed. We can therefore obtain performance index functions adapted to the regression problem by considering the class of performance index functions V_Σ and V_Σ^{exp} and discarding the terms linked with the dynamic of the system. Consequently, we obtain the functions $V_\Sigma^r : \mathbb{R}^m \times \mathbb{R}^n \to \mathbb{R}_{\geq 0}$

and $V_\Sigma^{r,\exp} : \mathbb{R}^m \times \mathbb{R}^n \to \mathbb{R}_{\geq 0}$ defined by

$$V_\Sigma^r(y,z) = \psi(y - Hz) \qquad V_\Sigma^{r,\exp}(y,z) = \sum_{j=0}^{m} e^{-\lambda\psi_j(y_j - h_j^\top z)} \tag{4.6}$$

where $h_j^\top$ designates the j-th row of H, ψ verifies properties (P2.1)–(P2.4) defined in Section 2.2.2, and ψ_j (j in $\mathbb{J}$) verifies properties (P3.1)–(P3.4) defined in Section 3.2.2. We can then define estimators $\mathcal{E}^r$ and $\mathcal{E}^{r,\exp}$ such that

$$\mathcal{E}^r(y) = \arg\min_{z\in\mathbb{R}^n} V_\Sigma^r(y,z) \qquad \mathcal{E}^{r,\exp}(y) = \arg\max_{z\in\mathbb{R}^n} V_\Sigma^{r,\exp}(y,z) \tag{4.7}$$

We notice that $\mathcal{E}^r$ is an adaptation of the class of estimators $\mathcal{E}$ as studied in Chapter 2, while $\mathcal{E}^{r,\exp}$ is an adaptation of class $\mathcal{E}^{\exp}$ as studied in Chapter 3. Formal resilient studies of such classes of estimators for regressive models can be found in the literature, see [Han19; Bak17] for $\mathcal{E}^r$ and [Bak18] for $\mathcal{E}^{r,\exp}$.

In the previous chapters, we made a marginal use of regressive models: indeed, in Section 2.4 for instance, we mentioned that when a dynamic system is assumed to not be disturbed by a noise in its dynamic equation, it can be rewritten as a regression model. If we consider System (1.1) on time-horizon T such that for all t in $\mathbb{T}$, $w_t = 0$, then it can be identified as a regression model (4.5)

$$\mathrm{vec}(Y) = Hx_0 + \mathrm{vec}(F)$$

where $\mathrm{vec}(Y)$ and $\mathrm{vec}(F)$ designates the vectorization of Y and $F = (\, f_0 \quad f_1 \quad \cdots \quad f_{T-1} \,)$, and where the regression matrix H is the observability matrix of the system over time-horizon T, *i.e.*

$$H = \begin{pmatrix} C_0 \\ C_1A_0 \\ C_2A_1A_0 \\ \vdots \\ C_{T-1}A_{T-2}...A_0 \end{pmatrix}.$$

In this particular case, where a state-space representation is reformulated into a regression model, the regression matrix has a very definite structure. However, in some applications, the regression matrix can be any matrix from $\mathbb{R}^{m\times n}$, and the lack of structure in H can potentially help the estimation process: for example, the use of random matrices are known to help improve the performances in several fields such as compressed sensing (see [Bar08]).

Sparsity test on a random regression matrix. To illustrate this concept, we introduce a randomly generated system H_{rand} of size $n = 4$ and $m = 100$ whose every component is the realisation of a zero mean Gaussian variable of variance 1. Moreover, the vector x is a random vector of $\mathbb{R}^n$ whose entries are also the realisation of a a zero mean Gaussian variable of variance 1.

We then perform a sparsity test similar to the one presented in the simulation sections of Chapters 2 and 3 (Sections 2.7 and 3.6 respectively): f is decomposed into two components such as $f = v + s$ where $v \in \mathbb{R}^m$ is a uniform noise with a SNR of 25dB and s a sparse noise in which the ratio of non-zero entries vary between 0 and 1. As previously, the index of the non-zero entries of s are uniformly selected, while their values are sampled from a Gaussian distribution of mean 0 and variance 100.

Three estimators were implemented to perform this test:

- $\mathcal{E}^r_{\ell_1}$ which implements the Estimator $\mathcal{E}^r$ as defined in (4.7) with $\psi = \|\cdot\|_1$.
- $\mathcal{E}^{r,\exp}$ which implements the estimator of the same name as defined in (4.7) with ψ_j equal to the square function for each j in $\mathbb{J}$ and $\lambda = 10$.
- Oracle[3] $\mathcal{E}^r_{\ell_2^2}$ which implements the Estimator $\mathcal{E}^r$ as defined in (4.7) with $\psi = \|\cdot\|_2^2$. It is therefore a Least Squares Estimator which will serve as a reference.

$\mathcal{E}^r_{\ell_1}$ and Oracle $\mathcal{E}^r_{\ell_2^2}$ were implemented by directly solving the underlying convex minimisation problem using CVX in MATLAB while $\mathcal{E}^{r,\exp}$ was implemented through an Iteratively Reweighted Least Squares Algorithm in a very similar fashion to $\mathcal{E}^\circ$ in Chapter 3 (see Algorithm C.1).

For each ratio of sparse noise, a hundred different noise configurations were simulated and the three aforementioned estimators were used in order to estimate the vector of parameters. The Relative Estimation Error (REE)

$$REE = \frac{\|x - \hat{x}\|_2}{\|x\|_2}$$

was then calculated for each noise configuration and averaged over the hundred obtained values. The results of this test can be found in Figure 4.2.

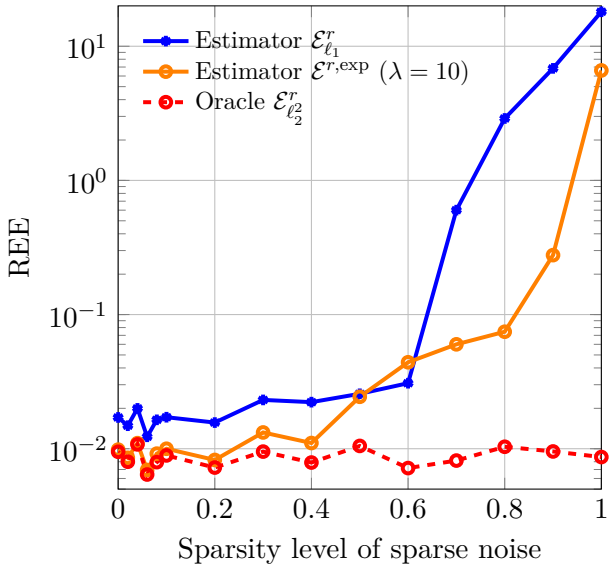

FIGURE 4.2: Averaged REE in function of sparse noise ratio for H_{rand}

The results obtained with this regressive model are fairly similar to the ones obtained for dynamic systems. For low ratios of sparse noise, *i.e.* up to 40% of non-zero entries of s for $\mathcal{E}^{r,\exp}$ and 60% for $\mathcal{E}^r$, the two estimators provide a reasonably bounded estimation error, with an averaged REE of up to 10^{-2} for $\mathcal{E}^{r,\exp}$ and $3 \cdot 10^{-2}$ for $\mathcal{E}^r$. $\mathcal{E}^{r,\exp}$ even maintains good performances up to 80% of sparse noise. For higher ratios of non-zero entries in s, both estimators fail to provide accurate estimation of the parameter vector x which is logical given that almost every component of y is disturbed by s.

[3]We remind the reader that the term "Oracle" refers to a version of the estimator which uses full knowledge of the sparse signal s containing the outliers.

Sparsity test on the IEEE 14-bus model. Performances heavily depend on the ratio m/n, *i.e.* the number of measurements per parameter. To assess this point, we introduce the regression model of an electrical network, the IEEE 14-bus system, which is part of an archive gathering different models of electrical networks [Chr99]. Those models consist in buses linked between each other through a specific configuration of branches: each bus can then be a generator, which supplies the network, or loads, which receives the power from the generators. There can also be shunt elements, such as condensers, within the system: Figure 4.3 presents the configuration of branches of the IEEE 14-bus system.

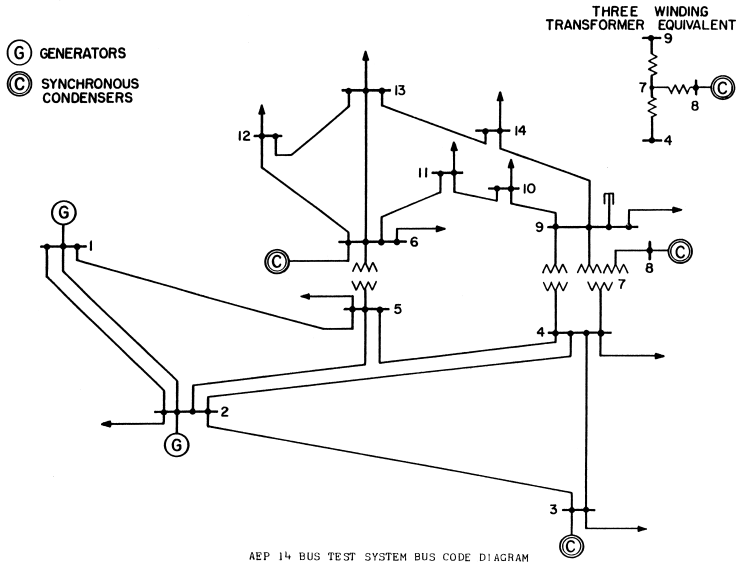

FIGURE 4.3: Structure of the IEEE 14-bus model [Chr99]

This model is commonly used as a benchmark for numerical examples in resilient estimation papers, such as [Faw14] or [Han19]. In this section, we will try to estimate states which are the voltage phase angle at each bus (except the first one which serves as a reference from which every other voltage phase angle is calculated) under the DC power flow model. This model is static and linear[4], and links the real power injections at each bus (14 measurements) as well as the real power flow at each branch (20 measurements) to the 13 states through a regression matrix H_{14} of size 34×13. To obtain H_{14}, we used MATPOWER [Zim11] which is an open-source MATLAB package designed to solve power flow problems: the resulting matrix can be found in Appendix D.1.

A sparsity test similar to the one conducted with H_{rand} was then performed on this system, with the difference that v is a random signal whose values are uniformly taken in $[-1, 1]$ and the values of f are the realisations of a Gaussian random variable of mean 0 and variance 10^4. Moreover, $\mathcal{E}^{r,\text{exp}}$ was implemented with $\lambda = 10^{-3}$.

The results of this test, presented in Figure 4.4, show that the performances of the estimators on the IEEE 14-bus model are much worse than on H_{rand}, especially for $\mathcal{E}^r$: we notice that its REE starts to drastically increase after more than two entries of s are nonzero, which represents a sparsity ratio of roughly 5%. The estimation error then continues to increase as the sparsity ratio increases, with an REE up to almost 10^3. On the other hand the averaged REE of $\mathcal{E}^{r,\text{exp}}$ seems to plateau at just below

[4]The model is actually affine because of a constant offset which was omitted for the sake of simplicity

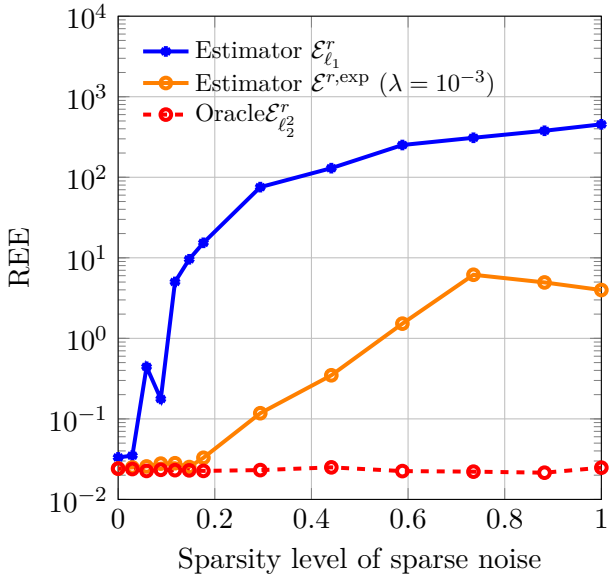

FIGURE 4.4: Averaged REE in function of sparse noise ratio for H_{14}

10. This might be due to the fact that the implementation of $\mathcal{E}^{r,\exp}$ goes through an iterative process which is known to improve the sparsity in estimation results [Dau10]. Overall, $\mathcal{E}^{r,\exp}$ provides a better estimation, with performances on par with the Oracle $\mathcal{E}^r_{\ell_2^2}$ for up to 20% of sparse noise. The REE does increase when the sparsity ratio increases but remains below 10^{-1} for up to 30% of non-zero entries of s. However, this is still worse than the case of H_{rand} where the REE remained below 10^{-1} for up to 80% of sparsity ratio.

An intuitive explanation for this difference in performances is the ratio m/n. Indeed, the IEEE 14-bus model, this ratio is equal to 2.6 measurements for one parameter. In comparison, H_{rand} has an m/n ratio of 25. The amount of information brought by each measurement is therefore greater for the IEEE 14-bus model, which explains why only one or two corrupted measurement is enough to disturb the performances of the estimators.

This is corroborated by the study presented in Chapter 2, where we exhibited an observability parameter, the r-th concentration ratio ν_r (see Eq. (2.55)), which guarantees the exact recoverability of the state of the system by estimator $\mathcal{E}$ if it is lower than 1/2. This ratio ν_r can easily be extended to regression models, and guarantees the exact recoverability of the parameter vector x by estimator $\mathcal{E}^r$ if $\nu_r < 1/2$. By using Lemma 2.6, we can then calculate an overestimation of ν_r which yields an underestimation of the number of outliers the estimators can handle.

By doing so, we observe that $\mathcal{E}^r$ can handle 12 outliers in the estimation process of the random system H_{rand} while it can only handle 1 outlier in the case of the IEEE 14-bus system model. These numbers, despite being an underestimation of the maximum number of outliers that $\mathcal{E}^r$ can handle for those systems, still show the gap in richness between the random system and the IEEE 14-bus system. Subsequently, this gap in richness explains the gap in performances of the estimators for the two considered systems.

Conclusion of the study. Our methods can be used to accurately estimate linear models in the presence of outliers. However, as any other estimation method, the

performances of our estimators deeply depend on the model itself. In particular, the r-th concentration ratio ν_r of a system is an important richness parameter to evaluate. This parameter gives knowledge about how an estimator is likely to be able to accurately estimate the parameter vector of a given system even in the presence of outliers disturbing the data.

4.3 Estimation of a switched system with an unknown switching signal

So far the sparse sequence in model (1.1) was viewed as part of sensor noise that is, a parasitic signal which is induced by imperfections of the measurement device. In this section, we illustrate, through an example, situations where the sparse additive signal affecting the system may be an intentional artefact used for methodological development.

For this purpose, consider a switched linear system, which is a particular case of a linear time-varying discrete system of the form

$$\Sigma : \left\{ \begin{array}{ll} x_{t+1} & = A_{\sigma(t)} x_t + w_t \\ y_t & = C_{\sigma(t)} x_t + v_t \end{array} \right. \tag{4.8}$$

where the matrices $A_{\sigma(t)}$ and $C_{\sigma(t)}$ are taken from two families of matrices $\{A_k\}$ and $\{C_k\}$ through a function $\sigma : \mathbb{N} \to \{1, ..., n_\sigma\}$, called the switching signal.

Each pair (A_k, C_k) is considered a mode of the system, and the switching signal σ indicates which one of the n_σ modes occurs at time t.

If we take mode (A_1, C_1) as a reference, we can reformulate the system as an LTI discrete-time state-space representation such that

$$\Sigma_s : \left\{ \begin{array}{ll} x_{t+1} & = A_1 x_t + w_t + o_t \\ y_t & = C_1 x_t + v_t + s_t \end{array} \right. \tag{4.9}$$

where $o_t = (A_{\sigma(t)} - A_1)x_t$ and $s_t = (C_{\sigma(t)} - C_1)x_t$.

$\{o_t\}$ and $\{s_t\}$ have the noticeable property that for every t such that $\sigma(t) = 1$, $o_t = s_t = 0$. This entails that $\{o_t\}$ and $\{s_t\}$ are sparse noises with a number of nonzero entries equal to the cardinality of $\{t \in \mathbb{T} : \sigma(t) \neq 1\}$. Consequently, the more System Σ is in mode (A_1, C_1) over $\mathbb{T}$, the sparser $\{o_t\}$ and $\{s_t\}$ are.

As a result, such a system fall under the scope of our resilient estimation methods. As long as the occurrences of t such that $\sigma(t) \neq 1$, and therefore the number of nonzero entries of o_t and s_t, remains as small as possible, the problem of estimating the state of the switched system (4.8) can be reduced to a robust state estimation problem for the LTI system (4.9).

The characteristics of System (4.9) also play a role in the performances of this approach. If it is observable in the sense presented in Chapters 2 and 3 (for instance, if it has a small p_r (see (2.26)) or a small $R_\Sigma(\rho)$ (see (3.24))), then the estimators will be more likely to provide an accurate estimation.

To illustrate this, we introduce the switched system with two states ($n = 2$), one measurement ($m = 1$), and two modes ($n_\sigma = 2$):

$$A_1 = \begin{pmatrix} 0.7 & 0.45 \\ -0.5 & 1 \end{pmatrix}, \quad A_2 = \begin{pmatrix} -0.65 & -0.7028 \\ 0.7028 & -0.65 \end{pmatrix}, \quad C_1 = C_2 = \begin{pmatrix} 1 & 2 \end{pmatrix} \tag{4.10}$$

with $x_0 = (1 \quad 2)$. It is worth noting that this switched system presents the same measurement matrix $C_1 = C_2 = C$ for both modes, but this is not an uncommon assumption to make, given that the way the system sensors perform measurements does not always change between the different modes of the system.

We will generate several switching signals throughout the experiments to follow. Those switching signals will be generated in order to set the *sparsity ratio* of $\{o_t\}$, *i.e.* its ratio of nonzero entries, to a certain value between 0 and 1. To do so, the number of occurrences of the reference mode will be set accordingly and then selected through a uniform distribution among all the time indexes.

The state estimation will be performed in an offline setting, with $T = 100$, and we will make use of three already defined batch estimators:

- Estimator $\mathcal{E}_{\ell_2,\ell_2^2}$ which implements Estimator $\mathcal{E}$ as defined in Chapter 2 (see (2.4)) with $\lambda = 10^{-4}$, and for all t, $\phi_t = \|\cdot\|_2$ and $\psi_t = \|\cdot\|_2^2$.
- Estimator $\mathcal{E}^{\text{exp}}$ as defined in Chapter 3 (see (3.4)) with $\lambda_\phi = 10^{-5}$, $\lambda_\psi = 1$ and for all t, $\phi_{t,i} = \psi_{t,j} = |\cdot|^2$ for each (i,j) in $\mathbb{I} \times \mathbb{J}$.
- Oracle $\mathcal{E}_{\ell_2^2,\ell_2^2}$ which implements Estimator $\mathcal{E}$ as defined in Chapter 2 (see (2.4)) with $\lambda = 10^{-1}$, and for all t, $\phi = \|\cdot\|_2^2$ and $\psi_t = \|\cdot\|_2^2$. This least squares estimator will be aware of the switching signal and will serve as a reference in terms of performances.

Remark 4.2. *The Estimator $\mathcal{E}_{\ell_2,\ell_2^2}$ has a fairly different choice of loss functions than what was previously implemented*[5]*, due to the process noise o_t being the only sparse noise present in System (4.10). This explains the choice of ϕ_t as a norm and ψ_t as a quadratic form.*

Moreover, when the system is not in the reference mode, every component of o_t is nonzero, which means that it is not sparse componentwise (see Section 1.4.2). The ℓ_2-norm is therefore more suited to this application than the ℓ_1-norm which is privileged for applications with componentwise sparse disturbances.

Sparsity ratio tests. In the first place, we will perform two tests with different sparsity ratios of $\{o_t\}$. One test will estimate System (4.10) with (A_1, C) as a reference mode, and the other will estimate it with (A_2, C) as reference. No dense noise, neither in the dynamic equation nor in the measurement equation, will be considered.

For each sparsity ratio, the tests consisted in generating a hundred different switching signals, simulating the corresponding state trajectories and measurement histories of System (4.10), and then reconstructing the state of the system through the aforementioned estimators. For each realisation, the Relative Estimation Error (see (2.80)) was computed and averaged for each ratio: the results of those tests are presented in Figure 4.5.

The first thing which can be observed from Figure 4.5 is that the reference mode used by the estimators plays a role in the performances of $\mathcal{E}_{\ell_2,\ell_2^2}$: for a sparsity ratio of 0.1, $\mathcal{E}$ indeed shows an averaged REE of 0.2 when (A_1, C) is the reference

[5] For instance, see $\mathcal{E}_{\ell_2^2,\ell_1}$ defined and studied in Section 2.7.

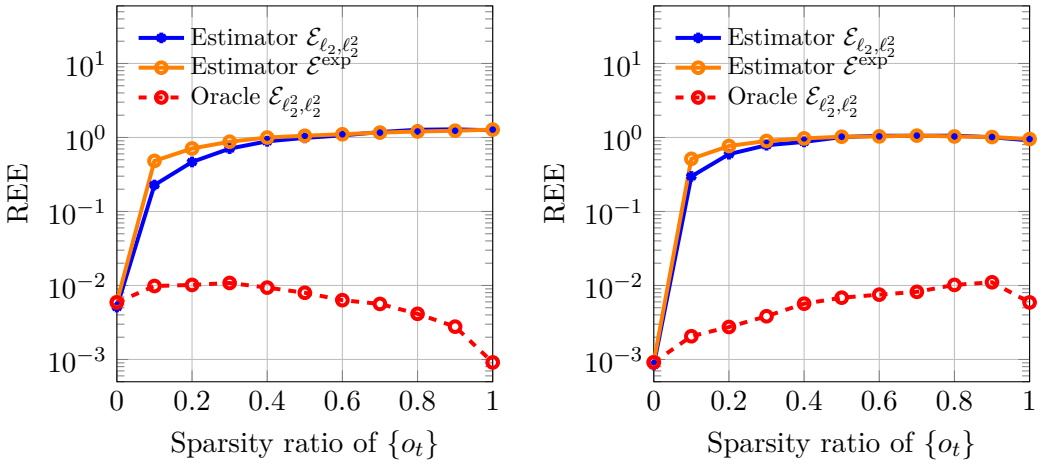

(A) Reference mode (A_1, C) (B) Reference mode (A_2, C)

FIGURE 4.5: Average REE of Estimators $\mathcal{E}_{\ell_2,\ell_2^2}$, $\mathcal{E}^{\exp}$ and Oracle $\mathcal{E}_{\ell_2^2,\ell_2^2}$ for System (4.10)

mode and a REE of 0.3 when (A_2, C) is the reference mode. This difference, albeit small, is consistent through the different values of sparsity ratios. An explanation for this phenomenon lies in the observability of (A_1, C) compared to the one of (A_2, C). Indeed, we recall p_r, defined in (2.26), an observability parameter of the system. If $p_r < 1/2$, then the estimation error of the class $\mathcal{E}$ is bounded in the presence of r outliers. Using the method proposed in Section 2.5.1, we can calculate p_1, which is equal to 0.0607 for (A_1, C) and 0.0672 for (A_2, C). This ensures that (A_1, C) is able to handle at least 8 outliers, while (A_2, C) handles at least 7 outliers. This small difference in observability can therefore explain the small difference in performances when using (A_1, C) or (A_2, C) as a reference mode for the estimation process.

Moreover, both estimators $\mathcal{E}_{\ell_2,\ell_2^2}$ and $\mathcal{E}^{\exp}$ reach an averaged REE of 1 for sparsity ratios of $\{o_t\}$ higher than 0.4. Below this value, their averaged REE is within the range of 10^{-1} which can be acceptable, given that the estimators do not take into account the occurrence of the other mode at all.

Study of state trajectories without dense noise. To further understand those numbers, Figure 4.6 presents the two state trajectories of System (4.10) for one specific switching signal σ, with a ratio of occurrence of 0.1. The switching signal is also represented. Alongside with the two state trajectories, the estimated trajectories returned by $\mathcal{E}_{\ell_2,\ell_2^2}$ and $\mathcal{E}^{\exp}$ (with (A_1, C) as a reference mode) are also represented.

We notice that $\mathcal{E}_{\ell_2,\ell_2^2}$ and $\mathcal{E}^{\exp}$ were able to accurately estimate the two states. For instance, they were both able to manage mode (A_2, C) occurring at $t = 6$ and $t = 15$. However, the resulting spike in the trajectory was better estimated by $\mathcal{E}_{\ell_2,\ell_2^2}$ than by $\mathcal{E}_{\exp}$ whose estimates present the same spike but with inaccurate amplitudes.

We also remark that both estimators lack precision when the non-reference mode occurs for several time indexes t within a short period of time: this can be seen around $t = 39$ or $t = 69$. Nevertheless, apart from those inaccuracies, the performances of $\mathcal{E}_{\ell_2,\ell_2^2}$ and $\mathcal{E}^{\exp}$ seem satisfactory, which is corroborated by the fact that their averaged REE[6] was equal to 0.3541 in the case of $\mathcal{E}_{\ell_2,\ell_2^2}$ and 0.6947 in the case of $\mathcal{E}^{\exp}$.

[6]We remind the reader that the REE is a relative indicator based on the whole trajectory, which explains why its values can be mistakenly interpreted as big.

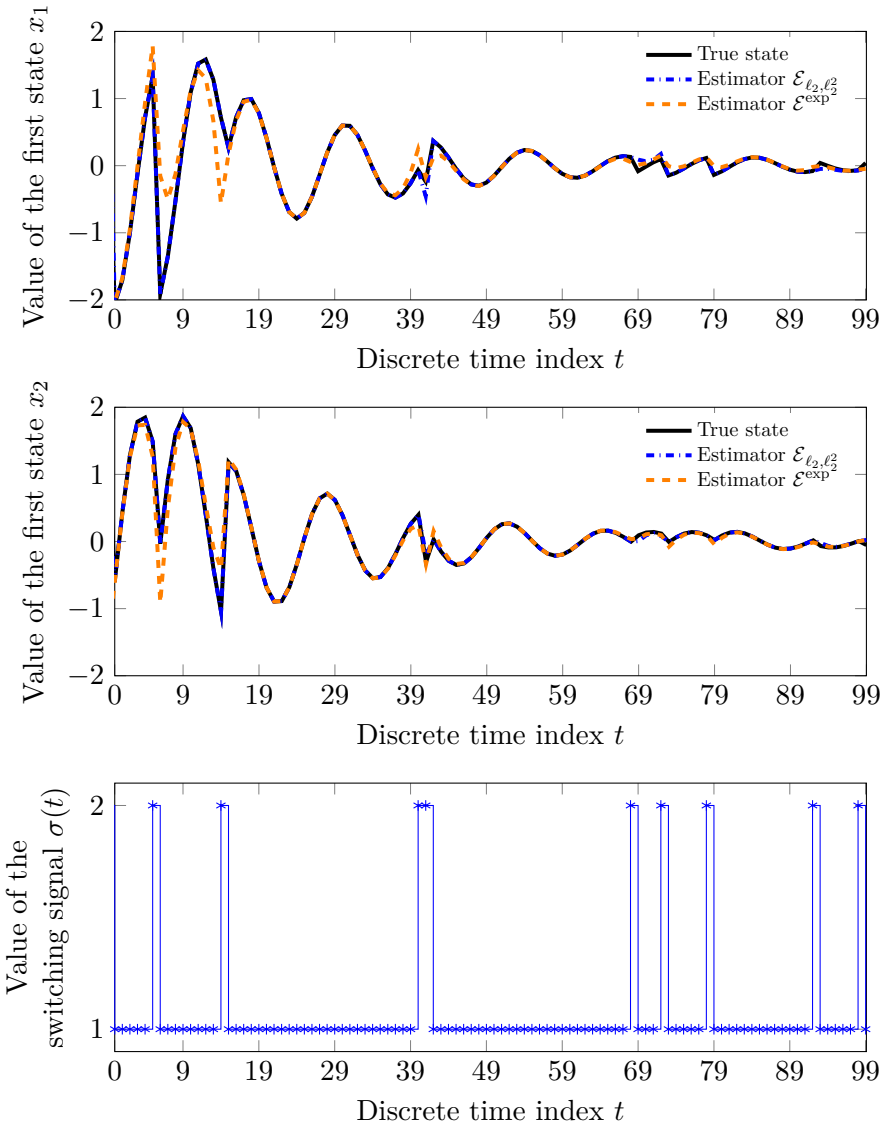

FIGURE 4.6: Trajectory of the states of the switched system (4.10) for a given switching signal (without noise) and the estimated trajectories returned by $\mathcal{E}_{\ell_2,\ell_2^2}$ and $\mathcal{E}^{\exp}$

Study of state trajectories with dense noise. Finally, we performed the exact same experience, *i.e.* simulating the switched system (4.10) for one specific switching signal σ, but in the presence of non-zero dense noises $\{w_t\}$ and $\{v_t\}$. For each t, w_t and v_t were chosen as the realisation of two uniform distribution laws between $[-0.5, 0.5]$ and $[-0.1, 0.1]$ respectively: this represents a Signal-to-Noise Ratio of around 10dB for the process noise and of 30dB for the measurement noise. Subsequently, the state trajectories were estimated through $\mathcal{E}_{\ell_2,\ell_2^2}$ and $\mathcal{E}^{\exp}$ (with reference mode (A_1, C)) and the real trajectories, the estimated trajectories and the switching signal σ were represented in Figure 4.7.

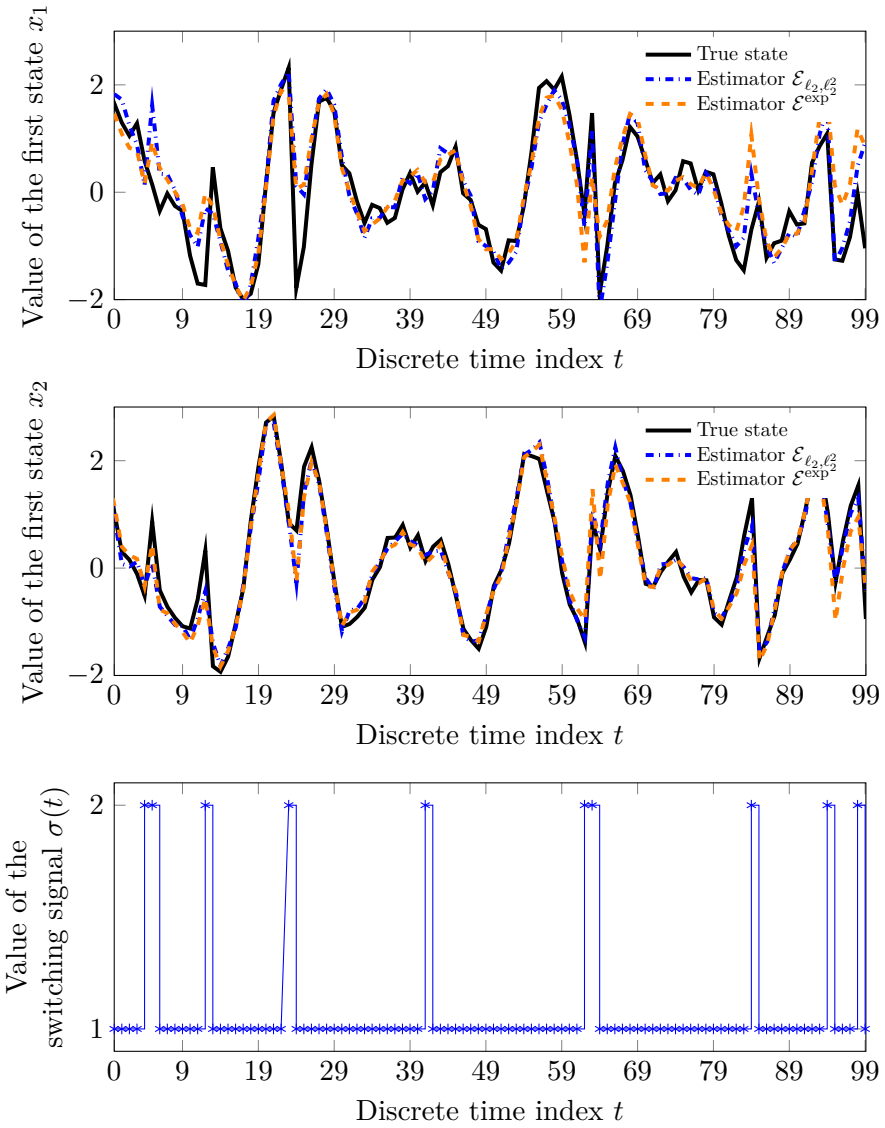

FIGURE 4.7: Trajectory of the states of the switched ystem (4.10) for a given switching signal (with noise) and the estimated trajectories returned by $\mathcal{E}_{\ell_2,\ell_2^2}$ and $\mathcal{E}^{\exp}$

The presence of the dense noises $\{w_t\}$ and $\{v_t\}$ does not seem to disturb the estimation process too much, and the conclusions of this test are fairly similar to the ones drawn from the noiseless test in Figure 4.6: both $\mathcal{E}_{\ell_2,\ell_2^2}$ and $\mathcal{E}^{\exp}$ manage to estimate the state trajectories well, but the estimate can be locally worse when the minor mode occurs a lot on a short period of time (*e.g.* $t = 10$ or $t = 60$). As a

comparison, the REE of $\mathcal{E}_{\ell_2,\ell_2^2}$ is 0.4170 for this simulation while the REE of $\mathcal{E}^{\text{exp}}$ is equal to 0.5133: those two values are close to the ones obtained for the previous test without any dense noise.

As a conclusion, it is possible to apply our estimation frameworks in order to estimate the state of a switched state system without knowing the switching signal between its different modes. The two key properties to ensure the good performances of such an application are:

- The reference mode used for the estimation must be visited as much as possible by the switched system.
- The LTI system formed by the reference mode (see (4.9)) needs to be as observable – in the terms presented in the analysis in Chapters 2 and 3 – as possible.

4.4 Position estimation of a quadrotor drone

In the recent years, *Unmanned Aerial Vehicles* (UAV), also known as drones, have become more and more utilised in order to perform several various tasks, such as medicine transportation [Eic19] or the scouting of agricultural fields [Tar20]. Their size, weight and remote control make them an interesting solution in applications where the presence of humans is dangerous.

Accurately operating a drone requires to know many variables such as its position. If the Global Positioning System (GPS) can be used to determine this position, the signals involved are very sensitive to interferences which makes it not suited in some cases such as indoor operations. In such cases, there is therefore a need to estimate this position, and this is most of the time performed through the knowledge of the initial position of the drone and the integration of its linear velocities. However, if accurate external sensors, such as radars, can measure these linear velocities, these measurements can be lost while being transmitted to the drone, which then sometimes needs to rely on internal and less accurate sensors.

FIGURE 4.8: Picture of the Crazyflie 2.0 (source: www.bitcraze.io/products/old-products/crazyflie-2-0/)

The goal of this section is to illustrate the estimation process of the position of a Crazyflie 2.0 (see Figure 4.8), an open-source quadrotor drone. This study will be performed based on a model and experimental data which are part of the PhD work of Jérémy Barra at the Ampère Laboratory and the CEA.

4.4.1 Model of the drone and settings of the experiment

In [Bar20], the following model was proposed for the drone dynamics:

$$\begin{pmatrix} \dot{v}_x \\ \dot{v}_y \\ \dot{v}_z \\ \dot{b}_{\text{acc},x} \\ \dot{b}_{\text{acc},y} \\ \dot{b}_{\text{acc},z} \end{pmatrix} = \begin{pmatrix} -0.32 & 0 & 0 & 0 & 0 & 0 \\ 0 & -0.32 & 0 & 0 & 0 & 0 \\ 0 & 0 & -4 & 0 & 0 & 0 \\ 0 & 0 & 0 & 0 & 0 & 0 \\ 0 & 0 & 0 & 0 & 0 & 0 \\ 0 & 0 & 0 & 0 & 0 & 0 \end{pmatrix} \begin{pmatrix} v_x \\ v_y \\ v_z \\ b_{\text{acc},x} \\ b_{\text{acc},y} \\ b_{\text{acc},z} \end{pmatrix} + \begin{pmatrix} 0 & -9.4 & 0 \\ 9.4 & 0 & 0 \\ 0 & 0 & -28.2 \\ 0 & 0 & 0 \\ 0 & 0 & 0 \\ 0 & 0 & 0 \end{pmatrix} \begin{pmatrix} \eta_1 \\ \eta_2 \\ T \end{pmatrix} \tag{4.11}$$

$$\begin{pmatrix} a_{\text{acc},x} \\ a_{\text{acc},y} \\ a_{\text{acc},z} \\ v_{\text{rdr},x} \\ v_{\text{rdr},y} \\ v_{\text{rdr},z} \end{pmatrix} = \begin{pmatrix} -1.2 \cdot 10^{-2} & 0 & 0 & -1.2 \cdot 10^{-2} & 0 & 0 \\ 0 & -1.2 \cdot 10^{-2} & 0 & 0 & -1.2 \cdot 10^{-2} & 0 \\ 0 & 0 & -6 \cdot 10^{-2} & 0 & 0 & -6 \cdot 10^{-2} \\ 1 & 0 & 0 & 0 & 0 & 0 \\ 0 & 1 & 0 & 0 & 0 & 0 \\ 0 & 0 & 1 & 0 & 0 & 0 \end{pmatrix} \begin{pmatrix} v_x \\ v_y \\ v_z \\ b_{\text{acc},x} \\ b_{\text{acc},y} \\ b_{\text{acc},z} \end{pmatrix} + f \tag{4.12}$$

This model is composed of $n = 6$ states and $m = 6$ measurements. Three states corresponds to the linear velocities v_x, v_y, v_z of the drone along the three dimensions of the space, while three others, $b_{\text{acc},x}$, $b_{\text{acc},y}$, $b_{\text{acc},z}$ are states aimed at describing a bias which was observed in one of the sensors.

Indeed, two sensors are present in the system:

- An on-board sensor, the *Inertial Measurement Unit* (IMU), measures its own accelerations which are linear combinations of the drone linear velocities (see [Lei14]), yielding $a_{\text{acc},x}$, $a_{\text{acc},y}$ and $a_{\text{acc},z}$. This sensor presents a bias in its measurements, which was considered constant in the model.
- A *radar*, which is off-board, measures the three linear velocities of the drone directly, yielding $v_{\text{rdr},x}$, $v_{\text{rdr},y}$ and $v_{\text{rdr},z}$.

It is worth noting that the drone is assumed to fly in a quasi-stationary mode, which means the dynamics of its rotation angles are neglected. This allows us to just consider η_1 and η_2, two of the three Euler angles of the drone, as an input of the system, alongside the thrust T induced by the four rotors of the drone.

Settings of the experiment. The experiment on which we base our study was performed in a room equipped with a motion capture system. Within this room, a Crazyflie 2.0 was flown and its linear accelerations and velocities measured by the two aforementioned sensors, while the motion capture system provided a reference of the position and the velocity of the drone during the experiment.

The radar has a much better accuracy than the IMU which presents very noisy measurements. However, in a normal setting, it is not rare that the radar loses track of the drone for a few moments. During those moments, the radar returns a default value which can completely disturb the estimation process. The goal is therefore to be able to handle those default values disturbing the estimation process while still trusting the radar measurements: this is all the more crucial as even the slightest mistake on the estimation of the velocity will create a permanent offset in the estimation of the drone position because of the integration.

4.4.2 Estimation setting

In order to simulate the normal operation of the drone, the estimation process must be performed online, as the position and velocities of the drone are needed in real time in order to control its trajectory. Moreover, the estimation process needs to take place in the drone on-board chip, which has limited resources. We therefore

cannot consider an application of the batch estimators, which are resources-heavy, to this setting, but will rather consider the recursive implementation of our optimal estimators presented in Section 2.6 and Section 3.5.3.

System (4.11)–(4.12) is a continuous-time LTI system. However, our estimation frameworks needs a discrete-time model. We therefore made use of MATLAB functions `ss` and `c2d` to obtain a discretisation of System (4.11)–(4.12) through the zero-order hold method [Mat]. As a result, when talking about System (4.11)–(4.12), we will now refer to the discretised version of the system. Three estimators were subsequently implemented:

- $\mathcal{E}_{\text{online}}$ which implements Algorithm 2.1 with $\lambda = 1$, $\varepsilon = 10^{-5}$, $\hat{x}_0 = 0_{6,1}$ and $P_0 = I_2$, and γ, Q such that

$$\gamma = \begin{pmatrix} 10 & 10 & 15 & 10 & 10 & 15 \end{pmatrix} \tag{4.13}$$

$$Q = \operatorname{diag}\left(10^{-4}, 10^{-4}, 10^{-4}, 4 \cdot 10^{-2}, 4 \cdot 10^{-2}, 6.4 \cdot 10^{-3}\right). \tag{4.14}$$

- $\mathcal{E}^{\text{exp}}_{\text{online}}$ which implements Algorithm D.1, a variation of Algorithm 3.2 as explained in Appendix D.2, with $\lambda_\phi = 1$, $\lambda_\psi = 10^{-1}$, $\hat{x}_0 = 0_{6,1}$, Q as in (4.14), $P_0 = I_2$ and

$$\{r_j\}_{j \in \mathbb{J}} = \left\{2.5 \cdot 10^{-3}, 2.5 \cdot 10^{-1}, 2.5 \cdot 10^{-3}, 4 \cdot 10^{-2}, 4 \cdot 10^{-2}, 10^{-2}\right\}.$$

4.4.3 Experimental results

The data which will be used in the estimation process are the three linear accelerations measured by the IMU and the three linear velocities measured by the radar. We aim at keeping track of the linear velocities of the drone in order to integrate them and reconstruct the trajectory of the drone.

The data of the experiment was recorded between $t_{\min} = 0$ s and $t_{\max} = 18$ s and sampled at a frequency of 500 Hz, for a total of $T = 9000$ samples. During the acquisition, an operator flew the drone back and forth along the y-axis while trying to maintain the movements along the x and z axis as small as possible.

The measurements of the radar gathered during the experiment did not natively present loss of measurements (refer to Figure D.1 from Appendix D.3 to see the raw measurements obtained from the experiment). To simulate this phenomenon, every 500 samples, we modified 50 consecutive samples of the three linear velocities returned by the radar, and replaced them by a saturated value of 10 m·s^{-1}.

Consequently, Figure 4.9 presents the three instantaneous estimation errors on the velocities $e_{t,x} = v_{\text{ref},t,x} - \hat{v}_{t,x}$, $e_{t,y} = v_{\text{ref},t,y} - \hat{v}_{t,y}$ and $e_{t,z} = v_{\text{ref},t,z} - \hat{v}_{t,z}$. Figure 4.10 displays the coordinates of the drone as measured by the motion capture system, as well as the coordinates of the drone obtained by integration of the estimated linear velocities.

In Figure 4.9, we see that $\mathcal{E}_{\text{online}}$ and $\mathcal{E}^{\text{exp}}_{\text{online}}$ filter out the outliers present in the measurements of the radar. This is particularly true for e_x and e_y, but we notice that the estimation error e_z of $\mathcal{E}_{\text{online}}$ presents spikes which correspond to the intervals of measurement loss.

However, those spikes seem to be small enough to not disturb the obtained trajectories in Figure 4.10, as $\mathcal{E}_{\text{online}}$ presents a very good estimation of the trajectory of the drone, with an error of the final position of the drone equal to 25 cm. $\mathcal{E}^{\text{exp}}_{\text{online}}$ obtains a drone trajectory which diverges more from the reference one, with a final

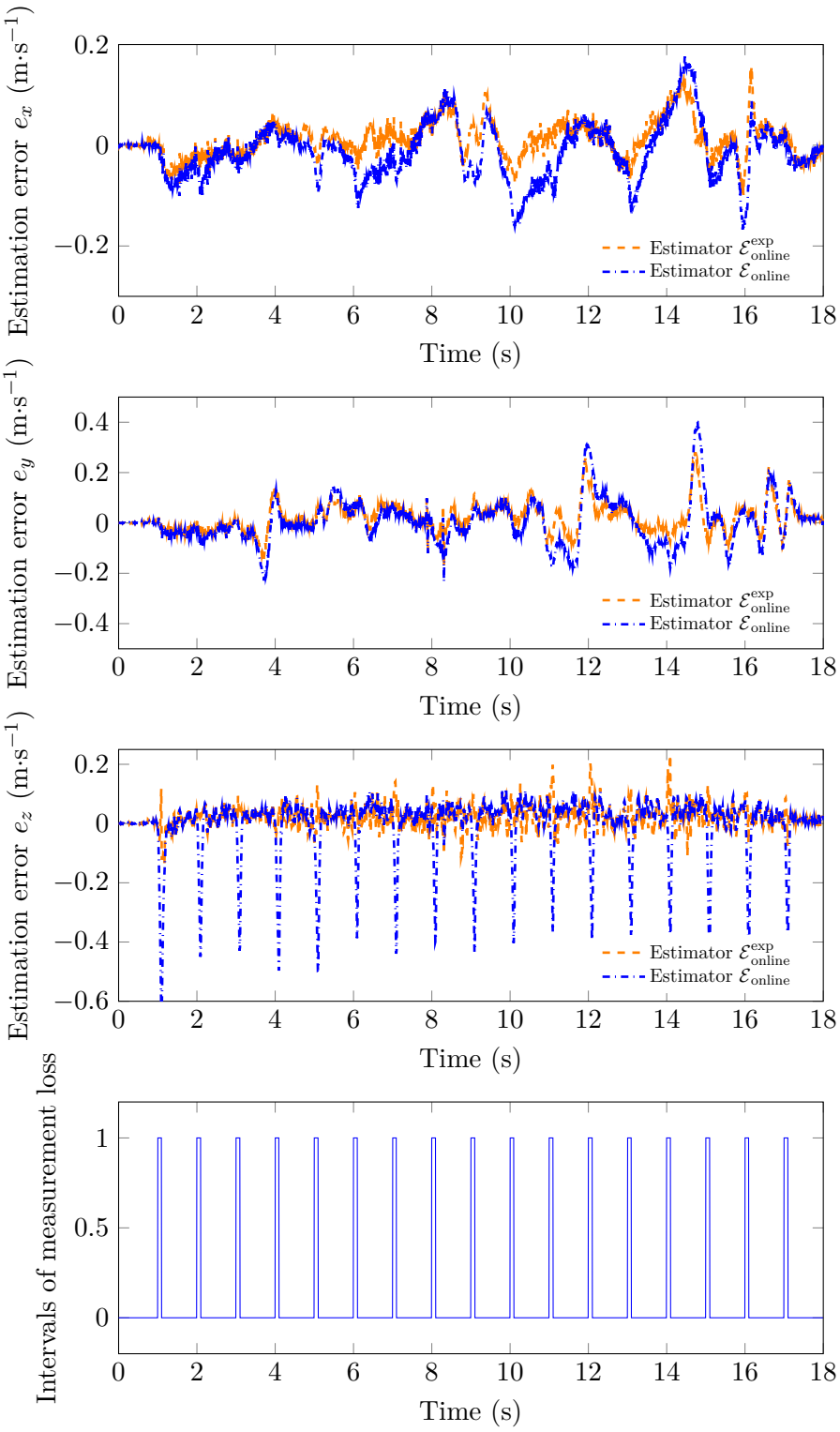

FIGURE 4.9: Estimation errors on the linear velocities of the drone for $\mathcal{E}_{\text{online}}$ and $\mathcal{E}_{\text{online}}^{\text{exp}}$

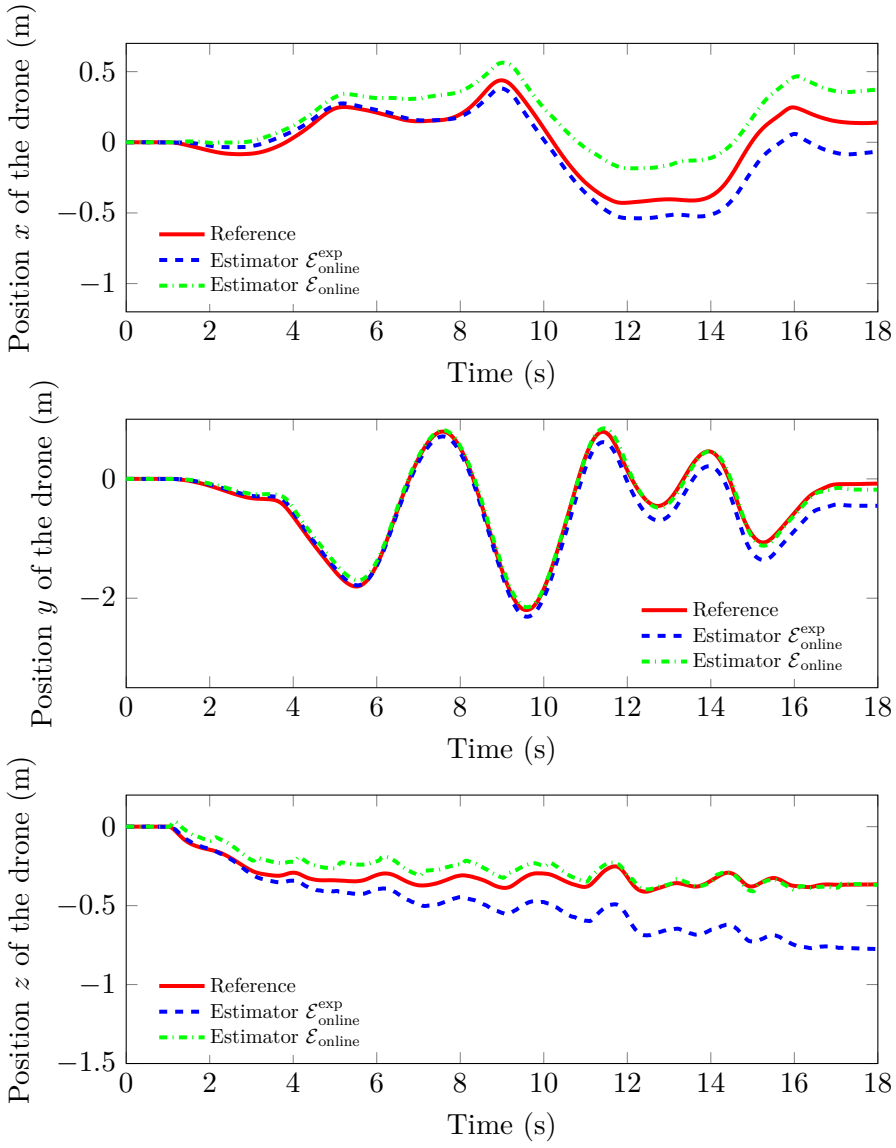

FIGURE 4.10: Reconstructed drone coordinates obtained from the linear velocities of the drone estimated by $\mathcal{E}_{\text{online}}$ and $\mathcal{E}_{\text{online}}^{\text{exp}}$

estimated position which is 59 cm away from the real one. This error is mainly due to the estimation of the z component where there is a 50 cm gap between the estimated and the real final positions. This might be explained by the limitations of some of the modelling assumptions.

Conclusion of this test. This test showed that the recursive implementations of our resilient optimal estimators were able to perform well in an online setting with temporary loss of measurements. $\mathcal{E}_{\text{online}}$ and $\mathcal{E}^{\text{exp}}_{\text{online}}$ were able to keep track of the drone velocities, and subsequently of the drone position.

However, both estimators rely on the update of the gain matrix at each time iteration. This heavier algorithmic complexity allows for a good handling of the measurement loss case, but we do acknowledge that it can be a problem if the estimators are to be implemented on devices with really limited resources.

Finally, it is also worth noting that we considered a simplified version of the model for drone dynamics. Several modifications, such as taking into account a bias on the radar measurements, could be done, which could also indirectly improve the performances of the estimator.

4.5 Conclusion

To conclude, we have presented four cases of application of the resilient estimation frameworks developed in Chapters 2 and 3. Those cases showed that there is a need for resilient estimation in many diverse fields, and that the developed frameworks are able to answer to that need in a satisfying manner:

- In Trend Filtering, the study led to the definition of an algorithm which successfully filters out outliers from time series without any assumption on their dynamics. This algorithm constitutes an interesting alternative to other outlier rejection methods, such as threshold methods, as it can simultaneously filter outliers out and provide a smooth trend.
- In linear regression, we showed that our resilient estimation framework can be successfully used when the available measurements are affected by impulsive noise.
- We provided simulation results to indicate that the estimators developed in Chapters 2 and 3 could estimate a switched system without knowing its switching signal. By assuming that the switching signal is such that one mode is preponderant over the others (in term of number of times it has been activated), the switched system can be represented as a linear system subject to sparse noise.
- We displayed accurate online estimation of a drone position in the presence of measurement loss based on actual measurements of linear velocities.

It is also worth noting that the application cases are not restricted to the ones presented in this chapter. Fault detection, robust control with faulty actuators, or hybrid system identification, are also cases to which the estimation frameworks developed in Chapters 2 and 3 could be applied.

Conclusion and perspectives

Summary of the dissertation

In this memoir, we have considered the design and the analysis of resilient optimal state estimators. These estimators are algorithms meant to perform the estimation of the state of Linear Time-Varying systems in the presence of impulsive noises, a type of noise which does not occur at all time but whose nonzero occurrences can have arbitrarily large magnitudes.

First of all, we defined an optimal state estimator as the mapping which associates to the measurements, the minimizing set of some performance index function. The main purpose of a performance index function is to discriminate potential state trajectories based on the knowledge of the system model and the output of the system. An optimal state estimator is then a mapping which returns the set of the most likely trajectories with respect to its defining performance index function.

The property of *resilience* is a specific notion of robustness. More precisely, we say that an estimator is *resilient* to a given set of disturbances if it induces an estimation error which is insensitive to any instance of those disturbances. Alternatively, we say that an estimator is *approximately resilient* to a given set of disturbances if the impact of those disturbances on its estimation error is bounded.

One of the very first issues tackled in this report is the question of designing a performance index function in order to produce an optimal state estimator which is *resilient* or *approximatively resilient*. Intuitively, this is achieved by ensuring that the image of the real state trajectory through the performance index function is somehow small and/or by designing the performance index function so that the estimated noises have a similar structure to the real ones. By reviewing the literature of resilient state estimation, we identified two types of interesting candidates for performance index functions: the ones using sparsity-inducing functions and the ones originating from the Maximum Correntropy Criterion (MCC) framework. By using these types of functions as a starting point, we designed two classes of performance index functions, and subsequently two classes of estimators. These classes are aimed at being as general as possible, which was achieved by defining their members through their properties rather than by a closed-form expression.

We then analysed the two resulting classes of estimators, in order to draw theoretical guarantees about their resilience or approximate resilience. The question of the implementation of those estimators was also considered.

Chapter 2 deals with a class of resilient state estimators, $\mathcal{E}$, based on *non-saturated* performance index functions. These functions, inspired by compressed sensing methods, are composed of smaller functions verifying properties generalising those of norms. This leads to consider a wide range of performance index functions, which can be convex or nonconvex, smooth or nonsmooth, etc.

After having formally defined the resilience property, we analysed the newly defined class of estimators $\mathcal{E}$. We proved that some of its elements are resilient if a parameter, p_r, linked with the observability of the system, is smaller than $1/2$. If this

condition is met, then the estimation error of these estimators is upper bounded by a bound which is independent of the extreme values of the measurement noise. This bound, albeit conservative, provides insight on how the different parameters of the system and of the estimators impact the quality of the estimation.

We also considered the problem of exact recoverability, *i.e.* when an estimator returns the exact state trajectory, in the absence of noise in the dynamic equation of the system. In this setting, we obtained that the estimator returns the exact state trajectory if and only if ν_r, another parameter linked with the observability of the system, is smaller than $1/2$.

As a result of this analysis, p_r and ν_r are two parameters of the system which would be interesting to assess. However, they can be hard to compute in practice since they are defined as the solution of a combinatorial nonconvex optimisation problem. We addressed this problem by stating two overestimation results, which we then used to perform several numerical tests on these parameters.

Finally, from an implementation perspective, $\mathcal{E}$ contains state estimators defined by convex performance index functions. This allowed us to use convex optimisation methods in order to directly solve the underlying optimisation problem of those estimators, yielding a direct batch implementation. We also proposed an approximate recursive implementation of some elements of $\mathcal{E}$ through the Forward Dynamic Programming (FDP) framework, resulting in a Kalman-like recursive algorithms.

In Chapter 3, we considered the class $\mathcal{E}^{\text{exp}}$, containing resilient state estimators based on *saturated* performance index functions. Inspired by the performance index functions in the MCC framework, these functions contain several exponential terms which induce a saturation when the magnitude of their argument grows towards infinity.

In the general case, we were able to provide theoretical results which showed that in the presence of arbitrary noise, a function of the estimation error is bounded if the system is observable enough. This result enabled a discussion on the impact of the parameters of the system and of the estimator on the estimation error.

By reformulating the estimators of $\mathcal{E}^{\text{exp}}$ in a regression-like framework, we were able to prove the approximate resilience of this newly defined class of estimators. Once again, this result ensures that the estimation error is bounded if a given condition on the observability of the system is verified and the number of "potentially unbounded" noise components is small enough. Interestingly enough, this condition entails that the more observable the system is, the larger the number of outliers the estimator will be able to handle. We numerically studied this condition, in order to assess the degree of observability, *i.e.* the observability parameter $R_\Sigma(\rho)$, that a system needed to verify in order to be approximately resilient.

Contrary to class $\mathcal{E}$, $\mathcal{E}^{\text{exp}}$ only contains estimators based on nonconvex performance index functions. To implement them, we derived heuristic batch and recursive algorithms based on solving a similar Least Squares optimisation problem. The batch algorithm was derived as an Iteratively Reweighted Least Squares algorithm, while the recursive implementation was obtained through another application of the FDP framework.

Finally, four cases of applications for the considered classes of estimators were studied in Chapter 4. These cases (Robust trend filtering, Linear regression problems, State estimation for switched linear systems, and Online estimation of the position of a drone) were aimed at showing the versatility of the estimation algorithms developed and studied in the previous three chapters. They gave a broad (but not exhaustive)

image of the potential of our methods, and in various estimation settings, both online and offline.

Potential perspectives

In this section, we will list and discuss a few potential leads for future works.

Improvement of the established analytical results

The main analytical results derived in this memoir proved that the estimation error of the considered classes of estimators is bounded when a given condition is met. These bounds and conditions have the advantage of directly involving the different parameters of the system and/or the estimator. We were therefore able to qualitatively interpret these quantities, and assess the critical parameters in the estimation process.

Nevertheless, we acknowledge that improving these results would be beneficial for our understanding and the instrumentation of resilient estimators. For instance, we could aim for a less conservative analysis in order to derive tighter conditions of resilience and tighter bounds on the estimation error. This improvement would give a more accurate depiction of the performances of resilient estimators.

In addition to this, one could also try to derive resilience-assessing indexes which are easier to evaluate in practice. Indeed, one of the drawbacks of the analysis we performed is that the obtained resilience-assessing indexes are hard to compute in practice. For instance, the r-Resilience index parameter p_r (see Eq. (2.26)) is defined as a solution of a combinatorial nonconvex optimisation problem. The advantage of having more easily computable resilience-assessing indexes would be the possibility of predicting the performances of the estimators in a given estimation setting.

Analysis of Resilience for recursive estimators

In this manuscript, we were able to obtain theoretical results on the resilience or the approximate resilience of some classes of state estimators. However, we were not able to derive recursive algorithms exactly implementing the state estimators theoretically studied. Indeed, the recursive estimators we derived were based on approximations of the original state estimators.

Consequently, the resilience study of the recursive estimators derived in this thesis remains an open question. It would be interesting to provide theoretical guarantees that these estimators are either resilient or approximately resilient in the presence of impulsive noise. We could consider two ways of conducting such an analysis:

- We could try to extend the theoretical results obtained on the exact estimators by quantifying the approximation brought by the recursive implementations.
- We could perform an entirely new analysis. For instance, we could try to analyse the optimal performance index functions introduced by the use of the FDP framework in order to derive an upper bound on the estimation error.

It is worth noting that Algorithm 3.1 is also an approximate (batch) implementation of class $\mathcal{E}^{\text{exp}}$, and its performances are therefore not guaranteed by the analysis of $\mathcal{E}^{\text{exp}}$ either. To theoretically analyse the performance of this batch algorithm, one could potentially study the critical points of functions V_Σ^{exp}, given that Algorithm 3.1 is designed to yield a critical point of V_Σ^{exp}, but not necessarily the one minimising the function.

Characterising a larger class of resilient estimators

The classes of estimators we defined cover a wide range of possible estimators defined through various performance index functions. We were then able to analyse these classes and subsequently proved the resilience or the approximate resilience of many estimators.

However, the estimators we considered in the present manuscript are not the only possible resilient estimators. Several other performance index functions, defining other state estimators, are very interesting candidates for the resilience (or approximate resilience) property. For instance, a class of estimators defined through cost functions with logarithmic loss functions of the form $a \mapsto \psi(a) - \log(1+\psi(a))$ (briefly presented in Subsection 1.5.4 for $\psi = |\cdot|$) can be a good candidate for resilient estimation. Our work therefore calls for the analysis of several more classes of estimators, in order to provide more and more solutions to the resilient state estimation problem.

Moreover, our work was focused on highlighting the key factors and properties which contribute to the resilience of estimators. We do acknowledge that there can be a tradeoff between the generality of the analysis and the fineness of the analysis results we obtain. Consequently, a possible extension of our analysis is to define new classes which would restrict the defined classes $\mathcal{E}$ or $\mathcal{E}^{\exp}$ by imposing more properties to the performance index functions. This could potentially help refining the analysis results which were obtained during this PhD thesis.

Appendix A

Appendices of Chapter 1

A.1 Proof of the coercivity of V_Σ as defined in (1.31)

In this appendix, we will prove that for any fixed Y (and μ_0), the function $V_\Sigma(Y,\cdot) : \mathbb{R}^{n\times T} \to \mathbb{R}_{\geq 0}$ such that for all $Z \in \mathbb{R}^{n\times T}$,

$$V_\Sigma(Y,Z) = \frac{1}{2}\|z_0-\mu_0\|^2_{S^{-1}} + \frac{1}{2}\sum_{t\in\mathbb{T}'}\|z_{t+1}-A_tz_t\|^2_{Q_t^{-1}} + \frac{1}{2}\sum_{t\in\mathbb{T}\setminus\{0\}}\|y_t-C_tz_t\|^2_{R_t^{-1}}$$

is coercive to the sense defined in Definition 1.4.

Proof. To do so, we consider a sequence $\{Z_k\}$ of matrices such that $\lim_{k\to+\infty}\|Z_k\| = +\infty$. First of all, we notice that for every definite positive matrix $M \in \mathbb{R}^{a\times a}$, we can write

$$\forall (z_1,z_2)\in\mathbb{R}^a\times\mathbb{R}^a,\ \|z_1-z_2\|^2_M \geq \frac{1}{2}\|z_1\|^2_M - \|z_2\|^2_M. \tag{A.1}$$

This follows from the convexity (see Definition 1.5) of the quadratic form $\|\cdot\|^2_M$. A formal derivation, in a more general case, can be found in Chapter 2 (see Lemma 2.1).

By applying (A.1) to $V_\Sigma(Y,Z)$, we obtain

$$\begin{aligned} V_\Sigma(Y,Z) \geq \frac{1}{2}\left(\frac{1}{2}\|z_0\|^2_{S^{-1}} - \|\mu_0\|^2_{S^{-1}}\right) + \frac{1}{2}\sum_{t\in\mathbb{T}'}\|z_{t+1}-A_tz_t\|^2_{Q_t^{-1}} \\ + \frac{1}{2}\sum_{t\in\mathbb{T}\setminus\{0\}}\left(\frac{1}{2}\|C_tz_t\|^2_{R_t^{-1}} - \|y_t\|^2_{R_t^{-1}}\right) \end{aligned} \tag{A.2}$$

This inequality can be written under the form

$$V_\Sigma(Y,Z) \geq F(Z) - \delta(\mu_0,Y), \tag{A.3}$$

with $\delta(\mu_0,Y)$ a quantity which does not depend on Z and $F : \mathbb{R}^{n\times T} \to \mathbb{R}_{\geq 0}$ such that

$$F(Z) = \frac{1}{4}\|z_0\|^2_{S^{-1}} + \frac{1}{2}\sum_{t\in\mathbb{T}'}\|z_{t+1}-A_tz_t\|^2_{Q_t^{-1}} + \frac{1}{4}\sum_{t\in\mathbb{T}\setminus\{0\}}\|C_tz_t\|^2_{R_t^{-1}}.$$

For every k in $\mathbb{N}$, we then have

$$V_\Sigma(Y,Z_k) \geq \|Z_k\|^2 F\left(\frac{Z_k}{\|Z_k\|}\right) - \delta(\mu_0,Y) \tag{A.4}$$

F is a continuous function, so it reaches its minimum over the compact set $\mathcal{S} = \{Z \in \mathbb{R}^{n\times T} : \|Z\| = 1\}$ according to the extreme value theorem (see [Rud76, Thm 4.16]): if we note $D = \min_{Z\in\mathcal{S}} F(Z)$, we notice that $D > 0$. Indeed, if $D = 0$, it means that

there exists $Z \in \mathcal{S}$ such that $F(Z) = 0$, and this entails

$$\begin{cases} z_0 = 0 \\ z_{t+1} = A_t z_t \qquad \forall t \in \mathbb{T}' \end{cases} . \tag{A.5}$$

Subsequently, $Z = 0$, which is not in $\mathcal{S}$. We therefore obtain

$$V_\Sigma(Y, Z_k) \geq D\|Z_k\|^2 - \delta(\mu_0, Y) \tag{A.6}$$

Given that $\lim_{k\to+\infty}\|Z_k\| = +\infty$, (A.6) is sufficient to prove that

$$\lim_{k\to+\infty}\|V_\Sigma(Y, Z_k)\| = +\infty,$$

and $V_\Sigma(Y, \cdot)$ is therefore coercive. □

A.2 Proof of Theorem 1.4

Proof. First of all, for a given measurement history $Y \in \mathbb{R}^{m\times T}$, given the definition (1.32) of the quadratic forms, we notice that the performance index function V_Σ can be rewritten as

$$V_\Sigma(Y,Z) = \frac{1}{2}z_0^\top S^{-1}z_0 - \mu_0^\top S^{-1}z_0 + \frac{1}{2}\sum_{t\in\mathbb{T}'}\begin{pmatrix} z_t \\ z_{t+1}\end{pmatrix}^\top \begin{pmatrix} A_t^\top Q_t^{-1}A_t & -A_t^\top Q_t \\ -Q_tA_t & Q_t\end{pmatrix}\begin{pmatrix} z_t \\ z_{t+1}\end{pmatrix} + \sum_{t\in\mathbb{T}\setminus\{0\}}\left(\frac{1}{2}z_t^\top C_t^\top R_t^{-1}C_tz_t - (C_t^\top R_ty_t)^\top z_t\right) + \delta(\mu_0,Y,S,\{R_t\}) \quad \text{(A.7)}$$

where $\delta(\mu_0,Y,S,\{R_t\})$ is a quantity which does not depend on Z. By defining $\mathcal{Q}$, $\mathcal{R}$ and $\tilde{Y}$ as in (1.35) and (1.36), we then obtain

$$V_\Sigma(Y,Z) = \frac{1}{2}\tilde{Z}^\top\mathcal{Q}\tilde{Z} + \frac{1}{2}\tilde{Z}^\top\mathcal{R}\tilde{Z} - \tilde{Y}^\top\tilde{Z} + \delta(\mu_0,Y,S,\{R_t\}) \quad \text{(A.8)}$$

with $\tilde{Z} = \mathrm{vec}(Z)$.

In the case of the Least Squares Estimator, V_Σ is differentiable with respect to Z. As V_Σ is convex (see Definition 1.5), its potential critical points, *i.e.* the values of Z for which the gradient of $V_\Sigma(Y,\cdot)$ is equal to the null vector, are global minimising arguments of V_Σ (for more information about the optimisation of Least-squares functions, refer to [Boy04, Sec. 1.2]).

As a result, finding the elements of $\mathcal{E}(Y)$, which is the set of minimising arguments of $V_\Sigma(Y,\cdot)$, is equivalent to finding the critical points of $V_\Sigma(Y,\cdot)$. By differentiating expression (A.8), given that $\mathcal{Q}$ and $\mathcal{R}$ are symmetric, we obtain

$$(\mathcal{Q}+\mathcal{R})\tilde{Z} - \tilde{Y} = 0. \quad \text{(A.9)}$$

(A.9) admits only one solution, which is $\hat{X}_T$. To finish the proof, we need to prove that the matrix $\mathcal{Q}+\mathcal{R}$ is invertible. Given that

$$\tilde{Z}^\top(\mathcal{Q}+\mathcal{R})\tilde{Z} = \|z_0\|^2_{S^{-1}} + \sum_{t\in\mathbb{T}'}\|z_{t+1}-A_tz_t\|^2_{Q_t^{-1}} + \sum_{t\in\mathbb{T}\setminus\{0\}}\|C_tz_t\|^2_{R_t^{-1}} \geq 0, \quad \text{(A.10)}$$

$\mathcal{Q}+\mathcal{R}$ is positive semidefinite. Moreover, $\tilde{Z}^\top(\mathcal{Q}+\mathcal{R})\tilde{Z} = 0$ implies $\tilde{Z} = 0$, which yields that $\mathcal{Q}+\mathcal{R}$ is positive definite, and therefore invertible. Consequently, the only solution of (A.9) can be expressed as

$$\mathrm{vec}(\hat{X}_T) = (\mathcal{Q}+\mathcal{R})^{-1}\tilde{Y},$$

which concludes the proof. □

A.3 Proof of Theorem 1.5

For any $T \in \mathbb{N}_{\neq 0}$, the goal of the proof is to obtain the relation

$$V^\star_{\Sigma,T}(Y_T, z) = \min_{s\in\mathbb{R}^n} \left\{ V^\star_{\Sigma,T-1}(Y_{T-1}, s) + \phi_{T-1}(z - A_{T-1}s) \right\} + \psi_T(y_T - C_T z)$$

with $Y_T = \begin{pmatrix} Y_{T-1} & y_T \end{pmatrix}$, $Y_{T-1} \in \mathbb{R}^{m\times T}$ and $y_T \in \mathbb{R}^m$.

According to the definition (1.29) of $V_{\Sigma,T}$,

$$V_{\Sigma,T}(Y_T, Z_T) = V_{\Sigma,T-1}(Y_{T-1}, Z_{T-1}) + \phi_{T-1}(z_T - A_{T-1}z_{T-1}) + \psi_T(y_T - C_T z_T) \quad \text{(A.11)}$$

By definition (1.39) of $V^\star_{\Sigma,T}$, we would then have

$$\begin{aligned}
V^\star_{\Sigma,T}(Y_T, z) &= \min_{\substack{Z_T\in\mathbb{R}^{n\times(T+1)} \\ z_T = z}} V_{\Sigma,T}(Y_T, Z_T) \\
&= \min_{\substack{Z_T\in\mathbb{R}^{n\times(T+1)} \\ z_T = z}} \{V_{\Sigma,T-1}(Y_{T-1}, Z_{T-1}) + \phi_{T-1}(z_T - A_{T-1}z_{T-1}) + \psi_T(y_T - C_T z_T)\} \\
&= \min_{Z_{T-1}\in\mathbb{R}^{n\times T}} \{V_{\Sigma,T-1}(Y_{T-1}, Z_{T-1}) + \phi_{T-1}(z - A_{T-1}z_{T-1})\} + \psi_T(y_T - C_T z) \\
&= \min_{s\in\mathbb{R}^n} \left\{ \min_{\substack{Z_{T-1}\in\mathbb{R}^{n\times T} \\ z_{T-1} = s}} V_{\Sigma,T-1}(Y_{T-1}, Z_{T-1}) + \phi_{T-1}(z - A_{T-1}s) \right\} + \psi_T(y_T - C_T z)
\end{aligned}$$

given that the order of minimisation is interchangeable [Roc98, Prop. 1.35]. This eventually yields

$$V^\star_{\Sigma,T}(Y_T, z) = \min_{s\in\mathbb{R}^n} \left\{ V^\star_{\Sigma,T-1}(Y_{T-1}, s) + \phi_{T-1}(z - A_{T-1}s) \right\} + \psi_T(y_T - C_T z)$$

which is the desired result.

□

A.4 Proof of Theorem 1.6

In the case of the Least Squares Estimator over time-horizon T, $V_{\Sigma,T}$ is such that for all $Z_T \in \mathbb{R}^{n\times T+1}$,

$$\begin{aligned} V_{\Sigma,T}(Y_T, Z_T) = &\frac{1}{2}(z_0-\mu_0)^\top S^{-1}(z_0-\mu_0) \\ &+ \sum_{t=0}^{T-1} \frac{1}{2}(z_{k+1}-A_k z_k)^\top Q_k^{-1}(z_{k+1}-A_k z_k) \\ &+ \sum_{t=0}^{T} \frac{1}{2}(y_k - C_k z_k)^\top R_k^{-1}(y_k - C_k z_k), \end{aligned}$$

To prove Theorem 1.6, we will proceed by recursion over T. For $T=0$, we have

$$V^\star_{\Sigma,0}(z) = V_{\Sigma,0}(z) = \frac{1}{2}(z-\mu_0)^\top S^{-1}(z-\mu_0). \tag{A.12}$$

Noting $P_0 = S$, $\hat{x}_0 = \mu_0$ and $r_0 = 0$, we can write

$$V^\star_{\Sigma,0}(z) = \frac{1}{2}(z-\hat{x}_0)^\top P_0^{-1}(z-\hat{x}_0) + r_0 \tag{A.13}$$

which is in accordance with the theorem.

Assuming now that the theorem is true for $T-1$, thanks to the Bellman equation (1.42), V_T can be written

$$\begin{aligned} V^\star_{\Sigma,T}(Y_T, z) = &\min_{s\in\mathbb{R}^n} \left\{ V^\star_{\Sigma,T-1}(Y_{T-1}, s) + \|z - A_{T-1}s\|^2_{Q_{T-1}^{-1}} \right\} + \|y_T - C_T z\|^2_{R_T^{-1}} \\ = &\min_{s\in\mathbb{R}^n} \left\{ \frac{1}{2}(s-\hat{x}_{T-1})^\top P_{T-1}^{-1}(s-\hat{x}_{T-1}) + r_T \right. \\ &\left. + \frac{1}{2}(z-A_{T-1}s)^\top Q_{T-1}^{-1}(z-A_{T-1}s) \right\} \\ &+ \frac{1}{2}(y_T - C_T z)^\top R_T^{-1}(y_T - C_T z) \\ = &\frac{1}{2}(s_{\min}-\hat{x}_{T-1})^\top P_{T-1}^{-1}(s_{\min}-\hat{x}_{T-1}) + r_{T-1} \\ &+ \frac{1}{2}(z-A_{T-1}s_{\min})^\top Q_{T-1}^{-1}(z-A_{T-1}s_{\min}) \\ &+ \frac{1}{2}(y_T - C_T z)^\top R_T^{-1}(y_T - C_T z) \end{aligned}$$

where $s_{\min}$ is equal to

$$s_{\min} = 2M_T^{-1}\left(P_{T-1}^{-1}\hat{x}_{T-1} + A_{T-1}^\top Q_{T-1}^{-1} z\right) \text{ with } M_T = P_{T-1}^{-1} + A_{T-1}^\top Q_{T-1}^{-1} A_{T-1}.$$

$s_{\min}$ is obtained by differentiating the function $s \mapsto \frac{1}{2}(s-\hat{x}_{T-1})^\top P_{T-1}^{-1}(s-\hat{x}_{T-1}) + r_{T-1} + \frac{1}{2}(z-A_{T-1}s)^\top Q_{T-1}^{-1}(z-A_{T-1}s)$ and then making it equal to zero, *i.e.*

$$\frac{1}{2}\left(P_{T-1}^{-1} + A_{T-1}^\top Q_{T-1}^{-1} A_{T-1}\right) s - P_{T-1}^{-1}\hat{x}_{T-1} - A_{T-1}^\top Q_{T-1}^{-1} z = 0$$

$$\Leftrightarrow\ s_{\min} = 2M_T^{-1}\left(P_{T-1}^{-1}\hat{x}_{T-1} + A_{T-1}^\top Q_{T-1}^{-1} z\right)$$

By replacing $s_{\min}$ by its expression in the latest one of $V_{\Sigma,T}^\star(Y_T, z)$, the latter can be reformulated such that

$$V_{\Sigma,T}^\star(Y_T, z) = \frac{1}{2} z^\top \Delta_t z - \rho_t^\top z + \theta_t \tag{A.14}$$

where $\Delta_{T-1} \in \mathbb{R}^{n\times n}$, $\rho_{T-1} \in \mathbb{R}^n$ and $\theta_{T-1} \in \mathbb{R}^n$ are equal to

$$\Delta_{T-1} = \left(Q_{T-1} + A_{T-1} P_{T-1} A_{T-1}^\top\right)^{-1} + C_T^\top R_T^{-1} C_T \tag{A.15}$$

$$\rho_{T-1} = \left(Q_{T-1} + A_{T-1} P_{T-1} A_{T-1}^\top\right)^{-1} A_{T-1}\hat{x}_{T-1} + C_T^\top R_T^{-1} y_T \tag{A.16}$$

$$\theta_{T-1} = r_{T-1} + \frac{1}{2} y_T^\top R_T^{-1} y_T + \frac{1}{2}\hat{x}_{T-1}^\top A_{T-1}^\top \left(Q_{T-1} + A_{T-1} P_{T-1} A_{T-1}^\top\right)^{-1} A_{T-1}\hat{x}_{T-1}. \tag{A.17}$$

Moreover, for all $z_1, z_2 \in \mathbb{R}^n$ and for all $M \in \mathcal{S}_n^+$, the square completion property states that

$$\frac{1}{2} z_1^\top M z_1 + z_2^\top z_1 = \frac{1}{2}(z_1 + M^{-1} z_2)^\top M (z_1 + M^{-1} z_2) - \frac{1}{2} z_2^\top M^{-1} z_2.$$

By using this property within (A.14), we then obtain

$$V_{\Sigma,T}^\star(Y_T, z) = \frac{1}{2}(z - \Delta_{T-1}^{-1}\rho_t)^\top \Delta_{T-1}^{-1}(z - \Delta_{T-1}^{-1}\rho_{T-1}) + r_{T-1} + \rho_{T-1}^\top \Delta_T^{-1}\rho_{T-1} + \theta_{T-1}.$$

By noting

$$P_T = \Delta_{T-1}^{-1} \tag{A.18}$$

$$\hat{x}_T = P_T \rho_{T-1} \tag{A.19}$$

$$r_T = r_{T-1} + \rho_{T-1}^\top \Delta_{T-1}^{-1}\rho_{T-1} + \theta_{T-1}, \tag{A.20}$$

we may now write

$$V_{\Sigma,T}^\star(z) = (z - \hat{x}_T)^\top P_T^{-1}(z - \hat{x}_T) + r_T \tag{A.21}$$

With these definitions, r_T is independent from z, and P_T verifies its defining equation (1.45). A little bit more developments are needed in order to verify that $\hat{x}_T$ respects its definition (1.44). Replacing ρ_{T-1} by its definition (A.16) in (A.19) yields

$$\hat{x}_T = P_T\left(Q_{T-1} + A_{T-1} P_{T-1} A_{T-1}^\top\right)^{-1} A_{T-1}\hat{x}_{T-1} + P_T^{-1} C_T^\top R_T^{-1} y_T \tag{A.22}$$

Using the definition of P_T and the Sherman-Morrison-Woodbury formula (see [Hor12, p. 0.7.4])

$$P_T\left(Q_{T-1} + A_{T-1} P_{T-1} A_{T-1}^\top\right)^{-1} A_{T-1} = A_{T-1} - P_T^{-1} C_T^\top R_T^{-1} C_T A_{T-1}$$

which directly yields the desired result.

Appendix B

Appendices of Chapter 2

B.1 A useful technical lemma

Lemma B.1. *Let $\xi_1, \xi_2 : \mathbb{R}^{a\times b} \to \mathbb{R}_{\geq 0}$ be two functions which satisfy properties (P2.1)–(P2.3) and let $\ell : \mathbb{R}^{c\times d} \to \mathbb{R}^{a\times b}$ be an injective linear mapping. Then $\xi_1 + \xi_2$ and $\xi_1 \circ \ell$ verify (P2.1)–(P2.3). In addition, the following holds:*

(j) *If ξ_1, ξ_2 verify (P2.4), then $\xi_1 + \xi_2$ and $\xi_1 \circ \ell$ verify (P2.4) .*

(jj) *If ξ_1, ξ_2 verify (P2.5), then $\xi_1 + \xi_2$ and $\xi_1 \circ \ell$ verify (P2.5) .*

The main point of interest of this lemma is that even if there are functions which satisfy properties (P2.4) and (P2.5) with different values of q and γ, their sum still verifies those properties.
To prove Lemma B.1, we will need the following result.

Lemma B.2 (Minimum function of two $\mathcal{K}_\infty$ functions)**.** *If q_1 and q_2 are two $\mathcal{K}_\infty$ functions, then so is the function q defined by*

$$\forall \lambda \in \mathbb{R}_{\geq 0},\ q(\lambda) = \min_{i\in\{1,2\}} q_i(\lambda) \tag{B.1}$$

Proof. We have to prove that q is continuous, strictly increasing and satisfies $q(0) = 0$ and $\lim_{\lambda\to+\infty} q(\lambda) = +\infty$.
First of all, it is clear that $q(0) = 0$. Also, continuity of q is immediate from that of q_1 and q_2 by noting that $q = (q_1 + q_2 - |q_1 - q_2|)/2$. To see the strict increasingness of q, consider λ_1 and λ_2 in $\mathbb{R}_{\geq 0}$ such that $\lambda_1 < \lambda_2$. Then $q(\lambda_1) \leq q_1(\lambda_1) < q_1(\lambda_2)$ and $q(\lambda_1) \leq q_2(\lambda_1) < q_2(\lambda_2)$. It follows that $q(\lambda_1) < \min_{i\in\{1,2\}} q_i(\lambda_2) = q(\lambda_2)$ and hence q is strictly increasing. We now show that $q(\lambda)$ tends to infinity when $\lambda \to +\infty$. Let $M > 0$ be an arbitrary positive number. Since q_1 and q_2 tend to infinity, there exist η_1 and η_2 such that $\lambda \geq \eta_1 \Rightarrow q_1(\lambda) \geq M$ and $\lambda \geq \eta_2 \Rightarrow q_2(\lambda) \geq M$. By taking $\eta = \max_{i\in\{1,2\}} \eta_i$, it holds that $q(\lambda) \geq M$ whenever $\lambda \geq \eta$, or equivalently that, $\lim_{\lambda\to+\infty} q(\lambda) = +\infty$. □

Proof of Lemma B.1: The sum $\xi_1 + \xi_2$ has clearly the properties (P2.1)–(P2.3) as a sum of continuous, even, positive definite functions. Moreover, the composition of a continuous, even, convex positive definite function with an injective linear mapping yields a continuous, even, positive definite function, so $\xi_1 \circ \ell$ satisfies properties (P2.1)–(P2.3) too.
Proof of (j): Assume that ξ_1 and ξ_2 satisfy (P2.4) with $\mathcal{K}_\infty$ functions q_1 and q_2 respectively. For all $\lambda \neq 0$ and all $Z \in \mathbb{R}^{a\times b}$, (2.6) yields

$$\xi_i(Z) \geq \min_{j\in\{1,2\}} q_j\left(\frac{1}{|\lambda|}\right) \xi_i(\lambda Z). \tag{B.2}$$

If we define q so that for all $\lambda \in \mathbb{R}_{\geq 0}$, $q(\lambda) = \min_{i\in\{1,2\}} q_i(\lambda)$, then q is a $\mathcal{K}_\infty$ function (see Lemma B.2 above) such that for all $\lambda \neq 0$ and $Z \in \mathbb{R}^{a\times b}$,

$$\xi_1(Z) + \xi_2(Z) \geq q\left(\frac{1}{|\lambda|}\right)(\xi_1(\lambda Z) + \xi_2(\lambda Z)) \tag{B.3}$$

therefore $\xi_1 + \xi_2$ verifies property (P2.4). Besides, for all $\lambda \neq 0$ and Z in $\mathbb{R}^{c\times d}$,

$$\xi_1(\ell(Z)) \geq q_1\left(\frac{1}{|\lambda|}\right)\xi_1(\lambda\ell(Z)) = q_1\left(\frac{1}{|\lambda|}\right)\xi_1(\ell(\lambda Z)) \tag{B.4}$$

given the linearity of ℓ. We can then conclude that $\xi_1 \circ \ell$ also verifies property (P2.4).
Proof of (jj): Assume that ξ_1 and ξ_2 satisfy (P2.5) for γ_1 and γ_2 respectively. Let $\gamma = \min_{i\in\{1,2\}} \gamma_i$. Similarly to the first case, for all Z_1, Z_2 in $\mathbb{R}^{a\times b}$ and i in $\{1,2\}$, (2.7) yields

$$\xi_i(Z_1 - Z_2) \geq \gamma\xi_i(Z_1) - \xi_i(Z_2) \tag{B.5}$$

which gives

$$\xi_1(Z_1 - Z_2) + \xi_2(Z_1 - Z_2) \geq \gamma\left(\xi_1(Z_1) + \xi_2(Z_1)\right) - \left(\xi_1(Z_2) + \xi_2(Z_2)\right) \tag{B.6}$$

therefore $\xi_1 + \xi_2$ satisfies property (P2.5). Moreover, for all Z_1 and Z_2 in $\mathbb{R}^{c\times d}$,

$$\xi_1(\ell(Z_1 - Z_2)) = \xi_1(\ell(Z_1) - \ell(Z_2)) \geq \gamma\xi_1(\ell(Z_1)) - \xi_1(\ell(Z_2)) \tag{B.7}$$

so $\xi_1 \circ \ell$ satisfies (P2.5) too.

□

B.2 Technical lemma for proving Theorem 2.1

This section contains a necessary lemma in order to prove Theorem 2.1.

Lemma B.3. *Given two $\mathcal{K}_\infty$ function q_1 and q_2. If we define q the function such that for all α in $\mathbb{R}_{\geq 0}$,*

$$q(\alpha) = \min\{q_1(\alpha), q_2(\alpha)\},$$

then q is invertible and for all α in $\mathbb{R}_{\geq 0}$,

$$q^{-1}(\alpha) = \max\{q_1^{-1}(\alpha), q_2^{(-1}(\alpha)\}$$

Proof. For the sake of simplicity, we will assume that one of the functions is always greater than the other, *i.e.* $q_1(\alpha) \leq q_2(\alpha)$ for all $\alpha \in \mathbb{R}_{\geq 0}$ with the possibility of switching notations between q_1 and q_2 is always greater than q_1. In the case where this assumption is not true, it means that the set $\mathcal{S} = \{\alpha \in \mathbb{R}_{\geq 0} \mid q_1(\alpha) = q_2(\alpha)\}$ is not reduced to the singleton $\{0\}$. The following reasoning can then be conducted on every segments of the form $[\alpha_1; \alpha_2]$ with α_1 and α_2 two consecutive values in $\mathcal{S}$ and then on $[\max_{\alpha \in \mathcal{S}} \alpha; +\infty[$, given that all those intervals form a partition of $\mathbb{R}_{\geq 0}$.

Let β be in $\mathbb{R}_{\geq 0}$, we shall prove that $q_2^{-1}(\beta) \leq q_1^{-1}(\beta)$.

Let α_2 be the value such that $q_2(\alpha_2) = \beta$: there also exists β_1 in $\mathbb{R}_{\geq 0}$ such that $q_1(\alpha_2) = \beta_1$, which leads to

$$\beta_1 = q_1(\alpha_2) \leq q_2(\alpha_2) = \beta.$$

As the inverse function of an increasing function, q_1^{-1} is increasing, $q_1^{-1}(\beta_1) \leq q_1^{-1}(\beta)$: however, by definition of β_1 and α_2,

$$q_1^{-1}(\beta_1) = \alpha_2 = q_2^{-1}(\beta),$$

which yields the desired result $q_2^{-1}(\beta) \leq q_1^{-1}(\beta)$. □

B.3 Technical results for proving Corollary 2.1.2

This section contains some technical steps of the proof of Corollary 2.1.2.

Lemma B.4. *If $\ell : \mathbb{R}^{n_y} \to \mathbb{R}_{\geq 0}$ satisfies (P2.1)–(P2.3) and (P2.5), then so does the function ψ defined by $\psi(y) = 1 - e^{-\ell(y)}$. Moreover if ℓ fulfills (P2.4), then ψ satisfies the same property but with a function q in $\mathcal{K}_{\mathrm{sat},a}$ for $a = 1$.*

Proof. It is straightforward to check that ψ obeys (P2.1)-(P2.3). By assumption, ℓ obeys (P2.5). Denote therefore the associated constant with γ_ℓ (which, by (2.7), is necessarily less than or equal to 1). To see then that (P2.5) is also satisfied by ψ, we just need to check that

$$\psi(a+b) - \bar{\gamma}_\ell \psi(a) - \bar{\gamma}_\ell \psi(b) \leq 0 \quad \forall (a,b) \in \mathbb{R}^{n_y} \times \mathbb{R}^{n_y} \tag{B.8}$$

with $\bar{\gamma}_\ell = \gamma_\ell^{-1} \geq 1$, which is equivalent to

$$1 - 2\bar{\gamma}_\ell + \bar{\gamma}_\ell e^{-\ell(a)} + \bar{\gamma}_\ell e^{-\ell(b)} - e^{-\ell(a+b)} \leq 0$$

Noting that $\ell(a+b) \leq \bar{\gamma}_\ell \ell(a) + \bar{\gamma}_\ell \ell(b)$, we have $-e^{-\ell(a+b)} \leq -e^{-\bar{\gamma}_\ell \ell(a) - \bar{\gamma}_\ell \ell(b)}$. From this it follows that for (B.8) to hold, it is enough that

$$1 - 2\bar{\gamma}_\ell + \bar{\gamma}_\ell e^{-\ell(a)} + \bar{\gamma}_\ell e^{-\ell(b)} - e^{-\bar{\gamma}_\ell \ell(a) - \bar{\gamma}_\ell \ell(b)} \leq 0$$

Posing $\alpha = e^{-\ell(a)}$ and $\beta = e^{-\ell(b)}$, it suffices that

$$1 - 2\bar{\gamma}_\ell + \bar{\gamma}_\ell \alpha + \bar{\gamma}_\ell \beta - (\alpha\beta)^{\bar{\gamma}_\ell} \leq 0 \quad \forall (\alpha, \beta) \in]0,1]$$

which can indeed be checked to be true by some differential calculations. In conclusion, (B.8) holds and therefore ψ satisfies (P2.5).
It remains now to check (P2.4). This follows directly from Lemma B.5 below, from which we know that $\psi(y) \geq q^\star(1/\lambda)\psi(\lambda y)$ with $q^\star$ is a saturated function in $\mathcal{K}_{\mathrm{sat},1}$. □

Lemma B.5. *Let $\ell : \mathbb{R}^{n_y} \to \mathbb{R}_{\geq 0}$ be a function satisfying properties (P2.1)–(P2.2) and (P2.4). In particular, assume that property (P2.4) is satisfied by ℓ with a $\mathcal{K}_\infty$ function q such that (2.6) is an equality relation. Let*

$$g(y,\lambda) = \frac{1 - e^{-\ell(y)}}{1 - e^{-\ell(y/\lambda)}}$$

for $\lambda \neq 0$ and $y \neq 0$. Then the function $q^\star : \mathbb{R}_{\geq 0} \to [0,1]$ defined by $q^\star(\lambda) = \inf_{y \neq 0} g(y,\lambda)$ for $\lambda > 0$ and $q^\star(0) = 0$, is well-defined, continuous and strictly increasing on $[0,1]$. Moreover we have

$$1 - e^{-\ell(y)} \geq q^\star(1/\lambda)(1 - e^{-\ell(\lambda y)}) \quad \forall (\lambda, y) \in \mathbb{R}_{>0} \times \mathbb{R}^{n_y}$$

Proof. Since g is positive on its domain (hence lower bounded), the defining infimum of $q^\star$ is well-defined. Pose $a = e^{-\ell(y)}$. Then by using the continuity property of ℓ and its radial unboundedness (see Lemma 2.2), we see that the range of a when y lives in $\mathbb{R}^{n_y} \setminus \{0\}$ is $]0,1[$. From the assumptions of the lemma, $\ell(y/\lambda) = q(1/\lambda)\ell(y)$ for all y and all $\lambda > 0$ and so, $q(1) = 1$ and $e^{-\ell(y/\lambda)} = a^{q(1/\lambda)}$. For all $\lambda > 0$ we can write

$$q^\star(\lambda) = \inf_{y \neq 0} g(y,\lambda) = \inf_{a \in]0,1[} \frac{1-a}{1 - a^{q(\frac{1}{\lambda})}}$$

with $q(1/\lambda) \geq 1$ for $0 < \lambda \leq 1$ and $q(1/\lambda) < 1$ for $\lambda > 1$. We therefore obtain

$$q^\star(\lambda) = \begin{cases} \dfrac{1}{q(1/\lambda)} & \text{if } 0 < \lambda \leq 1 \\ 1 & \text{otherwise} \end{cases}$$

The so obtained $q^\star$ is clearly continuous wherever it is well defined. Moreover, since $\lim_{\lambda \to 0} q^\star(\lambda) = q^\star(0) = 0$, we conclude that $q^\star$ is continuous on its entire domain. From the properties of q, we deduce that $q^\star$ is strictly increasing on $[0, 1]$. Lastly, we observe that the inequality in the statement of the lemma is a direct consequence of the definition of $q^\star$. □

B.4 Resilience to both process and measurement attacks

In this appendix, we will consider that the noise sequence $\{w_t\}$ is not bounded but arbitrary. In this case, $\{w_t\}$, much like $\{f_t\}$, can be decomposed for every $t \in \mathbb{T}$ as

$$w_t = g_t + o_t$$

with $\{g_t\}$ the bounded process noise sequence already present in most of the developments and $\{o_t\}$ a sparse noise sequence representing the potential outliers in $\{w_t\}$ much like the sparse noise sequence $\{s_t\}$ in $\{f_t\}$. Having such a process disturbance is indeed possible, in the case where the model takes into account actuators which can get either faulty or under attack.

We will assume the potential sparse noise affecting the actuators to be both temporally and component-wise sparse, which is a logical assumption to make when the attack or the fault occurring with one actuator is independent from the other potential disturbances. As a result, the family of loss functions $\{\phi_t\}$ need to be selected similarly to the family $\{\psi_t\}$ in Section 2.3.4. Therefore, if we assume that $\{\psi_t\}$ is defined as in (2.44) for every t in $\mathbb{T}$, ϕ_t will be defined in accordance with (2.2) such that for all t in $\mathbb{T}'$,

$$\phi_t(z) = \sum_{i \in \mathbb{I}} \phi_{t,i}(z[i]) \tag{B.9}$$

where $\phi_{t,i}(z[i]) = \phi_i^\circ(W_{t,i} z[i])$ with $W_{t,i} \in \mathbb{R}_{>0}$ and $\phi_i^\circ : \mathbb{R} \to \mathbb{R}_+$, $i = 1, \dots, n_y$, being some loss functions on $\mathbb{R}$ enjoying the properties (P2.1)–(P2.5).

To state the resilience property in this particular setting, we will need to partition both the index set $\mathbb{T}' \times \mathbb{I}$ and $\mathbb{T} \times \mathbb{J}$ with regards to the image of the arbitrary noise sequences $\{w_t\}$ and $\{f_t\}$, *i.e.*

$$\Pi_\varepsilon = \{(t,i) \in \mathbb{T}' \times \mathbb{I} \,:\, \phi_{t,i}(w_t[i]) \leq \varepsilon\} \tag{B.10}$$
$$\Pi_\varepsilon^c = \{(t,i) \in \mathbb{T}' \times \mathbb{I} \,:\, \phi_{t,i}(w_t[i]) > \varepsilon\} \tag{B.11}$$
$$\Lambda_\varepsilon = \{(t,j) \in \mathbb{T} \times \mathbb{J} \,:\, \psi_{t,j}(f_t[j]) \leq \varepsilon\} \tag{B.12}$$
$$\Lambda_\varepsilon^c = \{(t,j) \in \mathbb{T} \times \mathbb{J} \,:\, \psi_{t,j}(f_t[j]) > \varepsilon\} \tag{B.13}$$

As the analysis presented in Subsection 2.3.4 for attacks on individual sensors, the r-Resilience index needs to be redefined. However, contrary to the previous subsection, here this parameter needs to be function of two integer variables counting the possible error occurrences in the dynamic and in the measurement equations. Consequently, we define the (r, r')-Resilience index such that

$$\tilde{p}_{r,r'} = \sup_{\substack{Z \in \mathbb{R}^{n \times T} \\ Z \neq 0}} \sup_{\substack{\mathcal{T}' \subset \mathbb{T}' \times \mathbb{I} \\ |\mathcal{T}'| = r}} \sup_{\substack{\mathcal{T} \subset \mathbb{T} \times \mathbb{J} \\ |\mathcal{T}| = r'}} \frac{\bar{\lambda} \sum_{(t,i) \in \mathcal{T}'} \phi_{t,i}(z_{t+1}[i] - a_{t,i}^\top z_t) + \sum_{(t,j) \in \mathcal{T}} \psi_{t,j}(c_{t,j}^\top z_t)}{H_\Sigma(Z)} \tag{B.14}$$

with

$$\bar{\lambda} = \lambda \frac{1 + \gamma_\phi}{1 + \gamma_\psi} \tag{B.15}$$

where H_Σ is defined as in (2.25) from ψ_t in (2.44) and ϕ_t in (B.9), $z_{t+1}[i]$ is the i-th component of vector z_{t+1}, $a_{t,i}^\top$ is the i-th row of the state matrix A_t and $c_{t,j}^\top$ is i-th row of the observation matrix C_t.

Thanks to these notations, we can provide the following theorem which is the analog of Theorem 2.1 for abritrary disturbances in both state and measurement

equations under the componentwise and temporally sparse hypothesis.

Theorem B.1 (Upper bound on the estimation error with two arbitrary noises)**.** *Consider the system Σ defined by (1.1) with output Y together with the state estimator (2.4) in which the loss functions ϕ and ψ are assumed to obey (P2.1)–(P2.5). Denote with γ_ϕ and γ_ψ the constants associated with the GTI (P2.5) for ϕ and ψ respectively. Let $\varepsilon \geq 0$ and set $r = |\Pi_\varepsilon^c|$ $r' = |\Lambda_\varepsilon^c|$.*
If the system is observable on $[0, T-1]$ and $\tilde{p}_{r,r'} < 1/(1+\gamma_\psi)$, then for any norm $\|\cdot\|$ on $\mathbb{R}^{n\times T}$,

$$\|\hat{X} - X\| \leq h\left(\frac{2\beta_\Sigma(\varepsilon)}{D[1-\tilde{p}_{q,r}]} + \delta(\varepsilon)\right) \quad \forall \hat{X} \in \mathcal{E}(Y) \tag{B.16}$$

with X denoting the true state matrix from (1.1), $D = \min_{\|Z\|=1} H_\Sigma(Z) > 0$ and $\beta_\Sigma(\varepsilon)$, $\delta(\varepsilon)$ and h being defined by

$$\beta_\Sigma(\varepsilon) = \lambda \sum_{(t,i)\in\Pi_\varepsilon} \phi_{t,i}(w_t[i]) + \sum_{(t,j)\in\Lambda_\varepsilon} \psi_{t,j}(f_t[j]), \tag{B.17}$$

$$\delta(\varepsilon) = \frac{\lambda(1-\gamma_\phi)\sum_{(t,i)\in\Pi_\varepsilon^c} \phi_{t,i}(w_t[i]) + (1-\gamma_\psi)\sum_{(t,j)\in\Lambda_\varepsilon^c} \psi_{t,j}(f_t[j])}{D\left[1-\tilde{p}_{r,r'}\right]} \tag{B.18}$$

$$h(\alpha) = \max\left\{q_\phi^{-1}(\alpha), q_\psi^{-1}(\alpha)\right\}, \alpha \in \mathbb{R}_{\geq 0} \tag{B.19}$$

Remark. In this theorem, the threshold value ε used to separate the indexes of noises w_t and f_t is the same for both. It would be possible to define two threshold values, one for each, but this does not pose any additional theoretical problem given that it will only change the values of r and r'. As a result, it would only lead to an unnecessary additional notation.

Proof. Let $\hat{X}$ in $\mathcal{E}(Y)$. By definition of $\mathcal{E}$ in (2.4), we have $V_\Sigma(Y, \hat{X}) \leq V_\Sigma(Y, X)$, which gives explicitly

$$\begin{aligned}\lambda \sum_{(t,i)\in\mathbb{T}'\times\mathbb{I}} \phi_{t,i}(\hat{x}_{t+1}[i] - a_{t,i}^\top \hat{x}_t) + \sum_{(t,j)\in\mathbb{T}\times\mathbb{J}} \psi_{t,j}(y_t[j] - c_{t,j}^\top \hat{x}_t) \\ \leq \lambda \sum_{(t,i)\in\mathbb{T}'\times\mathbb{I}} \phi_{t,i}(w_t[i]) + \sum_{t\in\mathbb{T}\times\mathbb{J}} \psi_{t,j}(f_t[j])\end{aligned} \tag{B.20}$$

Using the fact that $x_{t+1}[i] = a_{t,i}^\top x_t + w_t[i]$, we can write

$$\phi_{t,i}(\hat{x}_{(t+1)}[i] - a_{t,i}^\top \hat{x}_t) = \phi_{t,i}(\hat{x}_{t+1}[i] - x_{t+1}[i] - a_{t,i}^\top(\hat{x}_t - x_t) + w_t[i]) \tag{B.21}$$

$$\tag{B.22}$$

Now, by applying the GTI and the symmetry properties of $\phi_{t,i}$, depending on whether (t,i) belongs to Π_ε or not, we have

$$\begin{aligned}\forall (t,i) \in \Pi_\varepsilon, \quad & \phi_{t,i}(\hat{x}_{t+1}[i] - a_{t,i}^\top \hat{x}_t) \geq \gamma_\phi \phi_{t,i}(e_{t+1}[i] - a_{t,i}^\top e_t) - \phi_{t,i}(w_t[i]) \\ \forall (t,i) \in \Pi_\varepsilon^c, \quad & \phi_{t,i}(\hat{x}_{t+1}[i] - a_{t,i}^\top \hat{x}_t) \geq \gamma_\phi \phi_{t,i}(w_t[i]) - \phi_{t,i}(e_{t+1}[i] - a_{t,i}^\top e_t),\end{aligned}$$

with $e_t = \hat{x} - x_t$. It follows that the first term on the left hand side of (B.20) is lower bounded as follows

$$\sum_{(t,i)\in\Pi_\varepsilon} \Big[\gamma_\phi \phi_{t,i}(e_{t+1}[i] - a_{t,i}^\top e_t) - \phi_{t,i}(w_t[i])\Big] + \sum_{(t,i)\in\Pi_\varepsilon^c} \Big[\gamma_\phi \phi_{t,i}(w_t[i]) - \phi_{t,i}(e_{t+1}[i] - a_{t,i}^\top e_t)\Big] \\ \leq \sum_{(t,j)\in\mathbb{T}\times\mathbb{I}} \phi_{t,i}(\hat{x}_{t+1}[i] - a_{t,i}^\top \hat{x}_t). \quad \text{(B.23)}$$

Similarly, by making use of the measurement equation in the model (1.1), observe that $\psi_{t,j}(y_t[j] - c_{t,j}^\top \hat{x}_t) = \psi_{t,j}(f_t[j] - c_{t,j}^\top e_t)$. We now apply the GTI and symmetry of ψ_t in two different ways depending on whether (t, j) belongs to Λ_ε or Λ_ε^c:

$$\begin{aligned} &\forall (t,j) \in \Lambda_\varepsilon, && \psi_{t,j}(y_t[j] - c_{t,j}^\top \hat{x}_t) \geq \gamma_\psi \psi_{t,j}(c_{t,j}^\top e_t) - \psi_{t,j}(f_t[j]) \\ &\forall (t,j) \in \Lambda_\varepsilon^c, && \psi_{t,j}(y_t[j] - c_{t,j}^\top \hat{x}_t) \geq \gamma_\psi \psi_{t,j}(f_t[j]) - \psi_{t,j}(c_{t,j}^\top e_t) \end{aligned}$$

These inequalities imply that the second term on the left hand side of (B.20) is lower bounded as follows

$$\sum_{(t,j)\in\Lambda_\varepsilon} \Big[\gamma_\psi \psi_{t,j}(c_{t,j}^\top e_t) - \psi_{t,j}(f_t[j])\Big] + \sum_{(t,j)\in\Lambda_\varepsilon^c} \Big[\gamma_\psi \psi_{t,j}(f_t[j]) - \psi_{t,j}(c_{t,j}^\top e_t)\Big] \\ \leq \sum_{(t,j)\in\mathbb{T}\times\mathbb{J}} \psi_{t,j}(y_t[j] - c_{t,j}^\top \hat{x}_t) \quad \text{(B.24)}$$

Combining (B.20), (B.23) and (B.24) gives

$$\begin{aligned} &\lambda\gamma_\phi \sum_{(t,i)\in\Pi_\varepsilon} \phi_{t,i}(e_{t+1}[i] - a_{t,i}^\top e_t) + \gamma_\psi \sum_{(t,j)\in\Lambda_\varepsilon} \psi_{t,j}(c_{t,j}^\top e_t) \\ &\quad - \lambda(1+\gamma_\phi) \sum_{(t,i)\in\Pi_\varepsilon^c} \phi_{t,i}(e_{t+1}[i] - a_{t,i}^\top e_t) - (1+\gamma_\psi) \sum_{(t,j)\in\Lambda_\varepsilon^c} \psi_{t,j}(c_{t,j}^\top e_t) \\ &\quad \leq 2\Big(\lambda \sum_{(t,i)\in\Pi_\varepsilon} \phi_{t,i}(w_t[i]) + \sum_{(t,j)\in\Lambda_\varepsilon} \psi_{t,j}(f_t[j])\Big) \\ &\quad + \lambda(1-\gamma_\phi) \sum_{(t,i)\in\Pi_\varepsilon^c} \phi_{t,i}(w_t[i]) + (1-\gamma_\psi) \sum_{(t,j)\in\Lambda_\varepsilon^c} \psi_{t,j}(f_t[j]) \quad \text{(B.25)} \end{aligned}$$

which, by using (2.25) and (B.17), can be written as

$$\begin{aligned} &H_\Sigma(E) - \lambda(1+\gamma_\phi) \sum_{(t,i)\in\Pi_\varepsilon^c} \phi_{t,i}(e_{t+1}[i] - a_{t,i}^\top e_t) - (1+\gamma_\psi) \sum_{(t,j)\in\Lambda_\varepsilon^c} \psi_{t,j}(c_{t,j}^\top e_t) \\ &\quad \leq 2\beta_\Sigma(\varepsilon) + \lambda(1-\gamma_\phi) \sum_{(t,i)\in\Pi_\varepsilon^c} \phi_{t,i}(w_t[i]) + (1-\gamma_\psi) \sum_{(t,j)\in\Lambda_\varepsilon^c} \psi_{t,j}(f_t[j]) \quad \text{(B.26)} \end{aligned}$$

with $E = \begin{pmatrix} e_0 & e_1 & \cdots & e_{T-1} \end{pmatrix}$. As Π_ε^c and Λ_ε^c have r and r' elements respectively, applying the definition of $\tilde{p}_{r,r'}$ gives

$$\lambda(1+\gamma_\phi) \sum_{(t,i)\in\Pi_\varepsilon^c} \phi_{t,i}(e_{t+1}[i] - a_{t,i}^\top e_t) + (1+\gamma_\psi) \sum_{(t,j)\in\Lambda_\varepsilon^c} \psi_{t,j}(c_{t,j}^\top e_t) \\ \leq (1+\gamma_\psi)\tilde{p}_{r,r'} H_\Sigma(E) \quad \text{(B.27)}$$

By the assumption that $\tilde{p}_{r,r'} < 1/(1+\gamma_\psi)$ we have

$$H_\Sigma(E) \leq \frac{1}{1-\tilde{p}_{r,r'}}\Big[2\beta_\Sigma(\varepsilon) + \lambda(1-\gamma_\phi)\sum_{(t,i)\in\Pi_\varepsilon^c}\phi_{t,i}(w_t[i]) + (1-\gamma_\psi)\sum_{(t,j)\in\Lambda_\varepsilon^c}\psi_{t,j}(f_t[j])\Big] \tag{B.28}$$

As it was already stated in the proof of Theorem 2.1, $H_\Sigma(\varepsilon)$ verifies properties (P2.1)–(P2.4) so apply Lemma 2.2 to conclude that for any norm $\|\cdot\|$, there exists a $\mathcal{K}_\infty$ function l such that

$$H_\Sigma(E) \geq Dq'(\|E\|) \tag{B.29}$$

with D defined by $D = \min_{\|Z\|=1} H_\Sigma(Z)$ and $q'(\alpha) = \min\{q_\phi(\alpha), q_\psi(\alpha)\}$. Finally, the result follows by selecting h to be $h = {q'}^{-1}$ with ${q'}^{-1}$ denoting the inverse of q', which can be simplified to match its definition in (2.31) through Lemma B.3 presented in Appendix B.2. □

Strict resilience. Just like the first scenario, this theorem does not provide any resilient proof yet as the bound still rely on the value of potentially large occurrences of the noises through $\delta(\varepsilon)$. However, there is a strict resilience result when all the class functions $\phi_{t,i}$ and $\psi_{t,j}$ satisfies the triangle inequality:

Corollary B.1.1 (Resilience property in presence of two arbitrary noises)**.** *Let the conditions of Theorem 2.1 hold with the additional requirement that* $\gamma_\phi = \gamma_\psi = 1$. *Then*

$$\|\hat{X} - X\| \leq h\Big(\frac{2\beta_\Sigma(\varepsilon)}{D(1-\tilde{p}_{r,r'})}\Big) \quad \forall \hat{X} \in \mathcal{E}(Y). \tag{B.30}$$

Proof. The proof is immediate by considering the bound in (B.16) and observing that $\delta(\varepsilon)$ expressed in (B.18) vanishes when $\gamma_\phi = \gamma_\psi = 1$, hence eliminating completely the contribution of the extreme values of $\{w_t[i]\}$ and $\{f_t[j]\}$ to the error bound. □

B.5 Calculability of p_r: a case not handled by the framework

This appendix deals with an estimator $\mathcal{E}$ such that for all t, $\phi_t = \|\cdot\|_2^2$ and $\psi_t = \|\cdot\|_1$. The following lemma can then be obtained:

Lemma B.6. *Let Σ be a system as in (1.1). Consider p_r as defined in (2.26) with $\{\phi_t\}$ and $\{\psi_t\}$ defined respectively by $\phi_t = \|\cdot\|_2^2$ and $\psi_t = \|\cdot\|_1$ for every t in $\mathbb{T}$. then $p_r = 1$ for every r in $\mathbb{N}_{\geq 0}$.*

Proof. First of all, given that for every r, $p_1 \leq p_r \leq 1$, we only need to prove that $p_1 = 1$.

In this configuration, p_1 is equal to

$$p_1 = \sup_{\substack{Z \in \mathbb{R}^{n\times T} \\ Z \neq 0}} \sup_{\tau \in \mathbb{T}} \frac{\|C_\tau z_\tau\|_1}{\lambda\gamma_\psi \sum_{t\in\mathbb{T}'} \|z_{t+1} - Az_t\|_2^2 + \sum_{t\in\mathbb{T}} \|C_t z_t\|_1} \tag{B.31}$$

For every τ in $\mathbb{T}$, we pose the following function

$$\forall Z \in \mathbb{R}^{n\times T},\ \Xi_\tau(Z) = \frac{\|C_\tau z_\tau\|_1}{\lambda\gamma_\psi \sum_{t\in\mathbb{T}'} \|z_{t+1} - Az_t\|_2^2 + \sum_{t\in\mathbb{T}} \|C_t z_t\|_1}. \tag{B.32}$$

This function verifies

$$p_1 = \sup_{\tau\in\mathbb{T}} \sup_{\substack{Z \in \mathbb{R}^{n\times T} \\ Z \neq 0}} \Xi_\tau(Z). \tag{B.33}$$

From the fact that for every μ in $\mathbb{R}$,

$$\Xi_\tau(\mu Z) = \frac{\|C_\tau z_\tau\|_1}{\mu\lambda\gamma_\psi \sum_{t\in\mathbb{T}'} \|z_{t+1} - Az_t\|_2^2 + \sum_{t\in\mathbb{T}} \|C_t z_t\|_1},$$

we verify that for every $Z \in \mathbb{R}^{n\times T}$,

$$\lim_{\mu\to 0} \Xi_\tau(\mu Z) = \frac{\|C_\tau z_\tau\|_1}{\sum_{t\in\mathbb{T}} \|C_t z_t\|_1}.$$

In particular, we define Z_τ the matrix from $\mathbb{R}^{n\times T}$ such that $\|z_\tau\|_2 = 1$ and every other columns are null. Z_τ is different from 0 and $\lim_{\mu\to 0} \Xi_\tau(\mu Z_\tau) = 1$.

By the definition of the limit, for every $\varepsilon > 0$, there exists μ_ε such that $|\mu| < \mu_\varepsilon$ implies $|\Xi_\tau(\mu Z_\tau) - 1| \leq \varepsilon$ which also implies $\Xi_\tau(\mu Z_\tau) \geq 1 - \varepsilon$. As a result, 1 is an upper bound of $\Xi_\tau(Z)$ and for every $\varepsilon > 0$, there exists Z in $\mathbb{R}^{n\times T}$ different from 0 such that $\Xi_\tau(Z) \geq 1 - \varepsilon$ (this is the case for any μZ_τ with $\mu > \mu_\varepsilon$): 1 is therefore the supremum by definition, *i.e.*

$$\sup_{\substack{Z \in \mathbb{R}^{n\times T} \\ Z \neq 0}} \Xi_\tau(Z) = 1. \tag{B.34}$$

This directly leads to $p_1 = 1$ given Equation (B.33) (the result is obtained if at least one τ verifies (B.34), but as a matter of fact, the reasoning can be applied to every τ in $\mathbb{T}$).

□

This lemma shows the limits of the framework developed in Chapter 2 in the sense that there are members of the class of estimators defined in Definition 2.1 for which

it is impossible to assess if they enjoy the resilience property through Theorem 2.1. It also suggests that the condition for the existence of the upper bound (2.28) is conservative, as we already knew given that it is merely a sufficient condition: however, we do not have any theoretical evidence to back this assumption up, as we do not know if the estimator described in Lemma B.6 actually enjoys the resilience property. It provides good simulation results, as it is the estimators $\mathcal{E}_{\ell_2^2,\ell_1}$ presented in Section 2.7, but this is indeed not enough to conclude about its theoretical performances.

B.6 Performance tests on an LTV system

In this appendix, we performed the tests presented in *Experiment 1: Sparsity Test* and *Experiment 2: SNR Test* on an LTV system to show that the class of estimators $\mathcal{E}$ can also handle such systems.

The studied system is a a two-states switched system, in the form

$$\Sigma_s : \begin{cases} x_{t+1} &= A_t x_t + g_t \\ y_t &= C_t y_t + f_t \end{cases} \tag{B.35}$$

where for every t in $\mathbb{T}$,

$$A_t = \mathcal{A}(\sigma(t)) \quad \text{and} \quad C_t = \mathcal{C}(\sigma(t)).$$

$\mathcal{A} : \{1,2\} \to \mathbb{R}^{2\times 2}$ and $\mathcal{C} : \{1,2\} \to \mathbb{R}^{1\times 2}$ are two functions such that

$$\mathcal{A}(1) = \begin{pmatrix} 0.7 & 0.45 \\ -0.5 & 1 \end{pmatrix}, \quad \mathcal{A}(2) = \begin{pmatrix} 0.75 & 0.65 \\ 0.65 & -0.75 \end{pmatrix}, \tag{B.36}$$

$$\mathcal{C}(1) = \begin{pmatrix} 1 & 2 \end{pmatrix}, \quad \mathcal{C}(2) = \begin{pmatrix} 0.15 & -0.1 \end{pmatrix}. \tag{B.37}$$

$\sigma : \mathbb{T} \to \{1,2\}$ is the switching signal, represented on Figure B.1. It was generated by initiating the states at 1 for $t = 0$ and then having a 0.3 probability of switching state at each time.

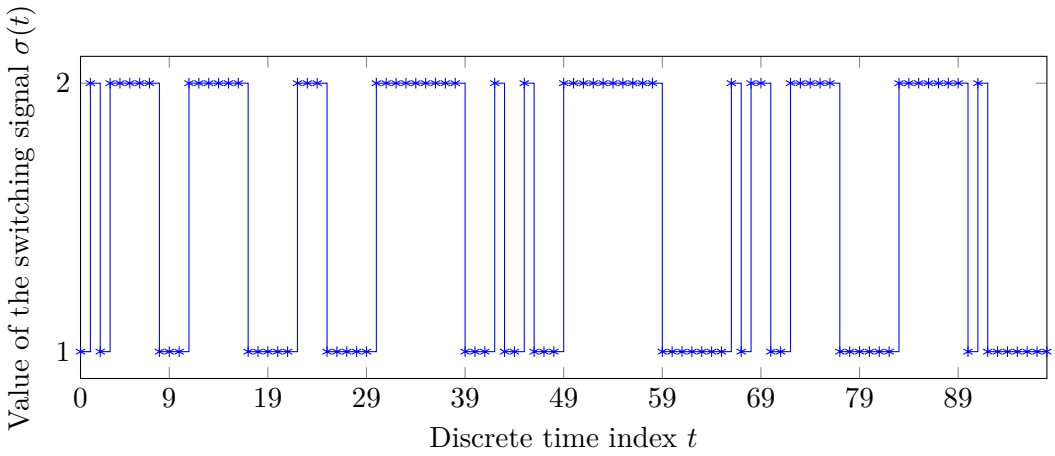

FIGURE B.1: State of System 2 throughout time

It can be interesting to compare the values of p_1 for the two system states $(\mathcal{A}(1), \mathcal{C}(1))$ (which is Sytem (1.21)) and $(\mathcal{A}(2), \mathcal{C}(2))$ to the one the overall System (B.35): we obtain $p_1 = 0.0607$ for state $(\mathcal{A}(1), \mathcal{C}(1))$, $p_1 = 0.0283$ for state $(\mathcal{A}(2), \mathcal{C}(2))$ and $p_1 = 0.0785$ for System (B.35). It seems hard to draw a conclusion on the link between the value of p_1 for system states and for the switched system, especially as the commutation signal σ plays a role in this value.

The results of the sparsity test and the SNR test are presented on Figure B.2: the conclusions of those tests are fairly similar to the ones drawn for the LTI case and System 1. The resilient estimators seem to be able to handle outliers in $\{f_t\}$ up to a given break point, and at a given ratio below that break point, the performances of those estimators are actually fairly close from the lower limit of performances indicated by Oracle $\mathcal{E}_{\ell_2^2,\ell_2^2}$. However, in that case, it can be noted that for lower ratios

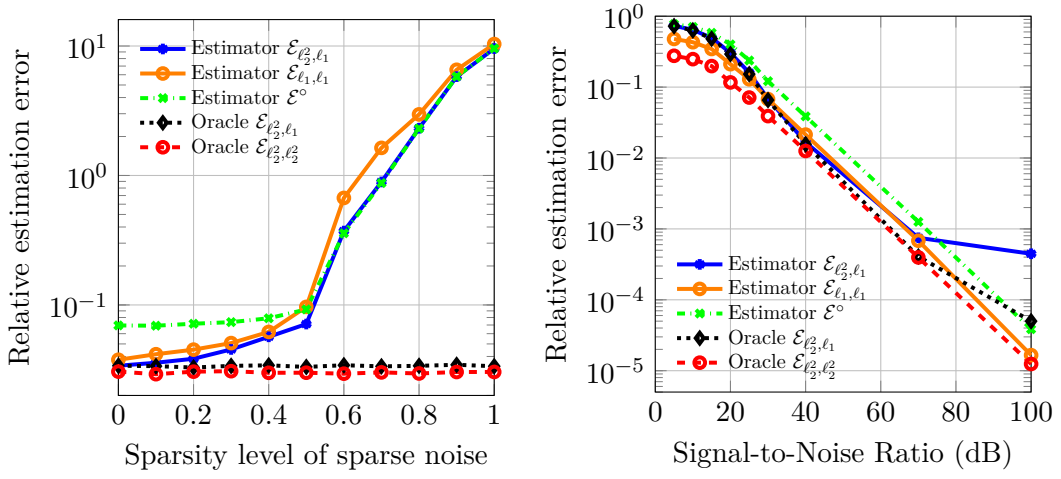

(A) Sparsity test (B) SNR test

FIGURE B.2: Performance tests of several different estimators for System 2

of sparsity, the obtained average REE is smaller, and the break point seems to be around 50% of non-zero entries for $\{s_t\}$ which is lower than for System (1.21).

Appendix C

Appendices of Chapter 3

C.1 Proof of Lemma 3.1

First of all, we notice that the expression

$$\left(\frac{1}{\rho}-1\right)e^{-2\lambda_\phi \varepsilon}-e^{-\lambda_\phi \varepsilon}+1$$

is a polynomial of degree 2 with respect to $e^{-\lambda_\phi \varepsilon}$. If we note $\xi : \mathbb{R} \to \mathbb{R}$ the polynomial function such that for all $a \in \mathbb{R}$,

$$\xi(a) = \left(\frac{1}{\rho}-1\right)a^2 - a + 1,$$

we can prove that (3.18) is true by verifying that for all $a \in [0,1]$,

$$0 \leq \xi(a) \leq \frac{1}{\rho}.$$

$\xi(a) \geq 0$**:** the polynomial discriminant of ξ is equal to $5-4/\rho$ which is nonpositive when $\rho < 4/5$. Consequently, $\xi(a)$ has the same sign as the leading coefficient of ξ, *i.e.* $(1/\rho - 1)$. This means that for all $a \in \mathbb{R}$, $\xi(a) \geq 0$.

$\xi(a) \leq \frac{1}{\rho}$**:** to assess this inequality, we will consider the polynomial $\xi - \frac{1}{\rho}$ and verify that for all $a \in [0,1]$, $\xi(a) - \frac{1}{\rho} \leq 0$. As the leading coefficient of this new polynomial is still $\left(\frac{1}{\rho}-1\right)$ which is nonnegative, $\xi(a) - \frac{1}{\rho} \leq 0$ for $a \in [a_1, a_2]$ if the roots $a_1 \leq a_2$ of the polynomial exist.

The discriminant of this new polynomial is equal to

$$\Delta = 1 + 4\left(\frac{1}{\rho}-1\right)^2 \geq 0,$$

so its two (real) roots are therefore equal to

$$a_1 = \frac{1-\sqrt{\Delta}}{2\left(\frac{1}{\rho}-1\right)} \qquad a_2 = \frac{1+\sqrt{\Delta}}{2\left(\frac{1}{\rho}-1\right)}.$$

Δ is strictly greater than 1 for every ρ, so it implies that $a_1 \leq 0$. Moreover, Δ is also strictly greater than $4(\frac{1}{\rho} - 1)^2$ so we notice that

$$a_2 \geq \frac{1 + \sqrt{4\left(\frac{1}{\rho} - 1\right)^2}}{2\left(\frac{1}{\rho} - 1\right)} \geq 1$$

As a result, we notice that $[0, 1] \subseteq [a_1, a_2]$, which ensures that $\xi(a) \leq \frac{1}{\rho}$.

C.2 Iterative Reweighted Least Squares algorithm in the case of $\mathcal{E}^{\circ,\exp}$

In the case of class $\mathcal{E}^{\circ,\exp}$, to approximately solve Problem (3.56) through an IRLS algorithm, we iteratively solve the optimisation problem

$$\hat{x}_0^{(k)} = \arg\min_{z\in\mathbb{R}^n} V_q^{\circ(k)}(Y,z)$$

with $V_q^{\circ(k)}$ the quadratic function such that for all (Y,z) in $\mathbb{R}^{m\times T}\times\mathbb{R}^n$,

$$V_q^{\circ(k)}(Y,z) = \sum_{(t,j)\in\mathbb{T}\times\mathbb{J}} \beta_{t,j}^{(k)} \left(y_{t,j} - \theta_{t,j}^\top z\right)^2. \tag{C.1}$$

The family of weights $\{\beta_{t,j}^{(k)}\}$ are recursively defined such that

$$\forall (t,j)\in\mathbb{T}\times\mathbb{J},\ \beta_{t,j}^{(k+1)} = e^{-\lambda_\psi\left(y_{t,j}-\theta_{t,j}^\top \hat{x}_0^{(k)}\right)^2},$$

and with the initial family $\{\beta_{t,j}^{(i)}\}$ such that

$$\forall (t,j)\in\mathbb{T}\times\mathbb{J},\ \beta_{t,j}^{(1)} = e^{-\lambda_\psi y_{t,j}^2}.$$

We use the stopping condition

$$\eta = \frac{\|\hat{X}^{(k)} - \hat{X}^{(k-1)}\|_2}{\|\hat{X}^{(k-1)}\|_2}$$

with $\hat{X}^{(k)}$ being the reconstructed state trajectory from $\hat{x}_0^{(k)}$ (see Eq. (3.20)). This stopping condition is compared to a threshold $\eta_{\min}$ indicating when the algorithm must stop. The resulting algorithm can be found in Algorithm C.1.

Algorithm C.1 Iterative Reweighted Least Squares (IRLS) Algorithm to approximately implement Problem (3.59)

Inputs: λ_ψ, Y, $k_{\max}$, $\eta_{\min}$
Initialisation:
$k \leftarrow 1$
$\eta \leftarrow 10^8$
$\forall (t,j)\in\mathbb{T}\times\mathbb{J},\ \beta_{t,j}^{(1)} \leftarrow e^{-\lambda_\psi y_{t,j}^2}$
$\hat{x}_0^{(1)} \leftarrow \arg\min_{z\in\mathbb{R}^n} V_q^{\circ(1)}(Y,z)$
$\forall (t,j)\in\mathbb{T}\times\mathbb{J},\ \beta_{t,j}^{(2)} \leftarrow e^{-\lambda_\psi (y_t[j]-\theta_{t,j}^\top \hat{x}_0^{(1)})^2}$
End of Initialisation.
while $\eta > \eta_{\min}$ **and** $k < k_{\max}$ **do**
  $k \leftarrow k+1$
  $\hat{x}_0^{(k)} \leftarrow \arg\min_{z\in\mathbb{R}^n} V_q^{\circ(k)}(Y,z)$
  $\forall (t,j)\in\mathbb{T}\times\mathbb{J},\ \beta_{t,j}^{(k+1)} \leftarrow e^{-\lambda_\psi (y_t[j]-\theta_{t,j}^\top \hat{x}_0^{(k)})^2}$
  $\eta \leftarrow \frac{\|\hat{X}^{(k)} - \hat{X}^{(k-1)}\|}{\|\hat{X}^{(k-1)}\|}$
end while
return $\hat{X}^{(k)}$

Appendix D

Appendices of Chapter 4

D.1 Regression matrix of the IEEE 14-bus system

The IEEE 14-bus system model which was used to illustrate the application of our estimation framework to regressive models in Section 4.2 is of the form

$$y = H_{14}x + f$$

with H_{14} the regression matrix from $\mathbb{R}^{34\times 13}$ such that

$$H_{14} = \begin{pmatrix}
-16.9 & 0 & 0 & -4.4835 & 0 & 0 & 0 & 0 & 0 & 0 & 0 & 0 & 0 \\
33.374 & -5.0513 & -5.6715 & -5.7511 & 0 & 0 & 0 & 0 & 0 & 0 & 0 & 0 & 0 \\
-5.0513 & 10.898 & -5.8469 & 0 & 0 & 0 & 0 & 0 & 0 & 0 & 0 & 0 & 0 \\
-5.6715 & -5.8469 & 42.011 & -23.747 & 0 & -4.8895 & 0 & -1.8555 & 0 & 0 & 0 & 0 & 0 \\
-5.7511 & 0 & -23.747 & 38.239 & -4.2574 & 0 & 0 & 0 & 0 & 0 & 0 & 0 & 0 \\
0 & 0 & 0 & -4.2574 & 20.871 & 0 & 0 & 0 & 0 & -5.0277 & -3.9092 & -7.6764 & 0 \\
0 & 0 & -4.8895 & 0 & 0 & 19.657 & -5.677 & -9.0901 & 0 & 0 & 0 & 0 & 0 \\
0 & 0 & 0 & 0 & 0 & -5.677 & 5.677 & 0 & 0 & 0 & 0 & 0 & 0 \\
0 & 0 & -1.8555 & 0 & 0 & -9.0901 & 0 & 26.478 & -11.834 & 0 & 0 & 0 & -3.6985 \\
0 & 0 & 0 & 0 & 0 & 0 & 0 & -11.834 & 17.041 & -5.2064 & 0 & 0 & 0 \\
0 & 0 & 0 & 0 & -5.0277 & 0 & 0 & 0 & -5.2064 & 10.234 & 0 & 0 & 0 \\
0 & 0 & 0 & 0 & -3.9092 & 0 & 0 & 0 & 0 & 0 & 8.9122 & -5.003 & 0 \\
0 & 0 & 0 & 0 & -7.6764 & 0 & 0 & 0 & 0 & 0 & -5.003 & 15.553 & -2.8734 \\
0 & 0 & 0 & 0 & 0 & 0 & 0 & -3.6985 & 0 & 0 & 0 & -2.8734 & 6.5719 \\
-16.9 & 0 & 0 & 0 & 0 & 0 & 0 & 0 & 0 & 0 & 0 & 0 & 0 \\
0 & 0 & 0 & -4.4835 & 0 & 0 & 0 & 0 & 0 & 0 & 0 & 0 & 0 \\
5.0513 & -5.0513 & 0 & 0 & 0 & 0 & 0 & 0 & 0 & 0 & 0 & 0 & 0 \\
5.6715 & 0 & -5.6715 & 0 & 0 & 0 & 0 & 0 & 0 & 0 & 0 & 0 & 0 \\
5.7511 & 0 & 0 & -5.7511 & 0 & 0 & 0 & 0 & 0 & 0 & 0 & 0 & 0 \\
0 & 5.8469 & -5.8469 & 0 & 0 & 0 & 0 & 0 & 0 & 0 & 0 & 0 & 0 \\
0 & 0 & 23.747 & -23.747 & 0 & 0 & 0 & 0 & 0 & 0 & 0 & 0 & 0 \\
0 & 0 & 4.8895 & 0 & 0 & -4.8895 & 0 & 0 & 0 & 0 & 0 & 0 & 0 \\
0 & 0 & 1.8555 & 0 & 0 & 0 & 0 & -1.8555 & 0 & 0 & 0 & 0 & 0 \\
0 & 0 & 0 & 4.2574 & -4.2574 & 0 & 0 & 0 & 0 & 0 & 0 & 0 & 0 \\
0 & 0 & 0 & 0 & 5.0277 & 0 & 0 & 0 & 0 & -5.0277 & 0 & 0 & 0 \\
0 & 0 & 0 & 0 & 3.9092 & 0 & 0 & 0 & 0 & 0 & -3.9092 & 0 & 0 \\
0 & 0 & 0 & 0 & 7.6764 & 0 & 0 & 0 & 0 & 0 & 0 & -7.6764 & 0 \\
0 & 0 & 0 & 0 & 0 & 5.677 & -5.677 & 0 & 0 & 0 & 0 & 0 & 0 \\
0 & 0 & 0 & 0 & 0 & 9.0901 & 0 & -9.0901 & 0 & 0 & 0 & 0 & 0 \\
0 & 0 & 0 & 0 & 0 & 0 & 0 & 11.834 & -11.834 & 0 & 0 & 0 & 0 \\
0 & 0 & 0 & 0 & 0 & 0 & 0 & 3.6985 & 0 & 0 & 0 & 0 & -3.6985 \\
0 & 0 & 0 & 0 & 0 & 0 & 0 & 0 & 5.2064 & -5.2064 & 0 & 0 & 0 \\
0 & 0 & 0 & 0 & 0 & 0 & 0 & 0 & 0 & 0 & 5.003 & -5.003 & 0 \\
0 & 0 & 0 & 0 & 0 & 0 & 0 & 0 & 0 & 0 & 0 & 2.8734 & -2.8734
\end{pmatrix} \tag{D.1}$$

D.2 Variation of Algorithm 3.2 used to implement $\mathcal{E}^{\text{exp}}_{\text{online}}$ in Section 4.4

In Section 4.4, we implemented a modified version of Algorithm 3.2 whose details can be found in Algorithm D.1.

Algorithm D.1 Fine-tuning variation of Algorithm 3.2

1: **Inputs:** A, C, $\lambda_\phi \in \mathbb{R}_{>0}$, $\lambda_\psi \in \mathbb{R}_{>0}$, $\hat{x}_0 \in \mathbb{R}^n$, $P_0 \in \mathcal{S}_n^+(\mathbb{R})$, $Q \in \mathcal{S}_n^+(\mathbb{R})$, $\{r_j\}_{j\in\mathbb{J}}$, $T_{\max} \in \mathbb{N}$, $Y \in \mathbb{R}^{m\times T_{\max}}$
2: **Initialization:**
3: $T \leftarrow 0$
4: **End of Initialization.**
5: **while** $T < T_{\max}$ **do**
6: $\quad \hat{x}_{T|T-1} \leftarrow A\hat{x}_{T-1}$
7: $\quad \forall j \in \mathbb{J},\ \hat{\beta}_{T,j} = \frac{\lambda_\psi}{r_j} e^{-\frac{\lambda_\psi}{r_j}\left(y_t[j]-c_j^\top \hat{x}_{T|T-1}\right)^2}$
8: $\quad R_T \leftarrow \text{diag}(1/\hat{\beta}_{T,1}, ..., 1/\hat{\beta}_{T,m})$
9: $\quad P_{T|T-1} \leftarrow AP_{T-1}A^\top + \frac{1}{\lambda_\phi}Q$
10: $\quad L_T \leftarrow P_{T|T-1}C^\top \left(CP_{T|T-1}C^\top + R_T\right)^{-1}$
11: $\quad \hat{x}_T \leftarrow \hat{x}_{T|T-1} + L_T(y_T - C\hat{x}_{T|T-1})$
12: $\quad P_T \leftarrow (I_n - LC)P_{T|T-1}$
13: $\quad T \leftarrow T + 1$
14: **end while**

The main difference between Algorithm 3.2 and Algorithm D.1 is that this one introduces weights in $\beta_{T,j}$ and replaces I_n on line 9 by a diagonal matrix Q from $\mathbb{R}^{n\times n}$. These additions enable us to weigh independently each term $\frac{\lambda_\psi}{r_j} e^{-\frac{\lambda_\psi}{r_j}\left(y_t[j]-c_j^\top \hat{x}_{T|T-1}\right)^2}$ in R_T, and also to weigh the confidence we have in each state of the system independently, in a very similar manner to how Q is designed in a Kalman Filter (see Section 1.3.2).

From a theoretical point of view, this online algorithm corresponds to the approximative implementation of the optimal estimator defined by the cost function such that for all (Y, Z) in $\mathbb{R}^{m\times T} \times \mathbb{R}^{n\times T}$,

$$V_\Sigma(Y,Z) = \sum_{(t,i)\in\mathbb{T}'\times\mathbb{I}} e^{-\frac{\lambda_\phi}{q_i}(z_{t+1}[i]-a_i^\top z_t)^2} + \sum_{(t,j)\in\mathbb{T}\times\mathbb{J}} e^{-\frac{\lambda_\psi}{r_j}(y_t[j]-c_j^\top z_t)^2}, \tag{D.2}$$

with $\{q_i\}$ the diagonal elements of Q. The reasoning performed in Section 3.5 to derive the offline and online algorithms could easily be extended to this cost function, which would eventually yield Algorithm D.1.

D.3 Raw measurements yielded by the accelerometer and the radar in the drone experiment

In Figure D.1, we see the measurements returned by the accelerometer and the radar alongside the reference returned by the motion capture system.

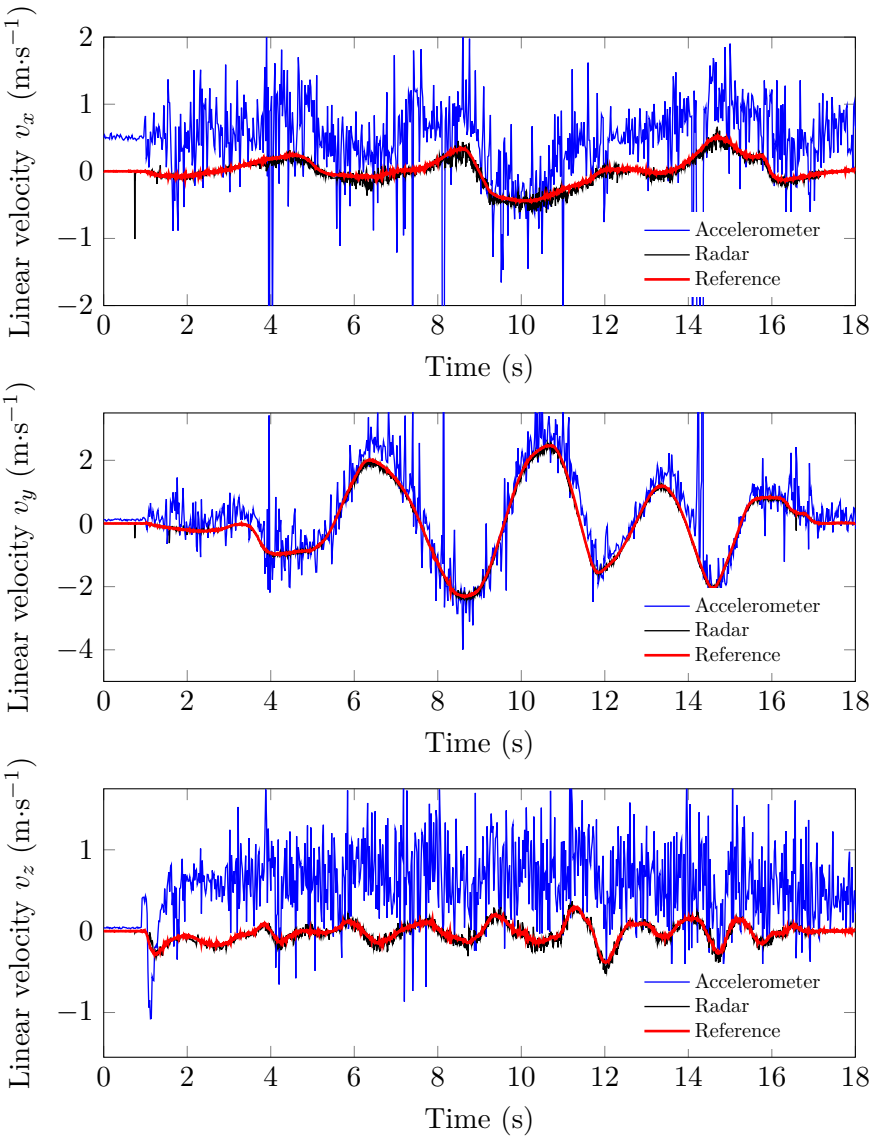

FIGURE D.1: Comparison of the linear velocities measured by the radar, the IMU, and the reference ones

Appendix E

Résumé étendu en français

E.1 Introduction

Dans ce mémoire, nous nous intéressons au problème de l'estimation de l'état d'un système.

Analytiquement, un système peut être décrit par un modèle, c'est-à-dire un ensemble d'équations et de paramètres décrivant le comportement interne du système ainsi que ses interactions avec son environnement. La classe de modèle que nous considérons est celle des représentations d'état, qui sont des modèles de la forme

$$\begin{aligned} x_{t+1} &= g(x_t, u_t, w_t) \\ y_t &= h(x_t, u_t, f_t), \end{aligned} \tag{E.1}$$

avec u_t les entrées connues du systèmes, w_t et f_t des entrées inconnues perturbant le système, y_t les sorties du système, g une fonction décrivant la dynamique du système et h décrivant le mécanisme de mesure. Dans cette structure, nous voyons que x_t joue un rôle central, faisant la connexion entre les entrées et les sorties du système tout en évoluant en accord avec la dynamique de ce dernier. x_t est ce que l'on appelle l'*état du système*, et il est propre à chaque représentation d'état.

Modéliser un système par une représentation d'état présente un grand intérêt du fait que ce type de modèle est au cœur de beaucoup de méthodes d'ingénierie, telles que le retour par contrôle d'état [AJ05], le suivi des systèmes [Sah09], la détection de faute [Man12] ou la poursuite de cible [Cha84]. Opérer efficacement un système requiert donc de connaître l'évolution du vecteur d'état afin de pouvoir utiliser ces méthodes.

Cependant, il n'est pas toujours possible de mesurer directement l'état d'un système, que ce soit par exemple parce qu'il n'existe pas de capteur adéquat ou encore que le nombre de capteurs nécessaire serait trop coûteux. Le problème de l'estimation d'état est donc de parvenir à reconstruire l'état du système sans le mesurer. Pour ce faire, on peut utiliser le modèle du système (connaissance *a priori*) et les sorties du systèmes (connaissance *a posteriori*. Cette reconstruction doit cependant se faire sans connaître les vraies valeurs des perturbations agissant dans le système.

Pour pouvoir concevoir un estimateur d'état de manière efficace, il est nécessaire de savoir de quel type sont les perturbations qui peuvent exister au sein du système considéré. Dans ce manuscrit, nous nous intéresserons principalement à l'estimation d'état en présence de *bruits impulsifs*, c'est-à-dire des bruits qui sont égaux à zéro la plupart du temps mais dont les occurrences non nulles peuvent prendre une amplitude arbitrairement grande. De tels bruits peuvent modéliser une grande variété

d'événements pouvant avoir lieu dans un système, tels que des défaillances capteurs ponctuels, des pertes de mesures momentanées, ou même le cas d'une attaque informatique où un attaquant détourne certaines mesures afin d'injecter des données aberrantes à l'entrée de l'estimateur.

Le problème que nous cherchons donc à résoudre est celui de l'estimation d'état en présence de bruits impulsifs. Notre but est donc de concevoir des estimateurs d'état capable de reconstruire l'état d'un système malgré la présence de tels bruits. Pour ce faire, nous allons étudier la *propriété de résilience* des estimateurs, qui caractérise la capacité d'un estimateur à être insensible à la présence d'une classe donnée de perturbations. Depuis dix ans, ce sujet de recherche suscite de plus en plus d'intérêt. Cet intérêt, relativement récent, peut s'expliquer par le développement, depuis le début des années 2000, des *systèmes cyber-physiques* qui sont des systèmes opérés par le biais de réseaux informatiques. Ce développement a même été encouragé par des programmes nationaux [Fou06] et internationaux [EC18].

Cependant, un problème majeur de ce type de système est leur vulnérabilité aux attaques informatiques [Inc17]. Si de telles attaques peuvent être partiellement endiguées par une meilleure sécurité informatique, il n'existe pas de risque zéro. Il est donc nécessaire de doter les systèmes cyber-physiques d'estimateurs pouvant gérer les attaques afin de protéger les infrastructures dont le contrôle se base sur l'estimation de l'état.

C'est ce contexte qui motive le travail présenté dans ce manuscrit. Son but est de concevoir des familles d'estimateurs d'état et d'analyser leurs propriétés de résilience afin d'apporter des garanties concernant leurs performances. Si ce travail est principalement théorique, une partie du présent document couvre également des aspects plus pratiques de l'estimation d'état résiliente, tels que la dérivation d'algorithmes récursifs, ou la présentation de plusieurs cas pratiques d'utilisation.

E.2 Rappels sur l'estimation d'état

E.2.1 Introduction

Avant d'aborder l'analyse des propriétés de résilience des estimateurs d'état par optimisation, il est nécessaire d'introduire quelques concepts clés sur lesquels les développements théoriques présentés dans ce manuscrit seront basés.

E.2.2 Le cadre de l'estimation d'état

Représentations d'état des systèmes

Un système décrit une portion de la réalité qui interagit avec son environnement par le biais de ses entrées et de ses sorties. La façon dont les entrées et les sorties interagissent dépend alors du fonctionnement interne du système que chaque modèle va représenter différemment. Pour cette étude, nous considèrerons uniquement les représentations d'état Linéaire Temps-Variantes (LTV) en temps discret, c'est-à-dire les modèles de la forme

$$\Sigma : \begin{cases} x_{t+1} &= A_t x_t + w_t \\ y_t &= C_t x_t + f_t \end{cases}, \tag{E.2}$$

avec $x_0 \in \mathbb{R}^n$ l'état initial du système.

Dans ces modèles, la variable (discrète) de temps t est un entier naturel. À tout instant $t \in \mathbb{N}$, les *variables d'entrée inconnues* $w_t \in \mathbb{R}^n$, $f_t \in \mathbb{R}^m$ et les *variables de sortie* (ou *mesures*) $y_t \in \mathbb{R}^m$ du modèle sont interconnectées à travers deux équations par le biais d'un ensemble de variables internes, les *états*, qui sont réunis dans le *vecteur d'état* $x_t \in \mathbb{R}^n$. La première équation, appelée l'*équation d'état* (ou *équation dynamique*), contient la dynamique du système et comment celle-ci évolue au cours du temps. La seconde, appelée *équation de sortie* (ou *équation de mesure*), modélise comment cette dynamique interne produit les sorties du système.

Les signaux $\{w_t\} \subset \mathbb{R}^n$ et $\{f_t\} \subset \mathbb{R}^m$ seront qualifiées de *perturbations*: ils représentent des quantités qui perturbent les deux équations du système, tels que du bruit de mesures ou des petites non-linéarités négligées par le modèle. Il est à noter qu'il est également très courant d'avoir des entrées connues dans le système, comme par exemple un signal de commande (voir Eq. (E.1)). Cependant, ces dernières n'induisent pas de difficulté particulière pour l'estimation d'état : pour des raisons de simplicité, les modèles considérés ne prennent donc pas en compte de telles entrées.

Les relations entre les variables x_t, y_t, w_t, f_t définies dans (E.2) sont *linéaires*. Plus précisément, elles sont liées par des matrices qui ne dépendent pas d'elles, notamment par la *matrice d'état* $A_t \in \mathbb{R}^{n\times n}$ et la *matrice de sortie* $C_t \in \mathbb{R}^{m\times n}$. Ces matrices peuvent varier au cours du temps, comme indiqué par la mention *Temps-variant*. Cependant, nous serons également amenés à considérer le cas temps-invariant, c'est-à-dire les représentations d'état de la forme

$$\Sigma : \begin{cases} x_{t+1} &= Ax_t + w_t \\ y_t &= Cx_t + f_t \end{cases}, \tag{E.3}$$

avec $x_0 \in \mathbb{R}^n$ l'état initial du système.

Le choix de considérer des représentations d'état en temps discret et de pouvoir facilement implémenter le processus d'estimation sur des puces électroniques du fait de l'omniprésence des outils numériques pour l'estimation d'état. Néanmoins, la plupart des systèmes d'ingénierie sont plus naturellement modélisés par des représentations d'état en temps continu. Ce problème peut être alors résolu en discrétisant les modèles en temps continu, ce qui peut être fait par de nombreuses méthodes telles que la méthode d'Euler ou la méthode par bloqueur d'ordre zéro [Mat].

Le problème de l'estimation d'état

Nous pouvons maintenant caractériser le problème de l'*estimation d'état*, qui consiste à estimer l'état interne du système modélisé par une représentation d'état. Le processus d'estimation de x_t doit s'effectuer uniquement grâce aux matrices du modèle A_t, C_t, aux mesures $\{y_t\}$, et sans la connaissance des valeurs des perturbations $\{w_t\}$ et $\{f_t\}$. Un *estimateur d'état* (ou *observateur*) est alors une méthode qui utilise toute la connaissance accessible afin d'obtenir une estimation du vecteur d'état (notée $\hat{x}_t$). Ce processus est résumé dans le diagramme par bloc présenté sur la Figure E.1.

Soit T un entier naturel désignant l'horizon de temps sur lequel on souhaite effectuer l'estimation d'état. Considérons les matrices $X_{T-1} \in \mathbb{R}^{n\times T}$, $\hat{X}_{T-1} \in \mathbb{R}^{n\times T}$ et $Y_{T-1} \in \mathbb{R}^{m\times T}$ définies par la concaténation respective des états, des états estimés et

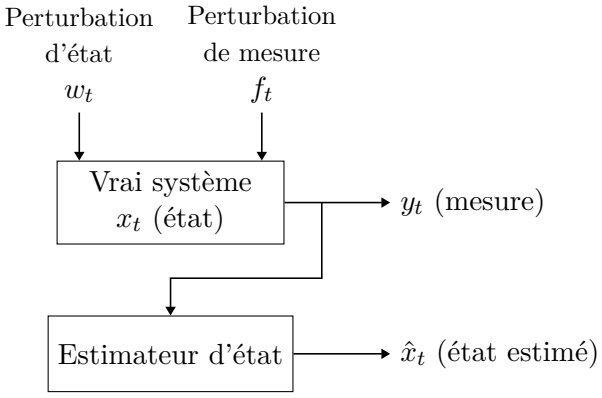

FIGURE E.1: Diagramme par bloc du principe de l'estimation d'état

des mesures entre $t = 0$ et $t = T - 1$, c'est-à-dire

$$X_{T-1} = \begin{pmatrix} x_0 & x_1 & \cdots & x_{T-1} \end{pmatrix}, \tag{E.4}$$

$$\hat{X}_{T-1} = \begin{pmatrix} \hat{x}_0 & \hat{x}_1 & \cdots & \hat{x}_{T-1} \end{pmatrix}, \tag{E.5}$$

$$Y_{T-1} = \begin{pmatrix} y_0 & y_1 & \cdots & y_{T-1} \end{pmatrix}. \tag{E.6}$$

X_{T-1} et $\hat{X}_{T-1}$ sont respectivement la *matrice de trajectoire d'état* et la *matrice de trajectoire d'état estimé*, tandis que Y_{T-1} est l'*historique des mesures*. Dans ce manuscrit, l'horizon de temps par défaut sera $T-1$ (pour que X_{T-1}, $\hat{X}_{T-1}$, et Y_{T-1} aient T colonnes). Par conséquent, lorsque l'indice de temps sera $T-1$, il sera souvent omis : ainsi, X, $\hat{X}$ et Y désignerons respectivement X_{T-1}, $\hat{X}_{T-1}$ et Y_{T-1}.

Estimer la trajectoire X sur l'horizon de temps $[0, T-1]$ dépend évidemment de la quantité de mesures accessible au moment de l'estimation. Par exemple, si l'on a accès aux mesures du système jusqu'à l'instant k, c'est-à-dire que nous avons accès à Y_k, pour estimer X_{T-1}, différentes valeurs de k entraînent différent scénarios d'estimation.

Pour exprimer ces nuances, l'horizon de mesure utilisé pour obtenir une estimation sera parfois indiqué via les notations $\hat{x}_{T-1|k}$ et $\hat{X}_{T-1|k}$, qui note que ces deux estimées ont été obtenues grâce à toutes les mesures du système jusqu'à l'instant k. Néanmoins, le présent document traite principalement le cas où l'horizon d'estimation et des mesures utilisées coïncident : $\hat{x}_t$ et $\hat{X}_T$ désigneront donc implicitement des estimées obtenues avec Y_t et Y_T respectivement.

Le concept d'observabilité

L'observabilité est un concept clé de l'estimation d'état. Il permet de savoir si un estimateur d'état sera capable de distinguer toutes les trajectoires d'état possibles d'un système. Pour les systèmes LTV qui nous intéressent, nous définissons la notion d'observabilité sur un horizon de temps donné :

Définition E.2.1 (Observabilité d'un système LTV sur un horizon de temps donné)**.** *Soit Σ un système de la forme (E.2) et $T \in \mathbb{N}_{\neq 0}$. Σ est observable sur l'horizon de temps $[0, T-1]$ si la matrice*

$$\mathcal{O}_{T-1} = \begin{pmatrix} C_0^\top & (C_1 A_0)^\top & \cdots & (C_{T-1} A_{T-2} \ldots A_0)^\top \end{pmatrix}^\top \in \mathbb{R}^{(mT)\times n} \tag{E.7}$$

est de rang colonne plein, c'est-à-dire de rang n.

Dans le cas des systèmes LTI, il est important de remarquer que pour tout $T > n$, l'observabilité d'un système sur $[0, T-1]$ peut être vérifiée de manière équivalente par l'étude la matrice $\mathcal{O}_{n-1}$:

Theorème E.2.1 (Condition d'observabilité pour les systèmes LTI [Oga06])**.** *Soit Σ un système LTI de la forme (E.3) et T un entier plus grand que n. Σ est alors observable sur $[0, T-1]$ si et seulement si la matrice*

$$\mathcal{O}_{n-1} = \begin{pmatrix} C^\top & (CA)^\top & \cdots & (CA^{n-1})^\top \end{pmatrix}^\top \tag{E.8}$$

est de rang colonne plein, c'est-à-dire de rang n.

Remarque E.2.1. *La matrice $\mathcal{O}_{n-1}$ dépend uniquement des matrics A et C. L'observabilité d'un système LTI peut donc être vue comme une propriété de la paire (A, C), et nous parlerons parfois de l'observabilité de la paire (A, C).*

Nous faisons également remarquer qu'il existe de nombreuses autres définitions de l'observabilité, qui peuvent être plus fortes, comme l'*observabilité complète uniforme* (voir [Bat17]), ou plus faibles, comme la notion de *détectabilité* (voir [Oga09, Sec. 9-7]), que celle présentée ici. Ces différentes notions confèrent logiquement différentes propriétés aux systèmes et par conséquent aux estimateurs d'état utilisés sur ces systèmes.

E.2.3 Le cadre de l'estimation d'état basée sur l'optimisation

La fonction de performance

Pour définir le cadre de l'estimation d'état basée sur l'optimisation, il est d'abord nécessaire de définir une mesure pouvant comparer quantitativement des trajectoires entre elles. Pour ce faire, nous définissons une fonction de performance qui va assigner une valeur réelle positive) à toutes les trajectoires hypothétiques que le système peut prendre.

Étant donné un système Σ de la forme (E.2),nous nous intéressons à l'estimation de la trajectoire sur un horizon de temps de taille $T-1$ avec l'aide de l'historique de mesure Y. La structure de la fonction de performance étudiée dans cette thèse est alors la suivante : pour tout $Z = \begin{pmatrix} z_0 & z_1 & \cdots & z_{T-1} \end{pmatrix}$ dans $\mathbb{R}^{n \times T}$,

$$V_{\Sigma,T-1}(Y, Z) = \chi(z_0 - \mu_0) + \sum_{t \in \mathbb{T}'} \phi_t(z_{t+1} - A_t z_t) + \sum_{t \in \mathbb{T}} \psi_t(y_t - C_t z_t) \tag{E.9}$$

avec $\mathbb{T} = \{0, 1, ..., T-1\}$, $\mathbb{T}' = \{0, ..., T-2\}$, $\mu_0 \in \mathbb{R}^n$, $\chi : \mathbb{R}^n \to \mathbb{R}_{\geq 0}$ une fonction et $\{\phi_t\}$, $\{\psi_t\}$ deux familles de fonctions de $\mathbb{R}^n$ vers $\mathbb{R}_{\geq 0}$ et $\mathbb{R}^m$ vers $\mathbb{R}_{\geq 0}$ respectivement. Comme précisé précédemment, $T-1$ est l'horizon de temps par défaut dans ce manuscrit, l'indice $T-1$ dans $V_{\Sigma,T-1}$ sera donc la plupart du temps omis, et V_Σ désignera $V_{\Sigma,T-1}$ par défaut.

Chaque terme de cette fonction de performance est destiné à évaluer à quel point la trajectoire hypothétique Z est plausible :

- $\chi(z_0 - \mu_0)$ évalue si l'état initial hypothétique z_0 est en accord avec une connaissance μ_0 *a priori* sur le vrai état initial .
- Les termes de la forme $\phi_t(z_{t+1} - A_t z_t)$ vérifient si la trajectoire hypothétique vérifie la dynamique du système. En effet, si elle vérifie l'équation dynamique (E.2),

alors pour tout t dans $\mathbb{T}'$, $z_{t+1} \approx A_t z_t + w_t$, ce qui implique que l'argument de chaque terme sera proche de w_t.

- Les termes de la forme $\psi_t(y_t - C_t z_t)$ vérifient si la trajectoire hypothétique permet d'expliquer les mesures obtenues à la sortie du vrai système. Si pour tout t dans $\mathbb{T}$, $C_t z_t \approx y_t - f_t$, alors la trajectoire Z produit des mesures proches des vraies, ce qui entraîne également que l'argument dans chaque terme sera proche de f_t.

Par conséquent, plus la trajectoire d'état hypothétique représentée par la matrice Z vérifie la dynamique du système et permet d'expliquer les mesures obtenues en sortie du système, plus $V_\Sigma(Y, Z)$ sera proche de $V_\Sigma(Y, X)$ avec X la vraie trajectoire d'état. Les fonctions coûts, c'est-à-dire la fonction χ et les membres des familles de fonctions $\{\phi_t\}$ et $\{\psi_t\}$, doivent être choisies afin que la valeur de $V_\Sigma(Y, X)$ soit petite par rapport aux autres.

A partir de cette structure de fonction de performance, nous sommes donc capables d'assigner une valeur à chaque trajectoire d'état potentielle afin de représenter sa vraisemblance. Le but de l'estimation optimale d'état est alors de sélectionner les trajectoires les plus vraisemblables au regard de la fonction de performance, c'est-à-dire les matrices Z qui minimisent V_Σ. Nous définissons un *estimateur optimal* Ψ comme étant l'application de $\mathbb{R}^{m\times T}$ vers $\mathcal{P}(\mathbb{R}^{n\times T})$ telle que pour tout $Y \in \mathbb{R}^{m\times T}$,

$$\Psi(Y) = \underset{Z\in\mathbb{R}^{n\times T}}{\arg\min}\, V_\Sigma(Y, Z) \tag{E.10}$$

Si les fonctions coûts sont bien définies, alors $V_\Sigma(Y, X)$ sera petit, ce qui entraîne que minimiser $V_\Sigma(Y, Z)$ par rapport à Z fournira des trajectoires d'état estimées proches de la vraie.

The Forward Dynamic Programming (FDP) framework

Le *Forward Dynamic Programming* (FDP) est un cadre qui propose une solution systématique mais théorique afin de passer d'un estimateur optimal par paquet – où l'estimation s'effectue sur tout un horizon de temps – à un estimateur optimal récursif – où l'état estimé à un instant t est calculé à partir de l'état estimé à l'instant précédent. Le but est donc d'obtenir $\hat{x}_T$, le dernier état de la trajectoire estimée $\hat{X}_T$ qui serait obtenue par la minimisation de la fonction de performance $V_{\Sigma,T}$.

Proposé dans les années 50 par Richard Bellman [Bel54], le FDP consiste à subdiviser un problème d'optimisation en plusieurs petit problèmes d'optimisation de complexité moindre.

Soit $V_{\Sigma,T} : \mathbb{R}^{m\times(T+1)} \times \mathbb{R}^{n\times(T+1)} \to \mathbb{R}_{\geq 0}$ une fonction de performance, nous définissons alors la *fonction de performance optimale* comme étant la fonction $V^\star_{\Sigma,T} : \mathbb{R}^{m\times(T+1)} \times \mathbb{R}^n \to \mathbb{R}_{\geq 0}$ telle que

$$V^\star_{\Sigma,T}(Y_T, z) = \min_{Z_T\in\mathbb{R}^{n\times(T+1)}} \{V_{\Sigma,T}(Y_T, Z_T) \ : \ z_T = z\}. \tag{E.11}$$

Pour un $Y_T \in \mathbb{R}^{m\times(T+1)}$ donné, $V^\star_{\Sigma,T}(Y_T, z)$ est la plus petite valeur de $V_{\Sigma,T}(Y_T, Z_T)$ qui peut être obtenue par une trajectoire hypothétique Z dont la dernière colonne est égale à z. Cela signifie que z est l'état à l'instant $t = T$ de cette trajectoire hypothétique. Autrement dit, la valeur $V^\star_{\Sigma,T}(Y_T, z)$ représente à quel point il est vraisemblable que le vecteur z soit l'état estimé à l'instant T au regard de $V_{\Sigma,T}$.

Pour mieux comprendre cette idée, il est possible d'interchanger l'ordre de minimisation dans la définition de la fonction $V^\star_{\Sigma,T}$ (voir [Roc98, Prop 1.35]), ce qui donne

$$\min_{z\in\mathbb{R}^n} V^\star_{\Sigma,T}(Y_T,z) = \min_{z\in\mathbb{R}^n}\left\{\min_{\substack{Z_T\in\mathbb{R}^{n\times T}\\ z_T=z}} V_{\Sigma,T}(Y_T,Z_T)\right\} = \min_{Z_T\in\mathbb{R}^{n\times T}} V_{\Sigma,T}(Y_T,Z_T). \quad \text{(E.12)}$$

La fonction de performance et la fonction de performance optimale partagent le même minimum, et les vecteurs minimisant $V^\star_{\Sigma,T}$ sont nécessairement les dernières colonnes des matrices minimisant $V_{\Sigma,T}$. Ainsi, les derniers états estimés $\hat{x}_T$ des trajectoires estimées $\hat{X}_T$ peuvent être théoriquement obtenus par la minimisation de $V^\star_{\Sigma,T}(Y_T,z)$, *i.e.*

$$\hat{x}_T \in \arg\min_{z\in\mathbb{R}^n} V^\star_{\Sigma,T}(Y_T,z). \quad \text{(E.13)}$$

Un des avantages du FDP, dans le cas où $V_{\Sigma,T}$ est de la forme (E.9), est le fait que la relation entre $V^\star_{\Sigma,T+1}$ et $V^\star_{\Sigma,T}$ peut être exprimée à travers ce que l'on appelle l'*équation de Bellman*:

Theorème E.2.2 (Equation de Bellman)**.** *Soit $V_{\Sigma,T}$ une fonction de performance définie par (E.9) et $V^\star_{\Sigma,T}$ la fonction de performance optimale associée à $V_{\Sigma,T}$ définie par (E.11). Pour tout $T\in\mathbb{N}_{\neq 0}$ et tout z dans $\mathbb{R}^n$, on a alors*

$$V^\star_{\Sigma,T}(Y_T,z) = \min_{s\in\mathbb{R}^n}\left\{V^\star_{\Sigma,T-1}(Y_{T-1},s) + \phi_{T-1}(z-A_{T-1}s)\right\} + \psi_T(y_T - C_T z), \quad \text{(E.14)}$$

avec $Y_T = \begin{pmatrix} Y_{T-1} & y_T \end{pmatrix}$ *($Y_{T-1}\in\mathbb{R}^{m\times T}$ et $y_T\in\mathbb{R}^m$).*

Même si T devient grand, il est théoriquement possible, grâce à l'équation de Bellman, d'obtenir la valeur de $V^\star_{\Sigma,T}(Y_T,z)$ sans avoir à résoudre le problème d'optimisation à $(n-1)T$ inconnues qui compose $V^\star_{\Sigma,T}$ tel que défini dans (E.11). Supposant que nous avons accès à la valeur de $V^\star_{\Sigma,T-1}(Y_{T-1},s)$ pour chaque $s\in\mathbb{R}^n$, obtenir la valeur $V^\star_{\Sigma,T}(Y_T,z)$ ne requerrait que la résolution d'un problème d'optimisation à n inconnues.

Cependant, le problème principale réside dans le fait de connaître $V^\star_{\Sigma,T-1}(Y_{T-1},s)$ pour tout $s\in\mathbb{R}^n$ sans résoudre le problème d'optimisation sous-jacent. En pratique, pour calculer $\hat{x}_t$, nous avons besoin d'une expression algébrique de $V^\star_{\Sigma,T}(Y_T,z)$, ce que l'équation de Bellman permet de construire récursivement. Le Théorème E.2.3 présente une façon de dériver l'implémentation récursive d'un estimateur des moindres carrés:

Theorème E.2.3 (Implémentation récursive d'un estimateur des moindres carrés par FDP)**.** *Soit Σ un système défini par (E.2), $T\in\mathbb{N}$ et $V_{\Sigma,T}$ une fonction de performance définie telle que pour tout (Y,Z) dans $\mathbb{R}^{m\times T}\times\mathbb{R}^{n\times T}$,*

$$V_\Sigma(Y,Z) = \frac{1}{2}\|z_0-\mu_0\|^2_{S^{-1}} + \frac{1}{2}\sum_{t\in\mathbb{T}'}\|z_{t+1}-A_t z_t\|^2_{Q_t^{-1}} + \frac{1}{2}\sum_{t\in\mathbb{T}\setminus\{0\}}\|y_t - C_t z_t\|^2_{R_t^{-1}}. \quad \text{(E.15)}$$

(i) Le coût optimal $V^\star_{\Sigma,T}$, défini par (E.11),est tel que pour tout z dans $\mathbb{R}^n$,

$$V^\star_{\Sigma,T}(Y_T,z) = \frac{1}{2}(z-\hat{x}_T)^\top P_T^{-1}(z-\hat{x}_T) + r_T \quad \text{(E.16)}$$

avec r_T une quantité connue qui ne dépend pas de z, $\hat{x}_T \in \mathbb{R}^n$ et $P_T \in \mathbb{R}^{n\times n}$ sont construits récursivement de telle sorte que $\hat{x}_0 = \mu_0$, $P_0 = S$, et

$$\hat{x}_T = A_{T-1}\hat{x}_{T-1} + P_T C_T^\top R_T^{-1}(y_T - C_T A_{T-1}\hat{x}_{T-1}) \tag{E.17}$$

$$P_T = \left((Q_{T-1} + A_{T-1}P_{T-1}A_{T-1}^\top)^{-1} + C_T^\top R_T^{-1} C_T\right)^{-1} \tag{E.18}$$

(ii) $\hat{x}_T$ est l'unique solution de (E.13), ce qui signifie que $\hat{x}_T$ est l'état estimé à l'instant T.

Les formules (E.17)–(E.18) construisant récursivement $\hat{x}$ et P_T ont le désavantage de présenter beaucoup d'inversions de matrice, qui demandent beaucoup de ressources lorsqu'on les implémente. Ces formules peuvent cependant être reformulées [Rei01, Eq. (22)–(24)], donnant l'Algorithme E.1.

Algorithme E.1 Implémentation récursive de l'estimateur des moindres carrés

Entrées: $\{A_T\}$, $\{C_T\}$, $\mu_0 \in \mathbb{R}^n$, $S \in \mathbb{R}^n$, $\{Q_T\}$, $\{R_T\}$, $T_{\max} \in \mathbb{N}$, $Y \in \mathbb{R}^{m\times T_{\max}}$
Initialisation:
$T \leftarrow 1$
$\hat{x}_0 \leftarrow \mu_0$
$P_0 \leftarrow S$
Fin de l'initialisation.
tant que $T < T_{\max}$
$\hat{x}_{T|T-1} \leftarrow A_{T-1}\hat{x}_{T-1}$
$P_{T|T-1} \leftarrow A_{T-1}P_{T-1}A_{T-1}^\top + Q_{T-1}$
$L_T \leftarrow P_{T|T-1}C_T^\top \left(C_T P_{T|T-1} C_T^\top + R_T\right)^{-1}$
$\hat{x}_T \leftarrow \hat{x}_{T|T-1} + L_T(y_T - C_T\hat{x}_{T|T-1})$
$P_T \leftarrow (I_n - L_T C_T)P_{T|T-1}$
$T \leftarrow T + 1$
fin tant que

L'algorithme E.1 est communément appelé un *filtre de Kalman*. Cet estimateur d'état a été initialement développé dans le cadre stochastique (voir [Kal60]). Dans un tel cadre, les signaux présents (x_t, y_t, w_t, f_t) sont supposés aléatoires, et l'estimateur est défini à travers la minimisation de la trace de la matrice de covariance de l'erreur d'estimation. Quand $\{w_t\}$ et $\{f_t\}$ sont des bruits blancs, indépendants entre eux et avec l'état initial du système, le filtre de Kalman est en effet l'estimateur qui produit l'estimée dont la matrice de covariance de l'erreur a la plus petite trace.

La méthode utilisée ici pour dériver l'Algorithme E.1 repose uniquement sur un cadre déterministe. Toutefois, nous pouvons constater que les matrices P_T définies dans (E.18) correspondent aux matrices de covariance de l'erreur d'estimation $e_T = \hat{x}_T - x_T$ dans le cadre stochastique. Par abus de langage, P_T sera parfois désigné comme la matrice de covariance de l'erreur d'estimation, même hors de toute considération stochastique. Même dans le cadre déterministe, P_T reste une image de l'amplitude de l'erreur d'estimation.

Introduction à l'estimation résiliente

La plupart des estimateurs d'état classiques sont conçus pour gérer des bruits relativement faibles qui ont lieu à tout instant. Cependant, ils présentent de bien moins bon résultats en présence d'autres bruits, tels que les bruits impulsifs, qui sont nuls la

plupart du temps mais peuvent prendre une amplitude arbitrairement grande quand ils ne le sont pas. Nous nous intéressons donc à des estimateurs qui seraient robustes à ces perturbations.

Perturbations arbitraires et le concept de résilience

Avant toute chose, nous devons spécifier les caractéristiques des perturbations dorénavant prises prises en compte. D'un point de vue physique, nous pouvons séparer les perturbations en deux grandes familles selon leur fréquence d'occurrence :

- Premièrement, nous considèrerons les **bruits denses**, qui ont lieu à chaque instant au sein du système. C'est le type de perturbation le plus classique et qui englobe de nombreux bruits tels que le bruit de capteur.
- Deuxièmement, il y a les **bruits creux**, aussi appelés *bruits impulsifs*, qui sont intermittents et n'ont pas lieu à tout instant dans le système. Ils modélisent une grande variété de perturbations qui modifient grandement le comportement du système lorsqu'ils sont non nuls. Ces derniers ne sont pas pris en compte par les estimateurs classiques, et notamment l'estimateur des moindres carrés.

Les bruits creux sont principalement la conséquence d'attaques ou de défaillances dans le système. Les défaillances sont la plupart du temps dues à un composant du système qui est soit cassé soit sur le point de casser : par exemple, un capteur défaillant peut produire du bruit creux dans la mesure, tandis qu'un actionneur défaillant peut amener du bruit creux dans l'équation d'état du système. Les attaques sont des actions entreprises par une personne extérieure au système afin de l'endommager sciemment ou de camoufler l'état.

Pouvoir estimer l'état d'un système dans de telles circonstances est essentiel, et ce pour plusieurs raisons :

- Dans le cas où le bruit creux est une contrainte du système et non pas la conséquence d'une défaillance ou d'une attaque, il reste nécessaire de fournir des moyens d'estimation d'état efficaces.
- Dans le cas où le bruit creux est induit par une défaillance, parvenir à estimer l'état permettrait de détecter plus facilement cette défaillance. Par exemple, cela peut permettre de détecter quel capteur est fautif pour pouvoir le remplacer.
- De nombreux processus vitaux pour le système, comme son contrôle, reposent sur l'estimation d'état. Par conséquent, si l'estimation commence à diverger, il y a un risque que ces processus divergent également, ce qui peut entraîner des dégâts sur le système.

Dans le contexte des systèmes LTV en temps discret (E.2), nous présentons maintenant les *bruits arbitraires*, qui peuvent présenter à la fois un comportement dense et un comportement creux. Pour simplifier, seul la perturbation de mesure $\{f_t\}$ sera considérée arbitraire sauf mention contraire.

Nous restreindrons les hypothèses entourant les bruits arbitraires au maximum. En particulier, il n'y aura pas d'hypothèse concernant la distribution de probabilité de ses valeurs. Néanmoins, des outils d'analyse seront utilisés afin de décrire les comportement du bruit arbitraire $\{f_t\}$: ces outils seront notamment les ensembles de la forme

$$\mathbb{T}_\varepsilon = \{t \in \mathbb{T} : \gamma_t(f_t) \leq \varepsilon\},$$

$$\mathbb{T}_\varepsilon^c = \mathbb{T} \setminus \mathbb{T}_\varepsilon = \{t \in \mathbb{T} : \gamma_t(f_t) > \varepsilon\},$$

où γ_t est une fonction de $\mathbb{R}^m$ vers $\mathbb{R}_{\geq 0}$, $\mathbb{T} = \{0, 1, ..., T-1\}$ et $\varepsilon > 0$ un paramètre d'analyse. γ_t sert à mesurer l'amplitude de f_t et les intervalles $\mathbb{T}_\varepsilon$ et $\mathbb{T}_\varepsilon^c$ partitionnent les indices de temps t en deux groupes selon si l'amplitude de f_t est plus petite ou plus grande que ε.

La décomposition obtenue par la définition des ensembles $\mathbb{T}_\varepsilon$ et $\mathbb{T}_\varepsilon^c$ sépare alors les occurrences de f_t en deux catégories : celles qui sont raisonnables au regard de ε, et les *valeurs aberrantes*. Cependant, il est important de comprendre que ε n'est pas une supposition de borne sur le bruit arbitraire $\{f_t\}$, mais est totalement libre, fournissant une multitude de décompositions de f possibles (voir Figure E.2 pour un exemple de comment différentes valeurs de ε entraînent différentes décompositions selon $\mathbb{T}_\varepsilon$ et $\mathbb{T}_\varepsilon^c$ lorsqu'il y a une sortie ($m = 1$) et $\gamma_t = |\cdot|$).

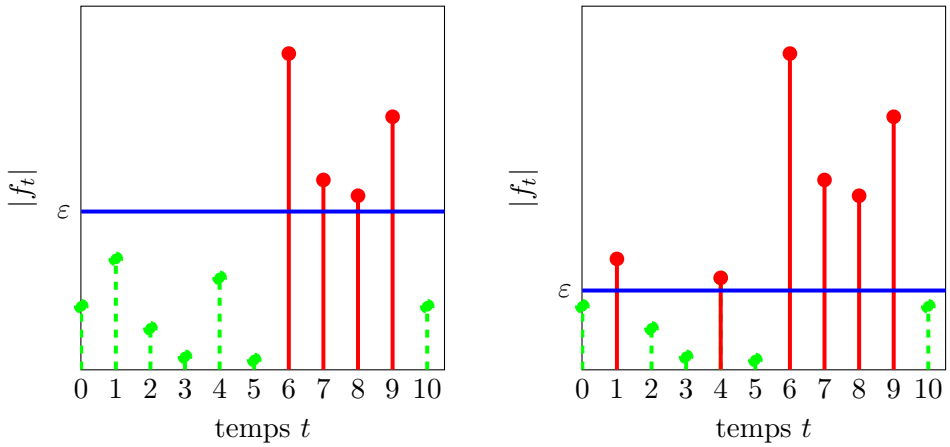

FIGURE E.2: Exemples de décomposition de $\{f_t\}$ ($\mathbb{T}_\varepsilon$ regroupe les indices de temps pour lesquels f_t est en pointillés verts, $\mathbb{T}_\varepsilon^c$ regroupe ceux pour lesquels f_t est en rouge) pour différentes valeurs de ε

Tout bruit peut être décomposé de sorte que

$$f_t = v_t + s_t \tag{E.19}$$

avec $\{v_t\}$ un bruit borné et $\{s_t\}$ un bruit *creux*. Lorsqu'on supposera explicitement une telle décomposition (*e.g.* lorsqu'on veut simuler f_t), v_t sera souvent désigné comme la *composante dense* de f_t, tandis que s_t sera appelé la *composante creuse* de f_t.

Le concept de *résilience*. Dans cette thèse, nous utiliserons le terme de *résilience* pour décrire une propriété de robustesse spécifique. Ainsi, nous dirons qu'un estimateur d'état est résilient à une classe donnée de perturbations $\mathcal{F}$ s'il produit une erreur d'estimation nulle lorsque $\{f_t\}$ appartient à cette classe de perturbations.

Nous utiliserons aussi la notion affaiblie de *résilience approximative*, qui caractérise un estimateur d'état produisant une erreur d'estimation bornée lorsque $\{f_t\}$ appartient à une certaine classe de perturbations $\mathcal{F}$.

E.2.4 Le problème de l'estimation d'état résiliente

Dans ce document, nous nous intéresserons à la conception et à l'analyse d'estimateurs d'états optimaux pouvant reconstruire la trajectoire d'état d'un système sur un horizon de temps donné $[0, T]$, et ce malgré la présence de bruits arbitraires. Plus exactement, si l'on reprend les équations d'un système LTV en temps-discret E.2, le bruit d'état w_t sera considéré dense tandis que le bruit de mesure f_t sera considéré comme une perturbation arbitraire. Dans cette configuration, nous tâcherons de vérifier si les estimateurs possèdent la propriété de résilience (ou de résilience approchée) par rapport aux bruits arbitraires, c'est-à-dire que ce type de perturbation a une influence nulle (ou bornée) sur leur erreur d'estimation.

En se basant sur une étude bibliographique du domaine de l'estimation d'état résiliente, nous avons défini deux familles d'estimateurs d'état optimaux à étudier. Les éléments de ces deux familles seront définis comme la minimisation d'un type particulier de fonction de performance V_Σ. Cependant, ces fonctions ne seront pas définies par une expression algébrique précise, mais par un ensemble de propriétés que ces dernières doivent vérifier, couvrant ainsi un large ensemble d'estimateurs d'état.

E.3 Estimateurs résilients optimaux basés sur des fonctions coûts non saturées

La première famille d'estimateurs d'état optimaux proposée pour répondre au problème d'estimation d'état résiliente présenté Section E.2.4 est une famille basée sur des fonctions de performance dont les propriétés sont similaires à celles de normes. Après avoir défini et discuté de ces propriétés, nous présenterons quelques-uns des résultats que nous avons obtenus sur cette famille ainsi que quelques résultats numériques.

E.3.1 Définition de la classe d'estimateurs étudiée

Pour définir formellement la famille d'estimateurs proposée, nous introduirons d'abord la fonction de performance qu'il faudra minimiser. Étant données les matrices $\{(A_t, C_t)\}$ du système et T mesures $Y = (\, y_0 \quad \cdots \quad y_{T-1} \,)$, nous définissons la fonction de performance $V_\Sigma : \mathbb{R}^{m\times T} \times \mathbb{R}^{n\times T} \to \mathbb{R}_{\geq 0}$ telle que

$$V_\Sigma(Y, Z) = \lambda \sum_{t\in\mathbb{T}'} \phi_t(z_{t+1} - A_t z_t) + \sum_{t\in\mathbb{T}} \psi_t(y_t - C_t z_t) \tag{E.20}$$

où $Z = (\, z_0 \quad \cdots \quad z_{T-1} \,) \in \mathbb{R}^{n\times T}$ est une trajectoire d'état potentielle, z_i représentant la i-ème colonne de Z; $\lambda > 0$ est un paramètre défini par l'utilisateur et visant à équilibrer la contribution des deux sommes présentes dans l'expression de $V_\Sigma(Y, Z)$. $\{\phi_t\}$ et $\{\psi_t\}$ sont deux familles de fonctions positives (les fonctions coût) définies sur $\mathbb{R}^n$ et $\mathbb{R}^m$ respectivement. Pour des raisons de simplicité, nous supposerons que pour tout t dans $\mathbb{T}$, ϕ_t et ψ_t s'expriment sous la forme

$$\phi_t(z) = \phi(W_t z) \quad \forall z \in \mathbb{R}^n \tag{E.21}$$

$$\psi_t(z) = \psi(V_t z) \quad \forall z \in \mathbb{R}^m, \tag{E.22}$$

où $\phi : \mathbb{R}^n \to \mathbb{R}_{\geq 0}$ et $\psi : \mathbb{R}^m \to \mathbb{R}_{\geq 0}$ sont deux fonctions coût temps-invariantes, et $\{W_t\}$, $\{V_t\}$ sont deux familles de matrices de pondération *non-singulières* de taille appropriée.

Nous définissons à présent formellement la classe d'estimateurs considérée :

Définition E.3.1. *Soit Σ un système de la forme (E.2) et étant donnée une matrice de mesure $Y \in \mathbb{R}^{m\times T}$. Nous définissons un estimateur d'état issu de la classe étudiée comme la fonction multivaluée $\mathcal{E} : \mathbb{R}^{m\times T} \to \mathcal{P}(\mathbb{R}^{n\times T})$ telle que*

$$\mathcal{E}(Y) = \underset{Z\in\mathbb{R}^{n\times T}}{\arg\min}\, V_\Sigma(Y, Z) \tag{E.23}$$

où V_Σ est une fonction de la forme (E.20).

Ainsi défini, un estimateur $\mathcal{E}$ est bien-défini si pour tout Y fixé, $V_\Sigma(Y, Z)$ admet un ensemble minimisant non vide, c'est-à-dire qu'il existe au moins un $Z^\star$ tel que $V_\Sigma(Y, Z) \geq V_\Sigma(Y, Z^\star)$ pour tout $Z \in \mathbb{R}^{n\times T}$. Pour s'assurer que les estimateurs sont tous bien-définis, nous allons avoir besoin de supposer que les systèmes utilisés vérifient une propriété d'observabilité. Nous requerrons également que certaines propriétés soient vérifiées par les fonctions coûts ϕ et ψ intervenant dans la fonction de performance V_Σ.

E.3.2 Estimateur bien-défini : propriétés de base des fonctions coûts

Nous commençons par établir les propriétés devant être vérifiées par les fonctions coût. Ainsi, une fonction coût $\xi : \mathbb{R}^{a\times b} \to \mathbb{R}_{\geq 0}$ pourra être vérifier une ou plusieurs des propriétés suivantes

(P3.1) **Définie positivité:** $\xi(0) = 0$ et $\xi(Z) > 0$ pour tout $Z \neq 0$

(P3.2) **Continuité:** ξ est continue

(P3.3) **Symétrie:** $\xi(-Z) = \xi(Z)$ pour tout $Z \in \mathbb{R}^{a\times b}$

(P3.4) **Homogénéité généralisée (HG):** Il existe une fonction $\mathcal{K}_\infty$ $q : \mathbb{R}_{\geq 0} \to \mathbb{R}_{\geq 0}$ telle que pour tout $\lambda \in \mathbb{R}$ non nul et pour tout $Z \in \mathbb{R}^{a\times b}$,

$$\xi(Z) \geq q\left(\frac{1}{|\lambda|}\right)\xi(\lambda Z). \tag{E.24}$$

(P3.5) **Inégalité Triangulaire Généralisée (ITG):** Il existe un nombre strictement positif γ_ξ tel que pour tout Z_1, Z_2 dans $\mathbb{R}^{a\times b}$

$$\xi(Z_1 - Z_2) \geq \gamma_\xi \xi(Z_1) - \xi(Z_2). \tag{E.25}$$

Remarque E.3.1. *En vertu de (E.21)-(E.22), les familles $\{\phi_t\}$ et $\{\psi_t\}$ vérifient (P3.1)–(P3.5) si ϕ et ψ vérifient les mêmes propriétés.*

Le lemme suivant, présenté et démontré dans [Kir20b], est une des propriétés fondamentale des fonctions coût. Ainsi, toute fonction coût vérifiant (P3.1)–(P3.2) et (P3.4) peut être bornée inférieurement par une image de la norme de son argument, ce qui justifie la définition des propriétés ci-dessus:

Lemme E.3.1 (Borne inférieure d'une fonction coût)**.** *Soit $\xi : \mathbb{R}^{a\times b} \to \mathbb{R}_{\geq 0}$ une fonction coût vérifiant (P3.1)–(P3.2) et (P3.4) avec une fonction $\mathcal{K}_\infty$ q donnée. Pour toute norme $\|\cdot\|$ de $\mathbb{R}^{a\times b}$, nous avons alors*

$$\xi(Z) \geq Dq(\|Z\|) \quad \forall Z \in \mathbb{R}^{a\times b} \tag{E.26}$$

où

$$D = \min_{\|Z\|=1} \xi(Z) > 0. \tag{E.27}$$

Ces propriétés permettent également d'assurer la bonne définition des estimateurs :

Proposition E.3.1 (Bonne-définition de l'estimateur)**.** *Soient ϕ et ψ définies dans* (E.21)-(E.22) *et satisfaisant (P3.1)–(P3.5).*

Si le système LTV (E.2) *est observable sur l'horizon de temps* $[0, T-1]$ *(voir Définition E.2.1),alors l'estimateur* (E.23) *est bien-défini, c'est-à-dire que la fonction de performance* $V_\Sigma(Y, \cdot)$ *atteint son minimum pour tout* Y *fixé.*

Les conditions présentes dans la proposition ci-dessus permettent ainsi de s'assurer que $\mathcal{E}(Y)$ est non vide pour tout $Y \in \mathbb{R}^{m\times T}$.

E.3.3 La propriété de résilience de la classe d'estimateurs proposée

Nous allons maintenant montrer que les estimateurs définis dans (E.23) présentent la propriété de résilience s'ils vérifient certaines conditions.

Définition formelle de la résilience

Nous commençons par donner une définition formelle de la résilience pour un estimateur d'état de la forme (E.23). Pour cela, $Y^\star = \begin{pmatrix} y_0^\star & \dots & y_{T-1}^\star \end{pmatrix}$ désigne la sortie idéale de(E.2), c'est-à-dire la sortie définie par $y_t^\star = C_t x_t^\star$, $t \in \mathbb{T}$, avec $x_{t+1}^\star = A_t x_t^\star$ et $x_0^\star = x_0$ (x_0 étant le vrai état initial de (E.2)).$\mathcal{F}_r$ désigne quant à lui un ensemble de matrices de perturbations potentielles, ce qui se correspond formellement à un sous-ensemble de $\mathbb{R}^{m\times T}$ contenant 0.

Définition E.3.2 (Résilience d'un estimateur)**.** *L'estimateur $\mathcal{E}$ défini par* (E.23) *est dit résilient par rapport à l'ensemble de perturbations de mesure $\mathcal{F}_r$ s'il existe une fonction $\mathcal{K}_\infty$ g telle que, lorsque le bruit d'état $\{w_t\}$ est nul, l'inégalité suivante est vérifiée pour toute matrice $F \in \mathbb{R}^{n_y\times T}$:*

$$\|\hat{X} - X\| \leq g\big(\inf_{\Omega\in\mathcal{F}_r} d(F-\Omega)\big) \quad \forall \hat{X} \in \mathcal{E}(Y^\star + F) \tag{E.28}$$

avec $\|\cdot\|$ désignant une norme quelconque, $d : \mathbb{R}^{m\times T} \to \mathbb{R}_{\geq 0}$ étant une fonction vérifiant (P3.1)-(P3.5), et $Y^\star = \begin{pmatrix} y_0^\star & \dots & y_{T-1}^\star \end{pmatrix}$ désignant la matrice de mesure idéale définie par $y_t^\star = C_t x_t^\star$, $t \in \mathbb{T}$, et $x_{t+1}^\star = A_t x_t^\star$, $x_0^\star = x_0$.

Ainsi, $\inf_{\Omega\in\mathcal{F}_r} d(F-\Omega)$ *désigne une pseudo distance de F par rapport à l'ensemble $\mathcal{F}_r$.*

Une conséquence clé de la condition (E.28) est que l'erreur d'estimation associée à un estimateur résilient est complètement insensible à toute matrice de bruit de mesure F appartenant à $\mathcal{F}_r$. En d'autres mots, $\mathcal{E}(Y^\star + F) = \{X\}$ pour toute perturbation de de mesure $F \in \mathcal{F}_r$.

Dans ce document, nous nous intéressons à une classe de perturbation $\mathcal{F}_r$ bien particulière. En effet, si l'on note $F = \begin{pmatrix} f_0 & \cdots & f_{T-1} \end{pmatrix} \in \mathbb{R}^{m\times T}$, $\mathbb{T}_0^c(F) = \{t \in \mathbb{T} : \psi_t(f_t) > 0\}$ et $\mathbb{T}_0(F) = \{t \in \mathbb{T} : \psi_t(f_t) = 0\}$, alors pour tout r entier strictement positif, $\mathcal{F}_r$ désignera l'ensemble des matrices de $\mathbb{R}^{m\times T}$ qui ont au plus r colonnes non nulles, c'est-à-dire

$$\mathcal{F}_r = \{F : |\mathbb{T}_0^c(F)| \leq r\}\,. \tag{E.29}$$

Afin de démontrer la propriété de résilience plus explicitement, nous aurons parfois besoin du lemme suivant qui s'applique uniquement à la classe de perturbations définie ci-dessus :

Lemme E.3.2. *Considérons l'ensemble de perturbations de mesure $\mathcal{F}_r$ défini par (E.29) et définissons la fonction/pseudo-distance $d : \mathbb{R}^{m\times T} \to \mathbb{R}_{\geq 0}$ telle que pour tout F dans $\mathcal{F}_r$, $d(F) = \sum_{t\in\mathbb{T}} \psi_t(f_t)$ avec ψ_t une fonction définie selon (E.22) et vérifiant (P3.1)-(P3.5). Ainsi, $\inf_{\Omega\in\mathcal{F}_r} d(F-\Omega)$ est égal à la somme des $T-r$ plus petits éléments de $\{\psi_t(f_t) : t \in \mathbb{T}\}$.*

La *résilience approchée* d'un estimateur $\mathcal{E}$ peut également être définie d'une manière similaire. En effet, si l'on reprend la Définition E.3.2, définir la résilience approchée revient à remplacer la droite de l'inégalité (E.28) par $g\big(\inf_{\Omega\in\mathcal{F}_r} d(F-\Omega)+\delta\big)$ avec δ un réel positif.

Notations pour l'analyse

Nous introduisons maintenant quelques notations supplémentaires pour simplifier l'écriture des résultats à venir.

Soit $\Phi : \mathbb{R}^{n\times T} \to \mathbb{R}_{\geq 0}$ et $\Psi_{\mathbb{T}} : \mathbb{R}^{n\times T} \to \mathbb{R}_{\geq 0}$ définis par

$$\Phi(Z) = \sum_{t\in\mathbb{T}'} \phi_t(z_{t+1} - A_t z_t) \tag{E.30}$$

$$\Psi_{\mathbb{T}}(Z) = \sum_{t\in\mathbb{T}} \psi_t(C_t z_t) \tag{E.31}$$

Nous définissons également la fonction de performance partielle $\Psi_{\mathcal{T}}$ telle que pour tout $\mathcal{T} \subset \mathbb{T}$, $\Psi_{\mathcal{T}}(Z) = \sum_{t\in\mathcal{T}} \psi_t(C_t z_t)$. Nous supposerons également que ϕ et ψ satisfont le sous-ensemble de propriétés (P3.1)–(P3.5). En outre, lorsqu'elles devront également satisfaire l'ITG (P3.5), nous noterons respectivement γ_ϕ et γ_ψ les constantes strictement positives associées.

Enfin, nous posons

$$H_\Sigma(Z) = \lambda\gamma_\phi \Phi(Z) + \gamma_\psi \Psi_{\mathbb{T}}(Z). \tag{E.32}$$

Preuve de résilience

Tout d'abord, il est nécessaire de présenter le concept d'indice de r-Résilience d'un estimateur de la forme (E.23). C'est une quantité qui va dépendre des matrices du système, de la structure de la fonction de performance V_Σ et des fonctions coût ϕ et ψ.

Définition E.3.3. *Soit r un entier positif. Supposons que le système Σ de la forme (E.2) est observable sur $[0, T-1]$. Nous définissons alors l'indice de r-Résilience de l'estimateur $\mathcal{E}$ défini par (E.23) (et appliqué à Σ) comme le nombre réel p_r tel que*

$$p_r = \sup_{\substack{Z\in\mathbb{R}^{n\times T}\\ Z\neq 0}} \sup_{\substack{\mathcal{T}\subset\mathbb{T}\\ |\mathcal{T}|=r}} \frac{\Psi_{\mathcal{T}}(Z)}{H_\Sigma(Z)} \tag{E.33}$$

avec H_Σ défini dans (E.32). Le supremum est considéré sur l'ensemble des matrices non nulles Z de $\mathbb{R}^{n\times T}$ et sur tous les sous-ensemble $\mathcal{T}$ de $\mathbb{T}$ qui ont une cardinalité égale à r.

p_r peut être interpreté comme une mesure quantitative de l'observabilité du système Σ. L'observabilité est par ailleurs nécessaire ici afin que le dénominateur $H_\Sigma(Z)$ de (E.33) soit toujours différent de zéro pour tout Z non nul. De plus, $\Psi_{\mathcal{T}}(Z) \leq H_\Sigma(Z)$ pour tout $\mathcal{T} \subset \mathbb{T}$, ce qui implique que les suprema définissant

p_r sont eux même bien définis. p_r est une fonction croissante de r et satisfait $p_0 = 0$ ainsi que $p_T = 1$.

Theorème E.3.1 (Borne supérieure de l'erreur d'estimation)**.** *Considérons le système Σ défini par (E.2) et une matrice de mesure Y, ainsi qu'un estimateur d'état (E.23) où les fonctions coût ϕ et ψ vérifient (P3.1)–(P3.5). Nous noterons γ_ϕ et γ_ψ les constantes associées à l'ITG (P3.5) et q_ϕ, q_ψ les fonctions $\mathcal{K}_\infty$ associées à l'HG (P3.4) pour ϕ et ψ respectivement. Soit $\varepsilon \geq 0$ quelconque, et nous posons $r = |\mathbb{T}_\varepsilon^c|$.*
Si le système est observable sur $[0, T-1]$ et $p_r < 1/(1+\gamma_\psi)$, alors pour toute norme $\|\cdot\|$ sur $\mathbb{R}^{n\times T}$,

$$\|\hat{X} - X\| \leq h\left(\frac{2\beta_\Sigma(\varepsilon)}{D[1-(1+\gamma_\psi)p_r]} + \delta(\varepsilon)\right) \quad \forall \hat{X} \in \mathcal{E}(Y) \tag{E.34}$$

avec X qui désigne la vraie trajectoire d'état de Σ, $D = \min_{\|Z\|=1} H_\Sigma(Z) > 0$, $\beta_\Sigma(\varepsilon)$, $\delta(\varepsilon)$ et h définis par

$$\beta_\Sigma(\varepsilon) = \lambda \sum_{t\in\mathbb{T}'} \phi_t(w_t) + \sum_{t\in\mathbb{T}_\varepsilon} \psi_t(f_t), \tag{E.35}$$

$$\delta(\varepsilon) = \frac{1-\gamma_\psi}{D\,[1-(1+\gamma_\psi)p_r]} \sum_{t\in\mathbb{T}_\varepsilon^c} \psi_t(f_t) \tag{E.36}$$

$$h(\alpha) = \max\left\{q_\phi^{-1}(\alpha), q_\psi^{-1}(\alpha)\right\}, \alpha \in \mathbb{R}_{\geq 0} \tag{E.37}$$

Ce théorème présente deux corollaires intéressants, l'un montrant la stricte résilience de certains membres de la famille d'estimateurs $\mathcal{E}$, l'autre montrant la résilience approchée d'autres de ses membres

Résilience stricte. Le résultat suivant est une conséquence du Théorème E.3.1 lorsque la fonction coût mesurant l'erreur sur la sortie ψ satisfait l'inégalité triangulaire stricte.

Corollaire E.3.1.1 (Propriété de résilience)**.** *Supposons que les conditions du Théorème E.3.1 sont vérifiées avec, de plus, $\gamma_\psi = 1$.*
On a alors

$$\|\hat{X} - X\| \leq h\Big(\frac{2\beta_\Sigma(\varepsilon)}{D(1-2p_r)}\Big) \quad \forall \hat{X} \in \mathcal{E}(Y). \tag{E.38}$$

La propriété de résilience de l'estimateur (E.23) tient ici du fait que, lorsque les conditions du Théorème E.3.1 et du Corollaire E.3.1.1 sont vérifiées, la borne (à droite dans (E.38)) sur l'erreur d'estimation ne dépend pas de l'amplitude des valeurs extrêmes du bruit $\{f_t\}_{t\in\mathbb{T}}$. En particulier, si l'on s'intéresse à $\beta_\Sigma(\varepsilon)$, nous remarquons qu'il est possible de surestimer ce terme par

$$\beta_\Sigma(\varepsilon) \leq \lambda \sum_{t\in\mathbb{T}'} \phi_t(w_t) + |\mathbb{T}_\varepsilon|\varepsilon. \tag{E.39}$$

Le premier terme à gauche dans (E.39) représente l'incertitude apportée par $\{w_t\}$ dans le processus d'estimation sur la totalité de l'horizon de temps. Ce terme est borné du fait que $\{w_t\}$ est borné par hypothèse. Le deuxième terme est une borne sur la somme des occurrences de f_t qui sont d'une amplitude plus petite que ε.
Etant donné que β_Σ est une fonction de ε, la borne dans (E.38) représente en réalité une famille de bornes paramétrées par ε. Or, ε n'est qu'une variable d'analyse : une

question qui peut alors se poser est celle de la sélection de ε afin d'obtenir la plus petite borne possible. Si l'on note $\varepsilon^\star$ une telle valeur, alors cette dernière satisfait

$$\varepsilon^\star \in \arg\min_{\varepsilon \geq 0} \left\{ h\Big(\frac{2\beta_\Sigma(\varepsilon)}{D(1-2p_r)}\Big) : r = |\mathbb{T}_\varepsilon^c|,\ p_r < 1/2 \right\}.$$

Nous observons également que plus l'indice p_r est petit, plus la borne sur l'erreur sera petite, ce qui suggère que l'estimateur sera plus résilient lorsque p_r est plus petit. On peut appliquer un raisonnement similaire pour D, qui a lui cependant besoin d'être grand pour que la borne sur l'erreur d'estimation soit petite.

Ces deux paramètres (p_r et D) reflètent les propriétés du système qui est en train d'être estimé. Ils peuvent être interprétés comme une mesure du degré d'observabilité de ce système. En conclusion, l'estimateur hérite une partie de sa propriété de résilience du système dont il doit reconstruire l'état. Ceci est en accord avec le fait bien connu que plus un système est observable, plus son état peut être estimé de manière robuste.

Enfin, on peut noter que la condition $p_r < 1/2$ permet de définir un nombre théorique de mesures corrompues que l'estimateur peut gérer selon le Théorème E.3.1 : ainsi, nous définirons $r_{\max}$ ce nombre maximum, c'est-à-dire le nombre r tel que

$$r_{\max} = \max_{r \in \mathbb{N}} r \quad \text{sujet à} \quad p_r < \frac{1}{2} \tag{E.40}$$

Approximate resilience. Comme discuté plus haut, il est fondamental que ψ vérifie l'inégalité triangulaire stricte pour avoir la stricte résilience de l'estimateur. Lorsque ψ ne vérifie pas cette propriété (c'est-à-dire $\gamma_\psi \neq 1$), il est peu probable que le terme $\delta(\varepsilon)$ dans (E.34) s'annule complètement. Cependant, nous pouvons l'empêcher de croître de manière excessive en choisissant ψ de manière appropriée dans (E.22). Pour illustrer cela, supposons, par exemple, que ψ est défini par $\psi(y) = 1 - e^{-\ell(y)}$. Ainsi, étant donné que $\psi(y) \leq 1$ pour tout y, $\delta(\varepsilon)$ sature jusqu'à une valeur constante, et ce quelque soit l'amplitude de f_t pour $t \in \mathbb{T}_\varepsilon^c$. Il est à noter que ce choix introduit un nouveau problème technique avec des fonctions qui ne sont plus des fonctions $\mathcal{K}_\infty$ mais des fonction bornées (et même qui saturent). Gérer ce cas de figure requiert des conditions supplémentaires.

En résumé, en sélectionnant ψcomme une fonction saturée, nous obtenons le résultat suivant sur la *résilience approchée*.

Corollaire E.3.1.2 (Cas où $\gamma_\psi \neq 1$)**.** *Supposons que les conditions du Théorème E.3.1 sont vérifiées. Supposons en outre que la fonction coût ψ dans (E.22) est définie par $\psi(y) = 1 - e^{-\ell(y)}$ où $\ell : \mathbb{R}^m \to \mathbb{R}_{\geq 0}$ vérifie (P3.1)–(P3.5). En particulier, nous supposons que la propriété (P3.4) est satisfaite par ℓ pour une fonction $\mathcal{K}_\infty$ q telle que (E.24) est une égalité.*

Enfin, nous supposons que $\varepsilon \geq 0$ vérifie

$$b(\varepsilon) \triangleq \frac{2\beta_\Sigma(\varepsilon) + r(1-\gamma_\psi) r^o(\varepsilon)}{D\left[1 - (1+\gamma_\psi)p_r\right]} < 1, \tag{E.41}$$

avec $r = r(\varepsilon) = |\mathbb{T}_\varepsilon^c|$ et $r^o(\varepsilon) = \max_{t \in \mathbb{T}_\varepsilon^c} \psi_t(f_t) \leq 1$. Il existe alors une fonction continue et strictement croissante $h_{\text{sat}} : [0,1] \to [0,1]$ (vérifiant $h_{\text{sat}}(0) = 0$ et $h_{\text{sat}}(1) = 1$) telle que pour toute norme $\|\cdot\|$ sur $\mathbb{R}^{n \times T}$,

$$\|\hat{X} - X\| \leq h_{\text{sat}}^{-1}(b(\varepsilon)) \quad \forall \hat{X} \in \mathcal{E}(Y). \tag{E.42}$$

avec D dans (E.41) défini tel que dans la preuve du Théorème E.3.1 (voir page 52) en utilisant la norme $\|\cdot\|$.

E.3.4 Discussions sur la propriété d'exacte recouvrabilité de l'estimateur

Quelques résultats supplémentaires peuvent être obtenus lorsque l'on restreint notre étude au cas où le bruit d'état $\{w_t\}$ est supposé nul et $\{f_t\}$ est supposé strictement creux sur l'intégralité de l'horizon de temps .

Dans cette configuration, nous pouvons obtenir un estimateur plus résilient (au bruit de mesure creux) que (E.23) en le redéfinissant pour qu'il intègre l'hypothèse sur l'absence de bruit d'état. Cela s'effecture en contraignant l'espace de recherche pour la trajectoire estimée : ainsi, on contraint cette trajectoire pour qu'elle soit dans l'ensemble $\mathcal{Z}_\Sigma \subset \mathbb{R}^{n\times T}$ défini par

$$\mathcal{Z}_\Sigma = \left\{ Z = \begin{pmatrix} z_0 & A_0 z_0 & \cdots & A_{T-1}\cdots A_1 A_0 z_0 \end{pmatrix} : z_0 \in \mathbb{R}^n \right\}, \tag{E.43}$$

qui est l'ensemble des trajectoires idéales du système se basant sur l'état initial $z_0 \in \mathbb{R}^n$. On considère alors l'estimateur $\mathcal{E}^\circ$ défini par

$$\mathcal{E}^\circ(Y) = \underset{Z\in\mathcal{Z}_\Sigma}{\arg\min}\, V_\Sigma(Y, Z).$$

$\mathcal{E}^\circ(Y)$ peut être réécrit plus simplement sous la forme

$$\mathcal{E}^\circ(Y) = \left\{ Z = \begin{pmatrix} z_0 & A_0 z_0 & \cdots & A_{T-1}\cdots A_1 A_0 z_0 \end{pmatrix} : z_0 \in \underset{z\in\mathbb{R}^n}{\arg\min}\, V^\circ_\Sigma(Y, z) \right\} \tag{E.44}$$

où

$$V^\circ_\Sigma(Y, z) = \sum_{t\in\mathbb{T}} \psi_t(y_t - M_t z) \tag{E.45}$$

avec

$$M_t = C_t A_{t-1}\cdots A_1 A_0 \tag{E.46}$$

pour tout $t \geq 1$ et $M_0 = C_0$. De cette façon, l'estimation de la trajectoire d'état revient à estimer l'état initial du système x_0. On peut l'interpréter comme un problème de régression robuste, comme ceux traités dans [Han19; Bak17]. En généralisant un résultat de [Bak17], nous obtenons le résultat suivant, qui est une condition nécessaire et suffisante pour recouvrer de manière exacte le vrai état du système Σ.

Afin de parvenir à ce résultat, nous allons d'abord présenter le concept de rapport de concentration, qui nécessite lui-même de poser, pour tout sous-ensemble $\mathcal{T}$ de $\mathbb{T}$, la notation suivante :

$$\Psi^\circ_\mathcal{T}(z) = \sum_{t\in\mathcal{T}} \psi_t(M_t z). \tag{E.47}$$

Définition E.3.4 (r-ème rapport de concentration)**.** *Soit $\{\psi_t\}$ une famille de fonctions coût définis par (E.22) et pour laquelle on suppose que ψ vérifie les propriétés (P3.1), (P3.3) et (P3.5) avec $\gamma_\psi = 1$. Soit $M = \{M_t\}_{t\in\mathbb{T}}$ une suite de matrices telle que la fonction $\Psi^\circ_\mathbb{T}$, définie par (E.47) avec $\mathcal{T} = \mathbb{T}$, est définie positive. Nous appelons le r-ème rapport de concentration de M le nombre réel tel que*

$$\nu_r(M) = \sup_{\substack{z\in\mathbb{R}^n \\ z\neq 0}} \sup_{\substack{\mathcal{T}\subset\mathbb{T} \\ |\mathcal{T}|=r}} \frac{\Psi^\circ_\mathcal{T}(z)}{\Psi^\circ_\mathbb{T}(z)} \tag{E.48}$$

Pour un r fixé, $\nu_r(M)$ quantifie une propriété de généricité de la suite $M = \{M_t\}_{t\in\mathbb{T}}$. Dans le cas de la structure particulière de M telle que définie dans (E.46), il est à noter que $\Psi^\circ_{\mathbb{T}}$ est définie positive si le système Σ est observable sur $\mathbb{T}$. De plus, $\nu_r(M)$ peut-être interprété, dans une certaine mesure, comme une mesure quantitative de l'observabilité d'un système. En effet, plus $\nu_r(M)$ est petit, plus le système est fortement observable.

Pour tout $(Y, z_0) \in \mathbb{R}^{m\times T} \times \mathbb{R}^n$ avec Y décomposé par colonne selon la forme $Y = (\, y_0 \quad \cdots \quad y_{T-1}\,)$, nous introduisons deux ensembles :

$$\mathcal{I}^0(Y, z_0) = \{t \in \mathbb{T} \,:\, y_t - M_t z_0 = 0\}$$
$$\mathcal{I}^c(Y, z_0) = \{t \in \mathbb{T} \,:\, y_t - M_t z_0 \neq 0\}.$$

Theorème E.3.2 (Condition d'exacte recouvrabilité)**.** *Considérons la fonction coût* (E.45) *avec* $M = \{M_t\}$ *une suite de matrice construite selon* (E.46) *à partir des matrices d'un système* Σ *de la forme* (E.2)*. Supposons également que les fonctions coût* $\{\psi_t\}$ *impliquées dans* (E.45) *sont définies par* (E.22) *où* ψ *vérifie (P3.1), (P3.3) et (P3.5) avec* $\gamma_\psi = 1$*. Soit* r *un entier strictement positif.*

Si le système Σ *est observable sur* $[0, T-1]$*, alors les deux propositions suivantes sont équivalentes :*

(i) *Pour tout* Y *dans* $\mathbb{R}^{m\times T}$ *et tout* z_0 *dans* $\mathbb{R}^n$*,*

$$|\mathcal{I}^c(Y, z_0)| \leq r \;\Rightarrow\; \operatorname*{arg\,min}_{z\in\mathbb{R}^n} V^\circ_\Sigma(Y, z) = \{z_0\} \tag{E.49}$$

(ii) *Le rapport de concentration* $\nu_r(M)$ *vérifie*

$$\nu_r(M) < 1/2 \tag{E.50}$$

Grâce au Théorème E.3.2, nous pouvons dire que dans l'hypothèse où le seul bruit présent dans le système est un bruit de mesure $\{f_t\}$ purement creux (ce qui implique qu'il n'y a aucun bruit dense dans la dynamique), $\mathcal{E}^\circ(Y) = \{X\}$ lorsque $\nu_r(M) < 1/2$, c'est-à-dire que l'estimateur $\mathcal{E}^\circ$ retourne le vrai état initial. Pour un système donné, si l'on était capable d'évaluer numériquement $\nu_r(M)$, il deviendrait alors possible d'évaluer le nombre maximal $r_{\max} \triangleq \max\{r : \nu_r(M) < 1/2\}$ d'erreurs aberrantes que l'estimateur $\mathcal{E}^\circ$ serait capable de gérer en estimant ce système.

On notera également que ce théorème peut être interprété comme une généralisation de la Proposition 6 issue de [Faw14] à une plus large classe de fonctions coût.

E.3.5 Quelques éléments sur la calculabilité de p_r et ν_r

Les analyses qui viennent d'être présentées se basent sur des conditions impliquant des quantités (p_r, ν_r) qui caractérisent l'observabilité du système à estimer. Une question qui peut alors se poser est : est-il possible de calculer ces quantités ? En effet, être capable de calculer p_r en amont permettrait de savoir à l'avance si l'estimateur sera résilient en vertu du Théorème E.3.1. De manière similaire, évaluer le rapport de concentration $\nu_r(M)$ permettrait de savoir si un estimateur donné serait capable de recouvrer exactement l'état d'un système en absence de bruit dense dans sa dynamique.

Cependant, calculer ces deux quantités s'avère compliqué, puisqu'elles sont basées sur la résolution de problèmes d'optimisation non convexes non triviaux et combinatoires. Il est à noter que c'est une caractéristique commune des quantités qui permettent d'évaluer la résilience ; par example, la constante de la Propriété d'Isométrie Restreinte (PIR) [Can08a] est tout aussi complexe à évaluer.

Il est néanmoins possible d'obtenir une surestimation des quantités p_r et ν_r avec un coût calculatoire acceptable. Nous présenterons deux méthodes d'optimisation convexe pour réaliser une telle surestimation.

L'indice de r-Résilience p_r

Pour discuter de la calculabilité de l'indice de r-Résilience p_r, nous rappelons sa définition :

$$p_r = \sup_{\substack{Z\in\mathbb{R}^{n\times T}\\ Z\neq 0}} \sup_{\substack{\mathcal{T}\subset\mathbb{T}\\ |\mathcal{T}|=r}} \frac{\sum_{t\in\mathcal{T}} \psi_t(C_t z_t)}{H_\Sigma(Z)}$$

Comme mentionné plus haut, calculer cette valeur requiert de résoudre deux problèmes d'optimisation reliés, l'un étant non convexe et l'autre étant combinatoire.

Cependant, il est possible de surestimer la valeur de p_r lorsque le système a un unique capteur ($m = 1$), notamment du fait que

$$p_r \leq r p_1 \tag{E.51}$$

Le lemme suivant décrit une façon de surestimer p_r lorsque $\{\phi_t\}$ est une famille de normes et ψ_t est égale à la norme ℓ_1 pour tout $t \in \mathbb{T}$:

Lemme E.3.3 (Une estimation de l'indice de r-Résilience p_r)**.** *Considérons p_r défini par (E.33) dans le cas où le système étudié n'a qu'une sortie ($m = 1$), où $\psi_t(e) = |e|$ pour tout $(t, e) \in \mathbb{T} \times \mathbb{R}$ et $\{\phi_t\}$ est une famille de normes quelconques. Nous avons alors*

$$p_r \leq \frac{r}{b_1} \tag{E.52}$$

where

$$b_1 = \inf_{t\in\mathbb{T}} \inf_{Z\in\mathbb{R}^{n\times T}} \left\{ H_\Sigma(Z) : c_t^\top z_\tau = 1 \right\} = \frac{1}{p_1}. \tag{E.53}$$

Lorsque les hypothèses du Lemme E.3.3 sont vérifiées, $\inf_{Z\in\mathbb{R}^{n\times T}} \left\{ H_\Sigma(Z) : c_t^\top z_\tau = 1 \right\}$ est un problème d'optimisation convexe pour tout t. Ainsi, calculer b_1 dans (E.53) revient à résoudre T problèmes d'optimisation convexe et à sélectionner la plus petite des T valeurs obtenues. Ce lemme permet donc bien d'obtenir une surestimation de p_r qui est facilement calculable numériquement.

Grâce à cette surestimation de p_r, nous pouvons assurer, par le Théorème E.3.1, qu'un estimateur (E.23) est résilient à r valeurs aberrantes si $r < b_1/2$. De plus, nous pouvons obtenir une sous-estimation du nombre maximum de valeurs aberrantes $r_{\max}$ (voir Eq. (E.40)) qu'un estimateur (E.23) peut gérer :

$$\tilde{r}_{\max} = \max \left\{ r : r < \frac{b_1}{2} \right\}. \tag{E.54}$$

Le rapport de concentration ν_r

Lorsque la dimension de l'état du système est suffisamment petite, $\nu_r(M)$ peut être calculé exactement en s'inspirant de la méthode présentée dans [Sha09] au prix d'un

grand coût de calcul. Une surestimation moins coûteuse en calcul peut toutefois être obtenue par optimisation convexe, comme suggéré par [Bak17]. Le lemme suivant explicite cette deuxième méthode et présente une surestimation de $\nu_r(M)$.

Lemme E.3.4. *Étant donné que toutes les quantités impliquées sont bien définies (voir les conditions des Définitions E.3.3 et E.3.4), les affirmations suivantes sont vraies :*

(a) $\nu_r \leq p_r$

(b) Si $\mu(M) \leq T-1$ *alors*

$$\nu_r(M) \leq \frac{r\nu^o}{1+\nu^o}, \tag{E.55}$$

où

$$\nu^o = \max_{t\in\mathbb{T}} \min_{\lambda_t\in\mathbb{R}^T} \left\{ \|\lambda_t\|_\infty : V_t M_t = \sum_{k\in\mathbb{T}} \lambda_t[k] V_k M_k, \lambda_t[t] = 0 \right\} \tag{E.56}$$

Dans (E.56), $\lambda_t[k]$ désigne les entrées du vecteur $\lambda_t \in \mathbb{R}^T$ et $\{V_t\}$ fait référence à la séquence de matrices de pondérations non singulières présentes dans (E.22).

E.3.6 Une implémentation récursive approchée

Jusqu'à maintenant, les estimateurs étudiés dans cette section ont été définis sur un horizon de temps complet, ce qui implique que pour avoir accès à l'estimée à l'instant T, il est nécessaire d'estimer toute la trajectoire de l'état sur l'horizon de temps $[0, T]$.

Or, ceci pose problème lorsque l'on estime un système sur une très longue période, puisque l'horizon de temps sur lequel on doit reconstruire la trajectoire d'état croît énormément. Cette implémentation devient alors très lourde et est peu pratique, notamment lorsque l'on veut mettre en œuvre l'estimateur sur une unité de calcul aux ressources limitées.

Nous allons présenter un algorithme mettant récursivement en œuvre une version approchée de l'estimateur E.23 obtenu par *Forward Dynamic Programming* (voir Section E.2.3). L'estimateur $\mathcal{E}$ considéré sera tel que pour tout $t \in \mathbb{N}$, $\phi_t = \|\cdot\|_{Q_t}^2$ avec $\{Q_t\}$ une suite de matrices définies positives, et $\psi_t = \|\cdot\|_1$.

Le but de l'estimation récursive est ici d'estimer l'état final de l'horizon de temps (qui n'est plus supposé constant), c'est-à-dire $\hat{x}_T$, sans avoir à recalculer toute la trajectoire d'état. Pour ce faire, nous allons nous intéresser à $V_\Sigma^\star$, la fonction de performance récursive introduite lors de la présentation du Forward Dynamic Programming (voir Eq. (E.11)). Ainsi, pour tout $T \in \mathbb{N}$, on a

$$\forall (Y, z) \in \mathbb{R}^{m\times T} \times \mathbb{R}^n,\ V_{\Sigma,T}^\star(Y, z) = \min_{\substack{Z\in\mathbb{R}^{n\times T} \\ z_T = z}} V_\Sigma(Y, Z).$$

Il est à noter que V_Σ, Y et Z dépendent toutes implicitement de T étant donné qu'elles sont définies sur l'horizon de temps T. À partir de $V_{\Sigma,T}^\star(Y, z)$, nous définissons maintenant l'estimateur récursif $\mathcal{E}_{\text{online}}$ tel que

$$\mathcal{E}_{\text{online}}(Y, T) = \arg\min_{z\in\mathbb{R}^n} V_{\Sigma,T}^\star(Y, z). \tag{E.57}$$

Étant donné la structure de V_Σ, l'équation de Bellman (E.14) donne une relation de récurrence entre $V^\star_{\Sigma,T+1}$ et $V^\star_{\Sigma,T}$:

$$V^\star_{\Sigma,T+1}(Y,z) = \min_{s\in\mathbb{R}^n} \left\{ V^\star_{\Sigma,T}(Y,s) + \lambda \|z - A_T s\|^2_{Q_T} \right\} + \|y_{T+1} - C_{T+1} z\|_1. \tag{E.58}$$

Cependant, il n'est pas possible d'implémenter directement l'estimateur $\mathcal{E}_{\text{online}}$ car il requiert une expression algébrique de $\min_{s\in\mathbb{R}^n} \left\{ V^\star_{\Sigma,T}(Y,s) + \lambda \|z - A_T s\|^2_{Q_T} \right\}$ par rapport à z et aux variables du système. Une telle relation semble très compliquée à obtenir, notamment du fait de la présence de $\psi_T = \|\cdot\|_1$, fonction coût non différentiable, au sein de $V^\star_{\Sigma,T}(Y,s)$.

Pour surmonter ce problème, nous allons approcher la norme ℓ_1 par une fonction quadratique, ce qui nous permettra par la suite d'avoir une expression algébrique de $V^\star_{\Sigma,T+1}$ en appliquant le Théorème E.2.3. Cette approximation se base sur le fait que pour tout a réel non nul,

$$|a| = \frac{a^2}{|a|}.$$

L'idée est alors d'estimer la valeur $|a|$ dans la partie droite de l'égalité et de la remplacer par une prédiction $|a|_{\text{pred}}$, de sorte que

$$|a| \approx \frac{a^2}{|a|_{\text{pred}}},$$

Ce principe permet d'approcher localement la valeur $\|y_T - C_T z\|_1$ par la fonction coût approchée $\psi_{T,\text{approx}}$ telle que pour tout T entier,

$$\psi_{T,\text{approx}}(y_T - C_T z) = \sum_{j=1}^{m} \frac{(y_T[j] - c_{T,j}^\top z)^2}{\gamma[j]\,|y_T[j] - c_{T,j}^\top \hat{x}_{T|T-1}| + \epsilon},$$

avec $\hat{x}_{T|T-1} = A_{T-1}\hat{x}_{T-1}$. Cette fonction coût peut se mettre sous une forme quadratique,

$$\forall z \in \mathbb{R}^m, \quad \psi_{T,\text{approx}}(z) = z^\top (\text{diag}(\gamma) R_T + \epsilon I_m)^{-1} z \tag{E.59}$$

avec $\gamma \in \mathbb{R}^m$ une vecteur de pondérations strictement positives, $\epsilon > 0$, et R_T une matrice symétrique définie positive telle que

$$R_T = \text{diag}(|y_T[1] - c_{T,1}^\top \hat{x}_{T|T-1}|, ..., |y_T[m] - c_{T,m}^\top \hat{x}_{T|T-1}|). \tag{E.60}$$

γ est un vecteur de paramètres qui permettent de réguler l'influence de chaque composante de $(y_T[j] - c_{T,j}^\top z)^2$ dans $\psi_{T,\text{approx}}$. ϵ est présent pour éviter tout problème de conditionnement lorsque la valeur $y_T - C_T \hat{x}_{T|T-1}$ est proche de 0.

Par application du Théorème E.2.3, nous sommes alors capables de dériver l'Algorithme E.2. Il est à noter que cet estimateur n'est pas strictement un estimateur de Kalman, car la matrice de pondération R_T à l'instant T dépend de l'estimée obtenue à l'instant $T-1$.

E.3.7 Résultats numériques

Cette section vise à donner un exemple de résultat numérique que l'on peut obtenir avec des estimateurs de la forme (E.23).

Le scénario que nous allons considérer est celui d'un système perturbé par un bruit d'état dense et un bruit de mesure présentant à la fois une composante dense et une

Algorithme E.2 Algorithme inspiré de Kalman pour implémenter $\mathcal{E}_{\text{online}}$ (E.57) de manière approchée

Entrées : $\{A_T\}$, $\{C_T\}$, $\lambda \in \mathbb{R}_{>0}$, $\gamma \in \mathbb{R}^m_{>0}$, $\epsilon \in \mathbb{R}_{>0}$, $\hat{x}_0 \in \mathbb{R}^n$, $\{Q_T\}$, $P_0 \in \mathcal{S}_n^+(\mathbb{R})$, $T_{\max} \in \mathbb{N}$, $Y \in \mathbb{R}^{m \times T_{\max}}$
Initialisation :
$T \leftarrow 0$
Fin de l'initialisation.
Tant que $T < T_{\max}$
$\hat{x}_{T|T-1} \leftarrow A_{T-1}\hat{x}_{T-1}$
$R_T \leftarrow \text{diag}(|y_T[1] - c_{T,1}^\top \hat{x}_{T|T-1}|, ..., |y_T[m] - c_{T,m}^\top \hat{x}_{T|T-1}|)$
$P_{T|T-1} \leftarrow A_{T-1}P_{T-1}A_{T-1}^\top + Q_{T-1}$
$L_T \leftarrow P_{T|T-1}C_T^\top \left(C_T P_{T|T-1} C_T^\top + \text{diag}(\gamma)R_T + \epsilon I_m\right)^{-1}$
$\hat{x}_T \leftarrow \hat{x}_{T|T-1} + L_T(y_T - C_T\hat{x}_{T|T-1})$
$P_T \leftarrow (I_n - L_T C_T)P_{T|T-1}$
$T \leftarrow T + 1$
Fin tant que

composante creuse. Nous nous intéresserons alors à l'erreur d'estimation, c'est-à-dire l'écart entre le vrai état du système et l'état estimé, pour plusieurs instances de la classe $\mathcal{E}$.

On considère le système LTV de la forme (E.2) avec

$$A = \begin{pmatrix} 0.7 & 0.45 \\ -0.5 & 1 \end{pmatrix}, \quad C = \begin{pmatrix} 1 & 2 \end{pmatrix}, x_0 = \begin{pmatrix} 1 \\ 2 \end{pmatrix}. \tag{E.61}$$

Les bruits denses qui perturbent ce système ($\{w_t\}$ et $\{v_t\}$ (voir Eq. (E.19))) sont supposés blancs, bornés et uniformément distribués. Pour cette expérience, les valeurs de ces perturbations seront en effet sélectionnées aléatoirement dans un intervalle de la forme $[-a, a]$.

Pour estimer l'état du système, nous avons implémenté les estimateurs suivants :

- L'estimateur $\mathcal{E}^\circ$qui instancie la classe définie par (E.44) pour $\phi = \|\cdot\|_1$.
- L'estimateur $\mathcal{E}_{\ell_2^2,\ell_1}$ qui instancie $\mathcal{E}$ defini par (E.23) pour $\phi = \|\cdot\|_2^2$, $\psi = \|\cdot\|_1$ et $\lambda = 1000$.
- L'estimateur $\mathcal{E}_{\ell_1,\ell_1}$ qui instancie $\mathcal{E}$ pour $\phi = \|\cdot\|_1$, $\psi = \|\cdot\|_1$ et $\lambda = 10$.

Pour avoir une base sur laquelle comparer les performances de ces estimateurs en présence de bruits aberrants, nous avons aussi implémenté des estimateurs oracles : le terme « oracle »indique que ces estimateurs basent leur estimation sur une version de la sortie qui n'est pas affectée par les valeurs aberrantes du bruit de mesure, c'est-à-dire $\tilde{y}_t = y - s_t$ avec s_t la composante creuse de f_t (voir Eq (E.19)). Ainsi, l'oracle $\mathcal{E}_{\ell_2^2,\ell_1}$ a été implémenté. De plus, pour avoir une idée des performances que l'on peut attendre d'un estimateur classique sur le même système, nous avons aussi implémenté un estimateur des moindres carrés oracle, aussi appelé oracle $\mathcal{E}_{\ell_2^2,\ell_2^2}$. Cet estimateur a été choisi du fait que c'est l'estimateur produisant la plus faible covariance de l'erreur d'estimation en présence de bruits gaussiens [Gee05, p. 1041] : il devrait donc fournir de bonnes performances en présence de bruits bornés.

L'ensemble de ces estimateurs a été implémenté en résolvant directement le problème d'optimisation convexe sous MATLAB.

L'indice de performance que nous utiliserons sera l'Erreur d'Estimation Relative (REE), c'est-à-dire la valeur

$$\text{REE} = \frac{\|\hat{X} - X\|_2}{\|X\|_2} \tag{E.62}$$

où X représente la vraie trajectoire d'état du système et $\hat{X}$ est la trajectoire estimée obtenue par l'estimateur. Dans chaque configuration, nous effectuerons une centaine de réalisations pour différentes valeurs de bruits, et les valeurs présentées seront les REE moyennées sur l'ensemble des réalisations.

Expérience 1 : test sur le nombre d'occurrences du bruit impulsif

Pour ce test, le Rapport Signal sur Bruit (RSB) des bruits denses (i.e., w_t et v_t) est fixé, avec une amplitude maximum de $a = 0.03$ pour w_t and de $a = 0.1$ pour v_t, ce qui donne un RSB d'environ 30 dB dans les deux cas. Le nombre de valeurs non nulles de $\{s_t\}$, quant à lui, varie de sorte à ce que le ratio d'occurrences non nulles varie entre 0 et 1. Pour le simuler, les indices temporels des occurrences non nulles sont sélectionnés uniformément sur l'ensemble des indices possibles, puis les valeurs de ces occurrences sont prises comme la réalisation d'une variable aléatoire gaussienne de moyenne nulle et de variance égale à 100. La REE (moyennée) de chaque estimateur pour ce test a enfin été représenté sur la Figure E.3a en échelle logarithmique.

Les résultats de ce test indiquent que malgré la présence du bruit impulsif s_t, les performances de l'estimateur (E.23) semblent rester stables jusqu'à ce qu'une condition de résilience (empirique) ne soit plus vérifiée, ce qui a lieu pour un ratio d'occurrences non nulles aux alentours de 60%. Ceci est cohérent avec la condition de résilience caractérisée par le Théorème E.3.1 qui indique que l'erreur d'estimation est insensible à la présence de s_t tant que le nombre d'occurrences non nulles de ce dernier est inférieur à un seuil ($r_{\max}$) qui dépend des propriétés du système.

Le Lemme E.3.3 permet de sous-estimer ce nombre $r_{\max}$ pour $\mathcal{E}_{\ell_1,\ell_1}$ dans cette configuration, ce qui donne $r_{\max} \geq 8$ (sur un total de 100 occurrences). On constate donc que cette sous-estimation est bien en deça de la limite empirique observée, qui semble être aux alentours de 40% pour $\mathcal{E}_{\ell_1,\ell_1}$. Cette différence peut être expliquée par le pessimisme de l'analyse présentée.

Expérience 2 : test sur le RSB. Pour ce second test, nous fixons le ratio d'occurrences non nulles de $\{s_t\}$ à 0.2 et faisons varier conjointement la puissance des bruits $\{(w_t, v_t)\}$ entre 5 dB et 100 dB en termes de RSB. Les résultats obtenus pour les estimateurs implémentés sont présentés Figure E.3b.

On observe donc que pour ce test, avec une quantité de données corrompues raisonnable (ici 20% des mesures disponibles), les estimateurs se comportent de la même façon que s'il n'y avait aucun bruit impulsif.

E.4 Estimateurs presque résilients basés sur des fonctions coût saturées

La seconde famille d'estimateurs d'état optimaux proposée pour répondre au problème d'estimation d'état résiliente présenté Section E.2.4 est une famille basée sur des fonctions de performance qui présentent une saturation. Cette saturation est induite par la présence d'une exponentielle négative dans la définition, de sorte qu'elle tend vers une valeur finie lorsque l'amplitude de son argument augmente.

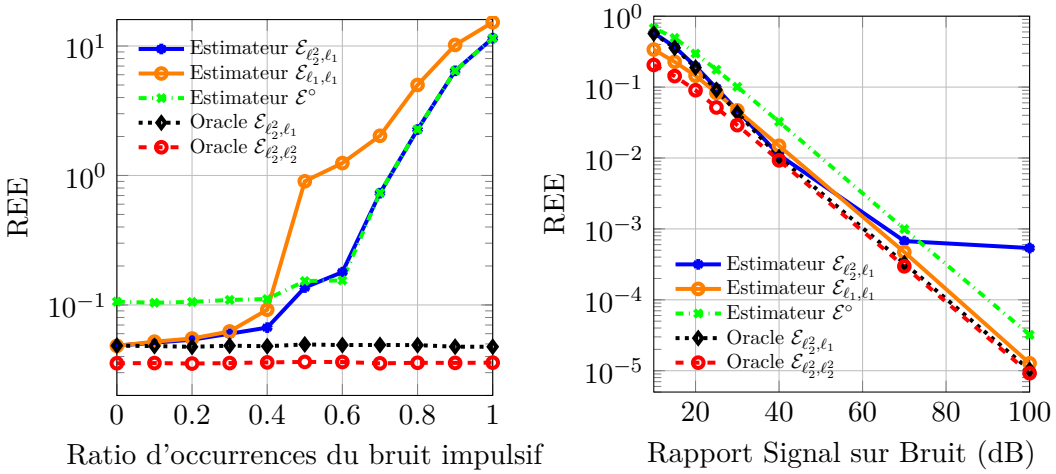

(A) Expérience 1 (B) Expérience 2

FIGURE E.3: Erreur d'estimation relative (en échelle logarithmique) obtenue pour différents estimateurs en fonction du ratio d'occurrences non nulles du bruit creux $\{s_t\}$ (gauche) et pour différents niveaux de bruits denses w_t et v_t (droite)

Comme pour la première famille d'estimateurs étudiée, après avoir défini et discuté de ces propriétés, nous présenterons quelques-uns des résultats que nous avons obtenus sur cette famille ainsi que quelques résultats numériques.

E.4.1 Définition de la classe d'estimateurs étudiée

Pour des raisons de simplicité, l'étude présentée ici sera dans le cadre des systèmes LTI, c'est-à-dire des systèmes de la forme (E.3)

$$\begin{cases} x_{t+1} &= Ax_t + w_t \\ y_t &= Cx_t + f_t \end{cases}$$

avec $x_0 \in \mathbb{R}^n$ l'état initial du système. Dans un premier temps, $\{w_t\}$ et $\{f_t\}$ seront tous les deux considérés comme des bruits arbitraires. Les développements présentés sont cependant facilement extensibles au cas LTV.

Pour résoudre le problème de l'estimation résiliente et estimer l'état d'un système LTI en temps-discret de la forme (E.3), nous proposons alors une autre solution basée sur l'optimisation d'une fonction de performance de la forme

$$V_\Sigma^{\exp}(Y,Z) = \sum_{(t,i)\in\mathbb{T}'\times\mathbb{I}} \left(1 - e^{-\lambda_\phi \phi\left(z_{t+1}[i] - a_i^\top z_t\right)}\right) + \sum_{(t,j)\in\mathbb{T}\times\mathbb{J}} \left(1 - e^{-\lambda_\psi \psi\left(y_t[j] - c_j^\top z_t\right)}\right) \tag{E.63}$$

avec $\lambda_\phi \in \mathbb{R}_{>0}$ et $\lambda_\psi \in \mathbb{R}_{>0}$ deux paramètres définis par l'utilisateur, $Z \in \mathbb{R}^{n\times T}$ la variable d'optimisation représente une trajectoire d'état potentielle, et $\mathbb{I} = \{1, ..., n\}$, $\mathbb{J} = \{1, ..., m\}$ les ensembles des indices pour l'état et les mesures respectivement. $\{a_i\}$, $\{c_j\}$ sont deux familles de vecteurs colonnes de $\mathbb{R}^n$ respectivement telles que

$$A = \begin{pmatrix} a_1 & \cdots & a_n \end{pmatrix}^\top$$

$$C = \begin{pmatrix} c_1 & \cdots & c_m \end{pmatrix}^\top.$$

Avec $\mathbb{T}' = \{1, .., T-2\}$ et $\mathbb{T} = \{1, .., T-1\}$, il y a un total de $|\mathbb{I}||\mathbb{T}'| + |\mathbb{J}||\mathbb{T}| = n(T-1)+mT$ termes au sein de $V_\Sigma^{\exp}$: par commodité, on pose $N = n(T-1)+mT$, et parfois, $V_\Sigma^{\exp}$ pourra être écrite de manière alternative

$$\forall Z \in \mathbb{R}^{n\times T},\ V_\Sigma^{\exp}(Y,Z) = N - \sum_{(t,i)\in\mathbb{T}'\times\mathbb{I}} e^{-\lambda_\phi \phi\left(z_{t+1}[i]-a_i^\top z_t\right)} - \sum_{(t,j)\in\mathbb{T}\times\mathbb{J}} e^{-\lambda_\psi \psi\left(y_t[j]-c_j^\top z_t\right)}.$$

Les fonctions ϕ et ψ sont définies de $\mathbb{R}$ vers $\mathbb{R}_{\geq 0}$ et leurs propriétés seront discutées dans la section suivante. Si l'on compare $V_\Sigma^{\exp}$ définie pour cette famille avec l'Équation (E.9) définissant la structure générale des fonctions de performance, nous observons que les familles de fonctions coût $\{\phi_t\}$ et $\{\psi_t\}$ correspondent, dans le cas présent, à

$$\phi_t(z) = \sum_{i\in\mathbb{I}} \left(1 - e^{-\lambda_\phi \phi(z[i])}\right) \quad \forall z \in \mathbb{R}^n, \tag{E.64}$$

$$\psi_t(z) = \sum_{j\in\mathbb{J}} \left(1 - e^{-\lambda_\psi \psi(z[j])}\right) \quad \forall z \in \mathbb{R}^m. \tag{E.65}$$

Remarque E.4.1. *Afin d'avoir des notations plus simples, les fonctions coût ϕ et ψ sont supposées indépendantes du temps. Les résultats présentés dans cette section peuvent cependant être étendus à des ϕ_t et ψ_t temps-variants. Par exemple, $\{\phi_t\}$ et $\{\psi_t\}$ peuvent être définis avec une structure similaire à (E.21)–(E.22), c'est-à-dire*

$$\phi_t(z) = \sum_{i\in\mathbb{I}} \left(1 - e^{-\lambda_\phi \phi(W_{t,i} z[i])}\right) \quad \forall z \in \mathbb{R}^n,$$

$$\psi_t(z) = \sum_{j\in\mathbb{J}} \left(1 - e^{-\lambda_\psi \psi(V_{t,j} z[j])}\right) \quad \forall z \in \mathbb{R}^m,$$

où pour tout $t \in \mathbb{T}$, $i \in \mathbb{I}$, $j \in \mathbb{J}$, $W_{t,i}$ et $V_{t,j}$ sont des réels strictement positifs.

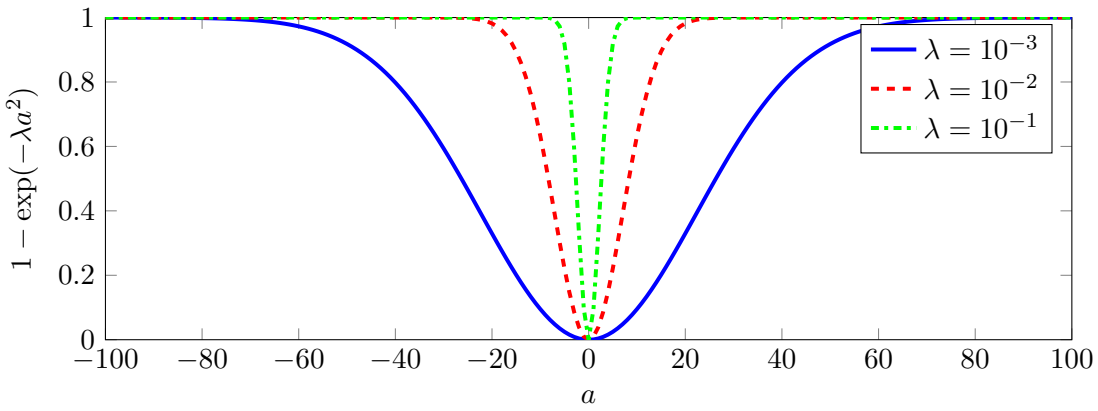

FIGURE E.4: Tracé de la fonction $a \mapsto 1 - \exp(-\lambda a^2)$ pour $\lambda \in \{10^{-1}, 10^{-2}, 10^{-3}\}$ sur $[-100, 100]$

Il est important de noter que les paramètres utilisateur λ_ϕ et λ_ψ impliqués dans les termes exponentiels de (E.63) jouent un rôle différent du paramètre utilisateur λ dans la fonction de performance V_Σ définie par (E.20). Dans les deux cas ((E.20) et (E.63)), les deux sommes impliquées dans V_Σ et $V_\Sigma^{\exp}$ évaluent deux choses différentes : la somme de gauche évalue l'adéquation entre la trajectoire d'état potentielle et la

dynamique du système, tandis que la somme de droite évalue la cohérence entre cette même trajectoire et les mesures obtenues en sortie du système. Ainsi, pour V_Σ, le paramètre λ sert à équilibrer la contribution de ces deux sommes dont les ordres de grandeur peuvent *a priori* être différents. En comparaison, un tel équilibrage n'est plus forcément nécessaire du fait que chaque terme présent dans $V_\Sigma^{\exp}$ est compris entre 0 et 1.

Cependant, le nouveau problème qui apparaît pour $V_\Sigma^{\exp}$ est la sensibilité de chaque terme exponentiel. En effet, l'intérêt de ces termes est que leur valeur tend vers 0 lorsque l'amplitude de leur argument tend vers l'infini, mais la rapidité avec laquelle ils tendent vers 0 doit être réglée. Pour l'illustrer, la Figure E.4 montre le tracé de la fonction $a \mapsto 1-\exp(-\lambda a^2)$ pour trois valeurs différentes du paramètre de réglage λ. Lorsque le paramètre de réglage diminue, la courbe correspondante devient plus plate, ce qui entraîne que même des arguments de grande amplitude vont avoir une image non nulle par ce terme exponentiel. Les deux paramètres utilisateur λ_ϕ et λ_ψ présents dans $V_\Sigma^{\exp}$ servent donc à définir un seuil au-delà duquel les arguments doivent être saturés.

À partir de $V_\Sigma^{\exp}$ (définie par (E.63)), nous pouvons définir l'estimateur $\mathcal{E}^{\exp}$: $\mathbb{R}^{m\times T} \to \mathcal{P}(\mathbb{R}^{n\times T})$ tel que

$$\mathcal{E}^{\exp}(Y) = \underset{Z\in\mathbb{R}^{n\times T}}{\arg\min}\, V_\Sigma^{\exp}(Y,Z). \tag{E.66}$$

E.4.2 Propriétés de base requises pour les fonctions coût

Les propriétés qui caractérisent les fonctions coût de cette section sont très similaires à celles utilisées dans la section précédente. Nous allons toutefois les réécrire ici par souci de clarté. Ainsi, dans cette section, le terme *fonction coût* fera référence à des fonctions de $\mathbb{R}$ vers $\mathbb{R}_{\geq 0}$ qui respectent les propriétés suivantes :

(P4.1) **Definie positivité :** $\psi(0) = 0$ et $\psi(a) > 0$ pour tout réel a non nul.

(P4.2) **Symétrie :** $\psi(-a) = \psi(a)$ pour tout $a \in \mathbb{R}$.

(P4.3) **Croissance :** pour tout a_1, a_2 dans $\mathbb{R}$, $|a_1| < |a_2|$ implique $\psi(a_1) \leq \psi(a_2)$.

(P4.4) **Inégalité Triangulaire Généralisée (ITG):** il existe $\gamma \in \mathbb{R}_{>0}$ tel que pour tout a_1, a_2 dans $\mathbb{R}$,

$$\psi(a_1 - a_2) \geq \gamma\psi(a_1) - \psi(a_2). \tag{E.67}$$

Dans le contexte des termes exponentiels formant les sommes impliquées dans $V_\Sigma^{\exp}$ (E.63), ces propriétés visent à généraliser l'approche utilisée dans le cadre du Critère de Correntropie Maximum (CCM). Cette approche se base sur le concept – issu de la théorie de l'information – de la correntropie, qui est définie comme une mesure de vraisemblance entre deux variables aléatoires.

L'intérêt de définir les fonctions coûts par leurs propriétés est alors que la classe $\mathcal{E}^{\exp}$ inclut de nombreux estimateurs d'état déjà étudiés dans la littérature sur le CCM (voir [Che17a] ou [Che17b] par exemple), mais elle inclut également des nouveaux estimateurs d'état qui n'ont pas encore été étudiés : par exemple, la classe $\mathcal{E}^{\exp}$ contient les estimateurs basés sur des coûts avec des exponentielles de la forme

$$\forall a \in \mathbb{R},\ \xi(a) = e^{-\frac{|a|^p}{2\sigma^p}}$$

$V_\Sigma^{\exp}$ avec $p \leq 1$ (voir [Bak18] pour la preuve que les fonctions de la forme $a \mapsto |a|^p$ vérifient (P4.1)–(P3.3)).

E.4.3 Étude de la résilience

La présente section a pour but de présenter quelques éléments concernant l'étude de la résilience de $\mathcal{E}^{\exp}$ dans les cas où les deux perturbations $\{w_t\}$ et $\{f_t\}$ présentent des valeurs aberrantes. Le résultat principal obtenu dans cette section est une borne supérieure sur une image de l'erreur d'estimation. Ce résultat ne permet pas de conclure à propos de la résilience ou de la résilience approchée de $\mathcal{E}^{\exp}$, mais il permet tout de même une analyse qualitative de l'influence des différents paramètres du système sur la performance de l'estimation.

Notations pour l'analyse

Pour mener à bien cette analyse, nous allons mettre en place quelques notations. Premièrement, on pose

$$\mathbb{S}_1 = \mathbb{I} \times \mathbb{T}' \qquad \mathbb{S}_2 = \mathbb{J} \times \mathbb{T}. \tag{E.68}$$

On va également supposer que ϕ et ψ vérifient les propriétés (P4.1)–(P4.4), et on pose respectivement γ_ϕ et γ_ψ les constantes avec lesquelles elles vérifient l'ITG (P4.4).

Enfin, pour $\mathcal{S}_1 \subseteq \mathbb{S}_1$ et $\mathcal{S}_2 \subseteq \mathbb{S}_2$, on définit $\Phi_{\mathcal{S}_1} : \mathbb{R}^{n\times T} \to \mathbb{R}_{\geq 0}$ et $\Psi_{\mathcal{S}_1} : \mathbb{R}^{n\times T} \to \mathbb{R}_{\geq 0}$ les deux fonctions telles que pour tout $Z \in \mathbb{R}^{n\times T}$,

$$\Phi_{\mathcal{S}_1}(Z) = \sum_{(i,t)\in\mathcal{S}_1} \left(1 - e^{-\gamma_\phi \lambda_\phi \phi\left(z_{t+1}[i] - a_i^\top z_t\right)}\right) \tag{E.69}$$

$$\Psi_{\mathcal{S}_2}(Z) = \sum_{(j,t)\in\mathcal{S}_2} \left(1 - e^{-\gamma_\psi \lambda_\psi \psi\left(c_j^\top z_t\right)}\right) \tag{E.70}$$

Résultat principal

Avant d'aborder le résultat principal, nous devons définir le paramètre suivant, qui a une structure comparable à l'indice de r-Résilience p_r qui avait été introduit dans la Section E.3 :

Définition E.4.1. *Soient r, r' deux entiers positifs. Supposons que le système LTI Σ défini par (E.3) est observable sur $[0, T-1]$. Nous définissons alors l'indice de (r, r')-Résilience de l'estimateur $\mathcal{E}^{\exp}$ dans (E.66) (appliqué à Σ) comme le réel $p_{r,r'}^{\exp}$ tel que*

$$p_{r,r'}^{\exp} = \sup_{\substack{Z\in\mathbb{R}^{n\times T}\\ Z\neq 0}} \sup_{\substack{\mathcal{S}_1\times\mathcal{S}_2\subset\mathbb{S}_1\times\mathbb{S}_1\\ |\mathcal{S}_2|=r\\ |\mathcal{S}_2|=r'}} \frac{\Phi_{\mathcal{S}_1}(Z) + \Psi_{\mathcal{S}_2}(Z)}{\Phi_{\mathbb{S}_1}(Z) + \Psi_{\mathbb{S}_2}(Z)} \tag{E.71}$$

où Φ et Ψ sont définis par (E.69)–(E.70).

$p_{r,r'}^{\exp}$, comme p_r précédemment, peut être interprété comme une mesure quantitative de l'observabilité du système Σ. La différence principale est que les paramètres utilisateur γ_ϕ et γ_ψ sont présents dans la définition de $p_{r,r'}^{\exp}$, du fait qu'ils sont impliqués dans les termes exponentiels de la fonction coût.

Nous avons aussi besoin de partitionner les ensembles $\mathbb{S}_1$ et $\mathbb{S}_2$. Plus précisément, nous considérons les sous-ensembles suivants :

$$\Pi_\varepsilon = \{(t,i) \in \mathbb{S}_1 \ : \ \phi(w_t[i]) \leq \varepsilon\} \tag{E.72}$$
$$\Pi^c_\varepsilon = \{(t,i) \in \mathbb{S}_1 \ : \ \phi(w_t[i]) > \varepsilon\} \tag{E.73}$$
$$\Lambda_{\varepsilon'} = \{(t,j) \in \mathbb{S}_2 \ : \ \psi(f_t[j]) \leq \varepsilon'\} \tag{E.74}$$
$$\Lambda^c_{\varepsilon'} = \{(t,j) \in \mathbb{S}_2 \ : \ \psi(f_t[j]) > \varepsilon'\} \tag{E.75}$$

avec $\varepsilon \geq 0$ et $\varepsilon' \geq 0$. Ces ensembles permettent de partitionner $\mathbb{S}_1$ et $\mathbb{S}_2$ par rapport aux valeurs raisonnables et aberrantes présentes dans $\{w_t\}$ et $\{f_t\}$. Les seuils ε et ε', qui sont des outils d'analyse, imposent la limite entre raisonnable et aberrant. Pour des raisons de simplicité, nous supposerons que les deux seuils vérifient $\lambda_\phi \varepsilon = \lambda_\psi \varepsilon'$. L'analyse peut être étendue au cas où cette hypothèse est fausse, notamment en redéfinissant $p_{r,r'}$ afin de prendre ε et ε' en compte.

Proposition E.4.1. *Soient Σ un système LTI défini par (E.3) de sortie Y, et un estimateur de la forme (E.66) pour lequel les fonctions coût ϕ et ψ sont supposées vérifier (P4.1)–(P4.4). Notons γ_ϕ et γ_ψ les constantes associées à l'IGT (P4.4). Soient $\varepsilon \geq 0$ et $\varepsilon' \geq 0$ tels que $\lambda_\phi \varepsilon = \lambda_\psi \varepsilon'$, et posons r et r' tels que $r = |\Pi^c_\varepsilon|$ et $r' = |\Lambda^c_{\varepsilon'}|$.*
Si le système est observable sur $[0, T-1]$ et $p^{\exp}_{r,r'} < 1$, alors pour tout $\hat{X} \in \mathcal{E}^{\exp}(Y)$,

$$\frac{1}{N}\left(\Phi_{\mathbb{S}_1}(\hat{X} - X) + \Psi_{\mathbb{S}_2}(\hat{X} - X)\right) \leq \frac{1}{1 - p^{\exp}_{r,r'}}\left[e^{-\lambda_\phi \varepsilon} - \left(1 - \frac{r + r'}{N}\right)\left(e^{-2\lambda_\phi \varepsilon} + e^{-\lambda_\phi \varepsilon} - 1\right)\right] \tag{E.76}$$

avec X la vraie trajectoire du système Σ et $N = n(T-1) + mT$.

De manière similaire à la Proposition E.3.1, cette proposition montre qu'on peut obtenir une image de l'erreur d'estimation qui est bornée par une valeur ne dépendant pas des valeurs extrêmes des bruits $\{w_t\}$ et $\{f_t\}$. Néanmoins, pour le cas de la borne supérieure présente dans (E.76), cette image, *i.e.* $\frac{1}{N}\left(\Phi_{\mathbb{S}_1}(E) + \Psi_{\mathbb{S}_2}(E)\right)$, n'est pas radialement non bornée mais est toujours entre 0 et 1 par définition.

Par conséquent, l'inégalité (E.76) n'a un intérêt que lorsque son côté droit est plus petit que 1. Ceci impose une contrainte supplémentaire sur l'indice de (r, r')-Résilience $p^{\exp}_{r,r'}$, qui doit donc en plus vérifier

$$p^{\exp}_{r,r'} \leq 1 - e^{-\lambda_\phi \varepsilon} + \left(1 - \frac{r + r'}{N}\right)\left(e^{-2\lambda_\phi \varepsilon} + e^{-\lambda_\phi \varepsilon} - 1\right). \tag{E.77}$$

En posant

$$r_\varepsilon = \frac{r + r'}{N},$$

qui n'est autre que le ratio de valeurs aberrantes parmi l'ensemble des occurences de $\{w_t\}$ et $\{f_t\}$ par rapport à ε, ε', la condition (E.77) peut être réécrite sous la forme

$$p^{\exp}_{r,r'} \leq (1 - r_\varepsilon)\, e^{-2\lambda_\phi \varepsilon} - r_\varepsilon e^{-\lambda_\phi \varepsilon} + r_\varepsilon. \tag{E.78}$$

Nous avons donc deux contraintes sur $p^{\exp}_{r,r'}$:

- $p^{\exp}_{r,r'} < 1$ afin que l'inégalité (E.76) soit vraie.

- $p^{\exp}_{r,r'}$ doit vérifier (E.78) pour que la partie droite de (E.76) soit plus petite que 1.

Seule la plus forte des deux contraintes doit être respectée, c'est-à-dire

$$p^{\exp}_{r,r'} < \min\left(1, (1-r_\varepsilon)\, e^{-2\lambda_\phi \varepsilon} - r_\varepsilon e^{-\lambda_\phi \varepsilon} + r_\varepsilon\right)$$

Le lemme suivant décrit sous quelles conditions (E.78) est la contrainte la plus forte :

Lemme E.4.1. *Supposons que les conditions de la Proposition E.4.1 sont vérifiées. Alors, si* $(r+r')/N = r_\varepsilon < 4/5$, *on a pour tout* $\varepsilon \geq 0$,

$$0 \leq r_\varepsilon \left[\left(\frac{1}{r_\varepsilon} - 1\right) e^{-2\lambda_\phi \varepsilon} - e^{-\lambda_\phi \varepsilon} + 1\right] \leq 1 \tag{E.79}$$

Le Lemme E.4.1 montre que si les valeurs extrêmes de $\{w_t\}$ et $\{f_t\}$ représentent moins de 80% de leurs occurrences totales, alors la condition la plus forte sur $p^{\exp}_{r,r'}$ est la condition (E.78). Si le ratio de valeurs extrêmes est plus grand que ce seuil de 80%, cette condition peut toujours avoir du sens mais seulement pour certaines valeurs de ε. Il est toutefois à noter que s'il y a plus de 80% de valeurs extrêmes, elles constitueraient plus la norme que l'exception au sein de $\{w_t\}$ et $\{f_t\}$ qui ne seraient donc plus vraiment des bruits aberrants.

Dans la plupart des cas, le résultat obtenu dans la Proposition E.4.1 ne permet pas de statuer sur la vraie valeur de l'erreur d'estimation du fait qu'il n'y pas de lien direct entre la norme de l'erreur d'estimation et la valeur de $\frac{1}{N}\left(\Phi_{\mathbb{S}_1}(E) + \Psi_{\mathbb{S}_2}(E)\right)$. Cependant, $\frac{1}{N}\left(\Phi_{\mathbb{S}_1}(E) + \Psi_{\mathbb{S}_2}(E)\right)$ reste une image de l'erreur d'estimation : elle est donc faible si l'erreur d'estimation est faible, et élevée si l'erreur d'estimation est élevée. Trois cas particuliers sont intéressants à mentionner :

- **Absence de bruit dense dans le système :** dans ce cas, on peut choisir $\varepsilon = \varepsilon' = 0$. Cela entraîne que $w_t[i]$ et $f_t[j]$ sont strictement creux ou bien que toute valeur non nulle peut être considérée comme aberrante. Si les conditions de la Proposition E.4.1 sont vérifiées, nous obtenons alors

$$\frac{1}{N}\left(\Phi_{\mathbb{S}_1}(\hat{X} - X) + \Psi_{\mathbb{S}_2}(\hat{X} - X)\right) \leq \frac{r_\varepsilon}{1 - p^{\exp}_{r,r'}}.$$

  Dans ce cas de figure, nous remarquons que la borne n'est pas égale à zéro, ce qui veut dire que les valeurs aberrantes ont un impact non nul mais borné sur cette borne supérieure. Ce constat semble donc indiquer que les estimateurs $\mathcal{E}^{exp}$ sont presque résilients mais pas strictement résilients.

- **Aucune valeur aberrante :** dans ce cas, nous avons $r_\varepsilon = r = r' = 0$. Seuls des bruits denses sont présents dans le système et les perturbations sont bornées, c'est-à-dire que $\phi_t(w_t[i]) \leq \varepsilon$ et $\psi_t(f_t[j]) \leq \varepsilon'$ pour tout $(t,i,j) \in \mathbb{T} \times \mathbb{I} \times \mathbb{J}$. Par définition, $p^{\exp}_{0,0} = 0$, donc les conditions de la Proposition E.4.1 sont forcément vérifiées, ce qui entraîne

$$\frac{1}{N}\left(\Phi_{\mathbb{S}_1}(\hat{X} - X) + \Psi_{\mathbb{S}_2}(\hat{X} - X)\right) \leq 1 - e^{-2\lambda_\phi \varepsilon}.$$

  Plus le seuil ε est petit, plus la borne sera resserrée.

- **Aucun bruit dans le système :** ce cas combine les deux cas précédents, à savoir $r_\varepsilon = 0$ et $\varepsilon = 0$. Il est alors évident que la partie droite de (E.76) est égale à zéro, ce qui donne

$$\frac{1}{N}\left(\Phi_{\mathbb{S}_1}(\hat{X} - X) + \Psi_{\mathbb{S}_2}(\hat{X} - X)\right) = 0.$$

Nous observons alors que $\Phi_{\mathbb{S}_1}(E) + \Psi_{\mathbb{S}_2}(E)$ est égal zéro, tous les termes exponentiels contenu dans l'expression (voir (E.69)–(E.70)) doivent être égaux à 1. Cela entraîne

$$\begin{aligned} &\forall (t,i) \in \mathbb{S}_1, && e_{t+1}[i] - a_i^\top e_t = 0 \\ &\forall (t,j) \in \mathbb{S}_2, && c_j^\top e_t = 0, \end{aligned}$$

qui implique $E = 0$, étant donné que le système est observable sur $[0, T-1]$. Par conséquent, lorsqu'il n'y a aucun bruit dans le système, si les conditions de la Proposition E.4.1 sont vérifiées, alors l'estimateur $\mathcal{E}^{\exp}$ renvoie la vraie trajectoire d'état du système, ce qui montre qu'il est bien défini.

E.4.4 Cas particulier de l'absence de bruit d'état

Cette section a pour but de montrer comment $\mathcal{E}^{\exp}$ peut être spécialisé pour gérer le cas d'un bruit d'état $\{w_t\}$ nul à tout instant, et présente un résultat sur la résilience approchée de cet estimateur spécialisé.

Dans une telle configuration, nous pouvons utiliser l'information quant à l'absence de bruit d'état pour restreindre l'espace de recherche pour les trajectoires d'état à l'ensemble $\mathcal{Z}_\Sigma$ défini par (E.43). Cet ensemble contient toutes les matrices de trajectoires Z qui respectent exactement la dynamique du système, c'est-à-dire que pour tout t dans $\mathbb{T}'$, $z_{t+1} = A_t z_t$. À partir de cet ensemble, on définit alors l'estimateur $\mathcal{E}^{\circ,\exp}$, minimisant $V_\Sigma^{\exp}$, telle que définie dans (E.63), sur l'ensemble $\mathcal{Z}_\Sigma$, c'est-à-dire

$$\mathcal{E}^{\circ,\exp}(Y) = \operatorname*{arg\,min}_{Z \in \mathcal{Z}_\Sigma} V_\Sigma^{\exp}(Y, Z). \tag{E.80}$$

Cette information permet également de se débarrasser de la somme de gauche dans $V_\Sigma^{\exp}$ étant donné qu'elle est égale à 0 pour tout Z dans $\mathcal{Z}_\Sigma$. $\mathcal{E}^{\circ,\exp}(Y)$ peut alors être réécrit plus simplement :

$$\mathcal{E}^{\circ,\exp}(Y) = \left\{\hat{X} = \begin{pmatrix}\hat{x}_0 & A\hat{x}_0 & \cdots & A^{T-1}\hat{x}_0\end{pmatrix} : \hat{x}_0 \in \operatorname*{arg\,min}_{z \in \mathbb{R}^n} V_\Sigma^{\circ,\exp}(Y, z)\right\} \tag{E.81}$$

avec

$$V_\Sigma^{\circ,\exp}(Y, z_0) = \sum_{(t,j) \in \mathbb{T} \times \mathbb{J}} \left(1 - e^{-\lambda_\psi \psi(y_t[j] - \theta_{t,j}^\top z_0)}\right) \tag{E.82}$$

où les $\theta_{t,j}^\top$ sont les lignes de la matrice d'observabilité définies par $\theta_{t,j}^\top = c_j^\top A^{t-1}$.

Ainsi, l'estimation de la trajectoire d'état peut être également réduite (comme avec $\mathcal{E}^\circ$ à la Section E.3.4) à l'estimation de l'état initial x_0. Adaptant un résultat issu de [Bak18] aux estimateurs d'états, nous allons étudier la résilience de cette nouvelle classe d'estimateurs. Après avoir présenté des remarques préliminaires et mis en place quelques notations, nous établirons le résultat principal, qui montre la résilience approchée de $\mathcal{E}^{\circ,\exp}$.

Remarques préliminaires

Sans perte de généralité, on peut supposer qu'il n'existe pas de (t, j) dans $\mathbb{T} \times \mathbb{J}$ tel que $\|\theta_{t,j}\|_2 = 0$.[1] On définit alors le paramètre suivante

$$\sigma_\Sigma = \min_{(t,j)\in\mathbb{T}\times\mathbb{J}} \|\theta_{t,j}\|_2 > 0 \tag{E.83}$$

De plus, étant donné ρ dans $[0, 1]$ et $z_0 \in \mathbb{R}^n$, on définit également l'ensemble d'indices (t, j) suivant :

$$\mathcal{J}_\Sigma(z_0, \rho) = \left\{(t, j) \in \mathbb{T} \times \mathbb{J} \ : \ |\theta_{t,j}^\top z_0| \geq \rho\|\theta_{t,j}\|_2\|z_0\|_2\right\} \tag{E.84}$$

Cet ensemble sélectionne les lignes de la matrice d'observabilité qui ont presque la même direction que z_0. (t, j) appartient à $\mathcal{J}_\Sigma(z_0, \rho)$ si et seulement si le vecteur $\theta_{t,j}$ est à l'intérieur du cône de direction z_0 et de demi-angle au sommet $\arccos(\rho)$. Si $\rho = 1$, alors $\mathcal{J}_\Sigma(z_0, \rho)$ collecte tous les $\theta_{t,j}$ qui sont colinéaires à z_0. À l'autre extrême, si $\rho = 0$, $\mathcal{J}_\Sigma(z_0, \rho)$ contient toutes les lignes de la matrice $\mathcal{O}_{T-1}$, *i.e.* $\mathcal{J}_\Sigma(z_0, \rho) = \mathbb{T} \times \mathbb{J}$. Comme nous allons le montrer via le Lemme E.4.2 ci-dessous, la cardinalité de $\mathcal{J}_\Sigma(z_0, \rho)$ peut-être considérée comme une mesure locale de l'observabilité en z_0, étant donné qu'elle représente combien de $\theta_{t,j}$ sont presque dans la direction de z_0 avec une tolérance de ρ. La Figure E.5 propose par ailleurs une représentation visuelle de $\mathcal{J}_\Sigma(z_0, \rho)$.

Idéalement, les $\theta_{t,j}$ couvrent finement toutes les directions de $\mathbb{R}^n$ afin que $\mathcal{J}_\Sigma(z_0, \rho)$ soit aussi grand que possible pour tout z_0. Cependant, il est à noter qu'une telle propriété est très forte. En identification des systèmes, par exemple, la matrice de données utilisée pour un tel type d'analyse peut en théorie être rendue aussi riche que nécessaire en générant un signal d'entrée approprié. En revanche, les propriétés de la matrice d'observabilité $\mathcal{O}_{T-1}$ sont bien moins contrôlables étant donné qu'elle est très structurée par la paire (A, C).

Nous définissons également le paramètre global d'observabilité suivant :

$$R_\Sigma(\rho) = \frac{1}{mT} \inf_{z_0\in\mathbb{R}^n} |\mathcal{J}_\Sigma(z_0, \rho)|. \tag{E.85}$$

R_Σ est un rapport, étant donné que pour tout ρ dans $[0, 1]$, $\mathcal{J}_\Sigma(z_0, \rho) \subseteq \mathbb{T} \times \mathbb{J}$ et $|\mathbb{T} \times \mathbb{J}| = mT$. Par conséquent, R_Σ est toujours compris entre 0 et 1. De plus, R_Σ est décroissant par rapport à ρ : en particulier, si $\rho = 0$, alors $R_\Sigma(\rho) = 1$. Plus $R_\Sigma(\rho)$ est proche de 1 pour des valeurs élevées de ρ, plus le système sera considéré observable.

Le lemme suivant donne un peu plus de contexte sur le lien entre $R_\Sigma(\rho)$ et l'observabilité du système :

Lemme E.4.2. *Soit Σ un système défini par (E.2). Les deux propositions suivantes sont équivalentes :*

(i) Le système est observable, soit $\text{rank}(\mathcal{O}_T) = n$.

(ii) Il existe $\rho \in]0, 1]$ tel que $R_\Sigma(\rho) \neq 0$.

Ce lemme montre que l'observabilité est une condition équivalente à l'existence d'un $\rho \in]0, 1]$ tel que $R_\Sigma(\rho) \neq 0$. Σ sera donc dorénavant supposé observable.

[1] Si la matrice d'observabilité $\mathcal{O}_{T-1}$ (voir Eq. (E.8)) contient des lignes nulles, la même analyse peut être menée avec une matrice contenant toutes les lignes non nulles de $\mathcal{O}_{T-1}$.

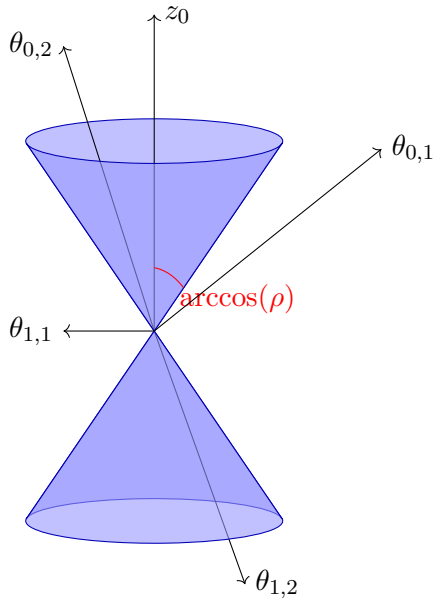

FIGURE E.5: Interprétation géomtrique de $\mathcal{J}_\Sigma(z_0, \rho)$: l'ensemble collecte tous les indices (t, j) tels que $\theta_{t,j}$ est à l'intérieur du cône bleu

Enfin, étant donné ε un réel positif, pour tout bruit $\{f_t[j]\}$, il est possible de partitionner $\mathbb{T} \times \mathbb{J}$ en deux ensembles disjoints

$$\mathcal{I}_\varepsilon = \{(t, j) \in \mathbb{T} \times \mathbb{J} \ : \ |f_t[j]| \leq \varepsilon\}, \tag{E.86}$$

qui réunit les indices de $f_t[j]$ tels que sa valeur absolue est plus petite que ε, et

$$\mathcal{I}_\varepsilon^c = \{(t, j) \in \mathbb{T} \times \mathbb{J} \ : \ |f_t[j]| > \varepsilon\}, \tag{E.87}$$

qui réunit les valeurs aberrantes par rapport à ε de $\{f_t[j]\}$. ε est donc un seuil que nous pouvons choisir et régler dans le cadre de notre analyse

Borne sur l'erreur d'estimation

Dans le théorème suivant, nous allons exprimer dans quelles circonstances la norme de l'erreur d'estimation sur l'état initial du système, c'est-à-dire $e_0 = \hat{x}_0 - x_0$, et par voie de conséquence celle de l'erreur d'estimation sur toute la trajectoire d'état $E = \hat{X} - X$, peut être bornée par des valeurs qui ne dépendent pas des occurrences aberrantes de f_t:

Theorème E.4.1. *Soit un estimateur d'état* (E.81)–(E.82) *défini pour le système* (E.2) *avec ψ qui vérifie les propriétés (P4.1)–(P4.3) ainsi que (P4.4) pour un $\gamma_\psi > 0$ donné. Soit $\varepsilon \geq 0$. Pour toute séquence de bruit $\{f_t\}$ et tout état initial x_0 dans* (E.2)*, générant une matrice de mesure Y, tels que*

$$\frac{1}{1 + e^{-\lambda_\psi \psi(\varepsilon)}} R_\Sigma(\rho) + e^{-\lambda_\psi \psi(\varepsilon)} \frac{|\mathcal{I}_\varepsilon|}{mT} > 1, \tag{E.88}$$

est vérifié pour un ρ dans $]0, 1]$, l'inégalité suivante est vraie :

$$\forall \hat{X} \in \mathcal{E}^{\circ,\exp}(Y), \ \psi(\rho \sigma_\Sigma \|e_0\|_2) \leq \frac{1}{\lambda_\psi \gamma_\psi} \ln(1/\mu) \tag{E.89}$$

avec $e_0 = \hat{x}_0 - x_0$ *et*

$$\mu = \frac{1 + e^{-\lambda_\psi \psi(\varepsilon)}}{\frac{|\mathcal{I}_\varepsilon|}{mT} + R_\Sigma(\rho) - 1} \left[\frac{1}{1 + e^{-\lambda_\psi \psi(\varepsilon)}} R_\Sigma(\rho) + e^{-\lambda_\psi \psi(\varepsilon)} \frac{|\mathcal{I}_\varepsilon|}{mT} - 1 \right] \tag{E.90}$$

De plus, si ψ *est strictement croissante sur* $\mathbb{R}_{\geq 0}$*, alors*

$$\mathfrak{N}(\hat{X} - X) \leq \frac{M_\Sigma}{\rho \sigma_\Sigma} \psi^{-1} \left(\frac{1}{\lambda_\psi \gamma_\psi} \ln(1/\mu) \right) \tag{E.91}$$

avec $\mathfrak{N}(\hat{X} - X) = \max_{t \in \mathbb{T}} \|\hat{x}_t - x_t\|_2$ *et* M_Σ *une constante dépendant de la dynamique du système.*

Le résultat de ce théorème est que l'estimateur $\mathcal{E}^{\circ,\exp}$ produit une erreur d'estimation qui est bornée malgré la présence d'un bruit de mesure arbitraire qui peut potentiellement prendre n'importe quelle valeur. Malheureusement, la condition (E.88) ne peut pas être facilement vérifiée étant donné que calculer $R_\Sigma(\rho)$ est un problème combinatoire et qu'avoir accès à $|\mathcal{I}_\varepsilon|$ demande de connaître à l'avance la proportion de valeurs aberrantes (par rapport à ε) dans $\{f_t[j]\}$. Toutefois, cette condition nous donne des informations pertinentes pour s'assurer que l'estimateur est bien approximativement résilient. En effet, l'inégalité est composée de trois termes. La gauche de l'inégalité est composée de deux termes, l'un qui dépend de l'observabilité du système par le biais de $R_\Sigma(\rho)$, et l'autre qui dépend du nombre de valeurs raisonnables du bruit de mesure par rapport à ε. La droite de l'inégalité présente un unique terme, constant, qui est égal au nombre total de mesures sur l'horizon de temps considéré. Pour augmenter les chances que cette condition soit vérifiée, il est donc nécessaire de s'intéresser à deux points importants :

- Il faut que le critère d'observabilité $R_\Sigma(\rho)$ soit aussi proche de 1 que possible pour un grand ρ.
- Le nombre de valeurs aberrantes doit être suffisamment faible, du fait que $|\mathcal{I}_\varepsilon^c|$ doit être petit.

L'interprétation qui peut être faite de la condition (E.88) est que l'erreur sur l'estimation d'état est bornée si le système est suffisamment observable, et plus il est observable, plus l'estimateur sera capable de gérer de valeurs aberrantes.

La borne présente dans (E.91) donne également des informations sur quels paramètres du système ont un impact sur la qualité de l'estimation : outre les conclusions obtenues par l'étude de la condition (E.88), on observe que les valeurs de ρ et ε jouent également un rôle dans la qualité de la borne. En effet, si l'on ne considère par leur influence sur $\mathcal{I}_\varepsilon$ et $R_\Sigma(\rho)$, alors la borne se resserre lorsque ρ croît et/ou lorsque ε décroît. Ainsi, étant donné que la borne existe pour tout couple (ρ, ε) qui vérifie la condition (E.88), la meilleure borne que l'on peut obtenir grâce au Theorème E.4.1 serait

$$\mathfrak{N}(E) \leq M_\Sigma \min_{\substack{(\rho,\varepsilon) \\ \mu > 0}} \left[\frac{1}{\rho \sigma_\Sigma} \psi^{-1} \left(\frac{1}{\lambda_\psi \gamma_\psi} \ln(1/\mu) \right) \right] \tag{E.92}$$

Il est cependant à noter que cette borne est sans doute très conservative du fait des nombreuses sous-estimations et surestimations utilisées afin de l' obtenir. Par conséquent, son intérêt principal repose moins sur sa valeur exacte que sur l'information qu'elle donne sur l'interaction entre les paramètres du système et la qualité de l'estimation. Cette interaction nous donne alors une idée de quels sont les paramètres clés à prendre en compte lorsqu'on estime l'état d'un système.

Cas d'un système avec un bruit d'état borné

On suppose à présent que le bruit d'état w_t présent dans (E.3) n'est plus égal à zéro mais est dorénavant dense. Bien que l'estimateur $\mathcal{E}^{\circ,\exp}$ ne soit pas conçu pour ce cas de figure, il peut quand même être appliqué au système Σ. En effet, nous remarquons que pour tout système Σ, il existe un système $\tilde{\Sigma}$ tel que

$$\tilde{\Sigma} : \begin{cases} \tilde{x}_{t+1} = A\tilde{x}_t \\ y_t = C\tilde{x}_t + \tilde{f}_t \end{cases} \tag{E.93}$$

avec $\tilde{x}_0 = x_0$, $\tilde{f}_t = C\tilde{w}_t + f_t$ et $\tilde{w}_t = \sum_{k=0}^{t-1} A^k w_k$. Ce nouveau système possède une structure de système LTI (E.3) et produit la même sortie que Σ mais présente un bruit d'état nul. De plus, l'écart entre x_t et $\tilde{x}_t$ peut être quantifié, et est égal à $x_t - \tilde{x}_t = A^t x_0 + \tilde{w}_t - A^t x_0 = \tilde{w}_t$. Ainsi, on peut obtenir le corollaire suivant à partir du Théorèm E.4.1 :

Corollaire E.4.1.1. *Considérons l'estimateur (E.81)–(E.82) pour un système (E.3) avec ψ une fonction inversible vérifiant les propriétés (P4.1)–(P4.4). Soit $\varepsilon \geq 0$. Pour tout bruit d'état $\{w_t\}$ borné, tout bruit de mesure $\{f_t\}$ et tout état initial x_0 dans (E.3), générant une matrice de mesure Y, tels que (E.88) est vérifiée pour un ρ dans $]0,1]$, l'inégalité suivante est vraie :*

$$\forall \hat{X} \in \mathcal{E}^{\circ,\exp}(Y), \qquad \mathfrak{N}(\hat{X} - X) \leq \frac{M_\Sigma}{\rho\sigma_\Sigma}\psi^{-1}\left(\frac{1}{\lambda_\psi \gamma_\psi}\ln(1/\mu)\right) + \max_{t\in\mathbb{T}}\|\tilde{w}_t\|_2 \tag{E.94}$$

avec $\tilde{w}$ tel que défini dans (E.93) et μ, $\mathfrak{N}$ et M_Σ tels que définis dans le Théorème E.4.1.

Ce corollaire montre que l'estimateur $\mathcal{E}^{\circ,\exp}$ reste résilient de manière approchée malgré la présence d'un bruit d'état dense dans le système.

E.4.5 Implémentation de $\mathcal{E}^{\exp}$ et $\mathcal{E}^{\circ,\exp}$

Contrairement à $\mathcal{E}$ et $\mathcal{E}^\circ$, il serait très compliqué d'implémenter $\mathcal{E}^{\exp}$ et $\mathcal{E}^{\circ,\exp}$ en résolvant le problème d'optimisation sous-jacent. En effet, si V_Σ peut être choisie convexe en sélectionnant les bonnes fonctions coût, $V_\Sigma^{\exp}$ (et $V_\Sigma^{\circ,\exp}$) ne peut pas l'être.

Par conséquent, nous avons développé des algorithmes heuristiques pour implémenter une version approchée du problème d'optimisation original définissant $\mathcal{E}^{\exp}$ et $\mathcal{E}^{\circ,\exp}$ dans le cas où ϕ et ψ sont toutes les deux égales à la fonction carrée, c'est-à-dire pour tout a dans $\mathbb{R}$, $\phi(a) = \psi(a) = a^2$. Dans un premier temps, nous expliciterons le problème d'optimisation convexe choisi, puis nous verrons deux algorithmes pour le résoudre, l'un par paquet, et l'autre récursif.

Problème d'optimisation convexe alternatif

L'objectif de cette section est de donner quelques éléments pour justifier le problème d'optimisation convexe utilisé pour remplacer celui définissant $\mathcal{E}^{\exp}$ et $\mathcal{E}^{\circ,\exp}$. Pour une question de simplicité, nous discuterons de ces éléments dans le cadre de $\mathcal{E}^{\circ,\exp}$. Le cas de l'estimateur $\mathcal{E}^{\exp}$ sera ensuite donné en remarque.

Pour $\hat{x}_0$ dans $\mathcal{E}^{\circ,\exp}(Y)$, si on définit $\{\beta_{t,j}\}$ une famille de pondérations réelles construite telle que

$$\forall (t,j) \in \mathbb{T}\times\mathbb{J}, \qquad \beta_{t,j} = \lambda_\psi e^{-\lambda_\psi\left(y_t[j] - \theta_{t,j}^\top \hat{x}_0\right)^2}, \tag{E.95}$$

alors la fonction quadratique V_q° telle que pour tout (Y, z) dans $\mathbb{R}^{m\times T} \times \mathbb{R}^n$,

$$V_q^\circ(Y, z) = \sum_{(t,j)\in\mathbb{T}\times\mathbb{J}} \beta_{t,j} \left(y_t[j] - \theta_{t,j}^\top z\right)^2, \tag{E.96}$$

a $\hat{x}_0$ comme unique vecteur minimisant si le système est observable [Boy04, Ex. 4.5]. Ceci peut être vérifié en considérant le gradient de $V_\Sigma^{\circ,\exp}$ qui est différentiable par rapport à z. En effet, en tant qu'argument minimisant de cette fonction, $\hat{x}_0$ est un point critique de $V_\Sigma^{\circ,\exp}$ et doit donc annuler son gradient. L'équation stationnaire résultante est alors la même que celle obtenue en différentiant V_q°, ce qui montre que les deux vecteurs minimisant coïncident.

Si nous avions accès en amont à toutes les valeurs de $\{\beta_{t,j}\}$, minimiser V_q° permettrait alors d'obtenir $\hat{x}_0$ sans avoir à minimiser V°. Néanmoins, $\{\beta_{t,j}\}$ dépend de $\hat{x}_0$ que l'on cherche à estimer en premier lieu : la démarche est alors de trouver une approximation $\{\hat{\beta}_{t,j}\}$ suffisamment bonne de la vraie famille de pondérations $\{\beta_{t,j}\}$ afin de résoudre le problème d'optimisation convexe

$$\arg\min_{z\in\mathbb{R}^n} \left\{ \sum_{(t,j)\in\mathbb{T}\times\mathbb{J}} \hat{\beta}_{t,j} \left(y_t[j] - \theta_{t,j}^\top z\right)^2 \right\}, \tag{E.97}$$

et d'obtenir une approximation de $\hat{x}_0$.[2] Les deux algorithmes que nous allons présenter ensuite seront deux façons différentes d'approcher les valeurs de $\{\beta_{t,j}\}$ pour résoudre le problème d'optimisation (E.97).

Remarque E.4.2. *Nous pouvons appliquer le même raisonnement à l'estimateur $\mathcal{E}^{\exp}$ défini par (E.66). Ainsi, on définit deux familles de pondérations strictement positives $\{\alpha_{t,i}\}$ et $\{\beta_{t,j}\}$ telles que*

$$\forall (t, i) \in \mathbb{T}' \times \mathbb{I}, \alpha_{t,i} = \lambda_\phi e^{-\lambda_\phi \left(\hat{x}_{t+1}[i] - a_i^\top \hat{x}_t\right)^2} \tag{E.98}$$

$$\forall (t, j) \in \mathbb{T} \times \mathbb{J}, \beta_{t,j} = \lambda_\psi e^{-\lambda_\psi \left(y_t[j] - c_j^\top \hat{x}_t\right)^2}, \tag{E.99}$$

avec $\hat{X} = (\,\hat{x}_0 \quad \cdots \quad \hat{x}_{T-1}\,)$ dans $\mathcal{E}^{\exp}(Y)$.

Le but de la méthode est alors de trouver deux familles d'approximations $\{\hat{\alpha}_{t,i}\}$ et $\{\hat{\beta}_{t,j}\}$ de sorte à résoudre

$$\arg\min_{Z\in\mathbb{R}^{n\times T}} \left\{ \sum_{(t,i)\in\mathbb{T}'\times\mathbb{I}} \hat{\alpha}_{t,i} \left(z_{t+1}[i] - a_i^\top z_t\right)^2 + \sum_{(t,j)\in\mathbb{T}\times\mathbb{J}} \hat{\beta}_{t,j} \left(y_t[j] - c_j^\top z_t\right)^2 \right\}, \tag{E.100}$$

et pouvoir ainsi obtenir une approximation de $\hat{X}$.[2]

Implémentation approchée par paquet : un algorithme des moindres carrés itératifs

La première approche que nous allons considérer consiste à résoudre itérativement le problème défini par (E.100) pour pouvoir ensuite mettre à jour les pondérations $\{\alpha_{t,i}\}$

[2] Tant que le système est observable, et $\{\hat{\alpha}_{t,j}\}$, $\{\hat{\beta}_{t,j}\}$ sont des familles de pondérations strictement positives, les problèmes d'optimisation (E.97) et (E.100) renverront un singleton. [Boy04, Ex. 4.5]

et $\{\beta_{t,j}\}$ grâce à la dernière estimée obtenue. L'Annexe C.2, quant à elle, présente l'utilisation de ce même méthode pour implémenter $\mathcal{E}^{\circ,\exp}$ de manière approchée.

Le principe de cette méthode repose sur le fait qu'à chaque itération, nous résolverons le problème d'optimisation

$$\{\hat{X}^{(k)}\} = \underset{Z\in\mathbb{R}^{n\times T}}{\arg\min}\, V_q^{(k)}(Y,Z), \tag{E.101}$$

avec $V_q^{(k)}$ la fonction quadratique telle que pour tout (Y,Z) dans $\mathbb{R}^{m\times T}\times\mathbb{R}^{n\times T}$,

$$V_q^{(k)}(Y,Z) = \sum_{(t,i)\in\mathbb{T}'\times\mathbb{I}} \alpha_{t,i}^{(k)} \left(z_{t+1}[i] - a_i^\top z_t\right)^2 + \sum_{(t,j)\in\mathbb{T}\times\mathbb{J}} \beta_{t,j}^{(k)} \left(y_t[j] - c_j^\top z_t\right)^2. \tag{E.102}$$

$\{\alpha_{t,i}^{(k)}\}$ et $\{\beta_{t,j}^{(k)}\}$ sont deux familles de pondérations strictement positives telles que pour tout $k\in\mathbb{N}$,

$$\forall (t,i)\in\mathbb{T}'\times\mathbb{I},\ \alpha_{t,i}^{(k+1)} = \lambda_\phi e^{-\lambda_\phi\left(\hat{x}_{t+1}^{(k)}[i] - a_i^\top \hat{x}_t^{(k)}\right)^2} \tag{E.103}$$

$$\forall (t,j)\in\mathbb{T}\times\mathbb{J},\ \beta_{t,j}^{(k+1)} = \lambda_\psi e^{-\lambda_\psi\left(y_t[j] - c_j^\top \hat{x}_t^{(k)}\right)^2}. \tag{E.104}$$

Enfin, les familles d'initialisation $\{\alpha_{t,i}^{(1)}\}$ et $\{\beta_{t,j}^{(1)}\}$ seront telles que

$$\forall (t,i)\in\mathbb{T}'\times\mathbb{I},\ \alpha_{t,i}^{(1)} = \lambda_\phi$$
$$\forall (t,j)\in\mathbb{T}\times\mathbb{J},\ \beta_{t,j}^{(1)} = \lambda_\psi e^{-\lambda_\psi y_t[j]^2}.$$

Le raisonnement derrière le choix de $\{\beta_{t,j}^{(1)}\}$ est de normaliser les contributions de chaque terme dans la somme de droite de $V_q^{(1)}$ (voir Eq. (E.102)). Cela empêche que les termes associés à une valeur de $y_t[j]$ grande comparée à d'autres (si elle est perturbée par une valeur aberrante du bruit de mesure, par exemple) ne prennent une place trop grande par rapport au reste des termes. En absence de connaissance *a priori*, chaque pondération $\alpha_{t,i}^{(1)}$ est choisie égale à λ_ϕ de sorte à pondérer uniformément tous les termes présents de la somme de gauche de (E.101). La valeur en elle-même λ_ϕ permet de maintenir l'équilibre entre les deux sommes (gauche et droite) de $V_q^{(1)}$ qui sont pondérées par λ_ϕ et λ_ψ respectivement.

La condition d'arrêt de l'algorithme consiste à vérifier si la trajectoire $\hat{X}^{(k)}$, obtenue à l'itération k, est vraiment différente de celle obtenue à $\hat{X}^{(k-1)}$, la trajectoire d'état estimée à la précédente itération : pour ce faire, nous calculons la *valeur d'arrêt*

$$\eta^{(k)} = \frac{\|\hat{X}^{(k)} - \hat{X}^{(k-1)}\|_2}{\|\hat{X}^{(k-1)}\|_2}$$

et arrêtons l'algorithme une fois que cette valeur est plus petite qu'un certain seuil $\eta_{\min}$ spécifié en entrée de l'algorithme.

Enfin, en plus de la condition d'arrêt, nous spécifions également un nombre maximum d'itérations $k_{\max}$ au-delà duquel nous arrêtons l'algorithme si la condition d'arrêt n'a pas été vérifiée.

L'algorithme obtenu est présenté dans l'Algorithme E.3.

Algorithme E.3 Algorithme des moindres carrés itératifs pour implémenter approximativement le problème (E.100)

Entrée: Σ, λ_ϕ, λ_ψ, Y, $k_{\max}$, $\eta_{\min}$
Initialisation:
$k \leftarrow 0$
$\eta^{(0)} \leftarrow 10^8$
$\forall (t,i) \in \mathbb{T} \times \mathbb{I}$, $\hat{x}_t^{(0)}[i] \leftarrow 10^5$
$\forall (t,i) \in \mathbb{T} \times \mathbb{I}$, $\alpha_{t,i}^{(1)} \leftarrow \lambda_\phi$
$\forall (t,j) \in \mathbb{T} \times \mathbb{J}$, $\beta_{t,j}^{(1)} \leftarrow \lambda_\psi e^{-\lambda_\psi y_t[j]^2}$
Fin de l'initialisation.
Tant que $\eta^{(k)} > \eta_{\min}$ **et** $k < k_{\max}$
$k \leftarrow k+1$
$\hat{X}^{(k)} \leftarrow \arg\min_{Z \in \mathbb{R}^{n \times T}} V_q^{(k)}(Y,Z)$
$\forall (t,i) \in \mathbb{T} \times \mathbb{I}$, $\alpha_{t,i}^{(k+1)} \leftarrow \lambda_\phi e^{-\lambda_\phi (\hat{x}_{t+1}^{(k)}[i] - a_i^\top \hat{x}_t^{(k)})^2}$
$\forall (t,j) \in \mathbb{T} \times \mathbb{J}$, $\beta_{t,j}^{(k+1)} \leftarrow \lambda_\psi e^{-\lambda_\psi (y_t[j] - c_j^\top \hat{x}_t^{(k)})^2}$
$\eta^{(k)} \leftarrow \frac{\|\hat{X}^{(k)} - \hat{X}^{(k-1)}\|}{\|\hat{X}^{(k-1)}\|}$
Fin tant que
Retourne $\hat{X}^{(k)}$

Implémentation récursive approchée : application du Forward Dynamic Programming

De manière similaire à la Section E.3.6, cette méthode consiste à utiliser le Forward Dynamic Programming (FDP) afin d'implémenter récursivement (E.100).

Pour ce faire, nous définissons la fonction $V_{q,T}^\star$ telle que pour tout $T \in \mathbb{N}$,

$$\forall (Y,z) \in \mathbb{R}^{m \times T} \times \mathbb{R}^n, \qquad V_{q,T}^\star(Y,z) = \min_{\substack{Z \in \mathbb{R}^{n \times T} \\ z_T = z}} V_q(Y,Z)$$

Encore une fois, Y, Z et V_q dépendent tous de T de manière implicite étant donné qu'elles ont été définies sur l'horizon de temps T.

L'équation de Bellman (E.14) donne la relation entre $V_{q,T+1}^\star$ et $V_{q,T}^\star$ qui est telle que pour tout T dans $\mathbb{N}$,

$$V_{q,T+1}^\star(z) = \min_{s \in \mathbb{R}^n} \left\{ V_{q,T}^\star(s) + \sum_{i \in \mathbb{I}} \alpha_{T,i} \left(z[i] - a_i^\top s \right)^2 \right\} + \sum_{j \in \mathbb{J}} \beta_{T+1,j} \left(y_{T+1}[j] - c_j^\top z \right)^2$$

Si nous avions connaissance des coefficients $\{\alpha_{T,i}\}$ et $\{\beta_{T+1,j}\}$ dans cette relation, nous pourrions appliquer le Théorème E.2.3. Le calcul de ces coefficients nécessite cependant la valeur de $\hat{x}_{T+1}$. Nous avons donc besoin d'une estimation *a priori* de $\hat{x}_{T+1}$, pour laquelle on choisit $\hat{x}_{T+1|T} = A_T \hat{x}_T$, afin d'approcher les valeurs de $\{\alpha_{T,i}\}$ et de $\{\beta_{T+1,j}\}$.

Nous définissons alors les familles $\{\hat{\alpha}_{T,i}\}$ et $\{\hat{\beta}_{T+1,j}\}$ pour tout T dans $\mathbb{N}$:

$$\forall i \in \mathbb{I}, \hat{\alpha}_{T,i} = \lambda_\phi e^{-\lambda_\phi \left(\hat{x}_{T+1|T}[i] - a_i^\top \hat{x}_T \right)^2} = \lambda_\phi \tag{E.105}$$

$$\forall j \in \mathbb{J}, \hat{\beta}_{T+1,j} = \lambda_\psi e^{-\lambda_\psi \left(y_{T+1}[j] - c_j^\top \hat{x}_{T+1|T} \right)^2}. \tag{E.106}$$

On peut noter qu'avec cette estimation *a priori* de $\hat{x}_T$, les pondérations $\{\hat{\alpha}_{T,i}\}$ sont toutes égales à λ_ϕ du fait que $\hat{x}_{T+1|T}[i] = a_i^\top \hat{x}_T$ pour tout (T,i) dans $\mathbb{N} \times \mathbb{I}$. Cela peut s'interpréter comme le fait qu'aucune information sur la valeur du bruit d'état w_T à l'instant T n'est contenue dans l'estimation *a priori* $\hat{x}_{T+1|T}$ puisque cette dernière est basée sur l'application de la dynamique exacte du système sur l'estimée $\hat{x}_T$.

C'est un problème courant lorsqu'on utilise des termes exponentiels dans les fonctions de performance, comme par exemple le filtre de correntropie dérivé dans [Iza16, Eq. (17)]. Une manière classique de le résoudre est d'itérer le processus d'estimation de $\hat{x}_T$ à la manière de la méthode du point fixe, de sorte à pouvoir mettre à jour les pondérations $\hat{\alpha}_{T,i}$ et $\hat{\beta}_{T+1,j}$ avec des estimations *a posteriori* de $\hat{x}_{T+1}$ et non plus a priori. Cette méthode a par exemple été utilisée dans [Che17a].

Avec les approximations (E.105)–(E.106), nous pouvons maintenant appliquer le Théorème E.2.3 avec les matrices $\{Q_T\}$ et $\{R_T\}$ telles que pour tout T dans $\mathbb{N}$,

$$Q_T = \frac{1}{\lambda_\phi} I_n \text{ and } R_T = \operatorname{diag}(1/\hat{\beta}_{T,1}, ..., 1/\hat{\beta}_{T,m})$$

L'algorithme obtenu correspond à l'Algorithme E.4. Ses entrées incluent les valeurs d'initialisation de $\hat{x}_0$ et P_0, ainsi qu'un horizon de temps maximal $T_{\max}$. Cet algorithme ressemble à la première itération de l'algorithme dérivé dans [Che17a] pour le *Maximum Correntropy Criterion Kalman Filter* (MCCKF). Leur façon de dériver leur algorithme est différente de celle présentée ici, mais repose sur ce même principe d'approcher le point critique d'une fonction de performance présentant des termes exponentiels en la différentiant.

Algorithme E.4 Algorithme récursif inspiré du Filtre de Kalman et implémentant de manière approchée le problème (E.100)

Entrées : A, C, $\lambda_\phi \in \mathbb{R}_{>0}$, $\lambda_\psi \in \mathbb{R}_{>0}$, $\hat{x}_0 \in \mathbb{R}^n$, $P_0 \in \mathcal{S}_n^+(\mathbb{R})$, $T_{\max} \in \mathbb{N}$, $Y \in \mathbb{R}^{m \times T_{\max}}$
Initialisation :
$T \leftarrow 0$
Fin de l'initialisation.
Tant que $T < T_{\max}$
$\hat{x}_{T|T-1} \leftarrow A\hat{x}_{T-1}$
$\forall j \in \mathbb{J}$, $\hat{\beta}_{T,j} = \lambda_\psi e^{-\lambda_\psi \left(y_t[j] - c_j^\top \hat{x}_{T|T-1}\right)^2}$
$R_T \leftarrow \operatorname{diag}(1/\hat{\beta}_{T,1}, ..., 1/\hat{\beta}_{T,m})$
$P_{T|T-1} \leftarrow AP_{T-1}A^\top + \frac{1}{\lambda_\phi} I_n$
$L_T \leftarrow P_{T|T-1}C^\top \left(CP_{T|T-1}C^\top + R_T\right)^{-1}$
$\hat{x}_T \leftarrow \hat{x}_{T|T-1} + L_T(y_T - C\hat{x}_{T|T-1})$
$P_T \leftarrow (I_n - LC)P_{T|T-1}$
$T \leftarrow T + 1$
Fin tant que

E.4.6 Résultats numériques

Comme la Section E.3.7, la présente section va illustrer les performances des estimateurs de la forme (E.66), et notamment les deux algorithmes par paquet que nous avons développés pour implémenter de manière approchée $\mathcal{E}^{\exp}$ et $\mathcal{E}^{\circ,\exp}$.

Le scénario considéré dans cette section est exactement le même que dans la Section E.3.7. Ainsi, nous allons à nouveau considérer le système (E.61)

$$A = \begin{pmatrix} 0.7 & 0.45 \\ -0.5 & 1 \end{pmatrix}, \quad C = \begin{pmatrix} 1 & 2 \end{pmatrix}, x_0 = \begin{pmatrix} 1 \\ 2 \end{pmatrix}.$$

perturbé par un bruit d'état dense et un bruit de mesure présentant à la fois une composante dense et une composante creuse. Les bruits denses qui perturbent ce système ($\{w_t\}$ et $\{v_t\}$ (voir Eq. (E.19))) sont supposés blancs, bornés et uniformément distribués. Pour cette expérience, les valeurs de ces perturbations seront en effet sélectionnées aléatoirement dans un intervalle de la forme $[-a, a]$. L'indice de performance que nous utiliserons sera encore l'Erreur d'Estimation Relative (REE)

$$\text{REE} = \frac{\|\hat{X} - X\|_2}{\|X\|_2}$$

où X représente la vraie trajectoire d'état du système et $\hat{X}$ est la trajectoire estimée obtenue par l'estimateur.

Les notations $\mathcal{E}^{\text{exp}}$ et $\mathcal{E}^{\circ,\text{exp}}$ désigneront les algorithmes obtenus Section 3.5 :

- l'estimateur $\mathcal{E}^{\text{exp}}$ désignera l'algorithme par paquet développé pour implémenter de manière approchée le problème (3.59). Cet algorithme, l'Algorithme E.3, sera implémenté avec $\eta_{\min} = 10^{-8}$ et $k_{\max} = 100$.
- l'estimateur $\mathcal{E}^{\circ,\text{exp}}$ désignera l'algorithme par paquet développé pour implémenter de manière approchée le problème (3.56), c'est-à-dire l'Algorithme C.1 présenté dans l'Annexe C.2.

Pour les deux estimateurs, les problèmes d'optimisation convexe seront résolus via MATLAB. De plus, les estimateurs $\mathcal{E}_{\ell_2^2,\ell_1}$ et oracle $\mathcal{E}_{\ell_2^2,\ell_2^2}$, qui ont été définis et étudiés dans la Section E.3.7, serviront de base de comparaison.

Il est à noter que les résultats qui vont être présentés ne correspondent pas nécessairement aux performances des estimateurs $\mathcal{E}^{\text{exp}}$ et $\mathcal{E}^{\circ,\text{exp}}$ que nous avons étudiés théoriquement dans la première partie de la présente section, puisque nous n'avons pas de garantie concernant l'équivalence numérique entre ces derniers et les algorithmes que nous avons développés. Cela constitue une différence majeure par rapport aux estimateurs étudiés dans la Section E.3 puisque nous avions pu étudier leurs performances exactes en résolvant directement le problème d'optimisation (convexe) les définissant.

Expérience 1 : test sur le nombre d'occurrences du bruit impulsif

Pour ce test, le Rapport Signal sur Bruit (RSB) des bruits denses (i.e., w_t et v_t) est fixé, avec une amplitude maximum de $a = 0.03$ pour w_t and de $a = 0.1$ pour v_t, ce qui donne un RSB d'environ 30 dB dans les deux cas. Le nombre de valeurs non nulles du bruit impulsif $\{s_t\}$, quant à lui, varie de sorte à ce que le ratio d'occurrences non nulles varie entre 0 et 1. Pour le simuler, les indices temporels des occurrences non nulles sont sélectionnés uniformément sur l'ensemble des indices possibles, puis les valeurs de ces occurrences sont prises comme la réalisation d'une variable aléatoire gaussienne de moyenne nulle et de variance égale à 100. La REE (moyennée) de chaque estimateur pour ce test a enfin été représenté sur la Figure E.6 en échelle logarithmique.

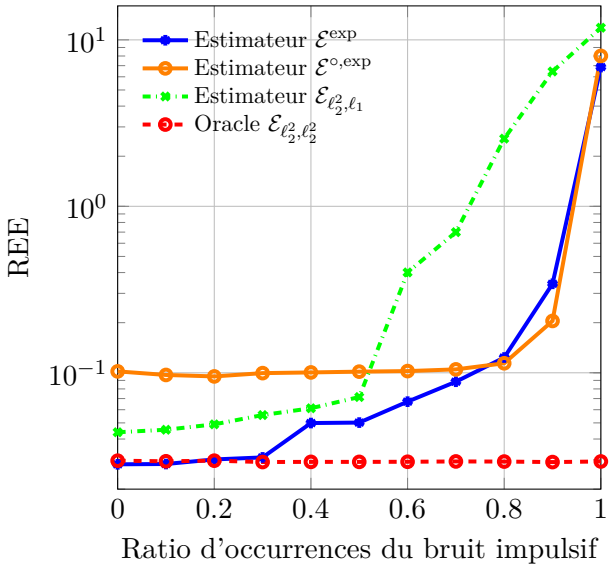

FIGURE E.6: Erreur d'estimation relative (en échelle logarithmique) obtenue pour différents estimateurs en fonction du ratio d'occurrences non nulles du bruit creux $\{s_t\}$

La Figure E.6 indique que l'erreur d'estimation de $\mathcal{E}^{\exp}$ et $\mathcal{E}^{\circ,\exp}$ est stable jusqu'à ce que le ratio des éléments non nulles de s_t soit trop important, ce qui correspond empiriquement à 30% pour l'estimateur $\mathcal{E}^{\exp}$ et 80% pour l'estimateur $\mathcal{E}^{\circ,\exp}$. Sur l'intervalle sur lequel son estimation est stable, $\mathcal{E}^{\exp}$ montre même des performances comparables à celle de l'oracle $\mathcal{E}_{\ell_2^2,\ell_2^2}$.

Par ailleurs, $\mathcal{E}^{\exp}$ donne de meilleurs résultats que l'estimateur $\mathcal{E}_{\ell_2^2,\ell_1}$, et ce pour tout ratio. La nature itérative de l'algorithme implémentant $\mathcal{E}^{\exp}$ (Algorithme E.3) joue certainement un rôle dans ces performances, notamment du fait que les processus itératifs sont connus pour améliorer la parcimonie d'une estimation [Dau10].

Enfin, nous remarquons que la REE de l'estimateur $\mathcal{E}^{\circ,\exp}$ comme à diverger pour des ratios bien plus élevés que $\mathcal{E}_{\ell_2^2,\ell_1}$ ou $\mathcal{E}^{\exp}$ dans cet exemple. Cependant, la REE d'$\mathcal{E}^{\circ,\exp}$ en elle-même est bien plus grande que celle des deux autres estimateurs, et notamment lorsqu'il n'y a pas d'occurrences non nulles dans le bruit creux.

Expérience 2 : test sur le RSB. Pour ce second test, nous fixons le ratio d'occurrences non nulles de $\{s_t\}$ à 0.2 et faisons varier conjointement la puissance des bruits $\{(w_t, v_t)\}$ entre 5 dB et 100 dB en termes de RSB. Les résultats obtenus pour les estimateurs implémentés sont présentés Figure E.7.

La Figure E.7 montre que chaque estimateur implémenté a des performances proches de l'oracle $\mathcal{E}_{\ell_2^2,\ell_2^2}$ (en terme de REE moyenné). Ainsi, $\mathcal{E}^{\exp}$, $\mathcal{E}_{\ell_2^2,\ell_1}$, et l'oracle $\mathcal{E}_{\ell_2^2,\ell_2^2}$ ont par exemple la même valeur de REE pour tout RSB entre 30dB to 50dB. $\mathcal{E}^{\circ,\exp}$ montre une REE deux fois plus large sur le même intervalle, mais cette valeur reste entre 10^{-1} et 10^{-2} ce qui est acceptable.

Néanmoins, les performances des estimateurs résilients sont moins bonnes que l'oracle pour des valeurs élevées de RSB, c'est-à-dire lorsque le système est très peu perturbé par les bruits denses. Dans ce cas de figure, l'écart entre les REE de $\mathcal{E}^{\exp}$ ou de $\mathcal{E}^{\circ,\exp}$ avec la REE de $\mathcal{E}_{\ell_2^2,\ell_2^2}$ est bien plus grand que pour des valeurs de RSB plus faibles. Ceci peut s'expliquer par le fait que les estimateurs résilients, afin de pouvoir gérer les valeurs aberrantes présentes dans le bruit de mesure, perdent en sensibilité au niveau des variations de l'état, ce qui est plus visible lorsque le bruit dense dans la dynamique du système est proche de 0.

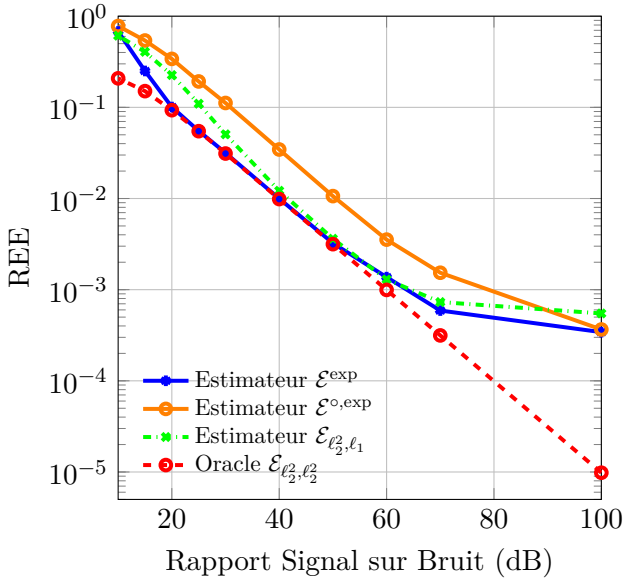

FIGURE E.7: Erreur d'estimation relative (en échelle logarithmique) obtenue pour différents estimateurs en fonction de différents niveaux de bruits denses w_t et v_t

E.5 Deux exemples d'application

Comme expliqué dans l'introduction, l'estimation d'état est au centre de nombreux aspects de l'ingénierie, et l'estimation d'état résiliente ne fait pas exception. Le but de cette section est de présenter deux cas d'application des estimateurs d'état résilient développés dans les deux précédentes sections. Pour chaque cas, nous décrirons le problème de base, et expliquerons en quoi le cadre de l'estimation d'état résiliente peut être utilisé pour construire une solution. Des tests numériques seront ensuite présentées afin de vérifier l'intérêt de mettre en place ces solutions.

Les deux exemples que nous étudierons seront les suivants :

- L'estimation de l'état d'un système à commutations sans connaître son signal de commutation.
- L'estimation en ligne de la position d'un drone avec des pertes de mesure intermittentes.

Il est à noter que dans le manuscrit complet, deux autres exemples sont traités : celui du filtrage de tendance sur des séries de mesure présentant des valeurs aberrantes et l'application de l'estimation résiliente aux problèmes de régression robuste.

E.5.1 Estimation de l'état d'un système avec signal de commutation inconnu

Dans la plupart des modèles de la forme (E.2) considérés jusqu'alors, le bruit creux était considéré comme faisant partie du bruit de mesure, c'est-à-dire un signal parasite dû aux imperfections de l'appareil de mesure. À travers cet exemple, nous allons illustrer une situation où le signal impulsif affectant le système est en réalité une partie nécessaire du système introduite pour certains développements méthodologiques.

Nous considérons un système linéaire à commutations, qui est un cas particulier des systèmes LTV, de la forme

$$\Sigma : \begin{cases} x_{t+1} &= A_{\sigma(t)}x_t + w_t \\ y_t &= C_{\sigma(t)}x_t + v_t \end{cases} \tag{E.107}$$

où les matrices $A_{\sigma(t)}$ et $C_{\sigma(t)}$ sont tirées de deux familles de matrices $\{A_k\}$ et $\{C_k\}$ via une fonction $\sigma : \mathbb{N} \to \{1, ..., n_\sigma\}$ que l'on appelle le signal de commutation.

Chaque paire (A_k, C_k) est considéré comme un mode du système, et le signal de commutation σ indique le mode dans lequel le système est à l'instant t parmi les n_σ modes possibles.

Si nous prenons le mode (A_1, C_1) comme un mode de référence, on peut reformuler le système sous la forme d'un système LTI en temps discret tel que

$$\Sigma_s : \begin{cases} x_{t+1} &= A_1 x_t + w_t + o_t \\ y_t &= C_1 x_t + v_t + s_t \end{cases} \tag{E.108}$$

avec $o_t = (A_{\sigma(t)} - A_1)x_t$ et $s_t = (C_{\sigma(t)} - C_1)x_t$.

$\{o_t\}$ et $\{s_t\}$ sont deux séquences de bruits qui ont la particularité que lorsque t est tel que $\sigma(t) = 1$, alors $o_t = s_t = 0$. Cela implique alors que $\{o_t\}$ et $\{s_t\}$ sont des bruits creux dont le nombre d'occurrences non nulles est égal à la cardinalité de l'ensemble $\{t \in \mathbb{T} : \sigma(t) \neq 1\}$. Par conséquent, plus le système Σ est dans le mode (A_1, C_1) sur $\mathbb{T}$, plus $\{o_t\}$ et $\{s_t\}$ seront creux.

Ce constat montre que l'estimation de l'état d'un tel système rentre dans le cadre de l'estimation d'état résiliente. Tant que le nombre d'occurrences de t telles que $\sigma(t) \neq 1$ reste faible, entraînant peu d'occurrences non nulles de o_t et s_t, le problème d'estimation de l'état du système à commutations (E.107) peut être réduit à l'estimation d'état robuste du système LTI (E.108).

Les caractéristiques du système (E.108) jouent évidemment un rôle dans les performances d'une telle approche. S'il est observable aux sens présentés dans les Sections E.3 et E.4 (c'est-à-dire s'il a par exemple un faible p_r (voir (E.33)) ou un faible $R_\Sigma(\rho)$ (voir (E.85))), alors l'estimateur aura plus de chances de produire une bonne estimation de l'état du système.

Pour illustrer ce principe, nous introduisons le système suivant à 2 états($n = 2$), 1 mesure ($m = 1$), et 2 modes ($n_\sigma = 2$):

$$A_1 = \begin{pmatrix} 0.7 & 0.45 \\ -0.5 & 1 \end{pmatrix}, \quad A_2 = \begin{pmatrix} -0.65 & -0.7028 \\ 0.7028 & -0.65 \end{pmatrix}, \quad C_1 = C_2 = \begin{pmatrix} 1 & 2 \end{pmatrix} \tag{E.109}$$

avec $x_0 = (\,1 \quad 2\,)$. Il est à noter que ce système présente la même matrice de mesure $C_1 = C_2 = C$ pour les deux modes. Ceci n'est cependant pas une hypothèse inhabituelle étant donné que les capteurs qui enregistrent les mesures ne changent pas forcément d'un mode à l'autre.

Nous allons générer plusieurs signaux de commutations dans les prochaines expériences. Ces signaux seront générés afin de pouvoir contrôler le ratio d'occurrences non nulles de $\{o_t\}$ à une certaine valeur entre 0 et 1. Pour ce faire, le nombre d'occurrences du mode de référence sera choisi à l'avance puis les occurrences en elles-mêmes seront sélectionnés uniformément sur l'ensemble des indices de temps.

L'estimation d'état sera effectuée hors ligne avec $T = 100$, et nous étudierons les estimateurs par paquets déjà étudiés :

- l'estimateur $\mathcal{E}_{\ell_2,\ell_2^2}$ qui implémente $\mathcal{E}$ tel que défini dans (E.23) avec $\lambda = 10^{-4}$, et pour tout t, $\phi = \|\cdot\|_2$ et $\psi_t = \|\cdot\|_2^2$.
- l'estimateur $\mathcal{E}^{\text{exp}}$ à travers l'algorithme par paquet développé (voire Algorithme E.3)avec $\lambda_\phi = 10^{-5}$, $\lambda_\psi = 1$ et pour tout t, $\phi_{t,i} = \psi_{t,j} = |\cdot|^2$ pour tout (i,j) dans $\mathbb{I} \times \mathbb{J}$.
- l'oracle $\mathcal{E}_{\ell_2^2,\ell_2^2}$ qui implémente l'estimateur $\mathcal{E}$ tel que défini dans (E.23)) avec $\lambda = 10^{-1}$, et pour tout t, $\phi_t = \|\cdot\|_2^2$ and $\psi_t = \|\cdot\|_2^2$. Cet estimateur des moindres carrés aura connaissance du signal de commutation et servira de référence en terme de performances.

Tests sur le nombre d'occurrences non nulles de $\{o_t\}$. Dans un premier temps, nous allons effectuer deux tests en fonction du nombre d'occurrences non nulles de $\{o_t\}$. L'un des deux tests estimera l'état du Système (E.109) avec (A_1, C) pour mode de référence, tandis que l'autre test estimera ce même état mais avec pour mode de référence (A_2, C). Aucun bruit dense, que ce soit dans l'équation d'état ou dans l'équation de mesure du système, ne sera considéré.

Pour chaque nombre d'occurrences non nulles de $\{o_t\}$, les tests consistent à générer 100 signaux de commutations, simuler la trajectoire d'état et la matrice de mesure correspondantes pour le Système (E.109), et reconstruire l'état du système par le biais des estimateurs définis plus haut. Pour chaque réalisation, la REE (voir (E.62)) a été calculée puis moyennée pour chaque ratio d'occurences et les résultats sont présentés Figure E.8.

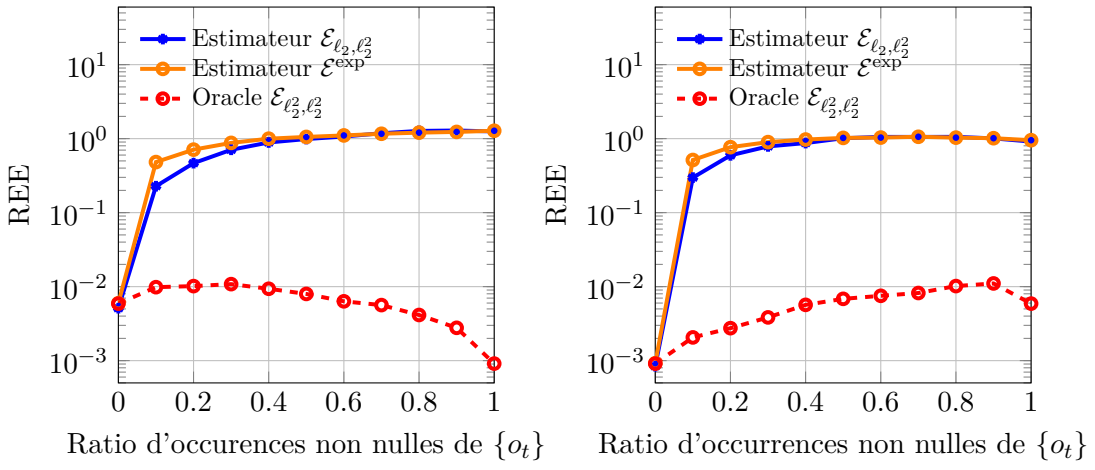

(A) Mode de référence (A_1, C)

(B) Mode de référence (A_2, C)

FIGURE E.8: REE moyennée pour les estimateurs $\mathcal{E}_{\ell_2,\ell_2^2}$, $\mathcal{E}^{\text{exp}}$ et oracle $\mathcal{E}_{\ell_2^2,\ell_2^2}$ appliqués au Système (E.109)

La première chose qui peut être constater est que le mode de référence utilisé pour l'estimation joue un rôle dans la qualité de l'estimation obtenue : en effet, lorsque le ratio d'occurrences non nulles de $\{o_t\}$ est égal à 0.1, $\mathcal{E}_{\ell_2,\ell_2^2}$ montre une REE de 0.2 lorsque (A_1, C) est le mode de référence et une REE de 0.3 lorsque (A_2, C) est le mode de référence. Bien que petite, cette différence se retrouve pour tous les ratios possibles. Elle peut être expliquée par le fait que le mode (A_1, C) est plus observable que le mode (A_2, C). En effet, si par exemple p_r, paramètre d'observabilité défini dans (E.33), est inférieur à 1/2, alors on sait que l'erreur d'estimation de la classe $\mathcal{E}$ est

bornée même en présence de r valeurs aberrantes. En utilisant la méthode présentée en Section E.3.5, on peut calculer p_1 qui est égal à 0.0607 pour (A_1, C) et 0.0672 pour (A_2, C). Cela assure que (A_1, C) est capable de gérer au moins 8 valeurs aberrantes, tandis que (A_2, C) peut en gérer au moins 7. Cette petite différence d'observabilité peut expliquer l'écart de performance suivant lequel de (A_1, C) ou (A_2, C) est utilisé comme mode de référence pour le processus d'estimation.

De plus, les deux estimateurs $\mathcal{E}_{\ell_2,\ell_2^2}$ et $\mathcal{E}^{\text{exp}}$ atteignent une REE moyennée de 1 pour un ratio d'occurrences non nulles de $\{o_t\}$ plus grand que 0.4. En dessous de cette valeur, leur REE moyennée a un ordre de grandeur de 10^{-1}, ce qui acceptable, étant donné que cette estimation a été effectuée sans prendre en compte du tout l'occurrence de l'autre mode du système.

Etude de l'estimation de la trajectoire d'état en absence de bruit dense. Pour étudier un peu plus en détail les chiffres présentés dans les deux premiers tests, la Figure E.9 présente une réalisation de la trajectoire des deux états du Système (E.109) pour un signal de commutation σ spécifique (également représenté sur la figure) avec un ratio d'occurrences non nulles de $\{o_t\}$ égal à 0.1. En plus des vraies trajectoires d'état et du signal de commutation, la figure présente les estimations des trajectoires d'état obtenues par $\mathcal{E}_{\ell_2,\ell_2^2}$ et $\mathcal{E}^{\text{exp}}$ avec (A_1, C) comme mode de référence.

Sur cette figure, nous observons que $\mathcal{E}_{\ell_2,\ell_2^2}$ et $\mathcal{E}^{\text{exp}}$ ont été capables d'estimer de manière correcte la trajectoire des deux états. Par exemple, ils ont tous les deux été capables de gérer l'apparition du mode (A_2, C) à $t = 6$ ou $t = 15$. On peut toutefois noter que la valeur du pic entraîné par cette commutation a été mieux estimé par $\mathcal{E}_{\ell_2,\ell_2^2}$ que par $\mathcal{E}_{\text{exp}}$ qui présente un pic mais d'une amplitude incorrecte.

Nous remarquons également que les deux estimateurs manquent de précision lorsque le mode non-utilisé (A_2, C) survient dans le système pendant plusieurs instants consécutifs, comme on peut le voir vers $t = 39$ ou vers $t = 69$. Néanmoins, mis à part ces deux inexactitudes, les performances de $\mathcal{E}_{\ell_2,\ell_2^2}$ et $\mathcal{E}^{\text{exp}}$ semblent satisfaisantes, ce qui est corroboré par le fait que pour le premier test (Figure E.8a), leur REE moyennée[3] étaient égales à 0.3541 pour $\mathcal{E}_{\ell_2,\ell_2^2}$ et 0.6947 pour $\mathcal{E}^{\text{exp}}$.

Etude de l'estimation de la trajectoire d'état en présence de bruit dense. Enfin, nous réalisons la même expérience que précédemment, mais cette fois-ci en prenant en compte la présence de bruits denses $\{w_t\}$ et $\{v_t\}$ non nuls. Pour tout t, w_t et v_t ont été obtenus par la réalisation de deux lois de distribution uniformes entre $[-0.5, 0.5]$ et $[-0.1, 0.1]$ respectivement, ce qui représente un RSB d'environ 10dB pour le bruit d'état et de 30dB pour le bruit de mesure. Les trajectoires d'état ont ensuite été estimées par $\mathcal{E}_{\ell_2,\ell_2^2}$ et $\mathcal{E}^{\text{exp}}$ (avec (A_1, C) pour mode de référence) et les vraies trajectoires, les trajectoires estimées et le signal de commutation ont tous été représentés sur la Figure E.10.

La présence des bruits denses $\{w_t\}$ et $\{v_t\}$ ne semble pas beaucoup perturber le processus d'estimation, car les conclusions de ce test sont sensiblement les mêmes que celles tirées dans le test sans bruit présenté Figure E.9 : les deux estimateurs $\mathcal{E}_{\ell_2,\ell_2^2}$ et $\mathcal{E}^{\text{exp}}$ parviennent à bien estimer les trajectoires d'état, mais cette estimation se dégrade localement lorsque le mode non-utilisé pour l'estimation survient à plusieurs instants consécutifs (par exemple vers $t = 10$ ou $t = 60$). Dans ce test, la REE de

[3] Nous rappelons au lecteur que la REE est une valeur qui est normalisée et calculée sur l'intégralité de la trajectoire, ce qui fait que sa valeur peut parfois – à tort – être considérée comme élevée.

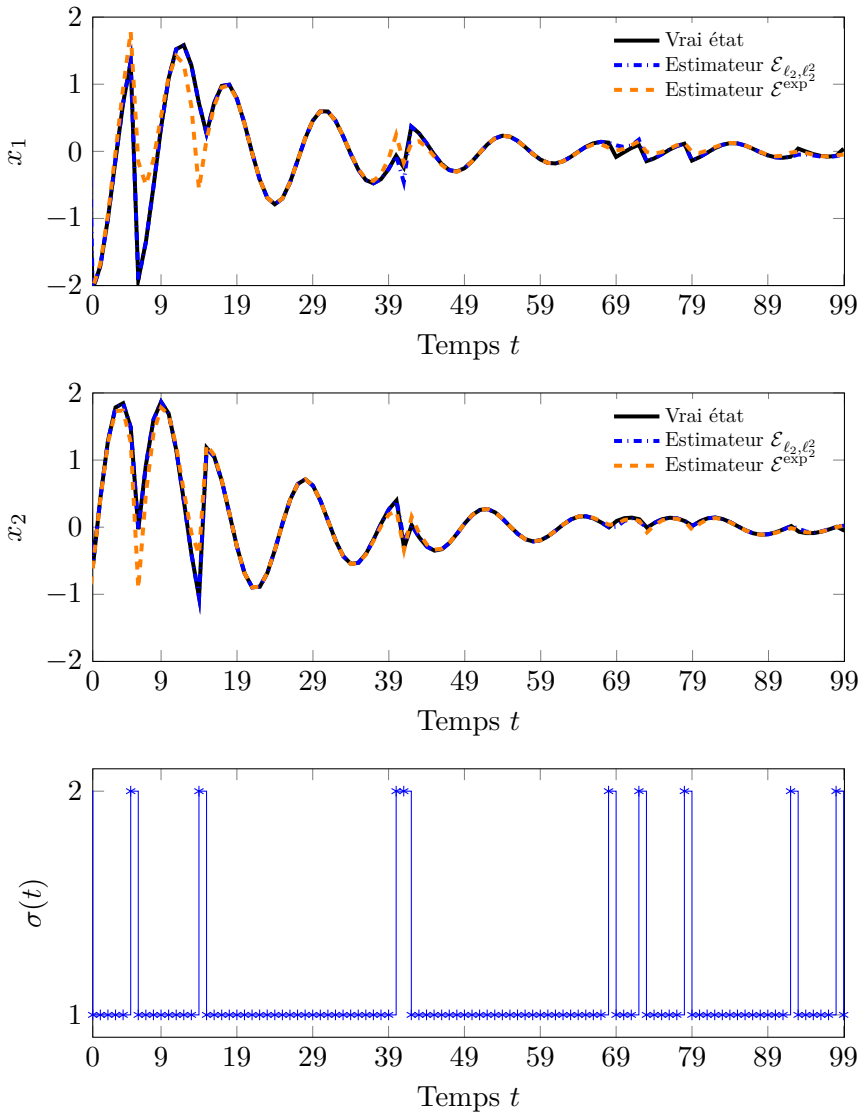

FIGURE E.9: Trajectoires d'état du système à commutations (E.109) pour un signal de commutation donné (sans bruit dense) et trajectoires d'états estimées par $\mathcal{E}_{\ell_2,\ell_2^2}$ et $\mathcal{E}^{\exp}$

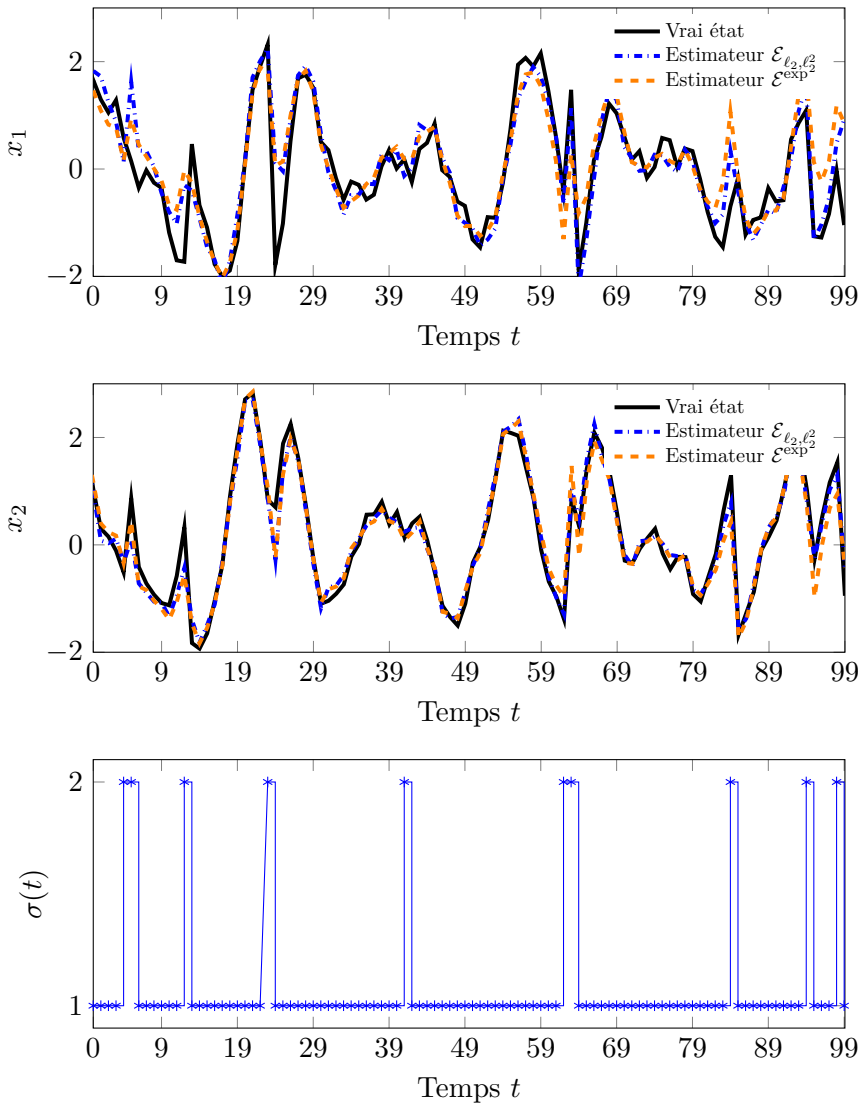

FIGURE E.10: Trajectoires d'état du système à commutation (E.109) pour un signal de commutation donné (avec bruit dense) et trajectoires d'états estimées par $\mathcal{E}_{\ell_2,\ell_2^2}$ et $\mathcal{E}^{\exp}$

$\mathcal{E}_{\ell_2,\ell_2^2}$ est de 0.4170 tandis que celle de $\mathcal{E}^{\text{exp}}$ est égale à 0.5133 : on constate que ces valeurs sont proches de celles obtenues dans le test sans bruit dense.

En conclusion, il est possible d'appliquer nos schémas d'estimation afin d'estimer l'état d'un système à commutations sans avoir connaissance du signal de commutation entre ses différents modes. Les deux propriétés qu'il semble primordial d'avoir pour assurer une bonne qualité d'estimation sont :

- que le mode de référence utilisé dans le processus d'estimation soit visité autant que possible par le système à commutations.
- Le système LTI que constitue ce mode de référence (voir (E.108)) doit être aussi observable que possible – aux sens présentés dans les sections E.3 et E.4.

E.5.2 Estimation de la position d'un drone quadrirotor

Récemment, les *véhicules aériens sans pilote*, aussi appelés drones, ont été de plus en plus utilisés pour effectuer de nombreuses tâches telles que le transport de médicaments [Eic19], ou la surveillance de champs agricoles [Tar20]. Leur petite taille, leur légèreté, ou encore le fait qu'ils sont commandés à distance en font une solution intéressante à des problèmes où la présence d'êtres humains serait dangereuse.

Opérer correctement un drone requiert de connaître de nombreuses variables telles que sa position. Si un GPS (*Global Positioning System*) peut être utilisé pour déterminer cette position, les signaux impliqués dans ce système sont très sensibles aux interférences et ne conviennent pas à toutes les interventions, notamment celles en intérieur. Dans de tels cas de figure, il y a une nécessité d'estimer la position du drone, ce qui est la plupart du temps effectué par le biais de la connaissance de sa position initiale et de l'intégration de ses vitesses linéaires. Cependant, si des capteurs externes, tels que des radars, sont capables de mesurer très précisément ces vitesses linéaires, les mesures obtenues peuvent être perdues durant la transmission au drone, qui doit alors compter sur des capteurs internes bien moins précis.

FIGURE E.11: Photographie du Crazyflie 2.0 (source: www.bitcraze.io/products/old-products/crazyflie-2-0/)

Le but de cette section est d'illustrer le processus d'estimation de la position d'un Crazyflie 2.0 (voir Figure E.11), un drone quadrirotor en open-source. Cette étude sera basée sur un modèle et des données expérimentales qui ont été obtenus dans le cadre du travail de thèse de Jérémy Barra au sein du Laboratoire Ampère et du CEA.

Modèle du drone et conditions de l'expérience

Dans [Bar20], le modèle suivant fut proposé pour modéliser la dynamique du drone :

$$\begin{pmatrix} \dot{v}_x \\ \dot{v}_y \\ \dot{v}_z \\ \dot{b}_{\text{acc},x} \\ \dot{b}_{\text{acc},y} \\ \dot{b}_{\text{acc},z} \end{pmatrix} = \begin{pmatrix} -0.32 & 0 & 0 & 0 & 0 & 0 \\ 0 & -0.32 & 0 & 0 & 0 & 0 \\ 0 & 0 & -4 & 0 & 0 & 0 \\ 0 & 0 & 0 & 0 & 0 & 0 \\ 0 & 0 & 0 & 0 & 0 & 0 \\ 0 & 0 & 0 & 0 & 0 & 0 \end{pmatrix} \begin{pmatrix} v_x \\ v_y \\ v_z \\ b_{\text{acc},x} \\ b_{\text{acc},y} \\ b_{\text{acc},z} \end{pmatrix} + \begin{pmatrix} 0 & -9.4 & 0 \\ 9.4 & 0 & 0 \\ 0 & 0 & -28.2 \\ 0 & 0 & 0 \\ 0 & 0 & 0 \\ 0 & 0 & 0 \end{pmatrix} \begin{pmatrix} \eta_1 \\ \eta_2 \\ T \end{pmatrix} \tag{E.110}$$

$$\begin{pmatrix} a_{\text{acc},x} \\ a_{\text{acc},y} \\ a_{\text{acc},z} \\ v_{\text{rdr},x} \\ v_{\text{rdr},y} \\ v_{\text{rdr},z} \end{pmatrix} = \begin{pmatrix} -1.2 \cdot 10^{-2} & 0 & 0 & -1.2 \cdot 10^{-2} & 0 & 0 \\ 0 & -1.2 \cdot 10^{-2} & 0 & 0 & -1.2 \cdot 10^{-2} & 0 \\ 0 & 0 & -6 \cdot 10^{-2} & 0 & 0 & -6 \cdot 10^{-2} \\ 1 & 0 & 0 & 0 & 0 & 0 \\ 0 & 1 & 0 & 0 & 0 & 0 \\ 0 & 0 & 1 & 0 & 0 & 0 \end{pmatrix} \begin{pmatrix} v_x \\ v_y \\ v_z \\ b_{\text{acc},x} \\ b_{\text{acc},y} \\ b_{\text{acc},z} \end{pmatrix} + f \tag{E.111}$$

Ce modèle est composé de $n = 6$ états et $m = 6$ mesures. Ces états correspondent aux trois vitesses linéaires v_x, v_y, v_z du drone selon les trois dimensions de l'espace, tandis que trois autres $b_{\text{acc},x}$, $b_{\text{acc},y}$, $b_{\text{acc},z}$ sont des états visant à décrire un biais observé dans les mesures retournées par les capteurs du système.

En effet, deux capteurs sont présents dans le système :

- Un capteur embarqué, l'*Unité de mesure inertielle* ou *IMU*, qui mesure ses propres accélérations linéaires qui peuvent s'exprimer comme une combinaison linéaires des vitesses linéaires du drone (voir [Lei14]), donnant $a_{\text{acc},x}$, $a_{\text{acc},y}$ et $a_{\text{acc},z}$. Ce capteur présente un biais dans ses mesures, qui a été considéré constant dans le modèle (E.110)–(E.111).
- Un *radar*, externe au drone, qui mesure directement les vitesses linéaires du drone, donnant $v_{\text{rdr},x}$, $v_{\text{rdr},y}$ et $v_{\text{rdr},z}$.

Les mesures sont perturbées par un bruit f, qui modélise à la fois le bruit de mesure des deux capteurs et le phénomène de perte de mesure. Enfin, il est important de noter que le drone est supposé voler en mode quasi-stationnaire, ce qui veut dire que la dynamique de sa rotation est totalement négligée. Cela nous permet de considérer que les seules entrées du système sont η_1 et η_2, deux des trois angles d'Euler du drone, ainsi que la poussées T induites par les quatre rotors présents sur le drone.

Conditions de l'expérience. L'expérience sur laquelle nous allons baser notre étude a été effectuée dans une salle équipée d'un système de capture de mouvement. A l'intérieur de cette salle, un opérateur a fait voler un Crazyflie 2.0 et ses accélérations et vitesses linéaires furent mesurées par les deux capteurs présentés ci-dessus (c'est-à-dire radar et IMU), tandis que le système de capture de mouvement a permis d'obtenir une référence quant à la position et à la vitesse du drone dans l'espace.

Le radar a une bien meilleure précision que l'IMU qui présente des mesures très bruitées. Cependant, dans une configuration réelle, il n'est pas rare que le drone perde la connexion avec le radar pendant quelques instants. Pendant ces instants, le radar retourne alors une valeur par défaut qui perturbe complètement le processus d'estimation. Notre but est donc de gérer ces valeurs par défaut tout en continuant à faire confiance aux mesures retournées par le radar. Ceci est d'autant plus crucial que même la plus petite erreur sur l'estimation de la vitesse entre un décalage permanent entraîne les positions supposées et réelles du drone du fait de l'intégration.

Paramètres de l'estimation

Afin de simuler une utilisation normale de drone, le processus d'estimation doit être effectué en ligne, ce qui veut dire estimer l'état au fur et à mesure que l'estimateur reçoit des informations en provenance du système, car nous avons besoin de la vitesse et de la position du drone en temps réel pour pouvoir contrôler sa trajectoire. De plus, l'estimation doit pouvoir avoir lieu sur le microprocesseur embarqué du drone, qui a des ressources de calcul très limitées. Par conséquent, les estimateurs par paquet utilisés jusqu'alors ne peuvent constituer une implémentation satisfaisante pour le problème posé. Nous implémenterons donc plutôt les algorithmes récursifs, qui demandent beaucoup moins de puissance de calcul.

Le système (E.110)–(E.111) est un système LTI en temps continu. Néanmoins, nos méthodes d'estimation ont besoin d'un modèle en temps discret. Nous avons donc utilisé les fonctions issues de MATLAB `ss` et `c2d` afin d'obtenir une discrétisation par la méthode du bloqueur d'ordre zéro [Mat] de (E.110)–(E.111). Par conséquent, la mention « système (E.110)–(E.111) » fera dorénavant référence à la version discrétisée du système. Trois estimateurs ont été implémentés :

- $\mathcal{E}_{\text{online}}$ qui implémente l'Algorithme E.2 avec $\lambda = 1$, $\varepsilon = 10^{-5}$, $\hat{x}_0 = 0_{6,1}$, $P_0 = I_2$, et γ, Q tels que

$$\gamma = \begin{pmatrix} 10 & 10 & 15 & 10 & 10 & 15 \end{pmatrix} \tag{E.112}$$

$$Q = \operatorname{diag}\left(10^{-4}, 10^{-4}, 10^{-4}, 4 \cdot 10^{-2}, 4 \cdot 10^{-2}, 6.4 \cdot 10^{-3}\right). \tag{E.113}$$

- $\mathcal{E}^{\text{exp}}_{\text{online}}$ qui implémente l'Algorithme D.1, une variation de l'Algorithm E.4 introduite dans l'Annexe D.2, avec $\lambda_\phi = 1$, $\lambda_\psi = 10^{-1}$, $\hat{x}_0 = 0_{6,1}$, Q donnée par (E.113), $P_0 = I_2$ et

$$\{r_j\}_{j \in \mathbb{J}} = \left\{2.5 \cdot 10^{-3}, 2.5 \cdot 10^{-2}, 2.5 \cdot 10^{-3}, 4 \cdot 10^{-2}, 4 \cdot 10^{-2}, 10^{-2}\right\}.$$

Résultats de l'expérience

Les données qui ont été utilisées pour l'estimation sont les trois accélérations mesurées par l'IMU ainsi que les trois vitesses mesurées par le radar. Nous cherchons à estimer la vitesse du drone de manière suffisamment précise pour pouvoir l'intégrer et ainsi reconstruire la trajectoire du drone.

Les données de cette expérience ont été mesurées entre $t_{\min} = 0$ s et $t_{\max} = 18$ s et échantillonnées à une fréquence de 500 Hz, pour un total de $T = 9000$ échantillons. Durant l'acquisition, l'opérateur pilote le drone pour qu'il effectue des allers-retours suivant l'axe y tout en essayant de restreindre au maximum les mouvements suivant les axes x et z.

Les données du radar obtenues durant l'expérience ne présentaient pas nativement de pertes de mesure (voir Figure D.1 dans l'Annexe D.3 pour les données brutes obtenues durant l'expérience). Pour simuler le phénomène de perte de capteurs, tous les 500 échantillons, nous avons donc modifié 50 échantillons consécutifs sur les trois vitesses linéaires mesurées par le radar, et les avons remplacés par la valeur par défaut 10 m·s^{-1}.

La Figure E.12 présente l'erreur d'estimation instantanée pour les trois vitesses linéaires du drone, c'est-à-dire $e_{t,x} = v_{\text{ref},t,x} - \hat{v}_{t,x}$, $e_{t,y} = v_{\text{ref},t,y} - \hat{v}_{t,y}$ et $e_{t,z} = v_{\text{ref},t,z} - \hat{v}_{t,z}$. La Figure E.13 montre les coordonnées mesurées par le système de

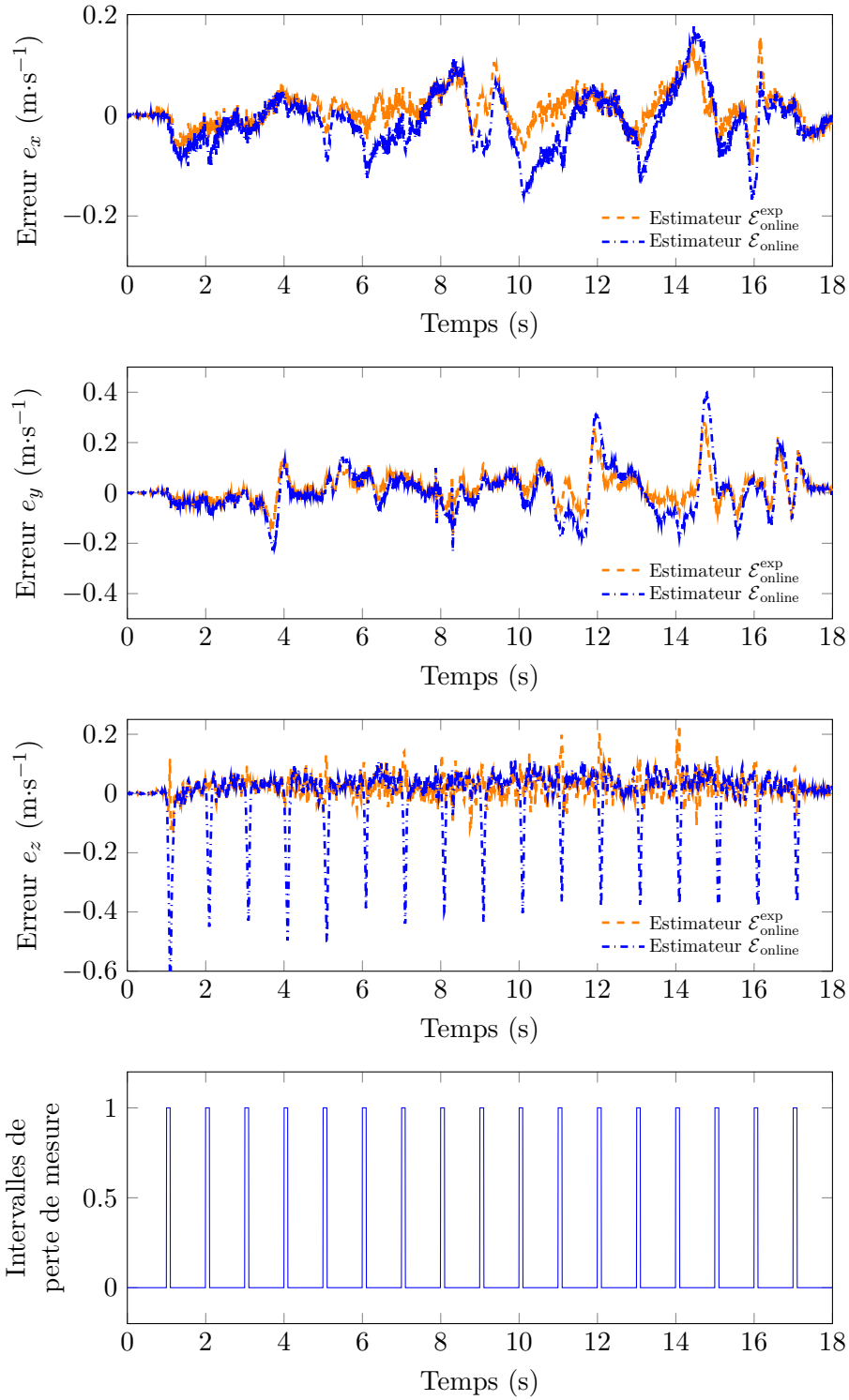

FIGURE E.12: Erreurs d'estimation sur les trois vitesses linéaires du drone pour $\mathcal{E}_{\text{online}}$ et $\mathcal{E}_{\text{online}}^{\text{exp}}$

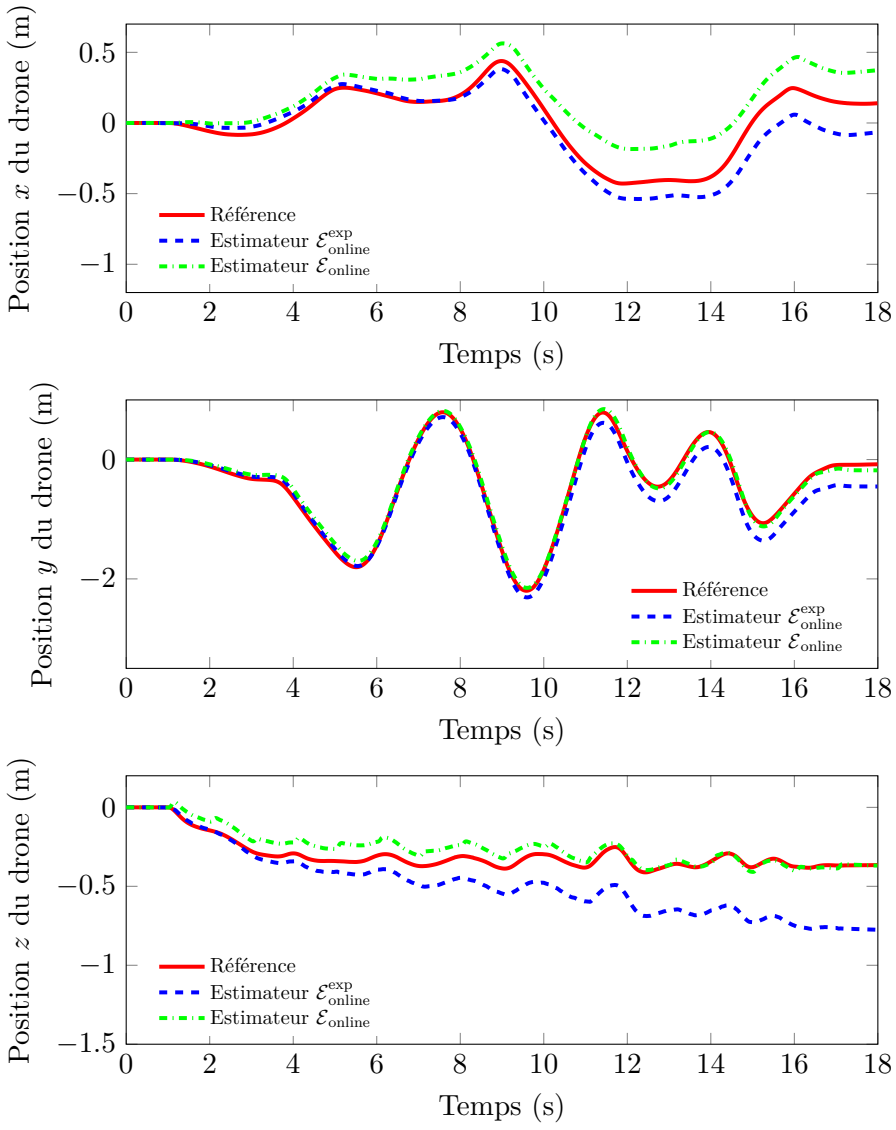

FIGURE E.13: Reconstruction des coordonnées du drone obtenues par intégration des vitesses linéaires estimées par $\mathcal{E}_{\text{online}}$ et $\mathcal{E}_{\text{online}}^{\text{exp}}$

capture de mouvement ainsi que les coordonnées estimées obtenues par l'intégration des vitesses linéaires du drone estimées par $\mathcal{E}_{\text{online}}$ et $\mathcal{E}^{\text{exp}}_{\text{online}}$.

Sur la Figure E.12, on peut voir que $\mathcal{E}_{\text{online}}$ et $\mathcal{E}^{\text{exp}}_{\text{online}}$ filtre les valeurs aberrantes présentes dans les données du radar. C'est notamment vrai pour e_x et e_y, mais nous remarquons que l'erreur e_z de $\mathcal{E}_{\text{online}}$ présente des pics correspondants aux intervalles sur lesquels l'estimateur a perdu les mesures du drone.

Ces pics sont toutefois suffisamment petits pour ne pas avoir un impact trop important sur les trajectoires obtenues et représentées sur la Figure E.13, étant donné que $\mathcal{E}_{\text{online}}$ montre de très bons résultats quant à l'estimation de la trajectoire du drone, avec une erreur sur la position finale de 25 cm. $\mathcal{E}^{\text{exp}}_{\text{online}}$ produit une trajectoire de drone qui diverge plus de la trajectoire de référence, avec une erreur sur la position finale égale 59 cm. Cette erreur est principalement due à la composante z où on observe déjà un écart de 50 cm entre les coordonnées réelle et estimée. Un tel écart peut être expliqué par des hypothèses de modélisation peut-être trop fortes.

Conclusion de ce test. Ce test a montré que les implémentations récursives de nos estimateurs optimaux étaient capables d'opérer de manière efficace en ligne et ce malgré un phénomène de perte de mesure. $\mathcal{E}_{\text{online}}$ et $\mathcal{E}^{\text{exp}}_{\text{online}}$ ont estimé précisément les vitesses linéaires du drone, et par conséquent sa position.

Cependant, les deux algorithmes implémentés sont basés sur une mise à jour de leur matrice de gain à chaque pas de temps. Cette complexité algorithmique permet de bien gérer le cas de la perte de mesure, mais il est à noter que cela peut poser problème pour des appareils avec des ressources de calcul extrêmement limitées.

Enfin, il est également à noter que nous avons considéré une version simplifiée du modèle du drone. Plusieurs modifications, telles que la prise en compte d'un biais de mesure pour le radar, pourraient être entreprises, ce qui pourrait aussi entraîner indirectement une amélioration des performances des estimateurs considérés.

Bibliography

[Aga11] Gabriel Agamennoni, Juan I. Nieto, and Eduardo M. Nebot. "An outlier-robust Kalman filter". In: 2011 IEEE International Conference on Robotics and Automation (ICRA). Shanghai, China, May 2011, pp. 1551–1558.

[Aga12] Gabriel Agamennoni, Juan I. Nieto, and Eduardo M. Nebot. "Approximate Inference in State-Space Models With Heavy-Tailed Noise". In: *IEEE Transactions on Signal Processing* 60.10 (Oct. 2012), pp. 5024–5037.

[AJ05] Nabil M. Abdel-Jabbar, Rami Y. Jumah, and Mohammad Q. Al-Haj Ali. "State estimation and state feedback control for continuous fluidized bed dryers". In: *Journal of Food Engineering* 70.2 (Sept. 1, 2005), pp. 197–203.

[Ale16] Angelo Alessandri and Moath Awawdeh. "Moving-horizon estimation with guaranteed robustness for discrete-time linear systems and measurements subject to outliers". In: *Automatica* 67 (May 1, 2016), pp. 85–93.

[Arg16] Reza Arghandeh, Alexandra von Meier, Laura Mehrmanesh, and Lamine Mili. "On the definition of cyber-physical resilience in power systems". In: *Renewable and Sustainable Energy Reviews* 58 (May 1, 2016), pp. 1060–1069.

[Ast21] Daniele Astolfi, Angelo Alessandri, and Luca Zaccarian. "Stubborn and Dead-Zone Redesign for Nonlinear Observers and Filters". In: *IEEE Transactions on Automatic Control* 66.2 (Feb. 2021), pp. 667–682.

[Bak17] Laurent Bako. "On a Class of Optimization-Based Robust Estimators". In: *IEEE Transactions on Automatic Control* 62.11 (Nov. 2017), pp. 5990–5997.

[Bak18] Laurent Bako. "Robustness analysis of a maximum correntropy framework for linear regression". In: *Automatica* 87 (Jan. 1, 2018), pp. 218–225.

[Bar08] Richard Baraniuk, Mark Davenport, Ronald DeVore, and Michael Wakin. "A Simple Proof of the Restricted Isometry Property for Random Matrices". In: *Constructive Approximation* 28.3 (Dec. 1, 2008), pp. 253–263.

[Bar20] Jérémy Barra, Gérard Scorletti, Suzanne Lesecq, Mykhailo Zarudniev, and Éric Blanco. "Attraction domain estimation of linear controllers for the attitude control of VTOL vehicles: P/PI control of a quadrotor". In: 2020 European Control Conference (ECC). May 2020, pp. 1644–1649.

[Bat17] Pedro Batista, Nicolas Petit, Carlos Silvestre, and Paulo Oliveira. "Relaxed conditions for uniform complete observability and controllability of LTV systems with bounded realizations". In: 20th IFAC World Congress 50.1 (July 1, 2017), pp. 3598–3605.

[Bel54] Richard Bellman. "The theory of dynamic programming". In: *Bulletin of the American Mathematical Society* 60.6 (1954), pp. 503–515.

[Ber09a] Dennis S. Bernstein. *Matrix Mathematics: Theory, Facts, and Formulas.* 2nd edition. Princeton University Press, July 6, 2009.

[Ber09b] Dimitri P. Bertsekas. *Convex optimization theory.* Optimization and computation series 1. Athena Scientific, 2009.

[Boy04] Stephen P. Boyd and Lieven Vandenberghe. *Convex optimization*. Cambridge, UK ; New York: Cambridge University Press, 2004. URL: https://web.stanford.edu/~boyd/cvxbook/bv_cvxbook.pdf.

[Can08a] Emmanuel J. Candès. "The restricted isometry property and its implications for compressed sensing". In: *Comptes-Rendus Mathématiques* 346.9 (May 1, 2008), pp. 589–592.

[Can08b] Emmanuel J. Candès and Paige A. Randall. "Highly Robust Error Correction byConvex Programming". In: *IEEE Transactions on Information Theory* 54.7 (July 2008), pp. 2829–2840.

[Car08] Alvaro Cardenas, Saurabh Amin, and Shankar Sastry. "Secure Control: Towards Survivable Cyber-Physical Systems". In: 2008 28th International Conference on Distributed Computing Systems Workshops (ICDCS Workshops). Beijing, China: IEEE, June 2008, pp. 495–500.

[Cav19] Ryan James Caverly and James Richard Forbes. "LMI Properties and Applications in Systems, Stability, and Control Theory". In: (June 12, 2019). URL: https://arxiv.org/pdf/1903.08599.pdf.

[Cha18] Young Hwan Chang, Qie Hu, and Claire J. Tomlin. "Secure estimation based Kalman Filter for cyber–physical systems against sensor attacks". In: *Automatica* 95 (Sept. 2018), pp. 399–412.

[Cha84] Chaw-Bing Chang and J. Tabaczynski. "Application of state estimation to target tracking". In: *IEEE Transactions on Automatic Control* 29.2 (Feb. 1984), pp. 98–109.

[Che17a] Badong Chen, Xi Liu, Haiquan Zhao, and Jose C. Principe. "Maximum correntropy Kalman filter". In: *Automatica* 76 (Feb. 1, 2017), pp. 70–77.

[Che17b] Yanbo Chen, Jin Ma, Pu Zhang, Feng Liu, and Shengwei Mei. "Robust State Estimator Based on Maximum Exponential Absolute Value". In: *IEEE Transactions on Smart Grid* 8.4 (July 2017), pp. 1537–1544.

[Che19] Badong Chen, Lei Xing, Haiquan Zhao, Shaoyi Du, and Jose C. Principe. "Effects of Outliers on the Maximum Correntropy Estimation: A Robustness Analysis". In: *IEEE Transactions on Systems, Man, and Cybernetics: Systems* (2019), pp. 1–6.

[Chr99] Richard Christie. *Power Systems Test Case Archive - UWEE*. 1999. URL: https://labs.ece.uw.edu/pstca/.

[Chu17] Charles K. Chui and Guanrong Chen. *Kalman Filtering: with Real-Time Applications*. 5th edition. Cham: Springer International Publishing, 2017.

[Dau10] Ingrid Daubechies, Ronald DeVore, Massimo Fornasier, and C. Siinan Güntürk. "Iteratively reweighted least squares minimization for sparse recovery". In: *Communications on Pure and Applied Mathematics* 63.1 (2010), pp. 1–38.

[Dua13] Guang-Ren Duan and Hai-Hua Yu. *LMIs in Control Systems: Analysis, Design and Applications*. CRC Press, Taylor & Francis Group, 2013.

[EC18] Cyber-Physical Systems for Europe (CPS4EU). 2018. URL: https://cps4eu.eu/.

[Eic19] Margaret Eichleay, Emily Evens, Kayla Stankevitz, and Caleb Parker. "Using the Unmanned Aerial Vehicle Delivery Decision Tool to Consider Transporting Medical Supplies via Drone". In: *Global Health: Science and Practice* 7.4 (Dec. 23, 2019), pp. 500–506.

[Eld09] Yonina C. Eldar and Helmut Bolcskei. "Block-sparsity: Coherence and efficient recovery". In: 2009 IEEE International Conference on Acoustics, Speech and Signal Processing. Apr. 2009, pp. 2885–2888.

[Faw14] Hamza Fawzi, Paolo Tabuada, and Suhas Diggavi. "Secure Estimation and Control for Cyber-Physical Systems Under Adversarial Attacks". In: *IEEE Transactions on Automatic Control* 59.6 (2014), pp. 1454–1467.

[Fou06] National Science Foundation. *Cyber-Physical Systems program*. 2006. URL: https://www.nsf.gov/funding/pgm_summ.jsp?pims_id=503286.

[Fou13] Simon Foucart and Holger Rauhut. *A Mathematical Introduction to Compressive Sensing*. Applied and Numerical Harmonic Analysis. New York, NY: Springer New York, 2013.

[Gee05] Sara A. van de Geer. "Least Squares Estimation". In: *Encyclopedia of Statistics in Behavioral Science*. American Cancer Society, 2005, pp. 1041–1045.

[Gra18] Michael C. Grant and Stephen P. Boyd. "The CVX Users' Guide". In: (2018).

[Han19] Duo Han, Yilin Mo, and Lihua Xie. "Convex Optimization Based State Estimation Against Sparse Integrity Attacks". In: *IEEE Transactions on Automatic Control* 64.6 (June 2019), pp. 2383–2395.

[He11] Ran He, Wei-Shi Zheng, and Bao-Gang Hu. "Maximum Correntropy Criterion for Robust Face Recognition". In: *IEEE Transactions on Pattern Analysis and Machine Intelligence* 33.8 (Aug. 2011), pp. 1561–1576.

[Hol18] Malorie Hologne. "Contribution to condition monitoring of Silicon Carbide MOSFET based Power Module". PhD thesis. Ampère Laboratory, University of Lyon, Dec. 13, 2018. URL: https://tel.archives-ouvertes.fr/tel-02061648/document.

[Hor12] Roger A. Horn and Charles R. Johnson. *Matrix Analysis*. 2nd edition. Cambridge University Press, 2012.

[Inc17] Dragos Inc. "CRASHOVERRIDE: Analysis of the threat to electric grid operations". In: (Mar. 2017). URL: https://www.dragos.com/wp-content/uploads/CRASHOVERRIDE.pdf.

[Iza16] Reza Izanloo, Seyed Abolfazl Fakoorian, Hadi Sadoghi Yazdi, and Dan Simon. "Kalman filtering based on the maximum correntropy criterion in the presence of non-Gaussian noise". In: 2016 Annual Conference on Information Science and Systems (CISS). Princeton, NJ, USA, Mar. 2016, pp. 500–505.

[Jaz07] Andrew H. Jazwinski. *Stochastic processes and filtering theory*. Dover Publications, 2007.

[Jeo16] Heegyun Jeon, Sungmin Aum, Hyungbo Shim, and Yongsoon Eun. *Resilient State Estimation for Control Systems Using Multiple Observers and Median Operation*. Mathematical Problems in Engineering. Mar. 7, 2016.

[Jor06] Murray Jorgensen. "Iteratively Reweighted Least Squares". In: *Encyclopedia of Environmetrics*. American Cancer Society, 2006.

[Kal60] Rudolf E. Kalman. "A new approach to linear filtering and prediction problems". In: *Journal of basic Engineering* 82.1 (1960), pp. 35–45.

[Kir20a] Alexandre Kircher, Laurent Bako, Éric Blanco, and Mohamed Benallouch. "On the resilience of a class of correntropy-based state estimators". In: IFAC World Congress (1st IFAC-V). Berlin, Germany, July 2020. URL: https://hal.archives-ouvertes.fr/hal-02903156.

[Kir20b] Alexandre Kircher, Laurent Bako, Éric Blanco, Mohamed Benallouch, and Anton Korniienko. "Analysis of resilience for a State Estimator for Linear Systems". In: American Control Conference (ACC). July 2020, pp. 1495–1500. URL: https://hal.archives-ouvertes.fr/hal-03181789.

[Kir21] Alexandre Kircher, Laurent Bako, Éric Blanco, and Mohamed Benallouch. "An optimization framework for resilient batch estimation in cyber-physical systems". In: *Transactions on Automatic Control* (2021). (Provisionally accepted). URL: https://arxiv.org/abs/1906.01714.

[Kul17] Maria V. Kulikova. "Square-root algorithms for maximum correntropy estimation of linear discrete-time systems in presence of non-Gaussian noise". In: *Systems & Control Letters* 108 (Oct. 1, 2017), pp. 8–15.

[Lei14] Robert C. Leishman, John C. Macdonald, Randal W. Beard, and Timothy W. McLain. "Quadrotors and Accelerometers: State Estimation with an Improved Dynamic Model". In: *IEEE Control Systems Magazine* 34.1 (Feb. 2014), pp. 28–41.

[Liu17] Xi Liu, Hua Qu, Jihong Zhao, and Badong Chen. "State space maximum correntropy filter". In: *Signal Processing* 130 (Jan. 1, 2017), pp. 152–158.

[Lue64] David G. Luenberger. "Observing the State of a Linear System". In: *IEEE Transactions on Military Electronics* 8.2 (1964), pp. 74–80.

[Ma15] Wentao Ma, Hua Qu, Guan Gui, Li Xu, Jihong Zhao, and Badong Chen. "Maximum correntropy criterion based sparse adaptive filtering algorithms for robust channel estimation under non-Gaussian environments". In: *Journal of the Franklin Institute* 352.7 (July 1, 2015), pp. 2708–2727.

[Man12] Rami S. Mangoubi. *Robust Estimation and Failure Detection: A Concise Treatment*. Springer Science & Business Media, Dec. 6, 2012.

[Mat] *Continuous-Discrete Conversion Methods*. MATLAB & Simulink. URL: https://mathworks.com/help/control/ug/continuous-discrete-conversion-methods.html.

[Mat04] John H. Mathews and Kurtis D. Fink. *Numerical methods using MATLAB*. 4th edition. Pearson, 2004.

[Mis17] Shaunak Mishra, Yasser Shoukry, Nikhil Karamchandani, Suhas N. Diggavi, and Paulo Tabuada. "Secure State Estimation Against Sensor Attacks in the Presence of Noise". In: *IEEE Transactions on Control of Network Systems* 4.1 (2017), pp. 49–59.

[Mo15] Yilin Mo and Bruno Sinopoli. "Secure Estimation in the Presence of Integrity Attacks". In: *IEEE Transactions on Automatic Control* 60.4 (Apr. 2015), pp. 1145–1151.

[Nie14] Peter C. Niedfeldt and Randal W. Beard. "Robust estimation with faulty measurements using recursive-RANSAC". In: 53rd IEEE Conference on Decision and Control. ISSN: 0191-2216. Dec. 2014, pp. 4160–4165.

[Oga06] Katsuhiko Ogata. *Discrete Time Control Systems*. 2nd edition. Dorling Kindersley Pvt Ltd, Dec. 1, 2006.

[Oga09] Katsuhiko Ogata. *Modern Control Engineering*. 5th edition. Pearson, 2009.

[O'R83] John O'Reilly. *Observers for linear systems*. Mathematics in science and engineering v. 170. London ; New York: Academic Press, 1983.

[Paj17] Miroslav Pajic, Insup Lee, and George J. Pappas. "Attack-Resilient State Estimation for Noisy Dynamical Systems". In: *IEEE Transactions on Control of Network Systems* 4.1 (Mar. 2017), pp. 82–92.

[Pas13] Fabio Pasqualetti, Florian Dorfler, and Francesco Bullo. "Attack Detection and Identification in Cyber-Physical Systems". In: *IEEE Transactions on Automatic Control* 58.11 (Nov. 2013), pp. 2715–2729.

[Pet99] Ian R. Petersen and Andrey V. Savkin. *Robust Kalman Filtering for Signals and Systems with Large Uncertainties*. Birkhäuser Basel, 1999.

[Pri10] Jose C. Principe. *Information theoretic learning: Renyi's entropy and kernel perspectives*. Information science and statistics. New York: Springer, 2010.

[Pri93] John Price and Terry Goble. "10 - Signals and noise". In: *Telecommunications Engineer's Reference Book*. Ed. by Fraidoon Mazda. Butterworth-Heinemann, Jan. 1, 1993, pp. 10–15.

[Rei01] Ian Reid and Hilary Term. "Estimation II". In: *University of Oxford, Lecture Notes* (2001). URL: https://www.robots.ox.ac.uk/~ian/Teaching/Estimation/LectureNotes2.pdf.

[Ren20] Xiaoqiang Ren, Yilin Mo, Jie Chen, and Karl H. Johansson. "Secure State Estimation with Byzantine Sensors: A Probabilistic Approach". In: *IEEE Transactions on Automatic Control* (2020), pp. 1–1.

[Roc70] Ralph T. Rockafellar. *Convex Analysis*. Princeton University Press, 1970.

[Roc98] Ralph T. Rockafellar and Roger J.-B. Wets. *Variational Analysis*. Grundlehren der mathematischen Wissenschaften. Berlin Heidelberg: Springer-Verlag, 1998.

[Rud76] Walter Rudin. *Principles of Mathematical Analysis*. 3rd Edition. 1976.

[Sah09] Bhaskar Saha, Kai Goebel, Scott Poll, and Jon Christophersen. "Prognostics Methods for Battery Health Monitoring Using a Bayesian Framework". In: *IEEE Transactions on Instrumentation and Measurement* 58.2 (Feb. 2009), pp. 291–296.

[Say14] Muhammed O. Sayin, N. Denizcan Vanli, and Suleyman S. Kozat. "A Novel Family of Adaptive Filtering Algorithms Based on the Logarithmic Cost". In: *IEEE Transactions on Signal Processing* 62.17 (Sept. 2014), pp. 4411–4424.

[Sha09] Yoav Sharon, John Wright, and Yi Ma. "Minimum sum of distances estimator: Robustness and stability". In: American Control Conference, 2009. ACC'09. IEEE, 2009, pp. 524–530.

[Sha10] Hua Shao and Norman C. Beaulieu. "Block Coding for Impulsive Laplacian Noise". In: 2010 IEEE International Conference on Communications. May 2010, pp. 1–6.

[Sho16] Yasser Shoukry and Paolo Tabuada. "Event-Triggered State Observers for Sparse Sensor Noise/Attacks". In: *IEEE Transactions on Automatic Control* 61.8 (2016), pp. 2079–2091.

[Sim06] Dan Simon. *Optimal state estimation: Kalman, H [infinity] and nonlinear approaches*. Hoboken, N.J: Wiley-Interscience, 2006.

[Sin04] Bruno Sinopoli, Luca Schenato, Massimo Franceschetti, Kameshwar Poolla, Michael I. Jordan, and Shankar S. Sastry. "Kalman Filtering With Intermittent Observations". In: *IEEE Transactions on Automatic Control* 49.9 (Sept. 2004), pp. 1453–1464.

[Szu09] Judit Szulágyi, Géza Kovács, and Doug Welch. "Application of the trend filtering algorithm to the MACHO database". In: *Astronomy & Astrophysics* 500.2 (June 1, 2009), pp. 917–927.

[Tü03] Reha H. Tütüncü, Kim C. Toh, and Michael J. Todd. "Solving semidefinite-quadratic-linear programs using SDPT3". In: *Mathematical Programming* 95.2 (Feb. 1, 2003), pp. 189–217.

[Tar20] *The Three Key Benefits of Drone Scouting*. Taranis. Apr. 20, 2020. URL: https://taranis.ag/2020/04/20/the-three-key-benefits-of-drone-scouting/.

[Thi19] John Thickstun. *Mercer's Theorem*. 2019. URL: https://homes.cs.washington.edu/~thickstn/docs/mercer.pdf.

[Tin07a] Jo-Anne Ting, Evangelos Theodorou, and Stefan Schaal. "A Kalman filter for robust outlier detection". In: 2007 IEEE/RSJ International Conference on Intelligent Robots and Systems. Oct. 2007, pp. 1514–1519.

[Tin07b] Jo-Anne Ting, Evangelos Theodorou, and Stefan Schaal. "Learning an Outlier-Robust Kalman Filter". In: *Machine Learning: ECML 2007*. Ed. by Joost N. Kok, Jacek Koronacki, Raomon Lopez de Mantaras, Stan Matwin, Dunja Mladenič, and Andrzej Skowron. Lecture Notes in Computer Science. Berlin, Heidelberg: Springer, 2007, pp. 748–756.

[Wan16] Yu-Xiang Wang, James Sharpnack, Alexander J. Smola, and Ryan J. Tibshirani. "Trend Filtering on Graphs". In: *Journal of Machine Learning Research* 17.105 (2016), pp. 1–41.

[Yam18] Hiroshi Yamada and Ruixue Du. "Some Results on ℓ_1 Polynomial Trend Filtering". In: *Econometrics* 6.3 (Sept. 2018), p. 33.

[Zim11] Ray D. Zimmerman, Carlos E. Murillo-Sánchez, and Robert J. Thomas. "MATPOWER: Steady-State Operations, Planning, and Analysis Tools for Power Systems Research and Education". In: *IEEE Transactions on Power Systems* 26.1 (Feb. 2011), pp. 12–19.